PATHOLOGIC CONDITIONS OF THE HUMAN NERVOUS AND MUSCULAR SYSTEMS ASSOCIATED WITH MUTANT CHAPERONES: MOLECULAR AND MECHANISTIC ASPECTS

EDITED BY: Alberto J. L. Macario and Everly Conway de Macario

PUBLISHED IN: Frontiers in Molecular Biosciences

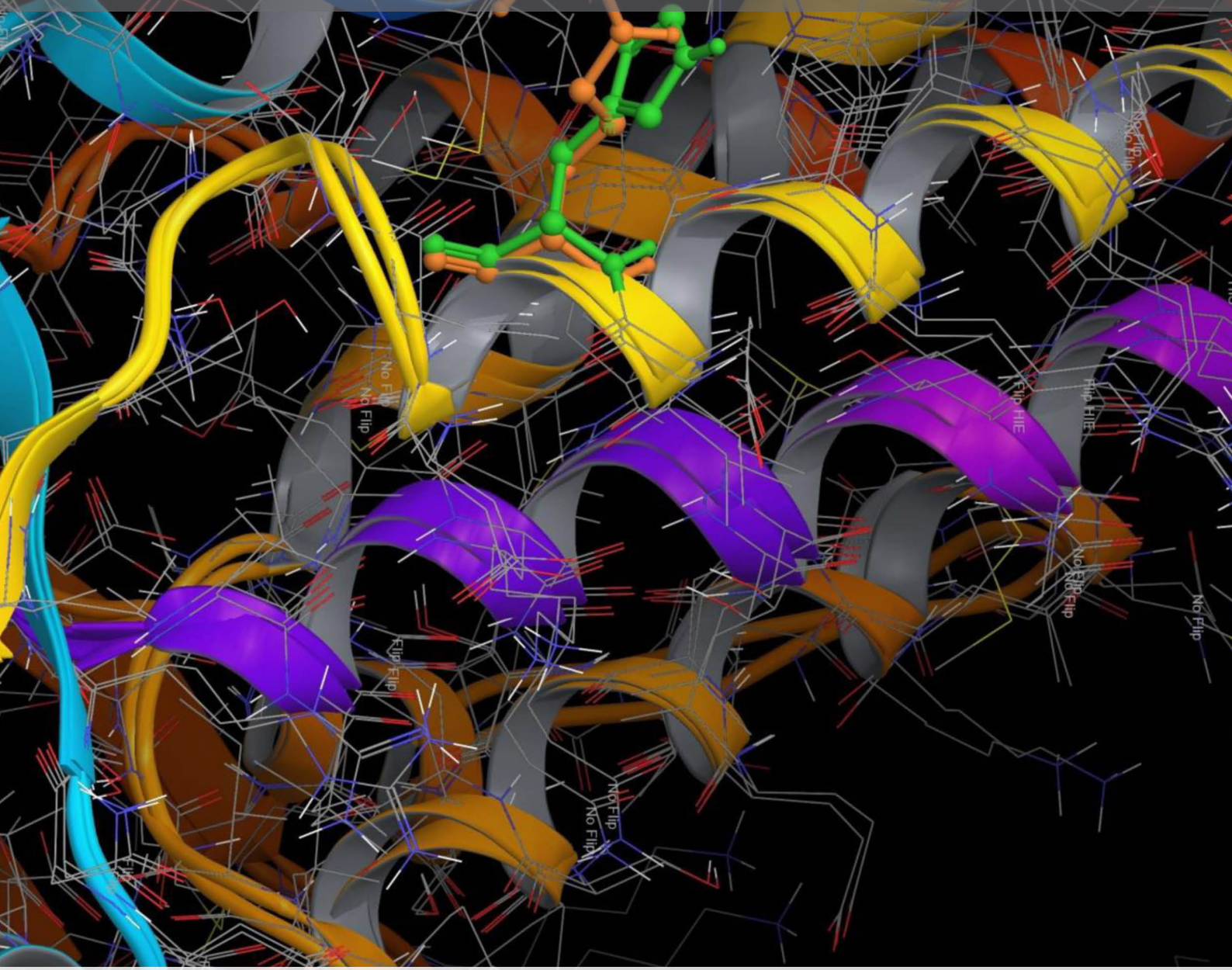

frontiers Research Topics

frontiers

ISSN 1664-8714
ISBN 978-2-88945-457-0
DOI 10.3389/978-2-88945-457-0

About Frontiers

Frontiers is more than just an open-access publisher of scholarly articles: it is a pioneering approach to the world of academia, radically improving the way scholarly research is managed. The grand vision of Frontiers is a world where all people have an equal opportunity to seek, share and generate knowledge. Frontiers provides immediate and permanent online open access to all its publications, but this alone is not enough to realize our grand goals.

Frontiers Journal Series

The Frontiers Journal Series is a multi-tier and interdisciplinary set of open-access, online journals, promising a paradigm shift from the current review, selection and dissemination processes in academic publishing. All Frontiers journals are driven by researchers for researchers; therefore, they constitute a service to the scholarly community. At the same time, the Frontiers Journal Series operates on a revolutionary invention, the tiered publishing system, initially addressing specific communities of scholars, and gradually climbing up to broader public understanding, thus serving the interests of the lay society, too.

Dedication to Quality

Each Frontiers article is a landmark of the highest quality, thanks to genuinely collaborative interactions between authors and review editors, who include some of the world's best academicians. Research must be certified by peers before entering a stream of knowledge that may eventually reach the public - and shape society; therefore, Frontiers only applies the most rigorous and unbiased reviews.
Frontiers revolutionizes research publishing by freely delivering the most outstanding research, evaluated with no bias from both the academic and social point of view.
By applying the most advanced information technologies, Frontiers is catapulting scholarly publishing into a new generation.

What are Frontiers Research Topics?

Frontiers Research Topics are very popular trademarks of the Frontiers Journals Series: they are collections of at least ten articles, all centered on a particular subject. With their unique mix of varied contributions from Original Research to Review Articles, Frontiers Research Topics unify the most influential researchers, the latest key findings and historical advances in a hot research area! Find out more on how to host your own Frontiers Research Topic or contribute to one as an author by contacting the Frontiers Editorial Office: **researchtopics@frontiersin.org**

PATHOLOGIC CONDITIONS OF THE HUMAN NERVOUS AND MUSCULAR SYSTEMS ASSOCIATED WITH MUTANT CHAPERONES: MOLECULAR AND MECHANISTIC ASPECTS

Topic Editors:
Alberto J. L. Macario, Department of Microbiology and Immunology, School of Medicine, University of Maryland at Baltimore-Institute of Marine and Environmental Technology (IMET), Columbus Center, Baltimore, MD, United States; Euro-Mediterranean Institute of Science and Technology (IEMEST), Palermo, Italy
Everly Conway de Macario, Department of Microbiology and Immunology, School of Medicine, University of Maryland at Baltimore-Institute of Marine and Environmental Technology (IMET), Columbus Center, Baltimore, MD, United States; Euro-Mediterranean Institute of Science and Technology (IEMEST), Palermo, Italy

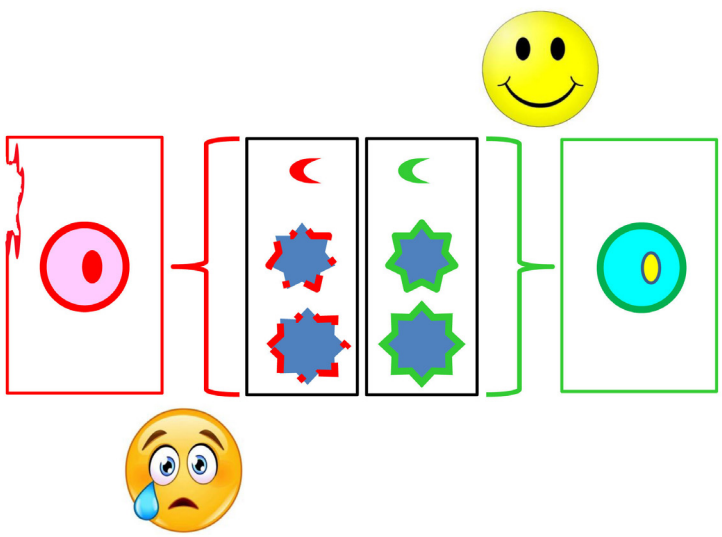

The chaperoning system of an organism (vertical rectangles in center, healthy right and sick left) consists of its entire set of chaperones, co-chaperones, and chaperone-cofactors (some of these are represented by the icons inside the center rectangles, e.g., CCT eight-pointed icon; Hsp60 seven-pointed icon; all others such as sHsp, or DnaJ/Hsp40, or Hsp10 small moon-like icon), and other molecules and structures closely interacting with them, such as chaperone receptors and interactors (not shown). Chaperones play key roles in the maintenance of normal cell physiology in tissues, e.g., the normal nervous and muscular tissues (right-most rectangle, in which a normal cell is represented as a circle with an oval inside as the nucleus). Genetic changes, for instance mutation can affect components of the chaperoning system and cause genetic chaperonopathies. Mutations can occur in the chaperone Hsp60;

or CCT; or any other, as shown in the center-left rectangle. A number of genetic chaperonopathies due to a mutation in one or the other of these chaperones affect primarily the nervous and muscular systems. In these cases, the genetically-defective chaperone has a deleterious impact on cells (red circle in left-most rectangle), for instance neurons, oligodendrocytes, Schwann cells, and myocytes. This, in turn, leads to tissue and organ abnormalities (represented by the red colored left-most rectangle with one broken side). Illustrative examples of these diseases are discussed in the eBook. The figure was created and drawn by Alberto J.L. Macario and Everly Conway de Macario.

Cover Image: Chaperonin CCT subunit 5 (CCT5) His147Arg pathogenic mutation discussed in this Research Topic (Conway de Macario et al., 2017, Front. Mol. Biosci. 3:84. doi: 10.3389/fmolb.2016.00084). Shown is a 3D image of Human CCT5, the experimental model chaperonin (Cpn) from *Pyrococcus furiosus* , and the template Cpn from the *Thermococcus* strain KS-1 crystal, superposed, and zoomed on the region in which the pathogenic mutation His147Arg occurs in the human CCT5, corresponding to position 138 in the archaeal sequences. More information is available in Sci Rep. 2014 Oct 27;4:6688. doi: 10.1038/srep06688. Image by Antonino Lauria, Anna Maria Almerico, Alberto J.L. Macario, and Everly Conway de Macario.

This eBook presents illustrative examples of genetic chaperonopathies affecting primarily nerves and muscles and discusses molecular mechanisms and treatment targeting chaperones, i.e., chaperonotherapy.

Citation: Macario, A. J. L., Conway de Macario, E., eds. (2018). Pathologic Conditions of the Human Nervous and Muscular Systems Associated with Mutant Chaperones: Molecular and Mechanistic Aspects. Lausanne: Frontiers Media. doi: 10.3389/978-2-88945-457-0

Table of Contents

frontiers in Molecular Biosciences

EDITORIAL
published: 16 February 2018
doi: 10.3389/fmolb.2018.00014

Editorial: Pathologic Conditions of the Human Nervous and Muscular Systems Associated with Mutant Chaperones: Molecular and Mechanistic Aspects

Alberto J. L. Macario [1,2]* *and Everly Conway de Macario* [1,2]

[1] *Department of Microbiology and Immunology, School of Medicine, University of Maryland at Baltimore-Institute of Marine and Environmental Technology (IMET), Columbus Center, Baltimore, MD, United States,* [2] *Euro-Mediterranean Institute of Science and Technology (IEMEST), Palermo, Italy*

Keywords: Genetic Chaperonopathies, Hsp60/CCT/BBS, Hsp40/DnaJ, small-Hsp, Indirect/Secondary Chaperonopathies, Chaperonotherapy

Editorial on the Research Topic

Pathologic Conditions of the Human Nervous and Muscular Systems Associated with Mutant Chaperones: Molecular and Mechanistic Aspects

This Research Topic focuses on genetic chaperonopathies (http://www.chaperones-pathology.org) affecting predominantly muscles and nerves. It should be useful to professionals in the medical and closely related sciences, particularly physicians and clinical pathologists in practice and in applied and basic research. These were the objectives outlined for the Research Topic (see About this Research Topic). By examining the current series of articles with their figures and tables, the references cited, and the diversity of contributors, one may say that the objectives have been attained at least in as much as the field covered is vast and the materials discussed varied. This cornucopia of information we hope will reach many for the ultimate benefit of a large number of patients and their families.

One of the important benefits of the notion that a chaperone can cause disease is that it alerts the researcher and the physician to the possibility that there is a pathogenic pathway, different from the others known to occur in any particular patient, which may be amenable to specific diagnostic and treatment procedures. This notion, in turn, engenders the idea that chaperones can be therapeutic targets or agents. For example, patients with chaperonopathies by defect may benefit from positive chaperonotherapy, namely from procedures aiming at correcting the deficiency by gene replacement or chaperone administration. Since developments in chaperonotherapy must be rooted in basic and clinical research, information in this Research Topic should be instrumental for investigators to find ways of preventing and curing chaperonopathies. Contributions are here presented in the order of their publication. All Figures and Tables cited in this Editorial can be found in the articles being discussed.

Accumulation of SOD1 (Superoxide Dismutase 1) mutant protein in neurons is pathogenic in some forms of amyotrophic lateral sclerosis (*SOD1*-ALS). Anzai et al. describe their attempts to find drugs that specifically interact with the misfolded SOD1 mutant molecules and suppress their pathologic aggregation. Their findings provide clues on which molecular structures should be further tested and modified to obtain efficacious drugs with minimal side effects.

Missense mutations in the *HSP60* gene cause SPG13 and MitCHAP-60 chaperonopathies, as discussed by Bross and Fernandez-Guerra. Figure 1 and Table 1 are excellent teaching tools that

Edited and reviewed by:
Vladimir N. Uversky,
University of South Florida,
United States

***Correspondence:**
Alberto J. L. Macario
ajlmacario@som.umaryland.edu

Specialty section:
This article was submitted to Protein Folding, Misfolding and Degradation, a section of the journal Frontiers in Molecular Biosciences

Received: *14 January 2018*
Accepted: *26 January 2018*
Published: *16 February 2018*

Citation:
Macario AJL and Conway de Macario E (2018) Editorial: Pathologic Conditions of the Human Nervous and Muscular Systems Associated with Mutant Chaperones: Molecular and Mechanistic Aspects. Front. Mol. Biosci. 5:14. doi: 10.3389/fmolb.2018.00014

can be used to spread knowledge not only on genetic HSP60 chaperonopathies, but also to explain what might happen to other chaperones if mutated at critical sites.

The article by Sorge and Brancaccio provides a useful review on the roles played by chaperones in the stressed heart, focusing on Melusin, and opening eyes as to possible developments in the treatment of heart diseases centered on this chaperone. Melusin is a muscle specific chaperone protein that induces adaptive hypertrophy and cardiomyocyte survival under stress.

Ruggieri et al. discuss DNAJB6 chaperonopathies and present an overview of the various mutations and phenotypes identified thus far (Table 1), focusing on limb girdle muscular dystrophy 1D. Fascinating questions that should stimulate future research emerge from the information provided, pertaining to tissue pathology differential distribution, mutations in DNAJ6 domains other than G/F, and chaperonotherapy using DNAJ gene/protein.

The contribution by Bie et al. represents the first ever description of an HSP10 chaperonopathy and offers a variety of starting points for future research not only on HSP10, but also on its functional partner, HSP60, and on mitochondrial disorders.

Tang and Xia review the pathogenic mutations of the human protein p97, including Multisystem Proteinopathies, Familial Amyotrophic Lateral Sclerosis, and Charcot-Marie-Tooth Disease Type 2Y (Table 1). Because of its many functions in various cellular locales, p97 interacts with a variety of co-factors and adaptors in a complex matrix, which is very difficult to elucidate. This article is very stimulating because it explains clearly the facts and the problems and suggests possible ways to advance the field.

Lupo et al. deal with pathogenic mutations in four chaperone genes (*DNAJB*, *HSPB1, HSPB3*, and *HSPB8*) that cause distal hereditary motor neuropathies (dHMN). Table 1 is a useful compendium of mutations, phenotypes, and bibliography. The connection between chaperones and chaperonopathies and the distinctive features of chaperonopathies as compared with proteinopathies are clearly explained.

Experimental models are necessary to study the molecular mechanisms that in chaperonopathies produce the abnormalities observed in tissues and organs, since work with human specimens is very limited. Conway de Macario et al. report on experimental models using archaea that possess chaperones very similar to those of humans. Studies on CCT chaperonopathies are reported along with a list of genes that may be affected and pathogenic mutations already identified (Tables 1, 2).

Pelizaeus-Merzbacher disease (PMD) is a hypomyelinating leukodystrophy associated with mutations in *PLP1*, which encodes a major myelin protein. Mutations in genes encoding membrane proteins (nicely explained in Figure 1, in the article by Inoue) may lead to the production of abnormal polypeptides that accumulate in the ER of the myelin-producing oligodendrocytes and, thereby, elicit the unfolded protein response (UPR), involving ER chaperones (explained in Figure 2). This would be an example of a secondary chaperonopathy, namely the mutated gene does not encode a chaperone but, ultimately, has an impact on chaperones, which become pathogenic. Suggestions for development of chaperonotherapy for PMD and other leukodystrophies are offered.

The article by Lanfranco et al. discusses Spinal Muscular Atrophy (SMA) and some of the molecular mechanisms of it that point toward a failure in chaperoning activity. The disease is directly associated with decreased levels of the Survival Motor Neuron (SMN) protein. This protein is part of a complex that functions as a molecular chaperone, interacting with and assisting in the assembly of small ribonuleoproteins (snRNPs). It is concluded that SMA may be considered a chaperonopathy and, consequently, amenable to chaperonotherapy. This is important because other disorders, such as adult-onset amyotrophic lateral sclerosis (ALS), show disturbance of snRNP assembly.

Bardet-Biedl syndrome (BBS) comprises a group of genetic diseases called ciliopathies since cell cilia are defective. The article by Alvarez-Satta et al. presents a subset of BBS as chaperonopathies because of the 21 or so genes whose mutations are currently known to be associated with BBS, three (BBS6, 10, and 12) belong to the family of CCT chaperonins. Other facts that argue in favor of considering some BBS as chaperonopathies are that over 50% of all BBS-affected families carry a pathogenic mutation in one of these three genes, and patients with mutations in any one of these three genes are more severely ill.

AUTHOR CONTRIBUTIONS

All authors listed have made a substantial, direct and intellectual contribution to the work, and approved it for publication.

ACKNOWLEDGMENTS

AJLM and ECdeM were partially supported by IMET. This work was done under the agreement between IEMEST (Italy) and IMET (USA) (this is IMET contribution number IMET 18-002).

Conflict of Interest Statement: The authors declare that the research was conducted in the absence of any commercial or financial relationships that could be construed as a potential conflict of interest.

frontiers in Molecular Biosciences

MINI REVIEW
published: 31 July 2017
doi: 10.3389/fmolb.2017.00055

Bardet-Biedl Syndrome as a Chaperonopathy: Dissecting the Major Role of Chaperonin-Like BBS Proteins (BBS6-BBS10-BBS12)

María Álvarez-Satta[1,2,3], *Sheila Castro-Sánchez*[1,2,3] *and Diana Valverde*[1,2,3]*

[1] Grupo de Biomarcadores Moleculares, Departamento de Bioquímica, Genética e Inmunología, Facultad de Biología, Universidad de Vigo, Vigo, Spain, [2] Grupo de Investigación en Enfermedades Raras y Medicina Pediátrica, Instituto de Investigación Sanitaria Galicia Sur (IIS Galicia Sur), SERGAS-UVIGO, Vigo, Spain, [3] Centro de Investigaciones Biomédicas (Centro Singular de Investigación de Galicia 2016–2019), Universidad de Vigo, Vigo, Spain

OPEN ACCESS

Edited by:
Alberto J. L. Macario, University of Maryland at Baltimore and Institute of Marine and Environmental Technology, United States; Istituto Euro-Mediterraneo di Scienza e Tecnologia, Italy

Reviewed by:
Luciano Brocchieri, TB-SEQ, Inc., United States
Adam Keith Walker, Macquarie University, Australia

***Correspondence:**
Diana Valverde
dianaval@uvigo.es

Specialty section:
This article was submitted to Protein Folding, Misfolding and Degradation, a section of the journal Frontiers in Molecular Biosciences

Received: 25 May 2017
Accepted: 13 July 2017
Published: 31 July 2017

Citation:
Álvarez-Satta M, Castro-Sánchez S and Valverde D (2017) Bardet-Biedl Syndrome as a Chaperonopathy: Dissecting the Major Role of Chaperonin-Like BBS Proteins (BBS6-BBS10-BBS12). Front. Mol. Biosci. 4:55. doi: 10.3389/fmolb.2017.00055

Bardet-Biedl syndrome (BBS) is a rare genetic disorder that belongs to the group of ciliopathies, defined as diseases caused by defects in cilia structure and/or function. The six diagnostic features considered for this syndrome include retinal dystrophy, obesity, polydactyly, cognitive impairment and renal and urogenital anomalies. Furthermore, three of the 21 genes currently known to be involved in BBS encode chaperonin-like proteins (MKKS/BBS6, BBS10, and BBS12), so BBS can be also considered a member of the growing group of chaperonopathies. Remarkably, up to 50% of clinically-diagnosed BBS families can harbor disease-causing variants in these three genes, which highlights the importance of chaperone defects as pathogenic factors even for genetically heterogeneous syndromes such as BBS. In addition, it is interesting to note that BBS families with deleterious variants in *MKKS/BBS6*, *BBS10* or *BBS12* genes generally display more severe phenotypes than families with changes in other *BBS* genes. The chaperonin-like BBS proteins have structural homology to the CCT family of group II chaperonins, although they are believed to conserve neither the ATP-dependent folding activity of canonical CCT chaperonins nor the ability to form CCT-like oligomeric complexes. Thus, they play an important role in the initial steps of assembly of the BBSome, which is a multiprotein complex essential for mediating the ciliary trafficking activity. In this review, we present a comprehensive review of those genetic, functional and evolutionary aspects concerning chaperonin-like BBS proteins, trying to provide a new perspective that expands the classical conception of BBS only from a ciliary point of view.

Keywords: ciliopathies, chaperonopathies, Bardet-Biedl syndrome, chaperonin-like BBS proteins, MKKS/BBS6, BBS10, BBS12

BARDET-BIEDL SYNDROME IN CONTEXT

The Bardet-Biedl syndrome (BBS; MIM#209900) is a multisystem, rare genetic disorder belonging to the group of ciliopathies, which encompasses several diseases that are caused by defects in cilia structure and/or function, especially affecting the primary cilium (reviewed in Hildebrandt et al., 2011; Mitchison and Valente, 2017). This highly conserved and dynamic organelle is considered

the sensorial antennae of the cell and also a central processing unit, since it captures and integrates all the extracellular signals with the cell cycle and metabolism (reviewed in Malicki and Johnson, 2017). Thus, primary cilia play a key role in coordinating the different cellular signaling pathways (reviewed in Cardenas-Rodriguez and Badano, 2009; Christensen et al., 2017), giving rise to biological responses related to the control of cell cycle, development and differentiation processes, migration and polarity, stimuli transduction or proliferation and maintenance of stem cells. Ciliopathies represent an expanding group of human inherited disorders that are valuable models to study several common conditions such as obesity, retinal dystrophy or renal cysts, considering their pleiotropic nature. Remarkably, more than 50 genes have been involved in ciliopathies (Mitchison and Valente, 2017), a number that continues to grow due to the new discoveries on ciliary proteome and ciliogenesis regulation (Mick et al., 2015; Wheway et al., 2015; Boldt et al., 2016), as well as the increasingly implementation of high-throughput sequencing technologies to ciliary disorders. Furthermore, it is important to highlight that ciliopathies are complex clinical entities with extensive genetic heterogeneity and also high phenotypic and genetic overlap among them. This, together with the progressive development of nearly all clinical features related to them, usually makes an early and specific diagnosis very difficult to establish.

BBS is considered a model disease to study the biology of the primary cilium, and is characterized by progressive retinal dystrophy, obesity, postaxial polydactyly, cognitive impairment and renal and urogenital anomalies as primary diagnostic features (reviewed in Forsythe and Beales, 2013). Furthermore, BBS is a genetically heterogeneous disorder with up to 21 genes (commonly known as *BBS* genes) described to date (Bujakowska et al., 2015; Heon et al., 2016; Khan et al., 2016 and references within). Intriguingly, although BBS is primarily inherited as an autosomal recessive disorder, a more complex model of oligogenic inheritance considering modifier *loci* and epistatic effects has been proposed for some families, trying to explain the high clinical variability reported for BBS patients (Katsanis, 2004; Badano et al., 2006). Regarding the functions of BBS proteins (reviewed in Novas et al., 2015), eight of them form a multimeric complex called BBSome, which plays a key role in mediating molecular/vesicular transport in and out of the primary cilium, and also in intraciliary trafficking as part of the intraflagellar transport machinery (Nachury et al., 2007; Loktev et al., 2008; Wei et al., 2012). Moreover, most of the remaining BBS proteins have functions related to BBSome assembly, cilia targeting of BBSome and proper recognition of BBSome cargoes, besides several extra-ciliary roles (Novas et al., 2015).

BARDET-BIEDL SYNDROME AS A CHAPERONOPATHY

Three of the main *BBS* genes, *MKKS*/*BBS6* (MIM*604896), *BBS10* (MIM*610148) and *BBS12* (MIM*610683), encode chaperonin-like proteins that localize to centrosomes and ciliary basal bodies (Kim et al., 2005; Marion et al., 2009). This implies that BBS would also be part of the emerging group of diseases called chaperonopathies, which are produced by defects in molecular chaperones or any other protein resembling their structure. In this regard, it is noteworthy that chaperonin-like BBS proteins, as will be explained later, are unlikely to display a folding activity but they have functions specifically related to the assembly of the BBSome.

Chaperonopathies represent an interesting subset of disorders that have so far received little attention, although they can provide useful models to better understand some of the molecular mechanisms necessary to maintain protein homeostasis (extensively reviewed in Macario and Conway de Macario, 2005, 2007a,b; Macario et al., 2005). Chaperonopathies often manifest themselves as complex phenotypes affecting multiple organs, possibly due to the ubiquitous localization of most chaperones, and may be of genetic or acquired origin. In this latter case, defects in chaperone post-translational modifications, distribution or quantity, together with other phenomena such as generation of antichaperone autoantibodies or aggregation of chaperones with deposits of abnormal proteins, all of them usually related to aging, could be the trigger rather than mutational events. Importantly, research on chaperones and their role in disease is opening a new field of therapeutic options (termed "chaperonotherapy") with interesting applications not only in chaperonopathies, but also in some processes such as cancer whereby chaperones may modulate the immune response against tumors (reviewed in Binder, 2008; Graner et al., 2015).

Contribution of *MKKS*/*BBS6, BBS10* and *BBS12* Genes to Bardet-Biedl Syndrome

Among ciliopathies, BBS represents a special case since as far as we know no other ciliopathy except the related McKusick-Kaufman syndrome (MKKS; MIM#236700) is caused by genetic defects in chaperone genes. At this point, it is appropriate to mention that MKKS is a monogenic ciliopathy caused by mutations in the *MKKS* gene leading to postaxial polydactyly, genital malformations (typically hydrometrocolpos in females) and also congenital heart disease (Schaefer et al., 2011). Furthermore, BBS is also a particular member of the chaperonopathies with regard to the very specific functions carried out by chaperonin-like BBS proteins within a ciliary context (explained in detail in the next section). In this sense, BBS constitutes a clear example of the great importance of chaperone defects as determinant pathogenic factors, taking into account that up to 50% of families clinically diagnosed with BBS can harbor pathogenic variants in *MKKS*/*BBS6*, *BBS10* and *BBS12* genes (Billingsley et al., 2010; Muller et al., 2010; Deveault et al., 2011). This data is even more relevant considering the high genetic heterogeneity of BBS with 21 genes currently identified, a number that is expected to grow as 20–30% of patients suspected to suffer BBS do not yet have molecular confirmation of their clinical diagnosis (Mitchison and Valente, 2017).

Chaperonin-like *BBS* genes are characterized by a relatively simple gene structure (**Figure 1**), with a low number of coding exons (one in *BBS12*, two in the case of *BBS10* and four exons in *MKKS*/*BBS6*), which make them ideal candidates for

a mutational screening previously to perform more complex and expensive analyses. Furthermore, a broad distribution of pathogenic variants throughout the coding sequence of chaperonin-like *BBS* genes has been reported. A brief summary of the most relevant genetic findings concerning each gene is presented below (see also **Table 1**).

MKKS/*BBS6* (chromosome 20p12.2) was the first gene coding a putative chaperonin to be associated with a human inherited disorder, the MKKS (Stone et al., 2000), being also involved in BBS shortly after (Katsanis et al., 2000; Slavotinek et al., 2000). To date, more than 50 deleterious variants have been described, predominantly missense and nonsense changes (Human Gene Mutation Database; Stenson et al., 2017). Regarding its contribution to the total load of BBS, *MKKS*/*BBS6* is a minor contributor with 3–5% of families harboring two disease-causing variants in the multiethnic cohorts reported worldwide (Beales et al., 2001; Muller et al., 2010; Deveault et al., 2011). Interestingly, the vast majority of causal variants described in this gene have been identified in BBS patients, so it has been proposed that both syndromes MKKS and BBS are different allelic forms of the same clinical entity (Katsanis et al., 2000; Schaefer et al., 2011). Thus, MKKS phenotypes would be linked to very rare, possibly hypomorphic alleles found in *MKKS*/*BBS6* gene.

The *BBS10* gene (chromosome 12q21.2) was first identified by Stoetzel et al. (2006) in a consanguineous pedigree of Lebanese origin. It is, together with *BBS1*, the major contributor to BBS accounting for 20% of all cases (Stoetzel et al., 2006; Forsythe and Beales, 2013), with remarkable exceptions in ethnically homogeneous groups such as Danish (43%; Hjortshøj et al., 2010) or Spanish BBS cohorts (8.3%; Álvarez-Satta et al., 2014). About 100 different disease-causing changes have been reported elsewhere (Human Gene Mutation Database; Stenson et al., 2017), of which the p.Cys91Leufs*5 allele represents a recurrent deleterious variant in BBS cohorts of European descent, reaching 26–48% of *BBS10* mutational load (Stoetzel et al., 2006; Billingsley et al., 2010; Muller et al., 2010).

Moreover, the *BBS12* gene (chromosome 4q27) was linked to BBS phenotypes a decade ago (Stoetzel et al., 2007). Its contribution to BBS has grown in importance over recent years, accounting for 8–11% of the total cases in most of the cohorts reported (Billingsley et al., 2010; Muller et al., 2010; Deveault et al., 2011; Álvarez-Satta et al., 2014). About 60 pathogenic variants have been currently identified in *BBS12* patients (Human Gene Mutation Database; Stenson et al., 2017), among which the nonsense change p.(Phe372*) could represent up to 20% of the mutated alleles found in this gene (Stoetzel et al., 2007).

Finally, it is also important to highlight some trends regarding the BBS phenotypes linked to changes in chaperonin-like *BBS* genes. Thus, there is a general consensus that BBS patients with pathogenic variants in *MKKS*/*BBS6*, *BBS10* and *BBS12* genes develop a more severe phenotype than those with changes affecting BBSome components such as BBS1 (Billingsley et al., 2010; Imhoff et al., 2011; Castro-Sánchez et al., 2015). In detail, they show an earlier disease onset (especially noted in *BBS10* patients), greater prevalence of all BBS primary diagnostic features and also a higher frequency of overlapping features with other ciliopathies, mainly MKKS and also Alström syndrome (MIM#203800), which is a closely related ciliopathy produced by mutations in the *ALMS1* gene and characterized by retinal dystrophy, sensorineural hearing loss, early-onset obesity with severe type 2 diabetes mellitus and metabolic syndrome, dilated cardiomyopathy and renal, hepatic and pulmonary injury with widespread fibrosis (reviewed in Marshall et al., 2011). One could hypothesize that differences in the severity of clinical presentation could be due to the distinct functional roles of chaperonin-like *BBS* genes when compared with the BBS proteins taking part of the BBSome. Thus, deleterious variants in some components of the BBSome might lead to the accumulation of intermediate complexes that maintain a residual or gain-of-function activity as compensating mechanism (Zhang et al., 2012), whereas the chaperonin-like BBS proteins are essential for the initial step of BBSome assembly (see below) so no functional complexes are formed if this subset of proteins is affected (Seo et al., 2010).

Structure and Function of Chaperonin-Like BBS Proteins: Comparison with Canonical CCT Chaperonins

The three chaperonin-like BBS proteins define a particular branch of proteins that have sequence homology to the chaperonin containing t-complex protein 1, CCT (also known

TABLE 1 | Summary of the main features related to chaperonin-like *BBS* genes.

Gene	Gene MIM number	Chromosome	Exons (Coding)	Pathogenic variants†	Mean contribution^(%)	Protein (aa)	Phenotype MIM number	References
MKKS/BBS6	*604896	20p12.2	6 (4)	57	3–5	570	#605231 (BBS) #236700 (MKKS)	Katsanis et al., 2000 Slavotinek et al., 2000; Stone et al., 2000
BBS10	*610148	12q21.2	2 (2)	99	20	723	#615987 (BBS)	Stoetzel et al., 2006
BBS12	*610683	4q27	2 (1)	59	8–11	710	#615989 (BBS)	Stoetzel et al., 2007

MIM, Mendelian Inheritance in Man® (online database of human genes and genetic diseases; https://www.omim.org/); aa, amino acids; BBS, Bardet-Biedl syndrome; MKKS, McKusick-Kaufman syndrome.

†*The number of pathogenic variants corresponds to the data obtained from the last version of the Human Gene Mutation Database (HGMD professional 2017.1; released on March 2017).*

^*The mean contribution for each chaperonin-like BBS gene was established from the values reported elsewhere (Beales et al., 2001; Stoetzel et al., 2006; Billingsley et al., 2010; Muller et al., 2010; Deveault et al., 2011; Forsythe and Beales, 2013; Álvarez-Satta et al., 2014).*

as TRiC) family of group II chaperonins (Kim et al., 2005; Stoetzel et al., 2006, 2007). CCT proteins are the eukaryotic cytosolic chaperonins of type II and play key roles in the folding of a wide range of newly translated proteins in an ATP-dependent manner, mainly soluble proteins related to cytoskeleton (actin and tubulin are the quantitative major substrates) (reviewed in Dunn et al., 2001; Spiess et al., 2004). Typically, they form a functional hetero-oligomeric complex of 16 subunits that consists of two stacked rings, each composed of eight CCT monomers radially arranged (CCT1-8). With regard to their specific roles in cilia, CCT subunits are required for ciliary assembly and maintenance of cilia tip integrity, as well as cytoskeleton structure, in the ciliate *Tetrahymena* (Seixas et al., 2010). In addition, it has been recently reported that CCT chaperonins are essential for the biogenesis of vertebrate photoreceptors' outer segment by mediating the BBSome assembly (Sinha et al., 2014).

Recent phylogenetic analyses have revealed that chaperonin-like BBS proteins represent a highly diverged, monophyletic group derived from a duplication event in the *CCT8* gene (Mukherjee et al., 2010). Remarkably, although *MKKS/BBS6*, *BBS10,* and *BBS12* genes were originally considered as vertebrate-specific, the finding of several orthologs in ancient eukaryotes clearly points to an earlier evolution (Mukherjee and Brocchieri, 2013). The high rate of divergence observed for chaperonin-like BBS proteins compared with those canonical CCT chaperonins is not reflected by their primary structure, which is mostly conserved. Thus, the typical chaperonin domain architecture consisting of apical, intermediate and equatorial domains is conserved in chaperonin-like BBS proteins (**Figure 1**); however, they have additional specific insertions (two in MKKS/BBS6, three for BBS10 and up to five in the BBS12 sequence) that are restricted to intermediate and equatorial domains (Kim et al., 2005; Stoetzel et al., 2006, 2007). Interestingly, the three insertions located in BBS10, as well as the insertions 1 and 3 of BBS12, protrude from the same face of the intermediate domain, which suggests they constitute an additional domain maybe with specific roles (Stoetzel et al., 2006, 2007). Furthermore, BBS12 seems to be the most divergent member since more differences in several secondary-structure motifs and also in the ATP-hydrolysis motif have been identified (Stoetzel et al., 2007; Mukherjee et al., 2010).

Despite structural similarities, solid evidences point out that chaperonin-like BBS proteins neither perform folding activity nor are able to form chaperonin oligomeric complexes like canonical CCT proteins do. Thus, the ATP hydrolysis motif in the equatorial domain (highly conserved in Group I and II chaperonins) is significantly different in MKKS/BBS6 and, above all, in BBS12 protein (Kim et al., 2005; Stoetzel et al., 2007), which suggests that the catalytic activity required for protein folding is missing; conversely, it would be conserved in BBS10 (Stoetzel et al., 2006). In addition, the existence of specific insertions in chaperonin-like BBS proteins covering potential monomer-monomer contact regions makes it unlikely that they can assemble in a functional CCT-like complex (Kim et al., 2005; Stoetzel et al., 2006, 2007; Mukherjee et al., 2010).

All these data suggest that the roles of chaperonin-like BBS proteins may differ from direct protein folding. Thus, recent work has demonstrated that MKKS/BBS6, BBS10 and BBS12 play a key role in the initial steps of BBSome assembly by stabilizing BBS7 (the first component to be incorporated) and mediating its interaction with six canonical CCT chaperonins (CCT1-5 and CCT8), which would actually accomplish the folding activity (Seo et al., 2010). This means that chaperonin-like BBS proteins act as an intermediate for the binding of CCT complex to its substrates, as part of the transient BBS/CCT/TRiC-chaperonin complex. Remarkably, BBS10 is not a structural member of this complex, but it regulates the interaction of the BBS6-BBS12-BBS7 intermediate with CCT proteins to form the BBS/CCT/TRiC-chaperonin complex (Zhang et al., 2012). It is also important to note that the second step in BBSome assembly, that is, the interaction between BBS2 and the stabilized BBS7 protein, is coupled with the release of BBS6-BBS12 from the complex, and that CCT/TRiC proteins are also released after the BBSome core complex (BBS2-BBS7-BBS9) is formed (Zhang et al., 2012). Accordingly, the BBS/CCT/TRiC-chaperonin complex would assist BBSome assembly only in the first steps, so the formation of mature BBSome complexes is finally completed by intrinsic protein-protein interactions among the BBSome components, which are known to contain β-propeller, tetratricopeptide repeats and pleckstrin homology domains that typically mediate these interactions (Zhang et al., 2012). Despite the significant progress made in deciphering the specific roles of chaperonin-like BBS proteins, details on how the BBS/CCT/TRiC-chaperonin complex is formed and completes the transition of BBS7 to BBSome remain to be elucidated.

Role of Other BBS Proteins in Protein Homeostasis

The cellular network for protein-quality control necessary to maintain protein homeostasis includes besides the chaperone machinery, which ensures proper protein folding and recognition of misfolded proteins (reviewed in Hartl et al., 2011), also two proteolytic machineries, the ubiquitin-proteasome system and the autophagy pathway, which play essential roles in removing irreversibly misfolded proteins (reviewed in Chen et al., 2011). In this regard, it is appropriate to remark on some findings involving several BBS proteins and their possible role in this field.

Several BBSome components such as BBS1-2, BBS4, and BBS7, as well as the BBS6 chaperonin-like protein, interact with proteasomal subunits and could be involved in the regulation of signaling pathways coordinated by the primary cilium (reviewed in Novas et al., 2015). It has been also speculated that TRIM32/BBS11 (MIM*602290) would be the putative E3-ubiquitin ligase that targets free BBS2 to be degraded by the ubiquitin-proteasome pathway (Zhang et al., 2012). Finally, there is also evidence that the *unfolded protein response* (UPR) of the endoplasmic reticulum can be a pathogenic mechanism related to BBS, as the UPR is triggered by protein accumulation in the photoreceptors of *Bbs12*-deficient models leading to apoptosis and subsequent retinal degeneration (Mockel et al., 2012). Interestingly, the light detection ability was restored by pharmacological modulation of the UPR, which highlights both the importance of identifying disease mechanisms that involve

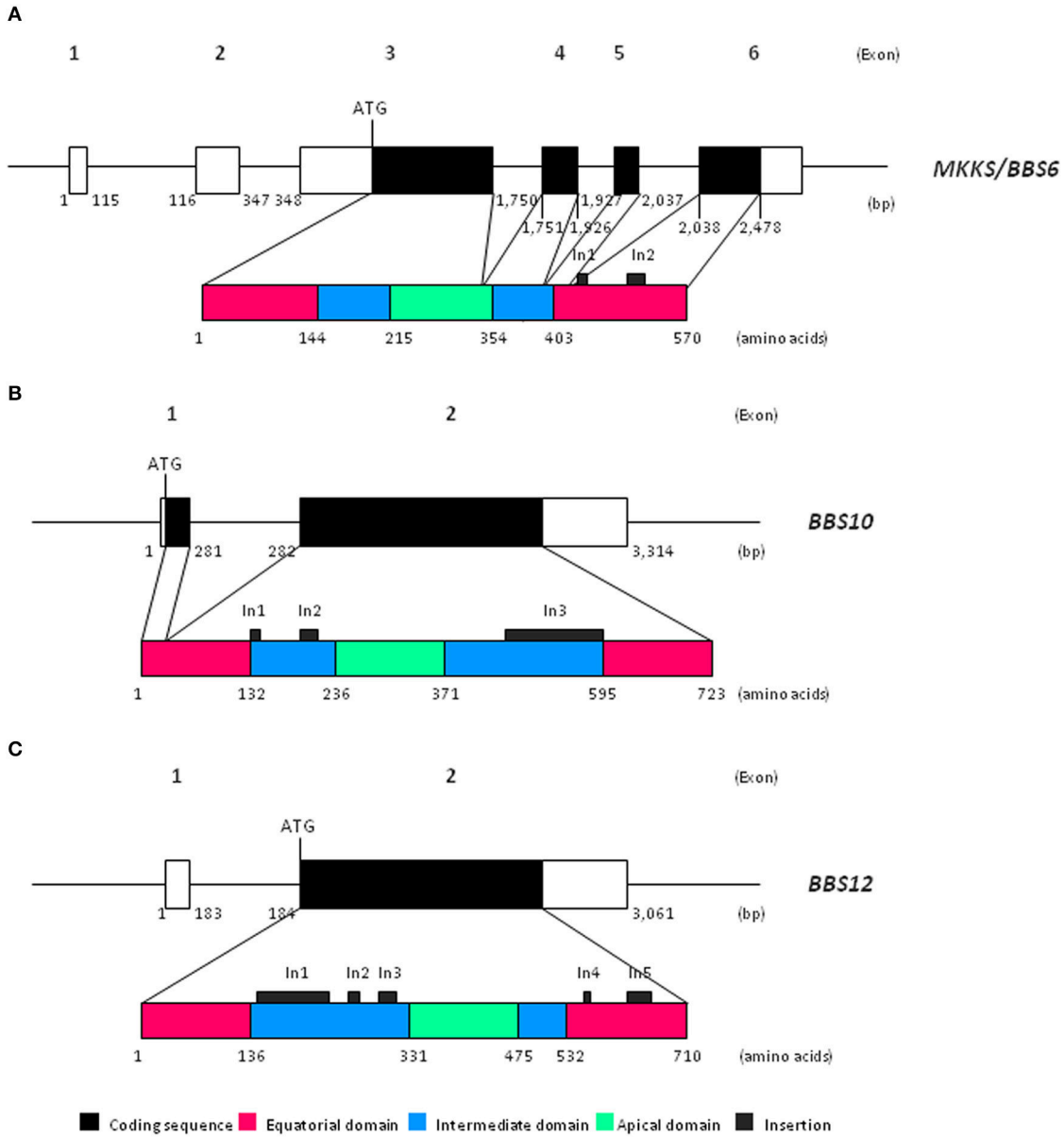

FIGURE 1 | Schematic view of both gene and protein structure of chaperonin-like BBS proteins. **(A)** Representation of *MKKS/BBS6* (reference transcript ENST00000347364.7); **(B)** Representation of *BBS10* (reference transcript ENST00000393262.3); **(C)** Representation of *BBS12* (reference transcript ENST00000314218.7). bp, base pairs.

proteostasis network components and their potential to develop new therapeutic strategies.

PERSPECTIVES

BBS is considered a model ciliopathy to study molecular mechanisms potentially involved in common disorders such as obesity, and also represents a singular component of the group of chaperonopathies. Unlike many of these clinical entities, the molecular basis underlying BBS is fairly well-known, just like the particular role of most BBS proteins in the primary cilium and also the cellular basis of several BBS phenotypes (reviewed in Novas et al., 2015). However, many mechanistic aspects remain to be uncovered, especially those concerning the particular molecular processes involved in initialization of BBsome assembly and also the role of protein degradation systems in BBS proteins turnover. In this sense, the use of prokaryotic chaperonins as models to investigate the impact of deleterious variants in chaperonin structure and function, as well as potential therapeutic strategies (Conway de Macario et al., 2017), could represent a promising tool not explored until now to further characterize chaperonin-like BBS proteins.

Moreover, a deeper understanding of the molecular mechanisms involving chaperonin-like BBS proteins could provide more opportunities to explore new therapies for BBS patients, currently unavailable. Thus, some BBSome components are found in monomeric form or aggregated with unidentified proteins in *Bbs6* null mice (Seo et al., 2010), which might suggest potential therapeutic targets related to the modulation of chaperone activity. In addition, identifying the specific chaperones and partners involved in the folding of BBSome components, not yet defined, could have a great impact on the development of new strategies in this field.

AUTHOR CONTRIBUTIONS

MA conceptualized the study, and drafted, reviewed and edited the manuscript. SC drafted and reviewed the manuscript. DV conceived of the study, critically revised the manuscript, acquired funds and supervised the work. All authors read and approved the final manuscript.

FUNDING

This work was supported by grants from Fondo de Investigación Sanitaria del Instituto de Salud Carlos III-FEDER (PI12/01853 and PI15/00049). MA (FPU12/01442) and SC (FPU13/01835) received graduate studentship awards (FPU fellowship) from the Spanish Ministry of Education, Culture and Sports.

ACKNOWLEDGMENTS

We would like to thank the Registro Español de los Síndromes de Wolfram, Bardet-Biedl y Alström (REWBA), the European Union Rare Diseases Registry for Wolfram syndrome, Alström syndrome, Bardet–Biedl syndrome and other rare diabetes syndromes (EURO-WABB), the Asociación Nacional de Ciliopatías (ANASBABI) and also to BIOCAPS Project (from European Commission under the 7th Framework Programme, FP-7-REGPOT 2012-2013-1, grant agreement no. FP7- 316265).

REFERENCES

Álvarez-Satta, M., Castro-Sánchez, S., Pereiro, I., Piñeiro-Gallego, T., Baiget, M., Ayuso, C., et al. (2014). Overview of Bardet-Biedl syndrome in Spain: identification of novel mutations in BBS1, BBS10 and BBS12 genes. *Clin. Genet.* 86, 601–602. doi: 10.1111/cge.12334

Badano, J. L., Leitch, C. C., Ansley, S. J., May-Simera, H., Lawson, S., Lewis, R. A., et al. (2006). Dissection of epistasis in oligogenic Bardet-Biedl syndrome. *Nature* 439, 326–330. doi: 10.1038/nature04370

Beales, P. L., Katsanis, N., Lewis, R. A., Ansley, S. J., Elcioglu, N., Raza, J., et al. (2001). Genetic and mutational analyses of a large multiethnic Bardet-Biedl cohort reveal a minor involvement of BBS6 and delineate the critical intervals of other loci. *Am. J. Hum. Genet.* 68, 606–616. doi: 10.1086/318794

Billingsley, G., Bin, J., Fieggen, K. J., Duncan, J. L., Gerth, C., Ogata, K., et al. (2010). Mutations in chaperonin-like BBS genes are a major contributor to disease development in a multiethnic Bardet-Biedl syndrome patient population. *J. Med. Genet.* 47, 453–463. doi: 10.1136/jmg.2009.073205

Binder, R. J. (2008). Heat-shock protein-based vaccines for cancer and infectious disease. *Expert. Rev. Vaccines* 7, 383–393. doi: 10.1586/14760584.7.3.383

Boldt, K., van Reeuwijk, J., Lu, Q., Koutroumpas, K., Nguyen, T. M., Texier, Y., et al. (2016). An organelle-specific protein landscape identifies novel diseases and molecular mechanisms. *Nat. Commun.* 7:11491. doi: 10.1038/ncomms11491

Bujakowska, K. M., Zhang, Q., Siemiatkowska, A. M., Liu, Q., Place, E., Falk, M. J., et al. (2015). Mutations in IFT172 cause isolated retinal degeneration and Bardet-Biedl syndrome. *Hum. Mol. Genet.* 24, 230–242. doi: 10.1093/hmg/ddu441

Cardenas-Rodriguez, M., and Badano, J. L. (2009). Ciliary biology: understanding the cellular and genetic basis of human ciliopathies. *Am. J. Med. Genet. C Semin. Med. Genet.* 151C, 263–280. doi: 10.1002/ajmg.c.30227

Castro-Sánchez, S., Álvarez-Satta, M., Cortón, M., Guillén, E., Ayuso, C., and Valverde, D. (2015). Exploring genotype-phenotype relationships in Bardet-Biedl syndrome families. *J. Med. Genet.* 52, 503–513. doi: 10.1136/jmedgenet-2015-103099

Chen, B., Retzlaff, M., Roos, T., and Frydman, J. (2011). Cellular strategies of protein quality control. *Cold Spring Harb. Perspect. Biol.* 3:a004374. doi: 10.1101/cshperspect.a004374

Christensen, S. T., Morthorst, S. K., Mogensen, J. B., and Pedersen, L. B. (2017). Primary Cilia and Coordination of Receptor Tyrosine Kinase (RTK) and Transforming Growth Factor β (TGF-β) Signaling. *Cold Spring Harb. Perspect. Biol.* 9:a028167. doi: 10.1101/cshperspect.a028167

Conway de Macario, E., Robb, F. T., and Macario, A. J. (2017). Prokaryotic chaperonins as experimental models for elucidating structure-function abnormalities of human pathogenic mutant counterparts. *Front. Mol. Biosci.* 3:84. doi: 10.3389/fmolb.2016.00084

Deveault, C., Billingsley, G., Duncan, J. L., Bin, J., Theal, R., Vincent, A., et al. (2011). BBS genotype-phenotype assessment of a multiethnic patient cohort calls for a revision of the disease definition. *Hum. Mutat.* 32, 610–619. doi: 10.1002/humu.21480

Dunn, A. Y., Melville, M. W., and Frydman, J. (2001). Review: cellular substrates of the eukaryotic chaperonin TRiC/CCT. *J. Struct. Biol.* 135, 176–184. doi: 10.1006/jsbi.2001.4380

Forsythe, E., and Beales, P. L. (2013). Bardet-Biedl syndrome. *Eur. J. Hum. Genet.* 21, 8–13. doi: 10.1038/ejhg.2012.115

Graner, M. W., Lillehei, K. O., and Katsanis, E. (2015). Endoplasmic reticulum chaperones and their roles in the immunogenicity of cancer vaccines. *Front. Oncol.* 4:379. doi: 10.3389/fonc.2014.00379

Hartl, F. U., Bracher, A., and Hayer-Hartl, M. (2011). Molecular chaperones in protein folding and proteostasis. *Nature* 475, 324–332. doi: 10.1038/nature10317

Heon, E., Kim, G., Qin, S., Garrison, J. E., Tavares, E., Vincent, A., et al. (2016). Mutations in C8ORF37 cause Bardet Biedl syndrome (BBS21). *Hum. Mol. Genet.* 25, 2283–2294. doi: 10.1093/hmg/ddw096

Hildebrandt, F., Benzing, T., and Katsanis, N. (2011). Ciliopathies. *N. Engl. J. Med.* 364, 1533–1543. doi: 10.1056/NEJMra1010172

Hjortshøj, T. D., Grønskov, K., Philp, A. R., Nishimura, D. Y., Riise, R., Sheffield, V. C., et al. (2010). Bardet-Biedl syndrome in Denmark-report of 13 novel sequence variations in six genes. *Hum. Mutat.* 31, 429–436. doi: 10.1002/humu.21204

Imhoff, O., Marion, V., Stoetzel, C., Durand, M., Holder, M., Sigaudy, S., et al. (2011). Bardet-Biedl syndrome: a study of the renal and cardiovascular phenotypes in a French cohort. *Clin. J. Am. Soc. Nephrol.* 6, 22–29. doi: 10.2215/CJN.03320410

Katsanis, N. (2004). The oligogenic properties of Bardet-Biedl syndrome. *Hum. Mol. Genet.* 13, R65–R71. doi: 10.1093/hmg/ddh092

Katsanis, N., Beales, P. L., Woods, M. O., Lewis, R. A., Green, J. S., Parfrey, P. S., et al. (2000). Mutations in MKKS cause obesity, retinal dystrophy and renal malformations associated with Bardet-Biedl syndrome. *Nat. Genet.* 26, 67–70. doi: 10.1038/79201

Khan, S. A., Muhammad, N., Khan, M. A., Kamal, A., Rehman, Z. U., and Khan, S. (2016). Genetics of human Bardet-Biedl syndrome, an updates. *Clin. Genet.* 90, 3–15. doi: 10.1111/cge.12737

Kim, J. C., Ou, Y. Y., Badano, J. L., Esmail, M. A., Leitch, C. C., Fiedrich, E., et al. (2005). MKKS/BBS6, a divergent chaperonin-like protein linked to the obesity

disorder Bardet-Biedl syndrome, is a novel centrosomal component required for cytokinesis. *J. Cell Sci.* 118, 1007–1020. doi: 10.1242/jcs.01676

Loktev, A. V., Zhang, Q., Beck, J. S., Searby, C. C., Scheetz, T. E., Bazan, J. F., et al. (2008). A BBSome subunit links ciliogenesis, microtubule stability, and acetylation. *Dev. Cell* 15, 854–865. doi: 10.1016/j.devcel.2008.11.001

Macario, A. J., and Conway de Macario, E. (2005). Sick chaperones, cellular stress, and disease. *N. Engl. J. Med.* 353, 1489–1501. doi: 10.1056/NEJMra 050111

Macario, A. J., and Conway de Macario, E. (2007a). Chaperonopathies by defect, excess, or mistake. *Ann. N.Y. Acad. Sci.* 1113, 178–191. doi: 10.1196/annals. 1391.009

Macario, A. J., and Conway de Macario, E. (2007b). Chaperonopathies and chaperonotherapy. *FEBS Lett.* 581, 3681–3688. doi: 10.1016/j.febslet.2007. 04.030

Macario, A. J., Grippo, T. M., and Conway de Macario, E. (2005). Genetic disorders involving molecular-chaperone genes: a perspective. *Genet. Med.* 7, 3–12.

Malicki, J. J., and Johnson, C. A. (2017). The cilium: cellular antenna and central processing unit. *Trends Cell Biol.* 27, 126–140. doi: 10.1016/j.tcb.2016. 08.002

Marion, V., Stoetzel, C., Schlicht, D., Messaddeq, N., Koch, M., Flori, E., et al. (2009). Transient ciliogenesis involving Bardet-Biedl syndrome proteins is a fundamental characteristic of adipogenic differentiation. *Proc. Natl. Acad. Sci. U.S.A.* 106, 1820–1825. doi: 10.1073/pnas.0812518106

Marshall, J. D., Maffei, P., Collin, G. B., and Naggert, J. K. (2011). Alström syndrome: genetics and clinical overview. *Curr. Genomics* 12, 225–235. doi: 10.2174/138920211795677912

Mick, D. U., Rodrigues, R. B., Leib, R. D., Adams, C. M., Chien, A. S., Gygi, S. P., et al. (2015). Proteomics of primary cilia by proximity labeling. *Dev. Cell.* 35, 497–512. doi: 10.1016/j.devcel.2015.10.015

Mitchison, H. M., and Valente, E. M. (2017). Motile and non-motile cilia in human pathology: from function to phenotypes. *J. Pathol.* 241, 294–309. doi: 10.1002/path.4843

Mockel, A., Obringer, C., Hakvoort, T. B., Seeliger, M., Lamers, W. H., Stoetzel, C., et al. (2012). Pharmacological modulation of the retinal unfolded protein response in Bardet-Biedl syndrome reduces apoptosis and preserves light detection ability. *J. Biol. Chem.* 287, 37483–37494. doi: 10.1074/jbc.M112.386821

Mukherjee, K., and Brocchieri, L. (2013). Ancient origin of chaperonin gene paralogs involved in ciliopathies. *J. Phylogenetics Evol. Biol.* 1:107. doi: 10.4172/2329-9002.1000107

Mukherjee, K., Conway de Macario, E., Macario, A. J., and Brocchieri, L. (2010). Chaperonin genes on the rise: new divergent classes and intense duplication in human and other vertebrate genomes. *BMC Evol. Biol.* 10:64. doi: 10.1186/1471-2148-10-64

Muller, J., Stoetzel, C., Vincent, M. C., Leitch, C. C., Laurier, V., Danse, J. M., et al. (2010). Identification of 28 novel mutations in the Bardet-Biedl syndrome genes: the burden of private mutations in an extensively heterogeneous disease. *Hum. Genet.* 127, 583–593. doi: 10.1007/s00439-010-0804-9

Nachury, M. V., Loktev, A. V., Zhang, Q., Westlake, C. J., Peränen, J., Merdes, A., et al. (2007). A core complex of BBS proteins cooperates with the GTPase Rab8 to promote ciliary membrane biogenesis. *Cell* 129, 1201–1213. doi: 10.1016/j.cell.2007.03.053

Novas, R., Cardenas-Rodriguez, M., Irigoín, F., and Badano, J. L. (2015). Bardet-Biedl syndrome: is it only cilia dysfunction? *FEBS Lett.* 589, 3479–3491. doi: 10.1016/j.febslet.2015.07.031

Schaefer, E., Durand, M., Stoetzel, C., Doray, B., Viville, B., Hellé, S., et al. (2011). Molecular diagnosis reveals genetic heterogeneity for the overlapping MKKS and BBS phenotypes. *Eur. J. Med. Genet.* 54, 157–160. doi: 10.1016/j.ejmg.2010.10.004

Seixas, C., Cruto, T., Tavares, A., Gaertig, J., and Soares, H. (2010). CCTalpha and CCTdelta chaperonin subunits are essential and required for cilia assembly and maintenance in Tetrahymena. *PLoS ONE* 5:e10704. doi: 10.1371/journal.pone.0010704

Seo, S., Baye, L. M., Schulz, N. P., Beck, J. S., Zhang, Q., Slusarski, D. C., et al. (2010). BBS6, BBS10, and BBS12 form a complex with CCT/TRiC family chaperonins and mediate BBSome assembly. *Proc. Natl. Acad. Sci. U.S.A.* 107, 1488–1493. doi: 10.1073/pnas.0910268107

Sinha, S., Belcastro, M., Datta, P., Seo, S., and Sokolov, M. (2014). Essential role of the chaperonin CCT in rod outer segment biogenesis. *Invest. Ophthalmol. Vis. Sci.* 55, 3775–3785. doi: 10.1167/iovs.14-13889

Slavotinek, A. M., Stone, E. M., Mykytyn, K., Heckenlively, J. R., Green, J. S., Heon, E., et al. (2000). Mutations in MKKS cause Bardet-Biedl syndrome. *Nat. Genet.* 26, 15–16. doi: 10.1038/79116

Spiess, C., Meyer, A. S., Reissmann, S., and Frydman, J. (2004). Mechanism of the eukaryotic chaperonin: protein folding in the chamber of secrets. *Trends Cell Biol.* 14, 598–604. doi: 10.1016/j.tcb.2004.09.015

Stenson, P. D., Mort, M., Ball, E. V., Evans, K., Hayden, M., Heywood, S., et al. (2017). The Human Gene Mutation Database: towards a comprehensive repository of inherited mutation data for medical research, genetic diagnosis and next-generation sequencing studies. *Hum. Genet.* 136, 665–677. doi: 10.1007/s00439-017-1779-6

Stoetzel, C., Laurier, V., Davis, E. E., Muller, J., Rix, S., Badano, J. L., et al. (2006). BBS10 encodes a vertebrate-specific chaperonin-like protein and is a major BBS locus. *Nat. Genet.* 38, 521–524. doi: 10.1038/ng1771

Stoetzel, C., Muller, J., Laurier, V., Davis, E. E., Zaghloul, N. A., Vicaire, S., et al. (2007). Identification of a novel BBS gene (BBS12) highlights the major role of a vertebrate-specific branch of chaperonin-related proteins in Bardet-Biedl syndrome. *Am. J. Hum. Genet.* 80, 1–11. doi: 10.1086/510256

Stone, D. L., Slavotinek, A., Bouffard, G. G., Banerjee-Basu, S., Baxevanis, A. D., Barr, M., et al. (2000). Mutation of a gene encoding a putative chaperonin causes McKusick-Kaufman syndrome. *Nat. Genet.* 25, 79–82. doi: 10.1038/75637

Wei, Q., Zhang, Y., Li, Y., Zhang, Q., Ling, K., and Hu, J. (2012). The BBSome controls IFT assembly and turnaround in cilia. *Nat. Cell. Biol.* 14, 950–957. doi: 10.1038/ncb2560

Wheway, G., Schmidts, M., Mans, D. A., Szymanska, K., Nguyen, T. M., Racher, H., et al. (2015). An siRNA-based functional genomics screen for the identification of regulators of ciliogenesis and ciliopathy genes. *Nat. Cell. Biol.* 17, 1074–1087. doi: 10.1038/ncb3201

Zhang, Q., Yu, D., Seo, S., Stone, E. M., and Sheffield, V. C. (2012). Intrinsic protein-protein interaction-mediated and chaperonin-assisted sequential assembly of stable bardet-biedl syndrome protein complex, the BBSome. *J. Biol. Chem.* 287, 20625–20635. doi: 10.1074/jbc.M112.341487

Conflict of Interest Statement: The authors declare that the research was conducted in the absence of any commercial or financial relationships that could be construed as a potential conflict of interest.

frontiers in Molecular Biosciences

MINI REVIEW
published: 08 June 2017
doi: 10.3389/fmolb.2017.00041

Spinal Muscular Atrophy: From Defective Chaperoning of snRNP Assembly to Neuromuscular Dysfunction

Maia Lanfranco[1,2,3], *Neville Vassallo*[1,2] *and Ruben J. Cauchi*[1,2]*

[1] Department of Physiology and Biochemistry, Faculty of Medicine and Surgery, University of Malta, Msida, Malta, [2] Center for Molecular Medicine and Biobanking, University of Malta, Msida, Malta, [3] Institut de Génétique Moléculaire de Montpellier, Center National de la Recherche Scientifique-UMR 5535, Université de Montpellier, Montpellier, France

OPEN ACCESS

Edited by:
Alberto J. L. Macario, University of Maryland at Baltimore and Institute of Marine and Environmental Technology, United States; Istituto Euro-Mediterraneo di Scienza e Tecnologia, Italy

Reviewed by:
Umesh K. Jinwal, University of South Florida, United States
Leonid Breydo, University of South Florida, United States

***Correspondence:**
Ruben J. Cauchi
ruben.cauchi@um.edu.mt

Specialty section:
This article was submitted to Protein Folding, Misfolding and Degradation, a section of the journal Frontiers in Molecular Biosciences

Received: 05 April 2017
Accepted: 26 May 2017
Published: 08 June 2017

Citation:
Lanfranco M, Vassallo N and Cauchi RJ (2017) Spinal Muscular Atrophy: From Defective Chaperoning of snRNP Assembly to Neuromuscular Dysfunction. Front. Mol. Biosci. 4:41. doi: 10.3389/fmolb.2017.00041

Spinal Muscular Atrophy (SMA) is a neuromuscular disorder that results from decreased levels of the survival motor neuron (SMN) protein. SMN is part of a multiprotein complex that also includes Gemins 2–8 and Unrip. The SMN-Gemins complex cooperates with the protein arginine methyltransferase 5 (PRMT5) complex, whose constituents include WD45, PRMT5 and pICln. Both complexes function as molecular chaperones, interacting with and assisting in the assembly of an Sm protein core onto small nuclear RNAs (snRNAs) to generate small nuclear ribonucleoproteins (snRNPs), which are the operating components of the spliceosome. Molecular and structural studies have refined our knowledge of the key events taking place within the crowded environment of cells and the numerous precautions undertaken to ensure the faithful assembly of snRNPs. Nonetheless, it remains unclear whether a loss of chaperoning in snRNP assembly, considered as a "housekeeping" activity, is responsible for the selective neuromuscular phenotype in SMA. This review thus shines light on *in vivo* studies that point toward disturbances in snRNP assembly and the consequential transcriptome abnormalities as the primary drivers of the progressive neuromuscular degeneration underpinning the disease. Disruption of U1 snRNP or snRNP assembly factors other than SMN induces phenotypes that mirror aspects of SMN deficiency, and splicing defects, described in numerous SMA models, can lead to a DNA damage and stress response that compromises the survival of the motor system. Restoring the correct chaperoning of snRNP assembly is therefore predicted to enhance the benefit of SMA therapeutic modalities based on augmenting SMN expression.

Keywords: survival motor neuron, SMN-Gemins complex, snRNP assembly, missplicing, motor neuron disease (MND), amyotrophic lateral sclerosis (ALS), spinal muscular atrophy (SMA), spliceosome

INTRODUCTION

Spinal Muscular Atrophy (SMA) is a neuromuscular disorder that can afflict both infants and adults. Patients present with loss of lower motor neurons and profound muscle weakness leading to immobility and, in severe cases, respiratory failure and death (Kolb and Kissel, 2011). The recent availability of an effective therapy is the culmination of more than two decades of research aimed

at characterizing the molecular genetics underlying the disease following the discovery that SMA is caused by mutation or homozygous deletion of the *survival motor neuron 1* (*SMN1*), a gene encoding the SMN protein. Due to a quirk in human evolution, SMN is also encoded by the highly homologous *SMN2* gene. Nonetheless, a single nucleotide substitution (C/T) in exon 7, converts an exon splicing enhancer to a silencer, hence inducing the omission of exon 7 from most of the *SMN2*-derived mRNA transcripts. This alteration leads to the production of an unstable truncated protein isoform (SMNΔ7) that is rapidly degraded, although in the absence of complete penetrance, full-length, functional SMN is still encoded by a small portion of *SMN2* transcripts that evade exon 7 skipping (reviewed in Burghes and Beattie, 2009). In the context of SMA, the levels of SMN are sufficient to prevent lethality yet not enough to fully compensate for the loss of *SMN1*. The inverse correlation between *SMN2* copy number and SMA severity elevated *SMN2* to the leading disease genetic modifier (Wirth et al., 2013). The antisense oligonucleotide (ASO) nusinersen (marketed as Spinraza), recently approved for a broad patient population, is the first successful output of a campaign aimed at identifying therapeutics that promote exon 7 inclusion in *SMN2* transcripts. The backdrop is a string of favorable results from animal models up to clinical trials, all showing that nusinersen enhanced SMN protein levels adequately enough to improve disease phenotypes (Faravelli et al., 2015; Farrar et al., 2016).

Interestingly, ASOs and other therapeutic approaches that treat SMA by augmenting SMN expression, including chief amongst others viral-mediated SMN gene delivery, and orally bioavailable small molecules that correct *SMN2* splicing, are not the obvious sequel to basic knowledge gained on SMN function. SMN, a ubiquitously expressed protein, is known to partner with Gemins 2–8 and Unrip to form a complex that is indispensable for chaperoning the assembly of small nuclear ribonucleoproteins (snRNPs), core elements of the spliceosome. In this review, we present a refined view of the key snRNP assembly events taking place within the crowded environment of cells, and evaluate the evidence favoring the classification of SMA as a chaperonopathy or a disorder arising from a disturbance in the chaperoning of snRNP assembly with the consequential transcriptome abnormalities as the primary drivers of neuromuscular degeneration in SMA patients. A better understanding of the mechanisms underpinning the disease can open up novel therapeutic routes that complement or accentuate the effect of the mainstream approach.

ANATOMY OF THE SMN-GEMINS COMPLEX CHAPERONE MACHINE

In its simplest version, the SMN-Gemins complex is composed of only SMN (Yab8p) and Gemin2 (Yip1p), a situation that is typical in the fission yeast *Schizosaccharomyces pombe* (Hannus et al., 2000). Complexity was gained in evolution through the incorporation of the remaining constituents (Kroiss et al., 2008; Cauchi, 2010). The fruit fly *Drosophila melanogaster* possesses a minimalistic complex that, in addition to SMN and Gemin2, also includes Gemin3 and Gemin5 (Cauchi et al., 2010). Besides physical associations (Cauchi et al., 2008; Kroiss et al., 2008; Shpargel et al., 2009; Guruharsha et al., 2011), genetic interactions between members of the *Drosophila* SMN-Gemins complex indicate that SMN and its Gemin associates were conserved during evolution not as independent entities but rather as a genetic network (Borg et al., 2015) (**Figure 1A**). Vertebrates, including humans, have the most elaborate SMN-Gemins complex counting SMN, seven Gemin proteins (Gemin2-Gemin8), and Unrip as its members. Comprehensive biochemical studies revealed a modular composition with the SMN-Gemin8-Gemin7 module placed at its center, thereby allowing the recruitment of the Gemin2-Gemin5 and Gemin6-Unrip subunits mainly via SMN and Gemin7, respectively. The Gemin3-Gemin4 block latches to the complex via both SMN and Gemin8 (Otter et al., 2007). Additional interactions are thought to further stabilize the complex (Otter et al., 2007; Ogawa et al., 2009) (**Figure 1A**). SMN, Gemin2, Gemin4, and Gemin8 can self-associate (Lorson et al., 1998; Young et al., 2000; Ogawa et al., 2007; Otter et al., 2007), hence their oligomerization propensity means that SMN-Gemins complexes can reach large macromolecular sizes, at least in vertebrates. Cell biology studies have confirmed the clustering of SMN-Gemins complex members to form membrane-less structures named Gems if nuclear (Liu and Dreyfuss, 1996; Cauchi, 2011) or U bodies if cytoplasmic (Liu and Gall, 2007; Cauchi et al., 2010).

It has long been known that loss of SMN is incompatible with life (reviewed in Burghes and Beattie, 2009). The same outcome applies to additional SMN-Gemins complex members investigated thus far. To this end, knockout or RNAi-mediated knockdown of Gemin2, Gemin3 or Gemin5 leads to lethality in various organisms (reviewed in Borg and Cauchi, 2014). This might indicate that the constituents of the SMN-Gemins complex are not redundant, hence, the function of one component cannot be covered by another. Alternatively, or additionally, an imbalance in the protein levels of its members can destabilize the SMN-Gemins complex. Experiments inducing a gain-of-function were revelatory in this regard. Indeed, overexpression of Gemin2 is deleterious in both yeast and flies (Borg et al., 2015). Furthermore, the upregulation of SMN or Gemin5 can have a negative impact on fly viability only when either perturbation is combined with a Gemin3 hypomorphic mutant (Borg et al., 2015). These findings are in line with studies that underscore the interdependence of constituent levels within the SMN-Gemins complex. Hence, cells with low amounts of SMN, including those derived from SMA patients, were found to have reduced protein levels of select Gemins (Jablonka et al., 2002; Helmken et al., 2003; Feng et al., 2005; Shpargel and Matera, 2005; Carissimi et al., 2006; Gabanella et al., 2007; Hao le et al., 2007). In agreement, severe SMA mice were also shown to have a significant reduction in the levels of a subset of Gemin proteins in the spinal cord (Gabanella et al., 2007; Zhang et al., 2008). A similar effect can be achieved on knockdown of select Gemins (Shpargel and Matera, 2005; Ogawa et al., 2007). Furthermore, the half-life of SMN was decreased by mutations interfering with its incorporation within the SMN-Gemins complex (Burnett et al., 2009).

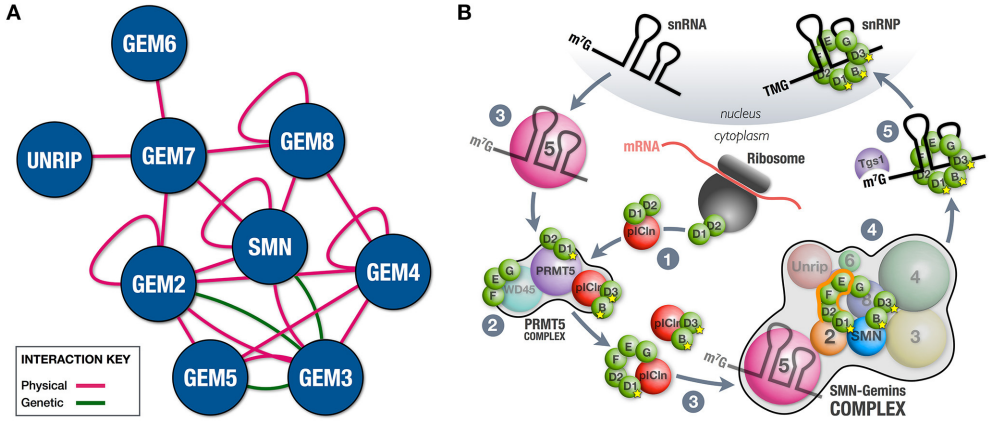

FIGURE 1 | SMN-Gemins complex and its role in chaperoning snRNP assembly. **(A)** Integration of physical and genetic interactions between the constituent members of the SMN-Gemins complex. Physical interactions were identified through various biochemical techniques including two-hybrid, pulldown and co-immunoprecipitation assays in multiple organisms (Lorson et al., 1998; Young et al., 2000; Ogawa et al., 2007, 2009; Otter et al., 2007; Cauchi et al., 2008; Kroiss et al., 2008; Shpargel et al., 2009; Guruharsha et al., 2011). Changes in the levels of SMN or Gemins enhanced viability and motor phenotypes of a hypomorphic Gemin3 mutant in *Drosophila*, thereby allowing the identification of genetic interactions (Borg et al., 2015). Interaction network was composed using the esyN tool. **(B)** Cooperation between the PRMT5 and SMN-Gemins complexes in the cytoplasm ensures the faithful assembly of snRNPs. (1) On translation, Sm D2 protein remains attached to the ribosome. Its release occurs subsequent to the formation of the Sm D2/D1 heterodimer and association with pICln. (2) Select Sm proteins are then post-translationally modified by the PRMT5 complex. (3) The SMN-Gemins complex receives pre-organized Sm subsets and snRNAs from pICln and Gemin5, respectively. (4) Within the SMN-Gemins complex, the majority of Sm proteins are handled by Gemin2 until their uploading onto the delivered snRNAs. (5) Tgs1 ensures cap hypermethylation of assembled snRNPs prior to their nuclear import.

A REFINED VIEW OF CHAPERONING ACTIVITIES DURING snRNP BIOGENESIS

In addition to being an essential step in gene expression, splicing of pre-mRNA transcripts is also crucial for the generation of diverse proteomes in eukaryotes. United in the major spliceosome, U1, U2, U4/U6, and U5 snRNPs catalyze the removal of the majority of pre-mRNA introns. The less abundant minor spliceosome, which processes a rare non-canonical group of introns is however composed of U11, U12, U4atac/U6atac and U5 snRNPs. Not considering the varying number of specific protein components, spliceosomal snRNPs are in essence composed of a short noncoding RNA (snRNA) bound to a heptameric Sm/Lsm protein ring (reviewed in Matera and Wang, 2014). Cells take numerous precautions to ensure the faithful assembly of snRNPs. Hence, key events of the snRNP production cycle take place in the cytoplasm to limit contact of partially assembled snRNPs with their nuclear substrates. Importantly, the process involves cooperation between the SMN-Gemins complex, and the protein arginine methyltransferase 5 (PRMT5) complex, whose constituents include WD45, PRMT5 and pICln. This brings the number of *trans*-acting assembly factors to at least twelve, a count far greater than the parts to be assembled (reviewed in Fischer et al., 2011). The mis-assembly evading measures put forward by cells most probably address the low intrinsic selectively of Sm proteins for snRNAs. As we discuss below, recent molecular and structural studies mostly focusing on Sm-class snRNPs have started to unravel the chaperoning activities of each factor during the uploading of the Sm ring onto a conserved short uridine-rich sequence motif, known as the Sm site, within snRNAs.

snRNP assembly is thought to occur during two phases, the early one dominated by the PRMT5 complex, whereas in the late one, the SMN-Gemins complex is central (**Figure 1B**). In the early assembly phase, the newly translated Sm D2 protein is thought to remain attached to the ribosome. Formation of the Sm D2/D1 dimer and its association with pICln ensures their release and the subsequent delivery to the PRMT5 complex (Paknia et al., 2016). Here, designated arginine residues of a bound Sm protein subset (B/B', D1, and D3) are symmetrically dimethylated by PRMT5 and, possibly PRMT7, a modification thought to enhance their affinity for the SMN-Gemins complex (reviewed in Fischer et al., 2011). The conclusion of this phase is marked by the formation of the Sm D1/D2/F/E/G and Sm B/D3 sub-complexes, each bound by pICln to prevent premature RNA interactions. Whereas pICln is dismissed, the pre-organized Sm proteins are handed over to the SMN-Gemins complex, a step that signals the initiation of the late assembly phase (Chari et al., 2008; Grimm et al., 2013). Gemin2 is the SMN-Gemins complex subunit that handles the majority of Sm proteins by hugging the crescent-shaped Sm D1/D2/F/E/G pentamer and blocking RNA binding capacity until delivery of snRNAs (Zhang et al., 2011; Grimm et al., 2013). The factor that channels snRNAs to the SMN-Gemins complex is Gemin5 (Battle et al., 2006; Yong et al., 2010), though U1-70K, a component of U1 snRNP, can substitute Gemin5 in a U1-exclusive snRNP assembly pathway (So et al., 2016). Gemin5 is capable of recognizing the Sm site and 7-methylguanosine (m^7G) cap of nuclear-exported snRNAs via the first and second WD40 repeat domains, respectively

(Lau et al., 2009; Jin et al., 2016; Tang et al., 2016; Xu et al., 2016). Although binding to both structures cannot be done simultaneously, this dual recognition tactic is thought to enhance stringency of snRNP assembly. The mechanism ensuring Sm ring closure remains unclear though Unrip and the Gemin6/Gemin7 dimer might have a leading role with the latter thought to act as a temporary substitute for the Sm B/D3 dimer (Ma et al., 2005; Ogawa et al., 2009).

The exact role of other SMN-Gemins complex members in snRNP assembly will probably be unraveled by future mechanistic and structure-based studies. Nevertheless, *in vitro* studies using purified reconstituted systems have recently shown that Gemins 3, 4 and even Gemin5 were dispensable for the assembly and proofreading of snRNAs (Neuenkirchen et al., 2015). This goes against findings by earlier reports demonstrating that snRNP assembly was disrupted on RNAi-mediated knockdown of Gemin3-8 and Unrip in cell culture (Feng et al., 2005; Grimmler et al., 2005; Shpargel and Matera, 2005; Carissimi et al., 2006). It could very well be argued that this outcome is an indirect effect brought about by the destabilization of the SMN-Gemins complex. In support, changes in the levels of its components are known to disrupt the function of the SMN-Gemins complex *in vivo* (Borg et al., 2015). However, it is highly likely that all components of the SMN-Gemins complex have key roles, at least *in vivo*, and their participation in chaperoning snRNP assembly drives the reaction forward in addition to increasing its efficiency. Hence, in an *in vivo* setting, ATP breakdown and RNA or RNP remodeling during snRNP biogenesis is a job most probably attributed to Gemin3, a well-known DEAD-box RNA helicase (Charroux et al., 1999; Yan et al., 2003). In a final step during the late assembly phase, the SMN-Gemins complex recruits trimethylguanosine synthase 1 (Tgs1), an enzyme that hypermethylates the 7-methylguanosine (m^7G) cap of assembled snRNPs to a 2,2,7-trimethylguanosine (TMG) cap (Mouaikel et al., 2002, 2003). Both the TMG cap and the Sm ring act as a localization signal for their import to the nucleus where they are expected to operate subsequent to a maturation stage in the Cajal body (reviewed in Stanek, 2016).

IN VIVO STUDIES LINKING snRNP ASSEMBLY DEFECTS TO NEUROMUSCULAR DYSFUNCTION

Several key studies making use of animal models strongly support the possibility that altered snRNP production due to defective chaperoning downstream to SMN deficiency can lead to the neuromuscular defects that are typical in SMA (**Table 1**). It has long been known that SMN levels strongly stipulate the snRNP assembly capacity of cell extracts (Wan et al., 2005; Boulisfane et al., 2011). In the spinal cord, maximal snRNP assembly chaperoning activity overlaps with the highest demands for SMN during the development of the neuromuscular system (Gabanella et al., 2005; Foust et al., 2010; Le et al., 2011; Lutz et al., 2011; Kariya et al., 2014). Importantly, snRNP assembly capacity in the spinal cord of SMA mouse models was found to determine disease severity, hence, the greatest perturbation was observed in severe SMA mice (Gabanella et al., 2007). In a reciprocal experiment, the disease phenotype was rescued in mice following the introduction of the SMN^{A111G} allele, which is capable of chaperoning snRNP assembly. Correction of SMA was dependent on snRNP assembly activity in the spinal cord (Workman et al., 2009). This study is in agreement with an earlier report demonstrating that motor neuron degeneration was rescued when purified snRNPs were injected in SMN-deficient zebrafish embryos (Winkler et al., 2005). Interestingly, in line with earlier findings demonstrating that knockdown of pICln or U1 snRNP leads to SMA-like defects in zebrafish (Winkler et al., 2005; Yu et al., 2015) (**Table 1**), disruption of either pICln or Tgs1 was found to result in motor defects that mirror those described on loss of SMN or Gemins in *Drosophila* (Borg et al., 2016). pICln and Tgs1 are two factors that are known to have a leading role in the early and late phase of snRNP assembly, respectively. Importantly, unlike the Gemins (reviewed in Cauchi, 2010), they have never been directly linked to the assembly and transport of messenger ribonucleoprotein (mRNP) complexes along axons, which is often considered as the primary non-canonical activity of the SMN-Gemins complex (reviewed in Donlin-Asp et al., 2016).

Consistent with a fundamental role for SMN in chaperoning snRNP assembly, several studies were successful in identifying splicing defects as a consequence of SMN loss and, importantly, explain how missplicing of specific transcripts leads to motor dysfunction in SMA. Whereas symptomatic SMA mice were shown to have widespread pre-mRNA splicing defects in numerous transcripts of diverse genes (Zhang et al., 2008; Baumer et al., 2009), at a pre-symptomatic stage, they exhibit dysregulation of genes that are critical for the function of the motor neuron and may thus contribute to SMA's signature pathology (Zhang et al., 2013). Similarly, in *Drosophila*, SMN deficiency perturbed the splicing and expression of several genes including that of *stasimon*, whose correct splicing is dependent on the minor spliceosome. Stasimon mRNA expression and splicing was also found perturbed in the constituent neurons of the sensory-motor circuit in SMA mice. Restoration of *stasimon* expression in the motor circuit was found to correct in part the motor system defects in *Drosophila Smn* mutants and *Smn*-deficient zebrafish, thus establishing stasimon as an SMN target gene (Lotti et al., 2012). Other studies have since focused on additional genes that are misspliced in SMA models including *Neurexin2* (See et al., 2014) and *Chondrolectin* (Sleigh et al., 2014), both of which are important for motor neuron axon outgrowth. Further still, following up on a previous study in a genetic model (Doktor et al., 2017), an ASO-inducible model of SMA was recently found to have widespread intron retention, particularly those spliced by the minor spliceosome, in spinal cord extracts. Importantly, these changes were rescued by a therapeutic ASO, thereby indicating that intron removal is directly correlated with SMN levels. Interestingly, intron retention was associated with a strong induction of the p53 pathway, and markers of DNA double-strand breaks were apparent in the neurons of the spinal cord and brain of SMA mice (Jangi et al., 2017). Thus, it is highly likely that instead of single gene effects, inefficiencies in pre-mRNA processing consequent

TABLE 1 | Key studies in animal models linking motor dysfunction to perturbation in snRNP biogenesis.

Organism	Genotype	Manipulation and/or findings	References
Drosophila	Loss-of-function Smn^{73Ao} mutants	Reduced snRNA levels; perturbation of the splicing and expression of genes with minor-class introns including *stasimon*	Lotti et al., 2012
Drosophila	Knockout of *Smn* (Smn^{X7} mutants)	Synaptic dysfunction and muscle growth defects are rescued by transgenic expression of *stasimon*, a minor-class intron containing gene	Lotti et al., 2012
Drosophila	pICln or Tgs1 disruption via RNAi-mediated knockdown or overexpression	SMA-like motor system defects	Borg et al., 2016
Zebrafish	Antisense morpholino knockdown of pICln or U1 snRNP components U1-70K or U1 snRNA	SMA-like motor axon degeneration	Winkler et al., 2005; Yu et al., 2015
Zebrafish	Antisense morpholino knockdown of SMN	Injection of purified snRNPs prevents motor neuron degeneration; injection of the mRNA of genes that are misspliced in SMA including *Stasimon*, *Chondrolectin* or *Neurexin 2,* results in correction of SMA-like motor axon defects	Winkler et al., 2005; Lotti et al., 2012; See et al., 2014; Sleigh et al., 2014
Mouse	Knockout of mouse *Smn* and manipulation of Smn levels through introduction of human *SMN2*, $SMN\Delta7$ and/or SMN^{A2G} transgenes	Degree of impaired snRNP assembly in spinal cord extracts is associated with disease severity; significant decrease in the levels of select snRNPs	Gabanella et al., 2007
Mouse	Knockout of mouse *Smn* and introduction of one or two copies of the human *SMN2* transgene	Introduction of the snRNP assembly competent human SMN^{A111G} transgene rescued the disease phenotype; reduced expression and splicing of *Neurexin 2* in spinal cord; elevated retention of minor class introns that is corrected by a therapeutic ASO	Workman et al., 2009; See et al., 2014; Doktor et al., 2017
Mouse	Knockout of mouse *Smn* and introduction of the human *SMN2* and $SMN\Delta7$ transgenes	Symptomatic mice have tissue-specific alterations in snRNA levels and widespread pre-mRNA splicing defects in gene transcripts with diverse roles; altered splicing and reduced expression of *Stasimon*, a minor-class intron containing gene, in motor neurons and proprioceptive neurons of early-symptomatic mice; splicing abnormalities and expression-level changes of specific mRNAs critical for motor neuron function including synaptogenesis in laser-capture micro-dissected motor neurons of pre-symptomatic mice	Zhang et al., 2008, 2013; Baumer et al., 2009; Lotti et al., 2012
Mouse	Knockout of mouse *Smn*, introduction of the human *SMN2* transgene (4 copies) and intracerebroventricular administration of an ASO mediating the skipping of exon 7 from the human *SMN2* transgene	Extensive intron retention, particularly minor-class introns, in spinal cord extracts that was corrected by a therapeutic ASO; p53 activation; markers of DNA double-strand breaks in neurons of brain and spinal cord	Jangi et al., 2017

$SMN^{\Delta7}$, predominant isoform produced by the human SMN2 gene.

to severe SMN deficiency lead to a DNA damage and stress response that compromises the survival of the motor neuron. Nonetheless, the reasons why the neuromuscular system remains highly vulnerable to damage warrants further investigation.

CONCLUSION

The ample evidence linking defective chaperoning of snRNP assembly to neuromuscular dysfunction is not only consistent with SMA being a chaperonopathy but also sets the scene for the discovery of therapies that target this pathway. Inhibition of RNA decay pathways to correct snRNP levels (Shukla and Parker, 2014) or suppression of genome instability induced by intron retention (Jangi et al., 2017) are two treatment routes that are successful, at least *in vitro*. Although the effectiveness of these and other approaches on animal models or humans, remains to be investigated, the suppression of snRNP hypo-assembly and splicing defects may provide benefits to SMA patients beyond the benefit of SMN restoration alone. Considering that distrubances in snRNP assembly are also a component of the pathogenesis of the adult-onset amyotrophic lateral sclerosis (ALS) (Cauchi, 2014; Sun et al., 2015; Yu et al., 2015), such therapeutic strategies are expected to have broad implications in motor neuron disease.

AUTHOR CONTRIBUTIONS

RC conceived the review focus; ML, NV, and RC conducted the literature review, wrote and edited the manuscript.

ACKNOWLEDGMENTS

The authors are grateful to Dr. Rémy Bordonné for his valuable collaboration and comments on the manuscript. Work in the authors' laboratory is supported by the University of Malta, the ALS Malta Foundation, and the Malta Council for Science and Technology. ML is supported by the Endeavor Scholarship Scheme (Malta), part-financed by the EU—European Social Fund under Operational Programme II—Cohesion Policy 2014-2020, "Investing in human capital to create more opportunities and promote the well-being of society."

REFERENCES

Battle, D. J., Lau, C. K., Wan, L., Deng, H., Lotti, F., and Dreyfuss, G. (2006). The Gemin5 protein of the SMN complex identifies snRNAs. *Mol. Cell* 23, 273–279. doi: 10.1016/j.molcel.2006.05.036

Baumer, D., Lee, S., Nicholson, G., Davies, J. L., Parkinson, N. J., Murray, L. M., et al. (2009). Alternative splicing events are a late feature of pathology in a mouse model of spinal muscular atrophy. *PLoS Genet.* 5:e1000773. doi: 10.1371/journal.pgen.1000773

Borg, R., and Cauchi, R. J. (2014). GEMINs: potential therapeutic targets for spinal muscular atrophy? *Front. Neurosci.* 8:325. doi: 10.3389/fnins.2014.00325

Borg, R. M., Bordonne, R., Vassallo, N., and Cauchi, R. J. (2015). Genetic interactions between the members of the SMN-gemins complex in Drosophila. *PLoS ONE* 10:e0130974. doi: 10.1371/journal.pone.0130974

Borg, R. M., Fenech Salerno, B., Vassallo, N., Bordonne, R., and Cauchi, R. J. (2016). Disruption of snRNP biogenesis factors Tgs1 and pICln induces phenotypes that mirror aspects of SMN-Gemins complex perturbation in Drosophila, providing new insights into spinal muscular atrophy. *Neurobiol. Dis.* 94, 245–258. doi: 10.1016/j.nbd.2016.06.015

Boulisfane, N., Choleza, M., Rage, F., Neel, H., Soret, J., and Bordonne, R. (2011). Impaired minor tri-snRNP assembly generates differential splicing defects of U12-type introns in lymphoblasts derived from a type I SMA patient. *Hum. Mol. Genet.* 20, 641–648. doi: 10.1093/hmg/ddq508

Burghes, A. H., and Beattie, C. E. (2009). Spinal muscular atrophy: why do low levels of survival motor neuron protein make motor neurons sick? *Nat. Rev. Neurosci.* 10, 597–609. doi: 10.1038/nrn2670

Burnett, B. G., Munoz, E., Tandon, A., Kwon, D. Y., Sumner, C. J., and Fischbeck, K. H. (2009). Regulation of SMN protein stability. *Mol. Cell. Biol.* 29, 1107–1115. doi: 10.1128/MCB.01262-08

Carissimi, C., Saieva, L., Baccon, J., Chiarella, P., Maiolica, A., Sawyer, A., et al. (2006). Gemin8 is a novel component of the survival motor neuron complex and functions in small nuclear ribonucleoprotein assembly. *J. Biol. Chem.* 281, 8126–8134. doi: 10.1074/jbc.M512243200

Cauchi, R. J. (2010). SMN and Gemins: 'we are family'... or are we? Insights into the partnership between Gemins and the spinal muscular atrophy disease protein SMN. *Bioessays* 32, 1077–1089. doi: 10.1002/bies.201000088

Cauchi, R. J. (2011). Gem formation upon constitutive Gemin3 overexpression in Drosophila. *Cell Biol. Int.* 35, 1233–1238. doi: 10.1042/CBI20110147

Cauchi, R. J. (2014). Gem depletion: amyotrophic lateral sclerosis and spinal muscular atrophy crossover. *CNS Neurosci. Ther.* 20, 574–581. doi: 10.1111/cns.12242

Cauchi, R. J., Davies, K. E., and Liu, J. L. (2008). A motor function for the DEAD-box RNA helicase, Gemin3, in Drosophila. *PLoS Genet.* 4:e1000265. doi: 10.1371/journal.pgen.1000265

Cauchi, R. J., Sanchez-Pulido, L., and Liu, J. L. (2010). Drosophila SMN complex proteins Gemin2, Gemin3, and Gemin5 are components of U bodies. *Exp. Cell Res.* 316, 2354–2364. doi: 10.1016/j.yexcr.2010.05.001

Chari, A., Golas, M. M., Klingenhager, M., Neuenkirchen, N., Sander, B., Englbrecht, C., et al. (2008). An assembly chaperone collaborates with the SMN complex to generate spliceosomal SnRNPs. *Cell* 135, 497–509. doi: 10.1016/j.cell.2008.09.020

Charroux, B., Pellizzoni, L., Perkinson, R. A., Shevchenko, A., Mann, M., and Dreyfuss, G. (1999). Gemin3: a novel DEAD box protein that interacts with SMN, the spinal muscular atrophy gene product, and is a component of Gems. *J. Cell Biol.* 147, 1181–1193. doi: 10.1083/jcb.147.6.1181

Doktor, T. K., Hua, Y., Andersen, H. S., Broner, S., Liu, Y. H., Wieckowska, A., et al. (2017). RNA-sequencing of a mouse-model of spinal muscular atrophy reveals tissue-wide changes in splicing of U12-dependent introns. *Nucleic Acids Res.* 45, 395–416. doi: 10.1093/nar/gkw731

Donlin-Asp, P. G., Bassell, G. J., and Rossoll, W. (2016). A role for the survival of motor neuron protein in mRNP assembly and transport. *Curr. Opin. Neurobiol.* 39, 53–61. doi: 10.1016/j.conb.2016.04.004

Faravelli, I., Nizzardo, M., Comi, G. P., and Corti, S. (2015). Spinal muscular atrophy–recent therapeutic advances for an old challenge. *Nat. Rev. Neurol.* 11, 351–359. doi: 10.1038/nrneurol.2015.77

Farrar, M. A., Park, S. B., Vucic, S., Carey, K. A., Turner, B. J., Gillingwater, T. H., et al. (2016). Emerging therapies and challenges in Spinal Muscular Atrophy. *Ann. Neurol.* 81, 355–368. doi: 10.1002/ana.24864

Feng, W., Gubitz, A. K., Wan, L., Battle, D. J., Dostie, J., Golembe, T. J., et al. (2005). Gemins modulate the expression and activity of the SMN complex. *Hum. Mol. Genet.* 14, 1605–1611. doi: 10.1093/hmg/ddi168

Fischer, U., Englbrecht, C., and Chari, A. (2011). Biogenesis of spliceosomal small nuclear ribonucleoproteins. *Wiley Interdiscip. Rev.* 2, 718–731. doi: 10.1002/wrna.87

Foust, K. D., Wang, X., McGovern, V. L., Braun, L., Bevan, A. K., Haidet, A. M., et al. (2010). Rescue of the spinal muscular atrophy phenotype in a mouse model by early postnatal delivery of SMN. *Nat. Biotechnol.* 28, 271–274. doi: 10.1038/nbt.1610

Gabanella, F., Butchbach, M. E., Saieva, L., Carissimi, C., Burghes, A. H., and Pellizzoni, L. (2007). Ribonucleoprotein assembly defects correlate with spinal muscular atrophy severity and preferentially affect a subset of spliceosomal snRNPs. *PLoS ONE* 2:e921. doi: 10.1371/journal.pone.0000921

Gabanella, F., Carissimi, C., Usiello, A., and Pellizzoni, L. (2005). The activity of the spinal muscular atrophy protein is regulated during development and cellular differentiation. *Hum. Mol. Genet.* 14, 3629–3642. doi: 10.1093/hmg/ddi390

Grimm, C., Chari, A., Pelz, J. P., Kuper, J., Kisker, C., Diederichs, K., et al. (2013). Structural basis of assembly chaperone-mediated snRNP formation. *Mol. Cell* 49, 692–703. doi: 10.1016/j.molcel.2012.12.009

Grimmler, M., Otter, S., Peter, C., Muller, F., Chari, A., and Fischer, U. (2005). Unrip, a factor implicated in cap-independent translation, associates with the cytosolic SMN complex and influences its intracellular localization. *Hum. Mol. Genet.* 14, 3099–3111. doi: 10.1093/hmg/ddi343

Guruharsha, K. G., Rual, J. F., Zhai, B., Mintseris, J., Vaidya, P., Vaidya, N., et al. (2011). A protein complex network of *Drosophila melanogaster*. *Cell* 147, 690–703. doi: 10.1016/j.cell.2011.08.047

Hannus, S., Buhler, D., Romano, M., Seraphin, B., and Fischer, U. (2000). The Schizosaccharomyces pombe protein Yab8p and a novel factor, Yip1p, share structural and functional similarity with the spinal muscular atrophy-associated proteins SMN and SIP1. *Hum. Mol. Genet.* 9, 663–674. doi: 10.1093/hmg/9.5.663

Hao le, T., Fuller, H. R., Lam le, T., Le, T. T., Burghes, A. H., and Morris, G. E. (2007). Absence of gemin5 from SMN complexes in nuclear Cajal bodies. *BMC Cell Biol.* 8:28. doi: 10.1186/1471-2121-8-28

Helmken, C., Hofmann, Y., Schoenen, F., Oprea, G., Raschke, H., Rudnik-Schoneborn, S., et al. (2003). Evidence for a modifying pathway in SMA discordant families: reduced SMN level decreases the amount of its interacting partners and Htra2-beta1. *Hum. Genet.* 114, 11–21. doi: 10.1007/s00439-003-1025-2

Jablonka, S., Holtmann, B., Meister, G., Bandilla, M., Rossoll, W., Fischer, U., et al. (2002). Gene targeting of Gemin2 in mice reveals a correlation between defects in the biogenesis of U snRNPs and motoneuron cell death. *Proc. Natl. Acad. U.S.A.* 99, 10126–10131. doi: 10.1073/pnas.152318699

Jangi, M., Fleet, C., Cullen, P., Gupta, S. V., Mekhoubad, S., Chiao, E., et al. (2017). SMN deficiency in severe models of spinal muscular atrophy causes widespread intron retention and DNA damage. *Proc. Natl. Acad. Sci. U.S.A.* 114, E2347–E2356. doi: 10.1073/pnas.1613181114

Jin, W., Wang, Y., Liu, C. P., Yang, N., Jin, M., Cong, Y., et al. (2016). Structural basis for snRNA recognition by the double-WD40 repeat domain of Gemin5. *Genes Dev.* 30, 2391–2403. doi: 10.1101/gad.291377.116

Kariya, S., Obis, T., Garone, C., Akay, T., Sera, F., Iwata, S., et al. (2014). Requirement of enhanced Survival Motoneuron protein imposed during neuromuscular junction maturation. *J. Clin. Invest.* 124, 785–800. doi: 10.1172/JCI72017

Kolb, S. J., and Kissel, J. T. (2011). Spinal muscular atrophy: a timely review. *Arch. Neurol.* 68, 979–984. doi: 10.1001/archneurol.2011.74

Kroiss, M., Schultz, J., Wiesner, J., Chari, A., Sickmann, A., and Fischer, U. (2008). Evolution of an RNP assembly system: a minimal SMN complex facilitates formation of UsnRNPs in Drosophila melanogaster. *Proc. Natl. Acad. Sci. U.S.A.* 105, 10045–10050. doi: 10.1073/pnas.0802287105

Lau, C. K., Bachorik, J. L., and Dreyfuss, G. (2009). Gemin5-snRNA interaction reveals an RNA binding function for WD repeat domains. *Nat. Struct. Mol. Biol.* 16, 486–491. doi: 10.1038/nsmb.1584

Le, T. T., McGovern, V. L., Alwine, I. E., Wang, X., Massoni-Laporte, A., Rich, M. M., et al. (2011). Temporal requirement for high SMN expression in SMA mice. *Hum. Mol. Genet.* 20, 3578–3591. doi: 10.1093/hmg/ddr275

Liu, J. L., and Gall, J. G. (2007). U bodies are cytoplasmic structures that contain uridine-rich small nuclear ribonucleoproteins and associate with P bodies. *Proc. Natl. Acad. Sci. U.S.A.* 104, 11655–11659. doi: 10.1073/pnas.0704977104

Liu, Q., and Dreyfuss, G. (1996). A novel nuclear structure containing the survival of motor neurons protein. *EMBO J.* 15, 3555–3565.

Lorson, C. L., Strasswimmer, J., Yao, J. M., Baleja, J. D., Hahnen, E., Wirth, B., et al. (1998). SMN oligomerization defect correlates with spinal muscular atrophy severity. *Nat. Genet.* 19, 63–66. doi: 10.1038/ng0598-63

Lotti, F., Imlach, W. L., Saieva, L., Beck, E. S., Hao le, T., Li, D. K., et al. (2012). An SMN-dependent U12 splicing event essential for motor circuit function. *Cell* 151, 440–454. doi: 10.1016/j.cell.2012.09.012

Lutz, C. M., Kariya, S., Patruni, S., Osborne, M. A., Liu, D., Henderson, C. E., et al. (2011). Postsymptomatic restoration of SMN rescues the disease phenotype in a mouse model of severe spinal muscular atrophy. *J. Clin. Invest.* 121, 3029–3041. doi: 10.1172/JCI57291

Ma, Y., Dostie, J., Dreyfuss, G., and Van Duyne, G. D. (2005). The Gemin6-Gemin7 heterodimer from the survival of motor neurons complex has an Sm protein-like structure. *Structure* 13, 883–892. doi: 10.1016/j.str.2005.03.014

Matera, A. G., and Wang, Z. (2014). A day in the life of the spliceosome. *Nat. Rev. Mol. Cell Biol.* 15, 108–121. doi: 10.1038/nrm3742

Mouaikel, J., Narayanan, U., Verheggen, C., Matera, A. G., Bertrand, E., Tazi, J., et al. (2003). Interaction between the small-nuclear-RNA cap hypermethylase and the spinal muscular atrophy protein, survival of motor neuron. *EMBO Rep.* 4, 616–622. doi: 10.1038/sj.embor.embor863

Mouaikel, J., Verheggen, C., Bertrand, E., Tazi, J., and Bordonne, R. (2002). Hypermethylation of the cap structure of both yeast snRNAs and snoRNAs requires a conserved methyltransferase that is localized to the nucleolus. *Mol. Cell* 9, 891–901. doi: 10.1016/S1097-2765(02)00484-7

Neuenkirchen, N., Englbrecht, C., Ohmer, J., Ziegenhals, T., Chari, A., and Fischer, U. (2015). Reconstitution of the human U snRNP assembly machinery reveals stepwise Sm protein organization. *EMBO J.* 34, 1925–1941. doi: 10.15252/embj.201490350

Ogawa, C., Usui, K., Aoki, M., Ito, F., Itoh, M., Kai, C., et al. (2007). Gemin2 plays an important role in stabilizing the survival of motor neuron complex. *J. Biol. Chem.* 282, 11122–11134. doi: 10.1074/jbc.M609297200

Ogawa, C., Usui, K., Ito, F., Itoh, M., Hayashizaki, Y., and Suzuki, H. (2009). Role of survival motor neuron complex components in small nuclear ribonucleoprotein assembly. *J. Biol. Chem.* 284, 14609–14617. doi: 10.1074/jbc.M809031200

Otter, S., Grimmler, M., Neuenkirchen, N., Chari, A., Sickmann, A., and Fischer, U. (2007). A comprehensive interaction map of the human survival of motor neuron (SMN) complex. *J. Biol. Chem.* 282, 5825–5833. doi: 10.1074/jbc.M608528200

Paknia, E., Chari, A., Stark, H., and Fischer, U. (2016). The ribosome cooperates with the assembly chaperone pICln to initiate formation of snRNPs. *Cell Rep.* 16, 3103–3112. doi: 10.1016/j.celrep.2016.08.047

See, K., Yadav, P., Giegerich, M., Cheong, P. S., Graf, M., Vyas, H., et al. (2014). SMN deficiency alters Nrxn2 expression and splicing in zebrafish and mouse models of spinal muscular atrophy. *Hum. Mol. Genet.* 23, 1754–1770. doi: 10.1093/hmg/ddt567

Shpargel, K. B., and Matera, G. (2005). Gemin proteins are required for efficient assembly of Sm-class ribonucleoproteins. *Proc. Natl. Acad. U.S.A.* 102, 17372–17377. doi: 10.1073/pnas.0508947102

Shpargel, K. B., Praveen, K., Rajendra, T. K., and Matera, A. G. (2009). Gemin3 is an essential gene required for larval motor function and pupation in Drosophila. *Mol. Biol. Cell* 20, 90–101. doi: 10.1091/mbc.E08-01-0024

Shukla, S., and Parker, R. (2014). Quality control of assembly-defective U1 snRNAs by decapping and 5′-to-3′ exonucleolytic digestion. *Proc. Natl. Acad. Sci. U.S.A.* 111, E3277–E3286. doi: 10.1073/pnas.1412614111

Sleigh, J. N., Barreiro-Iglesias, A., Oliver, P. L., Biba, A., Becker, T., Davies, K. E., et al. (2014). Chondrolectin affects cell survival and neuronal outgrowth in *in vitro* and *in vivo* models of spinal muscular atrophy. *Hum. Mol. Genet.* 23, 855–869. doi: 10.1093/hmg/ddt477

So, B. R., Wan, L., Zhang, Z., Li, P., Babiash, E., Duan, J., et al. (2016). A U1 snRNP-specific assembly pathway reveals the SMN complex as a versatile hub for RNP exchange. *Nat. Struct. Mol. Biol.* 23, 225–230. doi: 10.1038/nsmb.3167

Stanek, D. (2016). Cajal bodies and snRNPs - friends with benefits. *RNA Biol.* 14, 1–9. doi: 10.1080/15476286.2016.1231359

Sun, S., Ling, S. C., Qiu, J., Albuquerque, C. P., Zhou, Y., Tokunaga, S., et al. (2015). ALS-causative mutations in FUS/TLS confer gain and loss of function by altered association with SMN and U1-snRNP. *Nat. Commun.* 6:6171. doi: 10.1038/ncomms7171

Tang, X., Bharath, S. R., Piao, S., Tan, V. Q., Bowler, M. W., and Song, H. (2016). Structural basis for specific recognition of pre-snRNA by Gemin5. *Cell Res.* 26, 1353–1356. doi: 10.1038/cr.2016.133

Wan, L., Battle, D. J., Yong, J., Gubitz, A. K., Kolb, S. J., Wang, J., et al. (2005). The survival of motor neurons protein determines the capacity for snRNP assembly: biochemical deficiency in spinal muscular atrophy. *Mol. Cell. Biol.* 25, 5543–5551. doi: 10.1128/MCB.25.13.5543-5551.2005

Winkler, C., Eggert, C., Gradl, D., Meister, G., Giegerich, M., Wedlich, D., et al. (2005). Reduced U snRNP assembly causes motor axon degeneration in an animal model for spinal muscular atrophy. *Genes Dev.* 19, 2320–2330. doi: 10.1101/gad.342005

Wirth, B., Garbes, L., and Riessland, M. (2013). How genetic modifiers influence the phenotype of spinal muscular atrophy and suggest future therapeutic approaches. *Curr. Opin. Genet. Dev.* 23, 330–338. doi: 10.1016/j.gde.2013.03.003

Workman, E., Saieva, L., Carrel, T. L., Crawford, T. O., Liu, D., Lutz, C., et al. (2009). A SMN missense mutation complements SMN2 restoring snRNPs and rescuing SMA mice. *Hum. Mol. Genet.* 18, 2215–2229. doi: 10.1093/hmg/ddp157

Xu, C., Ishikawa, H., Izumikawa, K., Li, L., He, H., Nobe, Y., et al. (2016). Structural insights into Gemin5-guided selection of pre-snRNAs for snRNP assembly. *Genes Dev.* 30, 2376–2390. doi: 10.1101/gad.288340.116

Yan, X., Mouillet, J. F., Ou, Q., and Sadovsky, Y. (2003). A novel domain within the DEAD-box protein DP103 is essential for transcriptional repression and helicase activity. *Mol. Cell. Biol.* 23, 414–423. doi: 10.1128/MCB.23.1.414-423.2003

Yong, J., Kasim, M., Bachorik, J. L., Wan, L., and Dreyfuss, G. (2010). Gemin5 delivers snRNA precursors to the SMN complex for snRNP biogenesis. *Mol. Cell* 38, 551–562. doi: 10.1016/j.molcel.2010.03.014

Young, P. J., Man, N. T., Lorson, C. L., Le, T. T., Androphy, E. J., Burghes, A. H., et al. (2000). The exon 2b region of the spinal muscular atrophy protein, SMN, is involved in self-association and SIP1 binding. *Hum. Mol. Genet.* 9, 2869–2877. doi: 10.1093/hmg/9.19.2869

Yu, Y., Chi, B., Xia, W., Gangopadhyay, J., Yamazaki, T., Winkelbauer-Hurt, M. E., et al. (2015). U1 snRNP is mislocalized in ALS patient fibroblasts bearing NLS mutations in FUS and is required for motor neuron outgrowth in zebrafish. *Nucleic Acids Res.* 43, 3208–3218. doi: 10.1093/nar/gkv157

Zhang, R., So, B. R., Li, P., Yong, J., Glisovic, T., Wan, L., et al. (2011). Structure of a key intermediate of the SMN complex reveals Gemin2's crucial function in snRNP assembly. *Cell* 146, 384–395. doi: 10.1016/j.cell.2011.06.043

Zhang, Z., Lotti, F., Dittmar, K., Younis, I., Wan, L., Kasim, M., et al. (2008). SMN deficiency causes tissue-specific perturbations in the repertoire of snRNAs and widespread defects in splicing. *Cell* 133, 585–600. doi: 10.1016/j.cell.2008.03.031

Zhang, Z., Pinto, A. M., Wan, L., Wang, W., Berg, M. G., Oliva, I., et al. (2013). Dysregulation of synaptogenesis genes antecedes motor neuron pathology in spinal muscular atrophy. *Proc. Natl. Acad. Sci. U.S.A.* 110, 19348–19353. doi: 10.1073/pnas.1319280110

Conflict of Interest Statement: The authors declare that the research was conducted in the absence of any commercial or financial relationships that could be construed as a potential conflict of interest.

frontiers in Molecular Biosciences

MINI REVIEW
published: 24 February 2017
doi: 10.3389/fmolb.2017.00007

Cellular Pathology of Pelizaeus-Merzbacher Disease Involving Chaperones Associated with Endoplasmic Reticulum Stress

Ken Inoue *

Department of Mental Retardation and Birth Defect Research, National Institute of Neuroscience, National Center of Neurology and Psychiatry, Kodaira, Japan

Disease-causing mutations in genes encoding membrane proteins may lead to the production of aberrant polypeptides that accumulate in the endoplasmic reticulum (ER). These mutant proteins have detrimental conformational changes or misfolding events, which result in the triggering of the unfolded protein response (UPR). UPR is a cellular pathway that reduces ER stress by generally inhibiting translation, increasing ER chaperones levels, or inducing cell apoptosis in severe ER stress. This process has been implicated in the cellular pathology of many neurological disorders, including Pelizaeus-Merzbacher disease (PMD). PMD is a rare pediatric disorder characterized by the failure in the myelination process of the central nervous system (CNS). PMD is caused by mutations in the *PLP1* gene, which encodes a major myelin membrane protein. Severe clinical PMD phenotypes appear to be the result of cell toxicity, due to the accumulation of PLP1 mutant proteins and not due to the lack of functional PLP1. Therefore, it is important to clarify the pathological mechanisms by which the PLP1 mutants negatively impact the myelin-generating cells, called oligodendrocytes, to overcome this devastating disease. This review discusses how PLP1 mutant proteins change protein homeostasis in the ER of oligodendrocytes, especially focusing on the reaction of ER chaperones against the accumulation of PLP1 mutant proteins that cause PMD.

Keywords: unfolded protein response, hypomyelinating leukodystrophy, ER chaperone, point mutations, PLP1

OPEN ACCESS

Edited by:
Alberto J. L. Macario, School of Medicine, University of Maryland at Baltimore; and Institute of Marine and Environmental Technology (IMET), Baltimore, USA; and Euro-Mediterranean Institute of Science and Technology (IEMEST), Palermo, Italy

Reviewed by:
Stefan W. Vetter, North Dakota State University, USA
Leonid Breydo, University of South Florida, USA

***Correspondence:**
Ken Inoue
kinoue@ncnp.go.jp

Specialty section:
This article was submitted to Protein Folding, Misfolding and Degradation, a section of the journal Frontiers in Molecular Biosciences

Received: *27 December 2016*
Accepted: *09 February 2017*
Published: *24 February 2017*

Citation:
Inoue K (2017) Cellular Pathology of Pelizaeus-Merzbacher Disease Involving Chaperones Associated with Endoplasmic Reticulum Stress. Front. Mol. Biosci. 4:7. doi: 10.3389/fmolb.2017.00007

CLINICAL AND GENETIC BASIS OF PELIZAEUS-MERZBACHER DISEASE (PMD)

Pelizaeus-Merzbacher disease (PMD) is a pediatric inherited disorder of the central nervous system (CNS), mainly affecting oligodendrocytes, cells specialized in generating and maintaining myelin sheaths. Myelin is a membranous structure that wraps around the neuronal axons, enhancing the electronic conduction of neuronal circuits in the brain. Myelin also enables rapid and efficient movement of the body and cognitive function of the brain. Children with PMD thus show deficiencies in motor and intellectual development at an early stage of life, which usually continue thereafter. In addition, they present other neurological symptoms including nystagmus (involuntary rapid eye movement), spastic paraplegia (increased muscle tone and stiffness), ataxia (abnormal voluntary coordination of muscle movements), and dystonia (involuntary muscle contractions). PMD shows a wide range of clinical severity (**Figure 1A**). The most severe cases

(the connatal form) show the arrest of developmental milestones such as head control, and are often bedridden for their lifetime. Milder cases (the classic form) reveal delayed motor and cognitive development with different degrees; for example, some patients obtain the ability to walk independently or achieve head control, but are wheelchair-bound. In general, motor disability is more severe than cognitive dysfunction. The mildest cases display spastic paraplegia with mild cognitive impairment, often diagnosed as spastic paraplegia type 2 (SPG2). The incidence of PMD with *PLP1* mutations was estimated to be 1.45 and 1.9 per 100,000 male live births in Japan and USA, respectively (Bonkowsky et al., 2010; Numata et al., 2014).

The underlying cause of PMD is either an abnormal quality or quantity of the proteolipid protein 1 (PLP1), which is the most abundant myelin membrane lipid protein in the CNS (Inoue, 2005). *PLP1* is located at Xq22.1 on the long arm of the X chromosome and encodes tetra-span myelin membrane lipoprotein; hence PMD shows X-linked recessive pattern of inheritance. Two alternative splicing variants differ in the inclusion or exclusion of the latter half of exon 3, to produce either PLP1 or DM20 protein; the former composes the major portion in the mature myelin. (Griffiths et al., 1998; Yool et al., 2000).

Different *PLP1* mutations cause PMD through distinct molecular mechanisms (**Figure 1A**). Point mutations in the coding exons often lead to amino acid substitutions that alter protein conformation, resulting in a misfolded protein (Jung et al., 1996; Dhaunchak et al., 2011). Approximately 30–40% of PMD patients worldwide have point mutations in their *PLP1* gene (Numata et al., 2014). This review focuses on the molecular mechanisms underlying this class of mutations. Genomic duplication events of *PLP1* also cause the PMD phenotype (Inoue et al., 1996, 1999), due to the overexpression of the *PLP1* transcript. However, the exact cellular mechanism as to how an extra copy of the wild-type *PLP1* gene leads to a severe hypomyelinating phenotype, remains unknown. Duplication of the *PLP1* gene is the most common mutation that causes the PMD phenotype, since 60–70% of PMD patients have it and this proportion appears to be quite similar worldwide (Inoue, 2005; Numata et al., 2014). Rare *null* mutations, such as gene deletions or nonsense/frame shift mutations that result in premature terminations (presumably degraded by nonsense mediated mRNA decay) leading to no PLP1 production can cause a mild but slowly progressive PMD phenotype (Inoue et al., 2002; Garbern, 2007). Intronic and splicing mutations have been found in a considerable amount of patients, who also show variable PMD phenotype severity (Hobson et al., 2000, 2002; Laššuthova et al., 2013; Kevelam et al., 2015). Each of these mutations is associated with a specific clinical phenotype of PMD, as detailed in a previous review (Inoue, 2005).

Many *PLP1* point mutations cause amino acid substitutions, leading to the production of misfolded PLP1 that accumulates in the endoplasmic reticulum (ER) (Gow and Lazzarini, 1996; Swanton et al., 2005). In humans, production of wild-type PLP1 rapidly increases upon the maturation of oligodendrocytes in the process of myelination to produce massive amounts of myelin after birth. The secretory system runs at full capacity in the maturating oligodendrocytes to produce both myelin proteins and lipids. Therefore, in PMD patients, a large amount of PLP1 mutant proteins accumulates in the ER of oligodendrocytes, eventually leading to apoptotic cell death and myelination failure; however, the exact pathological mechanism is currently unknown. Mutant PLP1 proteins do not form aggregates or insoluble amyloid-like structures, but they form SDS-resistant homo oligomers, which is more prominent in mutations associated with severe clinical phenotype (Swanton et al., 2005).

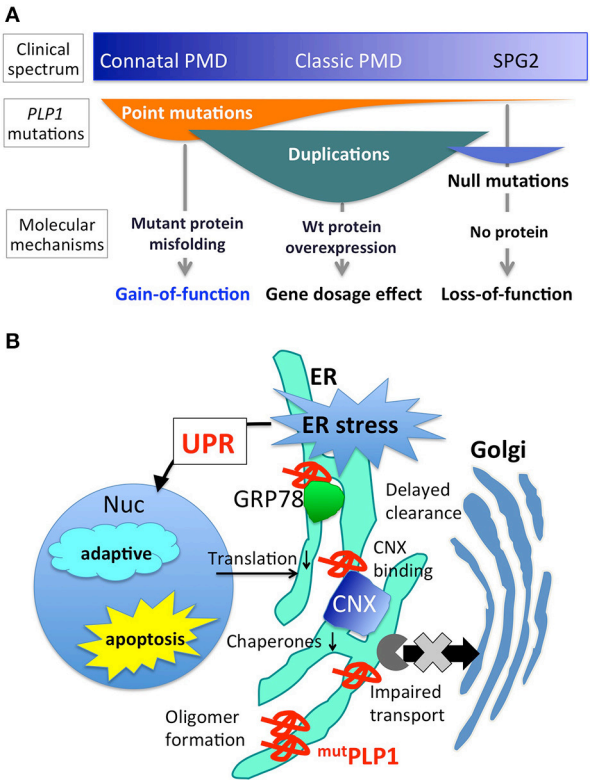

FIGURE 1 | *PLP1* mutations, associated phenotypes, and molecular mechanisms. (A) Different PLP1 mutations result in distinct molecular mechanisms underlying a wide variety of clinical phenotypes (Inoue, 2005). **(B)** Mutant PLP1 and associated cellular pathology. Misfolded mutant PLP1 (^{mut}PLP1) accumulates in the ER and evokes ER stress, which triggers unfolded protein response to rescue the cells by reducing translation and increasing ER chaperones, or to turn on the proapoptotic pathway to induce cell death (Southwood et al., 2002; D'Antonio et al., 2009; Clayton and Popko, 2016). Disease-causing mutations in PLP1 is known to cause oligomer formation in the ER (Swanton et al., 2005), binding to CNX and delayed clearance from the ER (Swanton et al., 2003), and impaired ER-Golgi trafficking (Numata et al., 2013).

ER STRESS AND UNFOLDED PROTEIN RESPONSE (UPR)

Recent studies have revealed that mutant PLP1 may cause PMD, not by lack of functional protein, but by eliciting a cytotoxic effect (Schneider et al., 1995; Swanton et al., 2005; Numata et al., 2013). Especially, unfolded protein response (UPR) has been

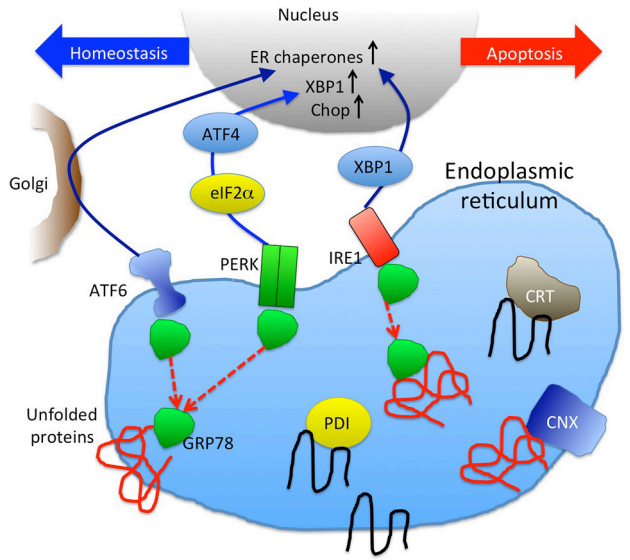

FIGURE 2 | A schematic picture of unfolded protein response and ER chaperones. GRP78 binding to unfolded proteins accumulated in ER results in dissociation from and activation of ER stress sensors, ATF6, PERK, and IRE1 (Szegezdi et al., 2006). Downstream signaling molecules function either to maintain cellular homeostasis or promote apoptosis. UPR result in increase of ER chaperones (CRT, CNX, GRP78, and PDI are depicted here) to enhance the protein folding capacity.

suggested to play a central role in the molecular pathology of PMD (**Figure 2**; Southwood et al., 2002; D'Antonio et al., 2009; Clayton and Popko, 2016). Regardless of the cell's pathological or physiological state, unfolded/misfolded proteins accumulate in the ER, causing ER stress; hence, these aberrant proteins need to be removed from the ER to maintain cellular homeostasis. The cellular signaling cascade that plays this role is the UPR, a stress-induced eukaryotic signaling cascade that serves as a cellular quality control (Walter and Ron, 2011). UPR protects cells from the toxicity of accumulated proteins in the ER by reducing translation, increasing retrotranslocation and degradation of ER-localized proteins, and bolstering the protein folding capacity of the ER to maintain cellular homeositasis. However, when the ER stress exceeds the capacity of this intrinsic quality control, apoptosis is induced through the up-regulation of the proapoptotic branch of the UPR pathway (Lin et al., 2007).

UPR activation is triggered by three distinct pathways: ATF6, IRE1, and PERK (Szegezdi et al., 2006) (**Figure 2**). These pathways are negatively regulated by GRP78 (also known as BiP), an ER chaperone that plays a critical role in the initiation of UPR (Schröder and Kaufman, 2005). When unfolded/misfolded proteins accumulate in the ER, GRP78 binds to these unfolded/misfolded proteins leading to the dissociation of the ER stress sensors (i.e., ATF6, IRE1, and PERK), thereby triggering UPR. ATF6 induces the transcription of major ER chaperones and XBP1 (Yamamoto et al., 2007). The endonuclease activity of IRE1 promotes the splicing of *XBP1* mRNA, producing its active form that encodes a transcription factor that regulates the expression of UPR-related genes (Calfon et al., 2002). ATF6 and IRE1-XBP1 axes promote the expression of ER chaperones, facilitating the correct folding and/or assembly of proteins in the ER, preventing ER protein aggregation, thereby improving cell survival (Yoshida et al., 2001; Szegezdi et al., 2006; Yamamoto et al., 2007). However, when this intrinsic quality control system fails to eliminate unfolded/misfolded proteins, UPR activates a proapoptotic signaling cascade, which is initiated by the dissociation of GRP78 from PERK. Phosphorylated PERK decreases global protein translation by phosphorylating the eukaryotic initiation factor 2α (eIF2α), reducing the ER protein load, while PERK also increases the translation of some UPR-related genes including ATF4, which leads to the transcriptional activation of CHOP. CHOP is a transcription factor that induces apoptosis by directly repressing the expression of anti-apoptotic factor Bcl-2 (Hetz, 2012).

The activation of the UPR-induced apoptotic pathway, caused by the accumulation of mutant PLP1, may cause massive cell death of oligodendrocytes, which is suspected to occur in the brains of patients with PMD.

ER STRESS AND UPR IN PMD

Clinical and genetic observations of patients with PMD have raised two questions in terms of the molecular pathology of *PLP1* point mutations. First, PMD patients with point mutations show a wide range of clinical severity; the mildest end of this clinical spectrum shows as spastic paraplegia type 2 (SPG2), which is considered to be milder disease than PMD, while the most severe end is the connatal form PMD, which can cause premature mortality (Inoue, 2005). The exact reason as to why different point mutations located in various positions of *PLP1* result in different clinical severity remains unknown. Second, it has been speculated that mutant PLP1 may act as gain-of-function proteins, because many patients with point mutations in *PLP1* show much severer phenotypes than those lacking a functional PLP1 protein, due to deletion or truncating mutations. However, the molecular basis by which mutant PLP1 elicits toxicity to oligodendrocytes remains to be determined.

The initial evidence addressing the question of cell toxicity due to the production of the mutant PLP1 was given by a cell biological study that demonstrated that the *PLP1* mutations associated with severe phenotypes led to the accumulation of both PLP1 and DM20 isoforms in the ER, while those associated with milder phenotypes resulted in the traverse of DM20 isoform through the secretory pathway to the cell surface (Gow and Lazzarini, 1996). Furthermore, the accumulation of mutant PLP1 was found to trigger ER stress and activate UPR (**Figure 1B**) (Southwood et al., 2002). During the maturation of oligodendrocytes, these cells produce a large amount of myelin sheath, and PLP1 abundance increases drastically. Nearly half of the entire protein content of mature oligodendrocytes is made up of PLP1. Therefore, it is not difficult to speculate that a significant amount of mutant PLP1 accumulates in the ER, causing an increased ER stress, resulting in the acute activation of the UPR apoptotic signaling cascade. In fact, CHOP, a proapoptotic transcription factor, is upregulated in the brains of patients with

PMD and mouse models (Southwood et al., 2002). Upregulation of UPR was also recapitulated in the PMD patient-derived iPS cells after differentiation into oligodendrocytes *in vitro* (Numasawa-Kuroiwa et al., 2014).

The genotype-phenotype correlation in *PLP1* mutations-PMD severity has been partly explained by studies showing how different mutations trigger UPR differently. In these studies, mouse models that recapitulate the different levels of PMD severity in humans have been utilized (Yool et al., 2000). The *myelin synthesis deficient* (*msd*) mice carry an A243V mutation, which results in a very severe phenotype in both humans and mice. The *rumpshaker* (*rsh*) mice with an I187T mutation serve as a model for the mildest end of the PLP1-associated severity spectrum, SPG2. These mutants, along with the classic PMD mouse model *jimpy (jp)*, have largely contributed to the understanding of the molecular pathogenesis of PMD. The mutant PLP1 protein associated with mild PMD phenotypes appear to be cleared quickly from the ER, via the proteasomal degradation pathway and/or ER exit, while the mutant PLP1 protein associated with severe PMD phenotypes is resistant to protein degradation and/or exclusion from the ER, triggering UPR activation (Roboti et al., 2009). The position of mutations in *PLP1* also contributes to the cellular pathology that triggers UPR. For example, the retention of the mutant PLP1 in the ER that carry mutations in the extracellular domain, where two disulfide bridges are located, depends on the cysteine residues that play a critical role in protein cross-linking (Dhaunchak and Nave, 2007).

It has been suggested that mutations leading to severe PMD phenotypes may enhance the CHOP proapoptotic pathway more markedly than mild PMD phenotype-associated mutations; hence, a more severe dysmyelinating phenotype may occur (McLaughlin et al., 2007; Roboti et al., 2009). If this is the case, the genetic removal of CHOP may rescue the PMD phenotype in the mouse model. However, this scenario was not that simple. Rather than rescuing the phenotype, *rsh* mice crossed with a *CHOP* null line revealed a higher premature mortality rate and an increased number of oligodendrocyte cell death (Southwood et al., 2002). The prominent worsening of PMD phenotype in mice lacking *CHOP* shows a sharp contrast in another disease model of peripheral demyelinating neuropathy, Charcot-Marie-Tooth disease (CMT), which is caused by mutations in the *MPZ* gene. The genetic removal of *CHOP* from the CMT model mice carrying S63del *MPZ* mutation ameliorated the demyelination and apoptotic cell death of Schwann cells (Pennuto et al., 2008). The exact reasons for these opposite outcomes resulting from *CHOP* ablation in central and peripheral myelin gene mutants remain unknown. One hypothesis is that the *CHOP* downstream genes in Schwann cells (and probably most other cell types) are maladaptive and CHOP induction leads to cell death and demyelination; however, CHOP may regulate a different set of downstream genes in oligodendrocytes, which presumably function as adaptive, or protective against cell death (Southwood et al., 2002; D'Antonio et al., 2009).

Interestingly, genetic ablation of ATF3 or caspase-12, both known to function in the proapoptotic pathway downstream of *CHOP*, showed no effect on disease severity in *msd* and *rsh* mice (Sharma and Gow, 2007; Sharma et al., 2007). The findings suggest that these genes are not related to oligodendrocyte survival in *PLP1* mutant mice.

CELLULAR PATHOLOGY BEYOND THE UPR

Although, the central role of UPR in the cellular pathology of PMD caused by point mutations in the *PLP1* gene is indisputable, the relationship between *CHOP* upregulation and the apoptotic cell death of oligodendrocytes in PMD should be reconsidered. In order to understand the effect of mutant PLP1 accumulating in the ER, studies beyond the UPR are required to elucidate specific characteristics of the mutant PLP1 molecule, especially its interaction with other ER proteins, such as ER chaperones.

If the activation of PERK-CHOP branch of UPR is not responsible for the oligodendrocyte cell death and dysmyelination, which is the major pathology in PMD, then, who is playing the major role? The answer to this question is still unknown, but some interesting findings suggest critical roles of ER chaperones in myelinating oligodendrocytes. Mice lacking *GRP78,* in either developing or mature oligodendrocytes, showed neurological phenotypes and dysmyelination accompanied by oligodendrocyte cell death, all of which are surprisingly similar to those observed in PMD mouse models (Hussien et al., 2015). GRP78 facilitates the proper protein folding and regulates UPR by keeping the three UPR sensors (PERK, IRE1, and ATF6) inactive. In fact, these mutant mice showed activation of PERK and ATF6, and induction of CHOP expression, suggesting that the genetic ablation of GRP78 leads to persistent activation of UPR (Hussien et al., 2015). It has not been elucidated if these drastic phenotypes are associated with a perturbed physiological function of GRP78, including protein folding or induction of CHOP-mediated apoptosis.

Another example showing the critical role of ER chaperones in myelination was demonstrated by deleting calnexin (CNX) in mice (Kraus et al., 2010). CNX is a lectin-like chaperone, and together with calreticulin (CRT), promotes the folding of glycosylated proteins (Caramelo and Parodi, 2015). Despite its critical role in quality control of the secretory pathway, the genetic ablation of CNX resulted in surprisingly limited peripheral and central myelin phenotypes. CNX-deficient mice are viable, with no discernible effects on other systems, presumably because of the functional redundancy of CRT. However, in myelin systems, the mice showed apparent dysmyelination in both CNS and PNS, indicating that CNX is essential for proper myelin formation (Kraus et al., 2010). At this point, it is not clear if CNX has unique functions in myelinating oligodendrocytes and Schwann cells, or increasing the protein load in the ER during the myelination process causing insufficient folding capacity by only CRT.

Mutant PLP1 not only triggers UPR but also changes the dynamics of ER chaperones. Although, PLP1 is not a glycosylated protein and normally is not a substrate for CNX/CRT, CNX, but not CRT, stably binds to the misfolded PLP1 mutant protein (Swanton et al., 2003). Surprisingly, this CNX-mutant PLP1

binding delays the elimination of mutant protein from the cells through the ER-associated degradation (ERAD), suggesting that this glycan-independent binding of ER chaperones possibly contributes to the pathology of PMD.

CNX may not be the only chaperone involved in the pathology of PMD. Our *in vitro* study showed that mutant PLP1 reduces the ER localization of GRP78, CRT, and PDI, but not CNX (Numata et al., 2013). The exact mechanism for this apparent reduction of ER chaperones from the ER, while the ER is under stress induced by the massive production of misfolded mutant PLP1, is unknown. It has become apparent that the mutant PLP1 not only accumulates in the ER but also inhibits the transport of other proteins in the secretory pathway from ER to the Golgi apparatus. This includes the KDEL receptor, which plays a critical role in carrying ER chaperones that contains the KDEL sequence (i.e., GRP78, CRT, and protein-disulfide isomerase (PDI), but not CNX) from the Golgi apparatus back to the ER after post-translational modifications. These findings highlight the effect of mutant PLP1 on global transport of secretory proteins.

IMPLICATION FOR POTENTIAL PMD TREATMENT

Considering the evidence in terms of the involvement of UPR and ER chaperones in the molecular pathology of PMD caused by mutant PLP1, some therapeutic interventions targeting the UPR and ER chaperones have been evaluated using cellular and animal models.

Curcumin, a polyphenol dietary compound derived from curry spice turmeric, has been evaluated for its therapeutic potential in some diseases in which ER stress and UPR have been implicated in the pathogenesis, such as cystic fibrosis (targeting *CFTR*), Charcot-Marie-Tooth disease (targeting *PMP22* and *MPZ*), retinitis pigmentosa (targeting *RHO*), and PMD (Egan et al., 2004; Khajavi et al., 2005, 2007; Vasireddy et al., 2011; Yu et al., 2012). *Msd* mice treated with oral curcumin showed an extended life span and a reduced number of apoptotic oligodendrocytes, showing an apparent but modest therapeutic effect. However, the expression of ER stress markers including CHOP, GRP78, myelin protein MBP, and motor function showed no change or improvement (Yu et al., 2012). Interestingly, curcumin also improved the PMD phenotype in PLP1 transgenic mouse, a model for *PLP1* duplication in patients with PMD (Epplen et al., 2015). Since the PLP1 overexpression does not involve ER stress or UPR, curcumin may also have different therapeutic targets other than UPR.

Chloroquine, an anti-malarial drug, was found to reduce the accumulation of the mutant PLP1 and attenuate ER stress by enhancing the phosphorylation of eIF2α (Morimura et al., 2014). Despite its drastic effects as an ER stress attenuator, the concentration to obtain this effect *in vitro* was relatively high (100 μM) for clinical application, considering its side effects.

Although, there is no clinically validated therapy for PMD to date, clarification of the molecular mechanism underlying the accumulation of the mutant PLP1 in the ER and its effect on cellular function and survival of oligodendrocytes, will help to identify the molecules that could rescue the cellular PMD phenotype. This could eventually lead to future treatment of patients with PMD. Enhancement of ER chaperones may serve as one possibility for the discovery of an effective treatment strategy for PMD.

AUTHOR CONTRIBUTIONS

The author confirms being the sole contributor of this work and approved it for publication.

FUNDING

This work was supported in part by research grants from Japan Agency of Medical Research and Development, AMED (Practical Research Project for Rare/Intractable Diseases: 16ek0109016) and Grant-in-Aid for Scientific Research (Kiban-B: 16H05361).

ACKNOWLEDGMENTS

The author thanks all patients and families who have contributed to our clinical and basic studies, as well as all colleagues and collaborators for their scientific contributions and valuable discussions.

REFERENCES

Bonkowsky, J. L., Nelson, C., Kingston, J. L., Filloux, F. M., Mundorff, M. B., and Srivastava, R. (2010). The burden of inherited leukodystrophies in children. *Neurology* 75, 718–725. doi: 10.1212/WNL.0b013e3181eee46b

Calfon, M., Zeng, H., Urano, F., Till, J. H., Hubbard, S. R., Harding, H. P., et al. (2002). IRE1 couples endoplasmic reticulum load to secretory capacity by processing the XBP-1 mRNA. *Nature* 415, 92–96. doi: 10.1038/415092a

Caramelo, J. J., and Parodi, A. J. (2015). A sweet code for glycoprotein folding. *FEBS Lett.* 589, 3379–3387. doi: 10.1016/j.febslet.2015.07.021

Clayton, B. L., and Popko, B. (2016). Endoplasmic reticulum stress and the unfolded protein response in disorders of myelinating glia. *Brain Res.* 1648(Pt B), 594–602. doi: 10.1016/j.brainres.2016.03.046

D'Antonio, M., Feltri, M. L., and Wrabetz, L. (2009). Myelin under stress. *J. Neurosci. Res.* 87, 3241–3249. doi: 10.1002/jnr.22066

Dhaunchak, A. S., Colman, D. R., and Nave, K. A. (2011). Misalignment of PLP/DM20 transmembrane domains determines protein misfolding in Pelizaeus-Merzbacher disease. *J. Neurosci.* 31, 14961–14971. doi: 10.1523/JNEUROSCI.2097-11.2011

Dhaunchak, A. S., and Nave, K. A. (2007). A common mechanism of PLP/DM20 misfolding causes cysteine-mediated endoplasmic reticulum retention in oligodendrocytes and Pelizaeus-Merzbacher disease. *Proc. Natl. Acad. Sci. U.S.A.* 104, 17813–17818. doi: 10.1073/pnas.0704975104

Egan, M. E., Pearson, M., Weiner, S. A., Rajendran, V., Rubin, D., Glockner-Pagel, J., et al. (2004). Curcumin, a major constituent of turmeric, corrects cystic fibrosis defects. *Science* 304, 600–602. doi: 10.1126/science.1093941

Epplen, D. B., Prukop, T., Nientiedt, T., Albrecht, P., Arlt, F. A., Stassart, R. M., et al. (2015). Curcumin therapy in a Plp1 transgenic mouse model of Pelizaeus-Merzbacher disease. *Ann. Clin. Transl. Neurol.* 2, 787–796. doi: 10.1002/acn3.219

Garbern, J. Y. (2007). Pelizaeus-Merzbacher disease: Genetic and cellular pathogenesis. *Cell. Mol. Life Sci.* 64, 50–65. doi: 10.1007/s00018-006-6182-8

Gow, A., and Lazzarini, R. A. (1996). A cellular mechanism governing the severity of Pelizaeus-Merzbacher disease. *Nat. Genet.* 13, 422–428.

Griffiths, I., Klugmann, M., Anderson, T., Thomson, C., Vouyiouklis, D., and Nave, K. A. (1998). Current concepts of PLP and its role in the nervous system. *Microsc. Res. Tech.* 41, 344–358.

Hetz, C. (2012). The unfolded protein response: controlling cell fate decisions under ER stress and beyond. *Nat. Rev. Mol. Cell Biol.* 13, 89–102. doi: 10.1038/nrm3270

Hobson, G. M., Davis, A. P., Stowell, N. C., Kolodny, E. H., Sistermans, E. A., de Coo, I. F., et al. (2000). Mutations in noncoding regions of the proteolipid protein gene in Pelizaeus-Merzbacher disease. *Neurology* 55, 1089–1096.

Hobson, G. M., Huang, Z., Sperle, K., Stabley, D. L., Marks, H. G., and Cambi, F. (2002). A PLP splicing abnormality is associated with an unusual presentation of PMD. *Ann. Neurol.* 52, 477–488. doi: 10.1002/ana.10320

Hussien, Y., Podojil, J. R., Robinson, A. P., Lee, A. S., Miller, S. D., and Popko, B. (2015). ER chaperone BiP/GRP78 is required for myelinating cell survival and provides protection during experimental autoimmune encephalomyelitis. *J. Neurosci.* 35, 15921–15933. doi: 10.1523/JNEUROSCI.0693-15.2015

Inoue, K. (2005). PLP1-related inherited dysmyelinating disorders: Pelizaeus-Merzbacher disease and spastic paraplegia type 2. *Neurogenetics* 6, 1–16. doi: 10.1007/s10048-004-0207-y

Inoue, K., Osaka, H., Imaizumi, K., Nezu, A., Takanashi, J., Arii, J., et al. (1999). Proteolipid protein gene duplications causing Pelizaeus-Merzbacher disease: molecular mechanism and phenotypic manifestations. *Ann. Neurol.* 45, 624–632.

Inoue, K., Osaka, H., Sugiyama, N., Kawanishi, C., Onishi, H., Nezu, A., et al. (1996). A duplicated *PLP* gene causing Pelizaeus-Merzbacher disease detected by comparative multiplex PCR. *Am. J. Hum. Genet.* 59, 32–39.

Inoue, K., Osaka, H., Thurston, V. C., Clarke, J. T., Yoneyama, A., Rosenbarker, L., et al. (2002). Genomic rearrangements resulting in PLP1 deletion occur by nonhomologous end joining and cause different dysmyelinating phenotypes in males and females. *Am. J. Hum. Genet.* 71, 838–853. doi: 10.1086/342728

Jung, M., Sommer, I., Schachner, M., and Nave, K. A. (1996). Monoclonal antibody O10 defines a conformationally sensitive cell-surface epitope of proteolipid protein (PLP): evidence that PLP misfolding underlies dysmyelination in mutant mice. *J. Neurosci.* 16, 7920–7929.

Kevelam, S. H., Taube, J. R., van Spaendonk, R. M., Bertini, E., Sperle, K., Tarnopolsky, M., et al. (2015). Altered PLP1 splicing causes hypomyelination of early myelinating structures. *Ann. Clin. Transl. Neurol.* 2, 648–661. doi: 10.1002/acn3.203

Khajavi, M., Inoue, K., Wiszniewski, W., Ohyama, T., Snipes, G. J., and Lupski, J. R. (2005). Curcumin treatment abrogates endoplasmic reticulum retention and aggregation-induced apoptosis associated with neuropathy-causing myelin protein zero-truncating mutants. *Am. J. Hum. Genet.* 77, 841–850. doi: 10.1086/497541

Khajavi, M., Shiga, K., Wiszniewski, W., He, F., Shaw, C. A., Yan, J., et al. (2007). Oral curcumin mitigates the clinical and neuropathologic phenotype of the Trembler-J mouse: a potential therapy for inherited neuropathy. *Am. J. Hum. Genet.* 81, 438–453. doi: 10.1086/519926

Kraus, A., Groenendyk, J., Bedard, K., Baldwin, T. A., Krause, K. H., Dubois-Dauphin, M., et al. (2010). Calnexin deficiency leads to dysmyelination. *J. Biol. Chem.* 285, 18928–18938. doi: 10.1074/jbc.M110.107201

Laššuthova, P., Žaliová, M., Inoue, K., Haberlová, J., Sixtová, K., Sakmaryová, I., et al. (2013). Three new PLP1 splicing mutations demonstrate pathogenic and phenotypic diversity of Pelizaeus-Merzbacher disease. *J. Child Neurol.* 29, 924–931. doi: 10.1177/0883073813492387

Lin, J. H., Li, H., Yasumura, D., Cohen, H. R., Zhang, C., Panning, B., et al. (2007). IRE1 signaling affects cell fate during the unfolded protein response. *Science* 318, 944–949. doi: 10.1126/science.1146361

McLaughlin, M., Karim, S. A., Montague, P., Barrie, J. A., Kirkham, D., Griffiths, I. R., et al. (2007). Genetic background influences UPR but not PLP processing in the rumpshaker model of PMD/SPG2. *Neurochem. Res.* 32, 167–176. doi: 10.1007/s11064-006-9122-y

Morimura, T., Numata, Y., Nakamura, S., Hirano, E., Gotoh, L., Goto, Y. I., et al. (2014). Attenuation of endoplasmic reticulum stress in Pelizaeus-Merzbacher disease by an anti-malaria drug, chloroquine. *Exp. Biol. Med. (Maywood).* 239, 489–501. doi: 10.1177/1535370213520108

Numasawa-Kuroiwa, Y., Okada, Y., Shibata, S., Kishi, N., Akamatsu, W., Shoji, M., et al. (2014). Involvement of ER stress in dysmyelination of Pelizaeus-Merzbacher disease with PLP1 missense mutations shown by iPSC-derived oligodendrocytes. *Stem Cell Reports* 2, 648–661. doi: 10.1016/j.stemcr.2014.03.007

Numata, Y., Gotoh, L., Iwaki, A., Kurosawa, K., Takanashi, J., Deguchi, K., et al. (2014). Epidemiological, clinical, and genetic landscapes of hypomyelinating leukodystrophies. *J. Neurol.* 261, 752–758. doi: 10.1007/s00415-014-7263-5

Numata, Y., Morimura, T., Nakamura, S., Hirano, E., Kure, S., Goto, Y. I., et al. (2013). Depletion of molecular chaperones from the endoplasmic reticulum and fragmentation of the Golgi apparatus associated with pathogenesis in Pelizaeus-Merzbacher disease. *J. Biol. Chem.* 288, 7451–7466. doi: 10.1074/jbc.M112.435388

Pennuto, M., Tinelli, E., Malaguti, M., Del Carro, U., D'Antonio, M., Ron, D., et al. (2008). Ablation of the UPR-mediator CHOP restores motor function and reduces demyelination in Charcot-Marie-Tooth 1B mice. *Neuron* 57, 393–405. doi: 10.1016/j.neuron.2007.12.021

Roboti, P., Swanton, E., and High, S. (2009). Differences in endoplasmic-reticulum quality control determine the cellular response to disease-associated mutants of proteolipid protein. *J Cell Sci.* 122(Pt 21), 3942–3953. doi: 10.1242/jcs.055160

Schneider, A. M., Griffiths, I. R., Readhead, C., and Nave, K. A. (1995). Dominant-negative action of the jimpy mutation in mice complemented with an autosomal transgene for myelin proteolipid protein. *Proc. Natl. Acad. Sci. U.S.A.* 92, 4447–4451.

Schröder, M., and Kaufman, R. J. (2005). The mammalian unfolded protein response. *Annu. Rev. Biochem.* 74, 739–789. doi: 10.1146/annurev.biochem.73.011303.074134

Sharma, R., and Gow, A. (2007). Minimal role for caspase 12 in the unfolded protein response in oligodendrocytes *in vivo*. *J. Neurochem.* 101, 889–897. doi: 10.1111/j.1471-4159.2007.04541.x

Sharma, R., Jiang, H., Zhong, L., Tseng, J., and Gow, A. (2007). Minimal role for activating transcription factor 3 in the oligodendrocyte unfolded protein response *in vivo*. *J. Neurochem.* 102, 1703–1712. doi: 10.1111/j.1471-4159.2007.04646.x

Southwood, C. M., Garbern, J., Jiang, W., and Gow, A. (2002). The unfolded protein response modulates disease severity in Pelizaeus-Merzbacher disease. *Neuron* 36, 585–596. doi: 10.1016/S0896-6273(02)01045-0

Swanton, E., High, S., and Woodman, P. (2003). Role of calnexin in the glycan-independent quality control of proteolipid protein. *EMBO J.* 22, 2948–2958. doi: 10.1093/emboj/cdg300

Swanton, E., Holland, A., High, S., and Woodman, P. (2005). Disease-associated mutations cause premature oligomerization of myelin proteolipid protein in the endoplasmic reticulum. *Proc. Natl. Acad. Sci. U.S.A.* 102, 4342–4347. doi: 10.1073/pnas.0407287102

Szegezdi, E., Logue, S. E., Gorman, A. M., and Samali, A. (2006). Mediators of endoplasmic reticulum stress-induced apoptosis. *EMBO Rep.* 7, 880–885. doi: 10.1038/sj.embor.7400779

Vasireddy, V., Chavali, V. R., Joseph, V. T., Kadam, R., Lin, J. H., Jamison, J. A., et al. (2011). Rescue of photoreceptor degeneration by curcumin in transgenic rats with P23H rhodopsin mutation. *PLoS ONE* 6:e21193. doi: 10.1371/journal.pone.0021193

Walter, P., and Ron, D. (2011). The unfolded protein response: from stress pathway to homeostatic regulation. *Science* 334, 1081–1086. doi: 10.1126/science.1209038

Yamamoto, K., Sato, T., Matsui, T., Sato, M., Okada, T., Yoshida, H., et al. (2007). Transcriptional induction of mammalian ER quality control proteins is mediated by single or combined action of ATF6α and XBP1. *Dev. Cell* 13, 365–376. doi: 10.1016/j.devcel.2007.07.018

Yool, D. A., Edgar, J. M., Montague, P., and Malcolm, S. (2000). The *proteolipid protein* gene and myelin disorders in man and animal models. *Hum. Mol. Genet.* 9, 987–992. doi: 10.1093/hmg/9.6.987

Yoshida, H., Matsui, T., Yamamoto, A., Okada, T., and Mori, K. (2001). XBP1 mRNA is induced by ATF6 and spliced by IRE1 in response to ER stress to produce a highly active transcription factor. *Cell* 107, 881–891. doi: 10.1016/S0092-8674(01)00611-0

Yu, L. H., Morimura, T., Numata, Y., Yamamoto, R., Inoue, N., Antalfy, B., et al. (2012). Effect of curcumin in a mouse model of Pelizaeus-Merzbacher disease. *Mol. Genet. Metab.* 106, 108–114. doi: 10.1016/j.ymgme.2012.02.016

Conflict of Interest Statement: The author declares that the research was conducted in the absence of any commercial or financial relationships that could be construed as a potential conflict of interest.

frontiers in Molecular Biosciences

REVIEW
published: 09 January 2017
doi: 10.3389/fmolb.2016.00084

Prokaryotic Chaperonins as Experimental Models for Elucidating Structure-Function Abnormalities of Human Pathogenic Mutant Counterparts

Everly Conway de Macario [1, 2], Frank T. Robb [1, 3] and Alberto J. L. Macario [1, 2]*

[1] Department of Microbiology and Immunology, School of Medicine, University of Maryland at Baltimore, Columbus Center; Institute of Marine and Environmental Technology, Baltimore, MD, USA, [2] Euro-Mediterranean Institute of Science and Technology, Palermo, Italy, [3] Institute for Bioscience and Biotechnology Research, University of Maryland, College Park, Rockville, MD, USA

OPEN ACCESS

Edited by:
Vladimir N. Uversky, University of South Florida, USA

Reviewed by:
Leonid Breydo, University of South Florida, USA
Martin M. Muschol, University of South Florida, USA
Nikolai B. Gusev, Moscow State University, Russia

***Correspondence:**
Everly Conway de Macario
econwaydemacario@som.umaryland.edu

Specialty section:
This article was submitted to Protein Folding, Misfolding and Degradation, a section of the journal Frontiers in Molecular Biosciences

Received: *30 September 2016*
Accepted: *12 December 2016*
Published: *09 January 2017*

Citation:
Conway de Macario E, Robb FT and Macario AJL (2017) Prokaryotic Chaperonins as Experimental Models for Elucidating Structure-Function Abnormalities of Human Pathogenic Mutant Counterparts. Front. Mol. Biosci. 3:84. doi: 10.3389/fmolb.2016.00084

All archaea have a chaperonin of Group II (thermosome) in their cytoplasm and some have also a chaperonin of Group I (GroEL; Cpn60; Hsp60). Conversely, all bacteria have GroEL, some in various copies, but only a few have, in addition, a chaperonin (tentatively designated Group III chaperonin) very similar to that occurring in all archaea, i.e., the thermosome subunit, and in the cytosol of eukaryotic cells, named CCT. Thus, nature offers a range of prokaryotic organisms that are potentially useful as experimental models to study the human CCT and its abnormalities. This is important because many diseases, the chaperonopathies, have been identified in which abnormal chaperones, including mutant CCT, are determinant etiologic-pathogenic factors and, therefore, research is needed to elucidate their pathologic features at the molecular level. Such research should lead to the clarification of the molecular mechanisms underlying the pathologic lesions observed in the tissues and organs of patients with chaperonopathies. Information on these key issues is necessary to make progress in diagnosis and treatment. Some of the archaeal organisms as well as some of the bacterial models suitable for studying molecular aspects pertinent to human mutant chaperones are discussed here, focusing on CCT. Results obtained with the archaeon *Pyrococcus furiosus* model to investigate the impact of a pathogenic CCT5 mutation on molecular properties and chaperoning functions are reviewed. The pathogenic mutation examined weakens the ability of the chaperonin subunit to form stable hexadecamers and as a consequence, the chaperoning functions of the complex are impaired. The future prospect is to find means for stabilizing the hexadecamer, which should lead to a recovering of chaperone function and the improving of lesions and clinical condition.

Keywords: chaperonopathies, Group II chaperonins, experimental models, archaea, CCT-like chaperonin in bacteria, CCT5 mutations, *Pyrococcus furiosus*, hexadecamer instability

INTRODUCTION

The realization that abnormal chaperones can be determinant etiologic-pathogenic factors has revealed the need to develop means for studying the molecular mechanisms involved. A number of questions still require answers if progress is to be made in the elucidation of the mechanism of disease and thereby, in early diagnosis and treatment. For instance: What is the impact of a pathogenic mutation on the intrinsic properties (e.g., stability in the face of stress, and flexibility) of the chaperone molecule? and What is the effect of these mutations on the chaperoning and non-chaperoning functions (e.g., protection of other proteins from denaturation by stressors, dissolution of fibrillar protein deposits, assistance in the folding of a nascent polypeptide, interaction with cells of the innate immune system) of the chaperone? In order to find answers to these key questions, experimental models are necessary. In this review, we provide information on archaeal organisms and on some exceptional bacteria that carry Groups I and II (or Group II-like) chaperonin genes, which have potential as experimental models to study human chaperonopathies.

SCOPE AND OBJECTIVE

This review encompasses the emerging field that comprises the use of archaeal organisms and some recently identified bacteria with archaeal-like chaperonins for studying issues directly relevant to human Medicine. The focus is on Group II chaperonins and associated genetic chaperonopathies. The main objective is to present this novel area of research to the scientific community so interest in these serious diseases might be ignited and projections into other similar disorders might be perceived. It is hoped that innovative research on these and many other conditions with comparable etiopathogenic characteristics, involving abnormal chaperones, will be initiated applying the prokaryotic models discussed.

CHAPERONE GENES AND ASSOCIATED CHAPERONOPATHIES

Diseases caused by mutations in molecular chaperone genes, the genetic chaperonopathies, are being diagnosed with increasing frequency and numerous examples representing the main chaperone families have been reported. For instance, concerning the chaperonins, among the latest reports of mutations associated with disease one pertains to HSPE1 (Bie et al., 2016) and another to the *cct2* gene (Minegishi et al., 2016). It may be assumed that many more cases of this kind of diseases will be found when the medical community becomes aware of the existence and high prevalence of chaperonopathies, genetic and acquired. To gain perspective on the potential scope of chaperonopathies one may recall the number of chaperone genes that have so far been identified in the human genome: at least 17 for Hsp70 (Brocchieri et al., 2008); 14 for CCT, and one for Hsp60 (HSPD1, Cpn 60) (Mukherjee et al., 2010; Bross and Fernandez-Guerra, 2016); 10 for the sHsp with the alpha-crystallin domain, one for Hsp10 (HSPE1, Cpn10), five for Hsp90, and nearly 50 for Hsp40/DnaJ (Kappé et al., 2003, 2010; Kampinga et al., 2009; Macario et al., 2013; Bross and Fernandez-Guerra, 2016). Furthermore, one has to include the many molecules such as co-chaperones and chaperone cofactors and closest interactors-receptors that, in addition to the chaperones themselves, integrate the chaperoning system. Thus, it is certain that there are many more diseases or syndromes associated with mutations or post-translational modifications of chaperones and closely associated molecules than those that have been identified to date.

In this article, we will focus on the chaperonins of Group II, namely the CCT chaperonins, since there are reports on diseases caused by mutations of human *cct* genes. Fourteen *cct* genes, including canonical and non-canonical family members, have been identified in the human genome (**Table 1**; Mukherjee et al., 2010), and mutations in several of them have been found to cause heritable disease (**Table 2**).

The clinical features and mode of inheritance of genetic chaperonopathies, including those caused by mutations of chaperonin genes, are in general well characterized (see for instance Bouhouche et al., 2006a; Bross and Fernandez-Guerra, 2016). However, the molecular mechanisms causing the cellular, tissue, and organ lesions observed in patients are still poorly understood. Likewise, the impact of these pathogenic mutations on the intrinsic properties and chaperoning functions of the chaperonin molecules has not yet been characterized *in vivo* or *in vitro* to a satisfactory extent. More research and especially, more experimental models are necessary to boost progress in this area of Medicine pertaining to chaperonopathies. In this regard, prokaryotes offer interesting possibilities. All bacteria possess chaperonins of Group I and some species also have chaperonins more closely related to Group II (Techtmann and Robb, 2010). All archaea have Group II chaperonins and some also possess chaperonins of Group I (**Table 3**; Deppenmeier et al., 2002; Galagan et al., 2002; Conway de Macario et al., 2003; Laksanalamai et al., 2004; Maeder et al., 2005; Large and Lund, 2009). In archaea, the chaperonins of Group II are present in various modes: some have only one gene/subunit while others have two, three, four, or five genes/subunits (**Figure 1**). As indicated in the figure, in all cases studied so far the archaeal Group II subunits associate to form hexadecamers made of two stacked octameric rings just like the human CCT subunits do.

BACTERIA WITH GROUP II-LIKE (GROUP III) CHAPERONINS

Many species of Bacteria have multiple Hsp60 (Cpn60) chaperonin genes. This is especially notable in the Agrobacterium group, in the Firmicutes, and in the Alphaproteobacteria (Lund, 2009). In these bacteria, the multiple GroEL/ES homologs presumably carry out complementary protein-folding and -quality control activities and in some cases for which genetic systems are available, the essential and nonessential copies of the Cpn60 gene could be identified (Lund, 2001). In addition, the two Cpn60 homologs of *Mycobacterium tuberculosis* can act as cytokines with modulation of inflammatory responses (Qamra

TABLE 1 | The human *hsp60-cct* gene extended family[a].

Name	Alternative names	St[b]	Chr	Ex	Is	aa
CCT1	TCP1, CCTa, CCTα, TCP-1α	−	6q25.3	12, 7	2	556, 401
CCT2	CCTβ, TCP-1β	+	12q15	14	1	535
CCT3	CCTγ, TCP-1γ	−	1q23.1	13, 13, 12	3	545, 544, 507
CCT4	CCTδ, TCPD, TCP-1δ	−	2p15	13	1	539
CCT5	CCTε, TCP1E, TCP-1ε	+	5p15.2	11	1	541
CCT6A	CCTζ, CCTζ1, TCP-1ζ, CCT6, Cctz, HTR3, TCP20, TCPZ, TTCP20	+	7p11.2	14, 13	2	531, 486
CCT6B	CCTζ-2, TCP-1ζ-2, Cctz2, TSA303, Tcp20	−	17q12	14	1	530
CCT7	CCTη, TCP-1η, Ccth, NIP7-1	+	2p13.2	12, 7	2	543, 339
CCT8	CCTθ, TCP-1θ, Cctq	−	21q21.3	15	1	548
CCT8L1	LOC155100	+	7q36.1	1	1	557
CCT8L2	GROL, CESK1	−	22q11.1	1	1	557
MKKS	BBS6	−	20p12.2	4, 4	2	570, 570
BBS10	C12orf58, FLJ23560	−	12q21.2	2	1	723
BBS12	C4orf24, FLJ35630, FLJ41559	+	4q27	1	1	710
HSPD1	GROEL, HSP60, Hsp60, SPG13, CPN60, Cpn60, HuCHA60	−	2q33.1	11, 11	2	573, 573
PIKFYVE	CFD, FAB1, PIP5K, PIP5K3	+	2q34	5	1	224

[a]*Source: Mukherjee et al., 2010.*

[b]*St, DNA strand with positive or negative signs indicating sequenced or complementary strand respectively; Chr, chromosome location; Ex, number of exons; Is, number of isoforms or mRNA variants, in which multiple numbers indicate the number of exons in each isoform; aa, total number of amino acids encoded in the gene; PIKFYVE, Fab1_TCP sequence domain of the PIKFYVE kinase, most similar to the apical domain of CCT3, in which features refer to the domain portion of the gene/protein.*

TABLE 2 | Diseases associated with mutations in genes encoding chaperonins and in genes phylogenetically related to the CCT family[a].

GENE/Name/HGNC/Gene ID/UniProtKB/Swiss-Prot/Accession number	Chaperonopathies. Mutations
CCT2/1615/10576/P78371/NM_006431	OMIM: 605139. Leber congenital amaurosis (LCA): hereditary, early-onset congenital retinopathy with macular degeneration. Mutations T400P and R516H. See Minegishi et al., 2016.
CCT4/1617/10575/P50991/NM_006430	OMIM: *605142. Distal hereditary sensory neuropathy (mutilated foot) in rat. Mutation C450Y.
CCT5/1618/22948/P48643/NM_012073.3	OMIM: *610150; #256840. Distal hereditary sensory-motor neuropathy. Mutation H147R. See description in this article.
MKKS/7108/8195/Q9NPJ1/NM_018848.2 & NM_170784.1	OMIM: 04896 gene; 209900 phenotype; 236700 phenotype; BBS6 605231; McKusick-Kaufman syndrome; MKKS hydrometrocolpos syndrome; hydrometrocolpos, postaxial polydactyly, and congenital heart malformation; HMCS Kaufman-Mckusick syndrome. Y37C (604896.0003), T57A (604896.0010), and C499S (604896.0013): increased MKKS degradation and reduced solubility relative to wildtype MKKS, and the mutant H84Y (604896.0001). R155L, A242S, and G345E mutations: increased MKKS degradation only.
BBS10/26291/79738/Q8TAM1/NM_024685.3	OMIM: 610148 gene; 209900 phenotype; BBS10 615987; Bardet-Biedl syndrome 10; ciliopathy with obesity, retinitis pigmentosa, polydactyly, hypogonadism, and renal failure. 209900) a 1-bp insertion at residue 91 leading to premature termination 4 codons later (C91fsX95). V11G; R34P; S303FS; S311A.
BBS12/26648/166379/Q6ZW61/NM_152618.2	OMIM: 610683 Phenotypes OMIN: BBS12 615989 Bardet-Biedl syndrome 12. A289P; R355T; 3-BP DEL, 335TAG; 2-BP DEL, 1114TT; 2-BP DEL, 1483GA; F372fsX373.
HSPD1/5261/3329/P10809/NM_199440.1 & NP_955472.1	OMIM: 605280 Spastic Paraplegia 13, autosomal dominant; SPG13, V98I; Q461E. See Bross and Fernandez-Guerra, 2016.
	OMIM: 612233 Leukodystrophy, Hypomyelinating, 4; HLD4; Mitochondrial HSP60 Chaperonopathy; MitCHAP60 Disease. Mutation D29G. See Bross and Fernandez-Guerra, 2016.
HSPE1/5269/3336/61604.2/NM_002157.2 & NP_002148.1	OMIM: *600141 Neurological and developmental disorder characterized by infantile spasms. Mutation L73F. See Bie et al., 2016.

[a]*Source: Macario and Conway de Macario, 2005; Mukherjee et al., 2010; Macario et al., 2013; Minegishi et al., 2016. Clinical and pathological features are described in the references cited and in the URLs shown.*

TABLE 3 | Examples of archaea with both, Group I and II chaperonin genes[a].

Organism	Chaperonin genes of Group:	
	I	II (subunits)
Methanococcus vannielii SB	1	1
Methanospirillum hungatei JF-1	1	2
Methanosarcina barkeri str. Fusaro	1	3
Methanosarcina mazei Go1	1	3
Methanosarcina acetivorans C2A	1	5

[a] *Source: Deppenmeier et al., 2002; Galagan et al., 2002; Conway de Macario et al., 2003; Maeder et al., 2005; Large and Lund, 2009.*

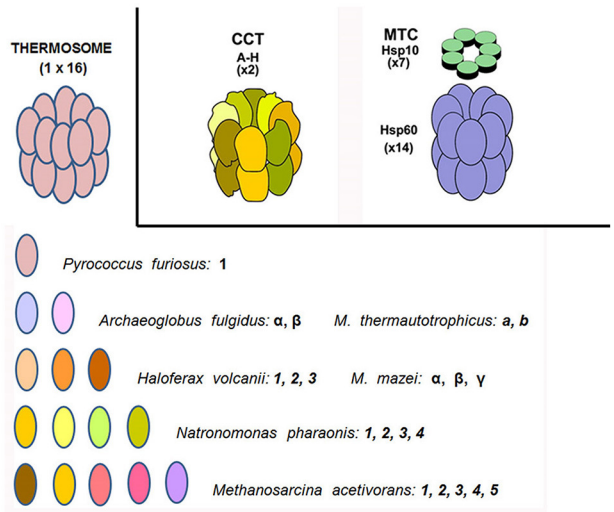

FIGURE 1 | Chaperonins of Group I and II in archaea and humans. Top left: archaeal CCT-complex equivalent, or thermosome; top center the CCT chaperonin of Group II complex typically resident of the eukaryotic-cell cytosol; and top right the chaperonin of Group I (Hsp60 or Cpn60) complex (with Hsp10 on top) characteristic of bacteria and eukaryotic-cell mitochondria (the former two are hexadecamers while the latter is a tetradecamer). Archaeal species vary in their content of chaperonin genes-proteins from only one through a maximum (at least from what we know at the present time) of five. These subunits are variously designated with Arabic numbers, English letters, or Greek letters. As far as we know, they all form a hexadecameric megadalton sized complex, the thermosome, of the type shown on top to the left, which is an example of a hexadecamer found in archaea encoding only one chaperonin subunit, e.g., *P. furiosus*. The composition of hexadecamers in all archaea that have two or more subunits is not yet fully elucidated. *M. thermautotrophicus*, *Methanothermobacter thermautotrophicus* ΔH, previously known as *Methanobacterium thermoautotrophicum* ΔH. *M. mazei*, *Methanosarcina mazei*. Source: Macario et al., 1999, 2004; Conway de Macario et al., 2003; Maeder et al., 2005; Large and Lund, 2009.

et al., 2005; Henderson et al., 2006, 2010). Given the predilection of *M. tuberculosis* for establishing cryptic infections, suppression of the inflammation response may be an important aspect of its molecular repertoire as a pathogen.

In a group of Bacteria with taxonomic common ground, an archaeal-type chaperonin occurs in addition to the canonical GroEL/ES operons. In these organisms, with one exception, the Group II-like proteins, tentatively named Group III chaperonins (**Figure 2**) are coded by genes that are embedded in the DnaK(Hsp70)/DnaJ(Hsp40) operon, which encodes the Hsp70, and DnaJ(Hsp40) homologs and the nucleotide exchange factor GrpE.

Prefoldin (or Gim C), a holdase chaperone complex found in the archaeal and eukaryal sequenced genomes, interacts directly with the charged residues located in the apical domain in Group II chaperonins (Vainberg et al., 1998; Sahlan et al., 2010; Zako et al., 2016). This is a favored mode of client protein delivery to the Group II chaperonin complex for refolding. The absence of Prefoldin in bacterial genomes may imply that another chaperone is partnering with the Group III chaperonin. It is tempting to speculate that DnaK(Hsp70), which is encoded in the same operon as most chaperonin III genes, and thus likely to be coregulated, is functioning as a direct delivery mechanism, a situation observed with eukaryotic homologs. Alternatively, the Group III chaperonins may be able to function efficiently without the assistance of a co-chaperone (Cuéllar et al., 2008). The working relationship, if any, between the chaperonins of Group I and Group III in bacteria that have both, in protein homeostasis is not characterized yet. The Group III chaperonins have been shown to provide robust resistance to lethal heat shock exposures in *Escherichia coli* when expressed as a single recombinant protein (Techtmann and Robb, 2010).

The crystal structure of the prototype Group III chaperonin from *Carboxydothermus hydrogenoformans* has recently been determined (An et al., 2016), and shows distinct structural differences, which probably reveal functional differences, between the Group II and Group III chaperonins (**Figure 3**). Based on both the phylogenetic and functional differences in the lid domain and the nucleotide-binding cavity (**Figure 4**), we have proposed that this class be called the Group III Cpn60 clade (Rowland, 2016). The apical domain of the Group III chaperonin was also shown to be divergent from Group II chaperonins (Techtmann and Robb, 2010). The Group III chaperonins may be thought to represent a remnant of the common ancestor of the Group I and Group II chaperonins (Techtmann and Robb, 2010). Alternatively, the genes may have diverged from an early lateral gene transfer of a Group II chaperonin from Archaea to Bacteria. In either event, the allosteric mechanism of the Group III chaperonins is similar to the Group II with the exceptions of divergence in the apical domain and the lack of a nucleotide sensing loop.

For the purposes of testing or mimicking the biochemical effects of pathological mutations affecting, for instance, human CCT genes, the Group III chaperonins may have unique advantages. These include the ability of the prototype to complement overtaxed stress responses of bacteria such as *E. coli*, as it is expressed in soluble form and at high levels in Bacteria (Techtmann and Robb, 2010). The crystal structure that has been produced from this prototype also provides a scaffold to determine the relative structural similarity to the regions of the CCT homologs affected by pathogenic mutations (An et al., 2016).

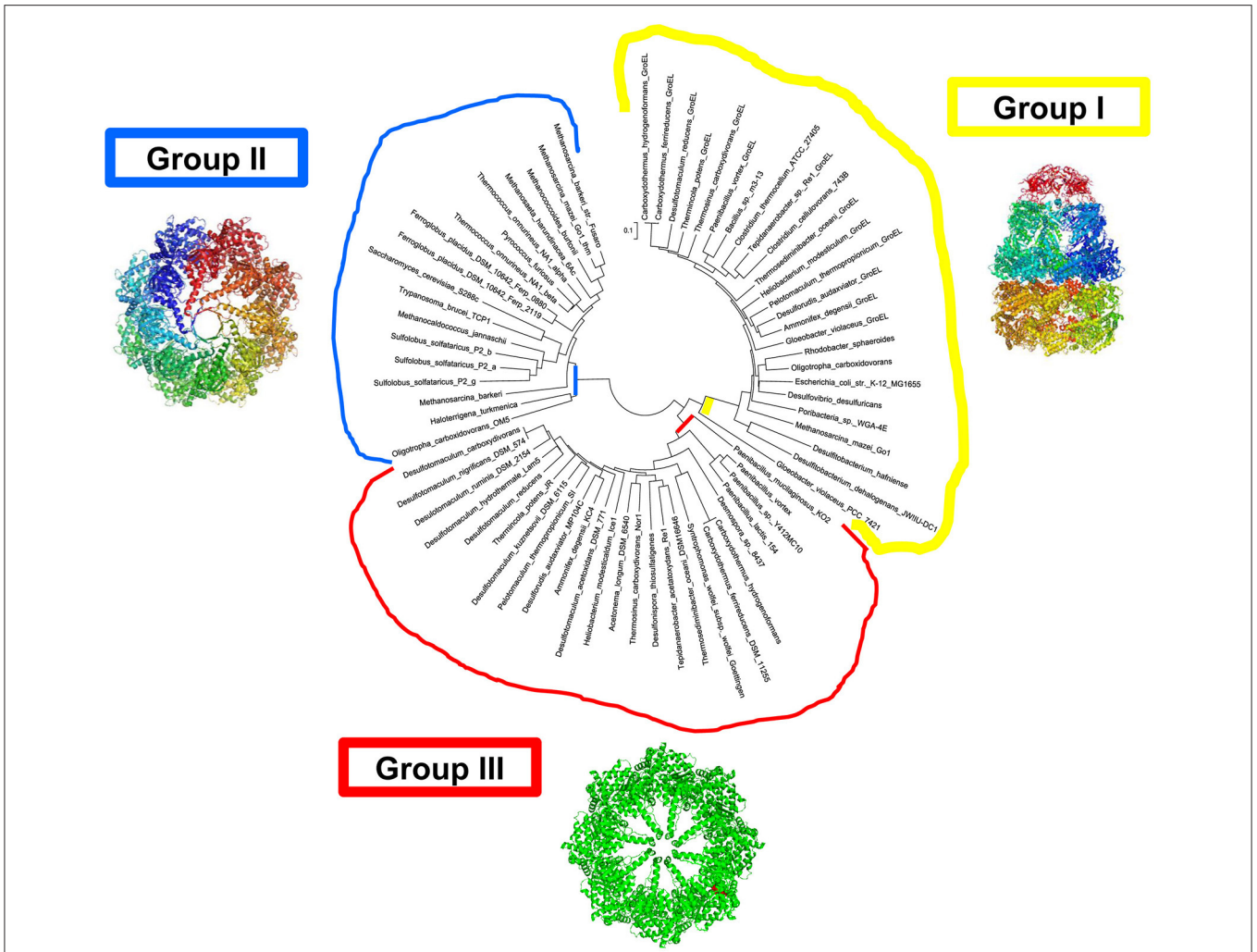

FIGURE 2 | Bacteria with chaperonins close to Group II (tentatively designated Group III). Molecular phylogenetic analysis by Maximum Likelihood methods. Groups I, II, and III, are in yellow, blue, and red, respectively. The evolutionary history was inferred by using the Maximum Likelihood method based on the JTT matrix-based model (Jones et al., 1992). A heuristic search was applied with Neighbor-Join and BioNJ algorithms to a matrix of pairwise distances estimated using a JTT model, and then selecting the topology with superior log likelihood value. The tree is drawn to scale, with branch lengths measured in the number of substitutions per site. The analysis involved 190 full-length chaperonin amino-acid sequences. All positions containing gaps and missing data were eliminated. There were a total of 370 positions in the final dataset. Evolutionary analyses were conducted in MEGA7. The intial alignment was constructed using ClustalW default settings.

CCT5 PATHOGENIC MUTATION

We have been working with archaeal stress proteins and chaperones for many years and are now using some archaea as experimental models to investigate molecular features of human chaperonopathies that are difficult to study directly, in human samples. Here, we will briefly discuss an archaeal experimental model that is providing interesting data pertaining to the impact of a pathogenic mutation on the properties of the chaperone molecule itself. The idea is that, by elucidating the molecular abnormalities caused by the mutation, the road will be opened to investigate the molecular mechanisms underlying the tissue lesions observed in the patients with chaperonopathies. Furthermore, biochemical and biophysical information insights that accrue from these studies will help in designing therapeutic strategies targeting the key steps of pathogenesis.

Along these lines, we are currently characterizing the molecular abnormalities involved in the causation of the pathological lesions observed in a human neuropathy associated with a mutation of the CCT5 subunit. This neuropathy was described in four members of a Moroccan family and was characterized as an autosomal recessive, mutilating, sensory neuropathy with spastic paraplegia (Bouhouche et al., 2006a,b). Onset occurred between 1 and 5 years of age and the clinical and pathological features were lower limb spasticity; hyperreflexia with clonus; positive Babinski; subtle distal amyotrophy with normal motor function; and distal sensory loss for all modalities in the upper and lower limbs, particularly in the feet.

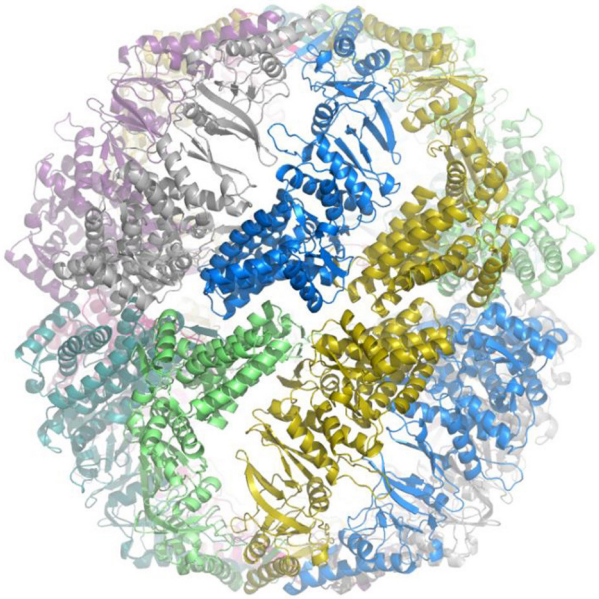

FIGURE 3 | Crystal structure of prototype of Group III chaperonin. Crystal structure of the prototype Group III chaperonin closed complex (hexadecamer) from *Carboxydothermus hydrogenoformans*. The view is along the equatorial plane and the individual, identical subunits are coded in different colors for contrast to visualize the intersubunit contacts. The structure reveals that the inter-ring contacts are formed by one-to-one associations between the subunits in the equatorial plane and that the configuration of the apical domain ("built-in lid") differs from the lid region of Group II chaperonin complexes. The method and preliminary structure have been described (An et al., 2016).

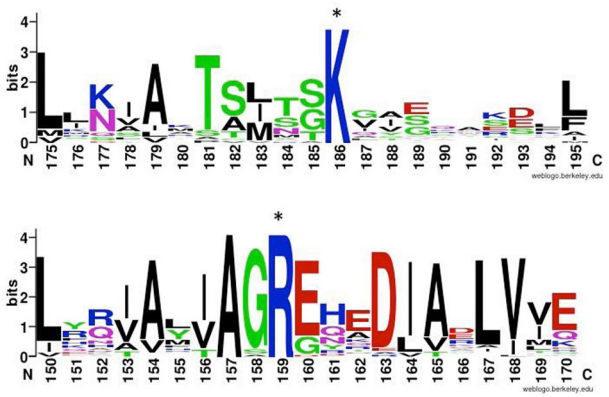

FIGURE 4 | ATP-binding sites of chaperonins of Group II and III. Comparison of highly conserved putative ATP gamma-phosphate interacting residue (denoted by asterisks) in group II (top) and group III (bottom) chaperonins. Top: Logo created using WebLogo (Schneider and Stephens, 1990; Crooks et al., 2004) and ClustalW amino-acid sequences alignment of 26 Group II chaperonins including representatives from all eight eukaryotic subunits and archaeal sequences. Bottom: Group III chaperonins alignment of 79 sequences pulled from NCBI database by BLAST against Ch cpn amino acid sequence (Altschul et al., 1990).

Deformities of the hands and feet were recorded in two patients, and most had deep perforating ulcers of the extremities. Progression of spasticity was slow but the sensory neuropathy

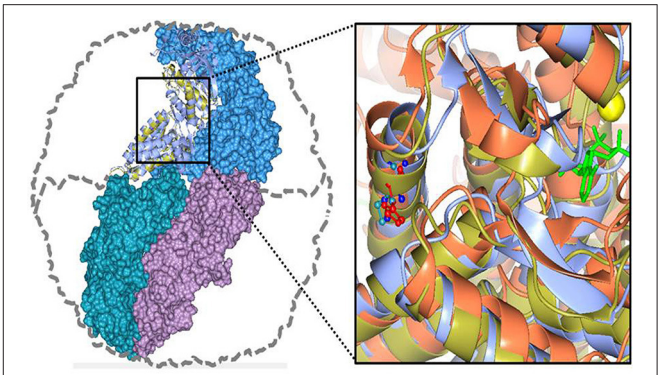

FIGURE 5 | Human CCT5 and *P. furiosus* Pf-Cpn (Pf-CD1) superposed onto the crystal structure of *Thermococcus* strain KS-1 subunit α (1Q3Q). Left. The Pf-CD1 graphic representation (gold ribbon) was obtained in Swiss-Model (http://swissmodel.expasy.org/) and superposed onto the crystal structure of KS-1 subunit α (monomers are displayed in marine blue, violet, and deep teal colors as surface, and in cyan color as ribbon). The whole hexadecamer double-ring structure is depicted by a dotted line. Right. Magnified image of the superposed structures of the Pf-CD1 (gold ribbon) and Human CCT5 (orange ribbon) onto the KS-1 α subunit crystal structure (1Q3Q; cyan ribbon). Side chains of isoleucine at 138 of Pf-CD1 (blue), isoleucine at 138 of KS-1 subunit α (deep teal), and histidine at 147 of human CCT5 (red) are represented as ball and stick. AMP-PNP (β,γ-Imidoadenosine 5′-triphosphate lithium salt hydrate; green stick) and magnesium ion (yellow ball). Source: Min et al., 2014.

was rapidly progressive and severe. Magnetic resonance imaging (MRI) of two patients showed severe atrophy of the spinal cord.

AN ARCHAEAL EXPERIMENTAL MODEL

Archaea have not been used as models to specifically study molecular aspects of human chaperonopathies until very recently (Min et al., 2014). However, studies on the structure and properties of the thermosome, the archaeal equivalent of the human CCT, have been going on for nearly 30 years. These studies of the thermosome have provided fundamental information useful also to understand the structure and mechanism of function of the eukaryotic counterpart. Here we will first present a few illustrative examples of structural studies of the thermosome and then, we will discuss the archaeal model we utilized to investigate molecular aspects of the chaperonopathy mentioned earlier, which is associated with mutations in the CCT5 submit.

THE STRUCTURE OF THE ARCHAEAL THERMOSOME

The archaeal thermosome has been the focus of study for elucidating the structure of the multisubunit chaperoning machine for many years and it continues to be a source of valuable information applicable to the human CCT complex (Waldmann et al., 1995; Ditzel et al., 1998; Bosch et al., 2000; Pereira et al., 2010, 2012; Zhang et al., 2010; Lund, 2011; Skjærven

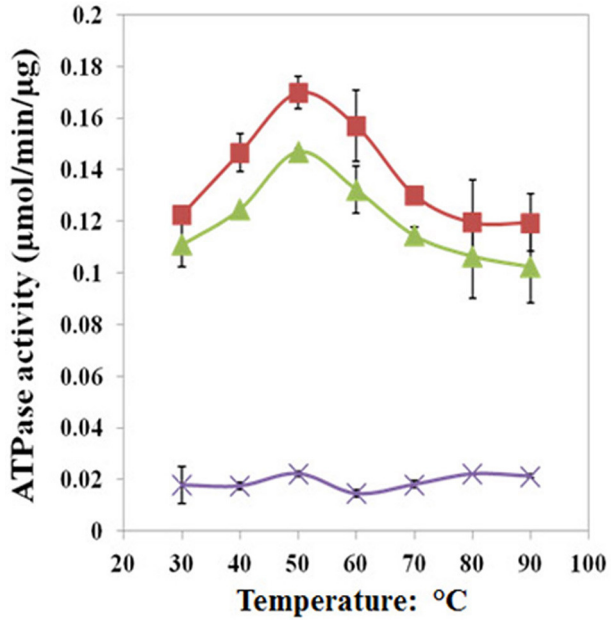

FIGURE 6 | The pathogenic mutant causes a loss of ATPase activity evidenced at various temperatures. Pf-CD1 (red squares), Pf-H (green triangles), and Pf-R (purple stars). The results shown are mean values (± standard deviations) and the experiments were carried out in triplicate. Source: Min et al., 2014.

et al., 2015). For example, data supporting the notion that the archaeal thermosome is the equivalent of the eukaryotic cytosolic chaperonin CCT, also named TRiC (t-complex polypeptide 1 ring complex), were obtained over two decades ago by studying the archaeon *Thermoplasma acidophilum* (Waldmann et al., 1995). This pioneering work provided impetus to subsequent investigations using the same organism to elucidate the functions and structure of the chaperonin complex. Two thermosome subunits are encoded in the *T. acidophilus*' genome (Ruepp et al., 2000, 2001; Large and Lund, 2009) termed a and b, or alpha and beta. A crystal structure revealed that the *T. acidophilus* thermosome is composed of two stacked octameric rings composed of alternating a (alpha) and b (beta) subunits, with the two rings being related by 2-fold symmetry, which generates a-a (alpha-alpha) and b-b (beta-beta) pairs and brings about an (ab)4(ab)4 arrangement with a 42-point symmetry (Ditzel et al., 1998). The domains in the monomers follow a topology similar to that of the GroEL monomer. The combined analysis of the crystal structure and of multiple alignments of extended primary sequences of various chaperonins helped to identify in the linear sequence the now well-known three domains, as follows, from the N to the C terminus: the N-terminal segment of the equatorial domain, the N-terminal portion of the apical domain, the intermediate domain, the C-terminal segment of the apical domain, and the C-terminal segment of the equatorial domain. This was a seminal contribution useful to many researchers since it was reported. The way rings make contact is different in the archaeal thermosome as compared with the GroEL complex. Most importantly, it was observed that the apical domains extend to build a sort of lid that can close the entrance to the central cavity, playing a similar role to that of GroES in the bacterial chaperonin complex. The central cavity was found to have a polar surface which suggested its implication in the process of substrate folding.

In subsequent work, the crystal structure of the beta-apical domain was determined at 2.8 Ångström resolution (Bosch et al., 2000). A comparative analysis with previously determined apical domain structures revealed in the *T. acidophilum* a segmental displacement of the protruding part of helix H10 via the hinge GluB276-ValB278. Furthermore, the portion of the molecule including the amino acids GluB245-ThrB253 was found to be in an extended beta-like conformation in contrast to the alpha-helix characteristic of the alpha-apical domain. These conformational features prompted the suggestion that apical domain projections could be the basis to provide a variety of context-dependent conformations during an open, substrate-accepting state during the ATP-dependent chaperoning cycle.

Other structural studies with the archaeal thermosome were carried out using *Methanococcus maripaludis* (Pereira et al., 2010, 2012). The genome of *M. maripaludis* encodes only one thermosome subunit (Hendrickson et al., 2004; Large and Lund, 2009). The crystal structures of both, the open (substrate acceptor) and closed (substrate folding) states were obtained (Pereira et al., 2010). It was observed that the *M. maripaludis* thermosome subunit remains rigid during the reorientation accompanying the cycling of the complex. This is in sharp contrast with what occurs with GroEL, in which the greatest motion occurs at the intermediate and apical domains while the equatorial domain conserves a similar conformation in the open and closed states. Interestingly, the rotation occurring from the open to the closed state decreases by 65% the volume of the folding chamber whose surface becomes highly hydrophilic.

In a subsequent study with *M. maripaludis*, the mechanism responsible for communicating the local changes in the ATP-binding site between subunits during the chaperoning cycle were investigated (Pereira et al., 2012). The data obtained provided fundamental information on the movements of the thermosome components as they are engaged in the various states of the chaperoning cycle. The crystal structures of several ATP-bound states were determined and it was observed that the amino acid Lys161, known to be much conserved among Group II chaperonins, interacts with the γ-phosphate of ATP and reorients in the presence of ADP. It was found that the loss of the interaction ATP- γ-phosphate in the ADP state is accompanied by considerably rearrangement of the loop including amino acids 160–169. It was proposed that Lys161 functions as an ATP sensor and the loop is a nucleotide-sensing device whose function would be to monitor the presence of γ-phosphate. Loop mutants had considerably lower ATPase activity than the wild type molecule, which suggested that the nucleotide-sensing loop plays a critical role in synchronizing the folding cycle.

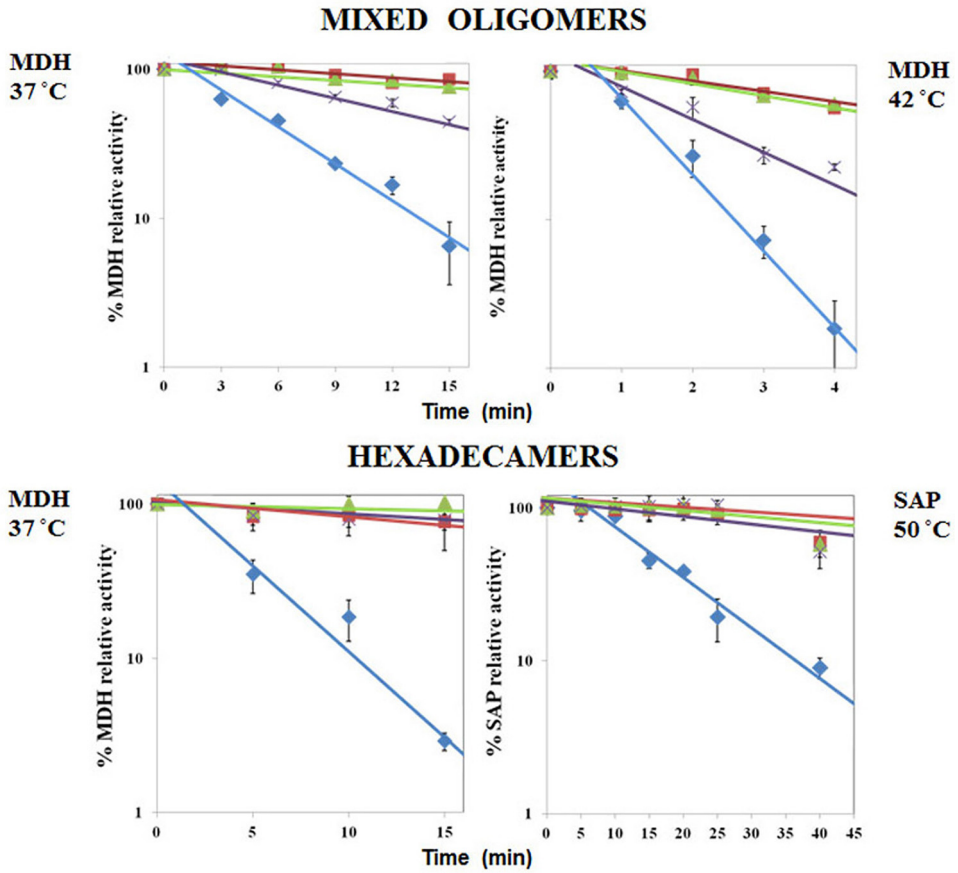

FIGURE 7 | Comparative analyses of protective capacity of mutant and wild type chaperonins. Protection from heat denaturation of malate dehydrogenase (MDH) by mixed oligomers of Pf-CD1 (red square), Pf-H (green triangle), and Pf-R (purple star) at 37°C (top left panel) and 42°C (top right panel); and protection of MDH at 37°C (bottom left panel) and shrimp alkaline phosphatase (SAP) at 50°C (bottom right panel) by pure hexadecamers. Negative control (no chaperonin added), i.e., MDH, or SAP in bottom right panel, alone: blue diamond. The results shown are mean values (±SD) of triplicate experiments. The loss of enzymatic activity caused by heat was impeded or considerably attenuated by the wild type and Pf-H molecules. In contrast, Pf-R did not have this protective effect, except when purified hexadecamers were used. Source: Min et al., 2014.

TABLE 4 | Summary of results showing the functional performance of the pathogenic mutant Pf-R in comparison with non-pathogenic counterparts[a].

Gene	*E. coli* exp.	Mixed oligomers				Hexadecamers			
		Heat res.	ATPase	Disperse fibrils	Form hexa-decamers	Protection			
						MDH		MDH	SAP
						37°C	42°C	37°C	50°C
Pf-CD1	100	100	100	100	100	100	100	100	100
Pf-H	100	100	100 or less	100 or less	100 or less	100	100	100	100
Pf-R	100	100	Low	Low	Low	Low	Low	100	100

[a]*Source: Min et al., 2014.*

exp, expression; res, resistance; 100, optimal; MDH, malate dehydrogenase; SAP, shrimp alkaline phosphatase.

THE THERMOSOME OF *PYROCOCCUS FURIOSUS*

We standardized an experimental model using the chaperonin molecule from the archaeon *Pyrococcus furiosus*. This organism has only one CCT ortholog (Robb et al., 2001) that forms an hexadecameric chaperoning machine, the thermosome, with the same overall structure as the human CCT complex, except that all 16 subunits are identical (**Figure 1**). Therefore, simulating a human CCT mutation on the *P. furiosus* chaperonin (Pf-Cpn)

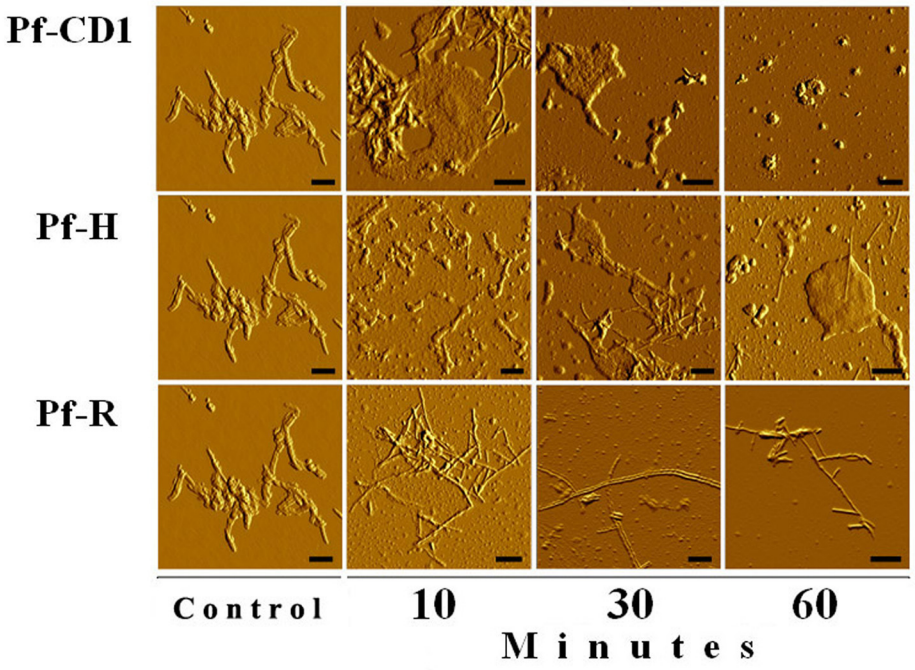

FIGURE 8 | The pathogenic mutant fails to disperse amyloid fibrils. Dispersion of amyloid fibrils by archaeal Pf-CD1 (top row of panels), partial dispersion by Pf-H (middle row of panels), and no dispersion by Pf-R (bottom row of panels). Atomic Force Microscopy (AFM) of bovine insulin amyloid fibrils treated with Cpn and Mg++, and ATP. Control panels, no added chaperonin. Scale bar: 250 nm. Source: Min et al., 2014.

subunit would amplify the impact of the human mutation 8-fold per octameric ring, and facilitate detection of subtle functional deficiencies caused by the mutation. Mutations causing major functional deficits in human CCT are most likely lethal because the chaperonin is essential for life; one can safely assume that no phenotypes will be found associated with mutations causing major, easily detectable functional failure of the chaperonin molecule *in vitro*, or *in vivo*. Therefore, this strategy for characterizing slight deficits in function may provide valuable insights into pathogenic mechanisms. It has to be borne in mind that if the mutation in one subunit of a hetero-oligomer such as the human CCT affects primarily the interaction of the non-identical subunits with each other, the use of an homo-oligomeric model like that of *P. furiosus* may not fully report on the impact of the mutation. This consideration must be taken into account in interpreting experimental results with the two types of oligomers.

We first established which amino acid position in the Pf-Cpn matches that in the human CCT5 in which the mutation is found, i.e., 147. In the wild type CCT5 the amino acid His is at this position but in the pathogenic mutant His is replaced by Arg. We found by a series of alignments and 3D modeling studies that position 138 in Pf-Cpn is equivalent to the 147 position in human CCT5 and it is occupied by Ile (**Figure 5**; information on the primary and secondary structures is available in Min et al., 2014). To examine the impact of the mutations we used Pf-CD1, which is the recombinant molecule Pf-Cpn lacking the last 22 amino acids that are involved in extreme heat resistance and have no match in the human CCTs. We introduced the pathogenic mutation Ile138Arg in Pf-CD1 to produce Pf-R, and then proceeded to test the mutant in comparison with the wild type to assess its properties and chaperoning capacity. We also made and used for comparison another mutant, not known to be pathogenic, Ile138His of Pf-CD1 (Pf-H).

We found that Pf-R had very low ATPase activity by comparison with Pf-CD1 and Pf-H (**Figure 6**). Likewise, mixed oligomers of Pf-R were deficient in protecting test enzymes from heat denaturation (**Figure 7**), and were incapable of dispersing amyloid fibrils in contrast to Pf-CD1 and Pf-H (**Figure 8**). Remarkably, purified hexadecamers from the three molecules had similar enzyme protection capability; namely, hexadecamers formed by Pf-R had a chaperoning ability comparable to that of Pf-CD1 and Pf-H (**Figure 7**). The summary of results obtained with assays aimed at measuring the chaperoning capacity of the mutant Pf-R are displayed in **Table 4**. In conclusion, the Arg mutation affects the formation and stability of functional hexadecamers. Indeed, in native PAGE, Pf-R appears predominantly as oligomers smaller than hexadecamers and as monomers in contrast to Pf-CD1 and Pf-H (Min et al., 2014).

It is possible that some part of the effects observed using Pf-R by comparison with PF-CD1 were magnified somewhat because in the archaeal mutant the wild type amino acid, Ile, is hydrophobic and the mutant amino acid, Arg, is charged, whereas in the human situation the two amino acids, wild type and mutant, are charged, i.e., they are similar in this regard. For this reason, we generated and characterized the Pf-H mutant as control for any change that this charged residue might bring to the stability of the complex, which turned out to be minimal (Min et al., 2014).

We could not yet test isolated monomers because they tend to oligomerize rapidly in solution. However, *in silico* analysis by molecular dynamics simulations revealed that Pf-R monomers are rigid at the physiological temperature whereas those of Pf-CD1 are flexible; namely, the Ile138Arg mutation causes a loss of flexibility in the chaperonin molecule, which is also the result we obtained for the human mutant CCT5 (Min et al., 2014).

Experimentally, by applying quantitative calorimetry, current experiments are showing that the Pf-R hexadecamers are less resistant to heat and dissociate faster and at lower temperatures as compared with Pf-CD1.

In conclusion, the use of the archaeal chaperonin provided information that reflects the anomalies of the human mutant CCT5, which has been studied *in vitro* (Sergeeva et al., 2014). In a pioneering study, the human CCT4, and CCT5 subunits have been shown to form homohexadecamer complexes after expression of the subunits in *E. coli* (Sergeeva et al., 2013). The chaperoning ability of wild type CCT4 and CCT5 was tested in comparison with CCT4 C450Y and CCT5 H147R mutants. The functional tests included the suppression of aggregation of γD-crystallin and mutant huntingtin, and the refolding of beta-actin. In all tests the mutant subunits formed complexes with slightly deficient folding activities compare to the wild-type counterpart, although these effects were minimal in the case of CCT5 H147R. Both of the mutants produced were able to form complexes, although CCT4 C450Y showed limited stability and formed fewer megadalton-size complexes than CCT5 H147R. This study reinforces our conclusion that the biochemical effects of human mutations affecting the CCT5 complex, yet permitting viability, must of necessity be slight, attesting to the central role that we believe this complex plays in human protein homeostasis and physiology.

PERSPECTIVES FOR THE FUTURE

In the particular case discussed above, future research ought to be directed to the development of agents, e.g., chemical compounds, with the ability to interact with the mutant chaperonin molecule and restore its proper, functional configuration and thus, boost its capacity to form stable hexadecamers. The screening of compounds and preclinical testing could utilize the same *P. furiosus* experimental model used to reveal the abnormal features of the mutant CCT5 molecule. The same approach would apply to chaperonopathies involving other mutations in CCT5 that might be discovered, or mutations in any other subunit. Likewise, the *P. furiosus* model, as well as any other based on the archaeal and bacterial organisms discussed here, could be standardized and applied to elucidate the abnormalities of pathogenic chaperone molecules due not only to mutations but also to post-translational modifications. For example, Group III chaperonins could be used for modeling defects in human chaperonins involving the nucleotide sensing domain which, as mentioned earlier, is divergent in the canonical and non-canonical orthologs.

AUTHOR CONTRIBUTIONS

ECdeM conceived the idea and outlined the project, participated in literature and databases searches, gathering and critical analysis of data, preparation of materials, and writing the manuscript. FTR participated in gathering of data and preparation of materials and writing the portions pertinent to chaperonins of Group III. AJLM participated in the outlining of the project and in literature and databases searches, gathering and critical analysis of data, preparation of materials, and writing the manuscript.

ACKNOWLEDGMENTS

AJLM and ECdeM were partially supported by the Institute of Marine and Environmental Technology (IMET, USA), and by the Euro-Mediterranean Institute of Science and Technology (IEMEST, Italy). FTR was supported by the US Air Force Office of Scientific Research (Grants AFOSR 03-S-28900 and 9550-10-1-0272. Part of this work was carried out at the Biomolecular Labeling Laboratory-National Institute of Standards and Technology, Rockville, USA. We thank Zvi Kelman for his hospitality and stimulating conversations during the sabbatical leave of FTR in his laboratory. We are also indebted and very grateful to Dr. Sara Rowland for discussion and assistance with the phylogenetic analysis of the Group III chaperonin. This is IMET contribution number IMET-16-185.

REFERENCES

Altschul, S. F., Gish, W., Miller, W., Myers, E. W., and Lipman, D. J. (1990). Basic local alignment search tool. *J. Mol. Biol.* 215, 403–410. doi: 10.1016/S0022-2836(05)80360-2

An, Y. J., Rowland, S. E., Robb, F. T., and Cha, S. S. (2016). Purification, crystallization and preliminary X-ray crystallographic analysis of Group III chaperonin from *Carboxydothermus hydrogenoformans*. *J. Microbiol.* 54, 440–444. doi: 10.1007/s12275-016-6089-5

Bie, A. S., Fernandez-Guerra, P., Birkler, R. I., Nisemblat, S., Pelnena, D., Lu, X., et al. (2016). Effects of a mutation in the HSPE1 gene encoding the mitochondrial co-chaperonin HSP10 and its potential association with a neurological and developmental disorder. *Front. Mol. Biosci.* 3:65. doi: 10.3389/fmolb.2016.00065

Bosch, G., Baumeister, W., and Essen, L. O. (2000). Crystal structure of the beta-apical domain of the thermosome reveals structural plasticity in the protrusion region. *J. Mol. Biol.* 301, 19–25. doi: 10.1006/jmbi.2000.3955

Bouhouche, A., Benomar, A., Bouslam, N., Chkili, T., and Yahyaoui, M. (2006a). Mutation in the epsilon subunit of the cytosolic chaperonin-containing t-complex peptide-1 (Cct5) gene causes autosomal recessive mutilating sensory neuropathy with spastic paraplegia. *J. Med. Genet.* 43, 441–443. doi: 10.1136/jmg.2005.039230

Bouhouche, A., Benomar, A., Bouslam, N., Ouazzani, R., Chkili, T., and Yahyaoui, M. (2006b). Autosomal recessive mutilating sensory neuropathy with spastic paraplegia maps to chromosome 5p15.31-14.1. *Eur. J. Hum. Genet.* 14, 249–252. doi: 10.1038/sj.ejhg.5201537

Brocchieri, L., Conway de Macario, E., and Macario, A. J. L. (2008). hsp70 genes in the human genome: conservation and differentiation patterns predict a wide array of overlapping and specialized functions. *BMC Evol. Biol.* 8:19. doi: 10.1186/1471-2148-8-19

Bross, P., and Fernandez-Guerra, P. (2016). Disease-associated mutations in the HSPD1 gene Encoding the large subunit of the mitochondrial HSP60/HSP10 chaperonin complex. *Front. Mol. Biosci.* 31:49. doi: 10.3389/fmolb.2016.00049

Conway de Macario, E., Maeder, D. L., and Macario, A. J. L. (2003). Breaking the mould: archaea with all four chaperoning systems. *Biochem. Biophys. Res. Commun.* 301, 811–812. doi: 10.1016/S0006-291X(03)00047-0

Crooks, G. E., Hon, G., Chandonia, J. M., and Brenner, S. E. (2004). WebLogo: a sequence logo generator. *Genome Res.* 14, 1188–1190. doi: 10.1101/gr.849004

Cuéllar, J., Martín-Benito, J., Scheres, S. H., Sousa, R., Moro, F., López-Vi-as, E., et al. (2008). The structure of CCT-Hsc70 NBD suggests a mechanism for Hsp70 delivery of substrates to the chaperonin. *Nat. Struct. Mol. Biol.* 15, 858–864. doi: 10.1038/nsmb.1464

Deppenmeier, U., Johann, A., Hartsch, T., Merkl, R., Schmitz, R. A., Martinez-Arias, R., et al. (2002). The genome of Methanosarcina mazei: evidence for lateral gene transfer between bacteria and archaea. *J. Mol. Microbiol. Biotechnol.* 4, 453–461.

Ditzel, L., Löwe, J., Stock, D., Stetter, K. O., Huber, H., Huber, R., et al. (1998). Crystal structure of the thermosome, the archaeal chaperonin and homolog of CCT. *Cell* 93, 125–138. doi: 10.1016/S0092-8674(00)81152-6

Galagan, J. E., Nusbaum, C., Roy, A., Endrizzi, M. G., Macdonald, P., FitzHugh, W., et al. (2002). The genome of M. acetivorans reveals extensive metabolic and physiological diversity. *Genome Res.* 12, 532–542. doi: 10.1101/gr.223902

Henderson, B., Allan, E., and Coates, A. R. (2006). Stress wars: the direct role of host and bacterial molecular chaperones in bacterial infection. *Infect. Immun.* 74, 3693–3706. doi: 10.1128/IAI.01882-05

Henderson, B., Lund, P. A., and Coates, A. R. (2010). Multiple moonlighting functions of mycobacterial molecular chaperones. *Tuberculosis (Edinb).* 90, 119–124. doi: 10.1016/j.tube.2010.01.004

Hendrickson, E. L., Kaul, R., Zhou, Y., Bovee, D., Chapman, P., Chung, J., et al. (2004). Complete genome sequence of the genetically tractable hydrogenotrophic methanogen *Methanococcus maripaludis*. *J. Bacteriol.* 186, 6956–6969. doi: 10.1128/JB.186.20.6956-6969.2004

Jones, D. T., Taylor, W. R., and Thornton, J. M. (1992).The rapid generation of mutation data matrices from protein sequences. *Comput. Appl. Biosci.* 8, 275–282. doi: 10.1093/bioinformatics/8.3.275

Kampinga, H. H., Hageman, J., Vos, M. J., Kubota, H., Tanguay, R. M., Bruford, E. A., et al. (2009). Guidelines for the nomenclature of the human heat shock proteins. *Cell Stress Chaperones.* 14, 105–111. doi: 10.1007/s12192-008-0068-7

Kappé, G., Boelens, W. C., and de Jong, W. W. (2010). Why proteins without an alpha-crystallin domain should not be included in the human small heat shock protein family HSPB. *Cell Stress Chaperones.* 15, 457–461. doi: 10.1007/s12192-009-0155-4

Kappé, G., Franck, E., Verschuure, P., Boelens, W. C., Leunissen, J. A., and de Jong, W. W. (2003). The human genome encodes 10 alpha-crystallin-related small heat shock proteins: HspB1-10. *Cell Stress Chaperones.* 8, 53–61. doi: 10.1379/1466-1268(2003)8<53:THGECS>2.0.CO;2

Laksanalamai, P., Whitehead, T. A., and Robb, F. T. (2004). Minimal protein-folding systems in hyperthermophilic archaea. *Nat. Rev. Microbiol.* 2, 315–324. doi: 10.1038/nrmicro866

Large, A. T., and Lund, P. A. (2009). Archaeal chaperonins. *Front. Biosci. (Landmark Ed).* 14, 1304–1324. doi: 10.2741/3310

Lund, P. A. (2001). Microbial molecular chaperones. *Adv. Microb. Physiol.* 44, 93–140. doi: 10.1016/S0065-2911(01)44012-4

Lund, P. A. (2009). Multiple chaperonins in bacteria–why so many? *FEMS Microbiol. Rev.* 33, 785–800. doi: 10.1111/j.1574-6976.2009.00178.x

Lund, P. A. (2011). Insights into chaperonin function from studies on archaeal thermosomes. *Biochem. Soc. Trans.* 39, 94–98. doi: 10.1042/BST0390094

Macario, A. J. L., and Conway de Macario, E. (2005). Sick chaperones, cellular stress, and disease. *N. Engl. J. Med.* 353, 1489–1501. doi: 10.1056/NEJMra050111

Macario, A. J. L., Conway de Macario, E., and Cappello, F. (2013). *The Chaperonopathies Diseases with Defective Molecular Chaperones.* Heidelberg; New York, NY; London: Springer Dordrecht: Library of Congress Control Number: 2013931840.

Macario, A. J. L., Lange, M., Ahring, B. K., and Conway de Macario, E. (1999). Stress genes and proteins in the archaea. *Microbiol. Mol. Biol. Rev.* 63, 923–967.

Macario, A. J. L., Malz, M., and Conway de Macario, E. (2004). Evolution of assisted protein folding: the distribution of the main chaperoning systems within the phylogenetic domain archaea. *Front. Biosci.* 9:1318–1332. doi: 10.2741/1328

Maeder, D. L., Macario, A. J. L., and Conway de Macario, E. (2005). Novel chaperonins in a prokaryote. *J. Mol. Evol.* 60, 409–416. doi: 10.1007/s00239-004-0173-x

Min, W., Angileri, F., Luo, H., Lauria, A., Shanmugasundaram, M., Almerico, A. M., et al. (2014). A human CCT5 gene mutation causing distal neuropathy impairs hexadecamer assembly in an archaeal model. *Sci. Rep.* 4:6688. doi: 10.1038/srep06688

Minegishi, Y., Sheng, X., Yoshitake, K., Sergeev, Y., Iejima, D., Shibagaki, Y., et al. (2016). CCT2 mutations evoke leber congenital amaurosis due to chaperone complex instability. *Sci Rep.* 6:33742. doi: 10.1038/srep33742

Mukherjee, K., Conway de Macario, E., Macario, A. J. L., and Brocchieri, L. (2010). Chaperonin genes on the rise: new divergent classes and intense duplication in human and other vertebrate genomes. *BMC Evol. Biol.* 10:64. doi: 10.1186/1471-2148-10-64

Pereira, J. H., Ralston, C. Y., Douglas, N. R., Kumar, R., Lopez, T., McAndrew, R. P., et al. (2012). Mechanism of nucleotide sensing in group II chaperonins. *EMBO J.* 31, 731–740. doi: 10.1038/emboj.2011.468

Pereira, J. H., Ralston, C. Y., Douglas, N. R., Meyer, D., Knee, K. M., Goulet, D. R., et al. (2010). Crystal structures of a group II chaperonin reveal the open and closed states associated with the protein folding cycle. *J. Biol. Chem.* 285, 27958–27966. doi: 10.1074/jbc.M110.125344

Qamra, R., Mande, S. C., Coates, A. R., and Henderson, B. (2005). The unusual chaperonins of *Mycobacterium tuberculosis*. *Tuberculosis (Edinb).* 85, 385–594. doi: 10.1016/j.tube.2005.08.014

Robb, F. T., Maeder, D. L., Brown, J. R., DiRuggiero, J., Stump, M. D., Yeh, R. K., et al. (2001). Genomic sequence of hyperthermophile, *Pyrococcus furiosus*: implications for physiology and enzymology. *Methods Enzymol.* 330, 134–157. doi: 10.1016/S0076-6879(01)30372-5

Rowland, S. E. (2016). *Structure and Function of Group III Chaperonins*. Ph.D. Dissertation, University of Maryland, College Park.

Ruepp, A., Graml, W., Santos-Martinez, M. L., Koretke, K. K., Volker, C., Mewes, H. W., et al. (2000). The genome sequence of the thermoacidophilic scavenger *Thermoplasma acidophilum*. *Nature* 407, 508–513. doi: 10.1038/35035069

Ruepp, A., Rockel, B., Gutsche, I., Baumeister, W., and Lupas, A. N. (2001). The chaperones of the archaeon *Thermoplasma acidophilum*. *J. Struct. Biol.* 135, 126–138. doi: 10.1006/jsbi.2001.4402

Sahlan, M., Zako, T., Tai, P. T., Ohtaki, A., Noguchi, K., Maeda, M., et al. (2010). Thermodynamic characterization of the interaction between prefoldin and group II chaperonin. *J. Mol. Biol.* 399, 628–636. doi: 10.1016/j.jmb.2010.04.046

Schneider, T. D., and Stephens, R. M. (1990). Sequence logos: a new way to display consensus sequences. *Nuc. Acids Res.* 18, 6097–6100. doi: 10.1093/nar/18.20.6097

Sergeeva, O. A., Chen, B., Haase-Pettingell, C., Ludtke, S. J., Chiu, W., and King, J. A. (2013). Human CCT4 and CCT5 chaperonin subunits expressed in *Escherichia coli* form biologically active homo-oligomers. *J. Biol. Chem.* 288, 17734–17744. doi: 10.1074/jbc.M112.443929

Sergeeva, O. A., Tran, M. T., Haase-Pettingell, C., and King, J. A. (2014). Biochemical characterization of mutants in chaperonin proteins CCT4 and CCT5 associated with hereditary sensory neuropathy. *J. Biol. Chem.* 289, 27470–27480. doi: 10.1074/jbc.M114.576033

Skjærven, L., Cuellar, J., Martinez, A., and Valpuesta, J. M. (2015). Dynamics, flexibility, and allostery in molecular chaperonins. *FEBS Lett.* 589(19 Pt A), 2522–2532. doi: 10.1016/j.febslet.2015.06.019

Techtmann, S., and Robb, F. T. (2010). Archaeal-like chaperones in bacteria. *Proc. Natl. Acad. Sci. U.S.A.* 107, 20269–20274. doi: 10.1073/pnas.1004783107

Vainberg, I. E., Lewis, S. A., Rommelaere, H., Ampe, C., Vandekerckhove, J., Klein, H. L., et al. (1998). Prefoldin, a chaperone that delivers unfolded proteins to cytosolic chaperonin. *Cell* 93, 863–873. doi: 10.1016/S0092-8674(00)81446-4

Waldmann, T., Nimmesgern, E., Nitsch, M., Peters, J., Pfeifer, G., Müller, S., et al. (1995). The thermosome of *Thermoplasma acidophilum* and its relationship to the eukaryotic chaperonin TRiC. *Eur. J. Biochem.* 227, 848–856. doi: 10.1111/j.1432-1033.1995.tb20210.x

Zako, T., Sahlan, M., Fujii, S., Yamamoto, Y. Y., Tai, P. T., Sakai, K., et al. (2016). Contribution of the C-terminal region of a Group II chaperonin to its interaction with prefoldin and substrate transfer. *J. Mol. Biol.* 428, 2405–2417. doi: 10.1016/j.jmb.2016.04.006

Zhang, J., Baker, M. L., Schröder, G. F., Douglas, N. R., Reissmann, S., Jakana, J., et al. (2010). Mechanism of folding chamber closure in a group II chaperonin. *Nature* 463, 379–383. doi: 10.1038/nature08701

Conflict of Interest Statement: The authors declare that the research was conducted in the absence of any commercial or financial relationships that could be construed as a potential conflict of interest.

The reviewer LB and handling Editor declared their shared affiliation, and the handling Editor states that the process nevertheless met the standards of a fair and objective review.

The reviewer MMM and handling Editor declared their shared affiliation, and the handling Editor states that the process nevertheless met the standards of a fair and objective review.

frontiers in Molecular Biosciences

MINI REVIEW
published: 14 December 2016
doi: 10.3389/fmolb.2016.00081

Chaperonopathies: Spotlight on Hereditary Motor Neuropathies

Vincenzo Lupo[1,2], *Carmen Aguado*[1,2,3], *Erwin Knecht*[1,2,3] *and Carmen Espinós*[1,2]*

[1] *Molecular Basis of Human Diseases Program, Centro de Investigación Príncipe Felipe, Valencia, Spain,* [2] *INCLIVA & IIS La Fe Rare Diseases Joint Units, Valencia, Spain,* [3] *Centro de Investigación Biomédica en Red, Valencia, Spain*

Distal hereditary motor neuropathies (dHMN) are a group of rare hereditary neuromuscular disorders characterized by an atrophy that affects peroneal muscles in the absence of sensory symptoms. To date, 23 genes are thought to be responsible for dHMN, four of which encode chaperones: *DNAJB2*, which encodes a member of the HSP40/DNAJ co-chaperone family; and *HSPB1, HSPB3,* and *HSPB8*, encoding three members of the small heat shock protein family. While around 30 different mutations in *HSPB1* have been identified, the remaining three genes are altered in many fewer cases. Indeed, a mutation of *HSPB3* has only been described in one case, whereas a few cases have been reported carrying mutations in *DNAJB2* and *HSPB8*, most of them caused by a founder c.352+1G>A mutation in *DNAJB2* and by mutations affecting the K141 residue in the HSPB8 chaperone. Hence, their rare occurrence makes it difficult to understand the pathological mechanisms driven by such mutations in this neuropathy. Chaperones can assemble into multi-chaperone complexes that form an integrated chaperone network within the cell. Such complexes fulfill relevant roles in a variety of processes, such as the correct folding of newly synthesized proteins, in which chaperones escort them to precise cellular locations, and as a response to protein misfolding, which includes the degradation of proteins that fail to refold properly. Despite this range of functions, mutations in some of these chaperones lead to diseases with a similar clinical profile, suggesting common pathways. This review provides an overview of the genetics of those dHMNs that share a common disease mechanism and that are caused by mutations in four genes encoding chaperones: *DNAJB2*, *HSPB1, HSPB3,* and *HSPB8*.

Keywords: Distal hereditary motor neuropathy, distal spinal muscular atrophy, DNAJB2, HSPB1, HSPB3, Chaperone, Heat shock protein

OPEN ACCESS

Edited by:
Alberto J. L. Macario, University of Maryland at Baltimore, USA

Reviewed by:
Eileen M. Lafer, University of Texas Health Science Center at San Antonio, USA
Davide Pareyson, Fondazione IRCCS, Istituto Neurologico Carlo Besta, Italy

***Correspondence:**
Carmen Espinós
cespinos@cipf.es

Specialty section:
This article was submitted to Protein Folding, Misfolding and Degradation, a section of the journal Frontiers in Molecular Biosciences

Received: *30 September 2016*
Accepted: *29 November 2016*
Published: *14 December 2016*

Citation:
Lupo V, Aguado C, Knecht E and Espinós C (2016) Chaperonopathies: Spotlight on Hereditary Motor Neuropathies. Front. Mol. Biosci. 3:81. doi: 10.3389/fmolb.2016.00081

CHAPERONES AND CHAPERONOPATHIES

Chaperones (Hartl et al., 2011; Smith et al., 2015) are proteins that, together with the protein degradation machinery (proteasomes, macroautophagy, etc.), contribute to the quality control apparatus and to the proteostasis of a cell. Typically, chaperones recognize other proteins (usually called their clients) to assist in their folding so that they attain their functional conformation at the sites where they must act. Most chaperones are promiscuous and they bind to many clients, although others (dedicated chaperones) restrict their associations to one or a few proteins. However, the information available on the molecules that interact with specific chaperones is still incomplete.

Chaperones also participate in other important processes, such as: (i) the reversion of erroneous folding of newly synthesized proteins; (ii) the prevention of the formation of improper protein aggregates and their disassembly; (iii) the escorting of proteins to their functional sites, including translocation across membranes and the assembly of functional protein-protein, protein-DNA or protein-RNA complexes; and (iv) the sequestering of proteins that are damaged or unable to fold properly to the intracellular protein degradation machinery for destruction. Most of these processes require energy and, therefore, some chaperones have ATP-binding sites and ATPase activity (e.g., Hsp90, Hsp70). By contrast, ATP-independent chaperones must cooperate with the former to carry out such functions. In fact, chaperones tend to assemble into synergistic multi-chaperone complexes of distinct sizes, containing chaperones from the same or different families, as well as other proteins that assist them in their functions, thereby forming an integrated chaperone network in the cell.

Chaperones can either be constitutively expressed, induced by stress (usually but not exclusively, heat shock) or both. Most chaperones induced by heat shock are frequently called heat shock proteins (HSPs). Chaperones, including HSPs, are sometimes classified into six major families according to their molecular mass, although a gross distinction is made between the larger (e.g., the Hsp100, Hsp90, Hsp70, Hsp60, and Hsp40 co-chaperones) and smaller (sHsp, 12–43 kDa, although the vast majority are 30 kDa or less) chaperones. Each group comprises various chaperones and in the human genome, for example, 10 different chaperones have been identified in the sHsp family (HspB1-HspB10). Thus, and although the total number of chaperones in humans is still expanding, an up to date and conservative estimate of their total number would be about 100 genes (Kakkar et al., 2014). Of course, these genes give rise to a much larger number of proteins due to the different transcriptional, translational and post-translational events and modifications they are subjected to. Given the range of activities undertaken by chaperones and the vast number of multimeric complexes that they form with other chaperones, some functional redundancies are likely to exist in their extended networks. Therefore, a single chaperone, or even of a group of dedicated chaperones, would not be expected to be exclusively responsible for a specific task with a particular client, and defects in one chaperone can usually be compensated by others, albeit more or less successfully. Together with the possible lethality associated with the loss of some important chaperones, this redundancy might explain the relatively low number of diseases known to be produced by mutations in genes encoding chaperones (Macario and Conway de Macario, 2007; Kakkar et al., 2014).

PROTEOPATHIES AND CHAPERONOPATHIES

There are many disorders, some that are well known, in which specific misfolded proteins aggregate and accumulate in cells (Walker et al., 2006). Classical examples are Huntington's, Parkinson's and Alzheimer's diseases, although they are not primarily due to defects in the machinery that assist proteins to fold properly but rather, to defects in the specific proteins that accumulate in each disease (e.g., huntingtin, alpha-synuclein, amyloid-beta peptide, and tau). Therefore, these diseases can be referred to as proteopathies or proteinopathies and in principle, they are not considered to be chaperonopathies.

Nevertheless, genetic or post-transcriptional defects in chaperones may be pathological given their role in protein folding. In fact, and despite the potential functional redundancy of chaperones, mutations in genes encoding these proteins have been associated with various disorders that can be collectively referred to as chaperonopathies (Macario and Conway de Macario, 2007). These mutations can affect different yet important domains of a chaperone (e.g., the ATP binding site, client recognition site, sites for interaction with other chaperones, etc.), but they can also affect other sites regulating the expression or the activity of the chaperone. The role of chaperones implies that chaperonopathies may be associated with the aggregation of misfolded proteins but, as mentioned above, such diseases differ from proteinopathies with respect to the protein that is altered (either chaperones or other proteins).

THE GROWING LIST OF CHAPERONES INVOLVED IN DISTAL HEREDITARY MOTOR NEUROPATHIES

Distal hereditary motor neuropathies (dHMN) or distal spinal muscular atrophies (dSMA) are a group of rare hereditary neuromuscular disorders characterized by an atrophy that affects peroneal muscles in the absence of sensory symptoms (Harding, 1993). Classically, patients experience progressive distal weakness and atrophy affecting the lower limbs, which subsequently spreads to the proximal muscles and ultimately reaches the upper limbs as the disease progresses, with the possible appearance of foot deformities. Other additional manifestations include ataxia or pyramidal tract signs, although these are unusual. These symptoms contrast with those of Charcot-Marie-Tooth disease (CMT) or hereditary motor sensory neuropathy (HMSN), conditions in which sensory involvement is also evident. However, there are some forms of CMT, in particular in axonal CMT or CMT type 2 (CMT2), in which only minor sensory involvement is recognized, and it is difficult to distinguish dHMN from CMT2 (Harding and Thomas, 1980). In fact, some genetic overlap is observed in CMT and dHMN as both conditions can be caused by mutations in the same gene, and even by the same mutation.

To date 23 genes associated with dHMN have been reported (Neuromuscular Disease Center, http://neuromuscular.wustl.edu/synmot.html), although no molecular diagnosis is available in most dHMN patients (Rossor et al., 2012a). Distinct activities are affected in motor-nerve disease, including: protein folding/misfolding (HSPB1, HSPB3, HSPB8, DNAJB2, and BSCL2), RNA metabolism (IGHMBP2, SETX, and GARS), axonal transport (DYNC1H1, DCTN1), cation channel activity (ATP7A, TRPV4), transcriptional control (FBXO38), etc. Here we will focus exclusively on dHMNs that

involve mutations in the chaperone genes *HSPB1, HSPB8, DNAJB2,* and *HSPB3*, all four encoding ATP-independent chaperones. Although, compensatory mechanisms driven by the relationships and redundancies within the chaperome can overcome specific chaperone defects, this does not appear to be the case here, as in other diseases. Indeed, even when this compensation occurs, the chaperone activity associated to the defective chaperones would be modified considerably.

The ***DNAJB2/HSJ1*** gene is a member of the HSP40/DNAJ co-chaperone family, characterized by a highly conserved domain of about 70 amino acids, the J domain. This domain allows proteins of this family to interact with Hsp70, and to regulate its ATPase-dependent activity in protein folding and in protein complex dissociation (Hageman et al., 2010). Moreover, spliced transcript variants have been described for the *DNAJB2* gene that encode different isoforms, one of which, DNAJB2a, participates in the resolution of protein aggregates associated with important neurodegenerative diseases (Chen et al., 2016 and references cited therein). Although this protein is mainly expressed in the brain, it has also been localized in normal and diseased skeletal muscle, where it is thought to influence protein turnover through the ubiquitin-proteasome pathway (Claeys et al., 2010). DNAJB2 interacts with ubiquitin chains and their fusion proteins, and since the proteasome mediates the degradation of selected proteins, it is possible that some of these proteins are related to the cytoskeleton (microtubules, intermediate filaments, and microfilaments), in accordance with the role of the other chaperones involved in dHMN (see below).

There are 10 cases where autosomal recessive inheritance has been associated to mutations in the *DNAJB2* gene (**Table 1**). The first mutation was reported in homozygosis, *DNAJB2* c.352+1G>A, and it was identified in a Moroccan family with a dHMN phenotype (dHMN5) by genome wide mapping (Blumen et al., 2012). In this case, the expression of DNAJB2 was dampened in fibroblasts from the patients and overexpression of the protein reduced the formation of inclusions in a neuronal cellular model, suggesting DNAJB2 is active in motor neurons and/or muscle (Blumen et al., 2012). Two additional homozygous mutations were later described in the *DNAJB2* gene, c.229+1G>A and c.14A>G (p.Y5C), in a family diagnosed with dHMN (dHMN5) and another with CMT2 (CMT2T), respectively (Gess et al., 2014). More recently, a homozygous large deletion was reported in a family with spinal muscular atrophy and parkinsonism, broadening the clinical spectrum of *DNAJB2* related neuropathies (Sanchez et al., 2016).

To date, the remaining known patients with mutations in the *DNAJB2* gene carry the c.352+1G>A mutation in homozygosis: 5 families from Spain (Frasquet et al., 2016; Lupo et al., 2016) and one from Brazil (Teive et al., 2015). These Spanish families were investigated by haplotype analysis and they carried the same homozygous haplotype. Hence, the *DNAJB2* c.352+1G>A mutation appears to be a founder event (Lupo et al., 2016), and it is shared with a family reported elsewhere (Blumen et al., 2012). The patients in Spain displayed a dHMN or CMT2 phenotype and, in some cases, initial clinical manifestations that were consistent with dHMN and that subsequently evolved to CMT2 (Frasquet et al., 2016). Moreover, the peripheral motor neuropathy recently described in a Brazilian family carrying the *DNAJB2* c.352+1G>A mutation was associated with parkinsonism and cerebellar ataxia (Teive et al., 2015). Some patients show parkinsonian symptoms (Frasquet et al., 2016; Sanchez et al., 2016; Teive et al., 2015), which probably are due to the DNAJB2 mutations. Other additional symptoms such as cerebellar ataxia may be coincidental. Further studies of a larger analytical series will be necessary to define the clinical manifestations associated with *DNAJB2* mutations in more depth.

HSPB1, HSPB3, and **HSPB8** are the three other chaperones associated with dHMNs, and they are all members of the sHsp family. These proteins are characterized by a highly conserved α-crystallin domain that is related to their chaperone activity, which is more closely associated with an 80–100 amino acid domain in the C- rather than the N-terminal region of the protein (Nefedova et al., 2015). These chaperones are normally found as monomers, but under stress, they tend to also interact with each other to form large, labile homo- and hetero-oligomeric complexes of more than twenty identical or different subunits, driving their recognition and interaction with new protein clients (Arrigo, 2013). Certain sHsp are tissue specific, while others are more ubiquitously expressed in function of the tissue and conditions. The main role of sHsps is to carry their denatured clients to ATP-dependent chaperones for renaturation or to the cell's protein degradation machinery (proteasomes and autophagosomes). In terms of dHMN and HMSN, sHsps stabilize the activities of the cell cytoskeleton, interacting with most of its proteins components, as well as preventing oxidative stress (Nefedova et al., 2015).

Autosomal dominant mutations in the ***HSPB1/HSP27*** gene were first described in four families with dHMN (dHMN2B) and in one family with CMT2 (CMT2F) (Evgrafov et al., 2004). More than 30 different mutations causing dHMN or CMT2 have since been described in the *HSPB1* gene, some of which also produce other manifestations (**Table 1**; Evgrafov et al., 2004; Kijima et al., 2005; Tang B. et al., 2005; Chung et al., 2008; Houlden et al., 2008; James et al., 2008; Ikeda et al., 2009; Luigetti et al., 2010; Mandich et al., 2010; Solla et al., 2010; Murphy et al., 2012; Rossor et al., 2012b; Sivera et al., 2013; Ylikallio et al., 2014, 2015). An autosomal recessive mutation in the *HSPB1* gene was identified in a consanguineous family with a similar clinical profile (Houlden et al., 2008). On the whole, *HSPB1* mutations are inherited dominantly and while most involve a change in one codon, they may also produce a frameshift or premature stop codons. The protein encoded by this gene is ubiquitously expressed and it is induced by environmental stress, translocating from the cytoplasm to the nucleus to influence stress resistance and produce other changes. The known mutations are located in all three domains of the protein: N-terminus, α-crystallin and C-terminus. These *HSPB1* mutations mostly modify the oligomeric state of the protein, usually negatively but also positively (certain mutations in the α-crystallin domain), altering its chaperone activity and in both cases affecting normal cytoskeletal function. HSPB1 is involved in the organization of the neurofilament network, which is important to maintain the axonal cytoskeleton and transport, and indeed, overexpression of HSPB1 mutants

TABLE 1 | Mutations reported in *DNAJB2*, *HSPB1*, *HSPB3* and *HSPB8* involved in hereditary neuropathies.

Gene	HGVS (nucleotide)	HGVS (protein)	Disease/Phenotype	References
DNAJB2	c.352+1G>A	donor site	dHMN/CMT2	Blumen et al., 2012; Frasquet et al., 2016; Lupo et al., 2016
	c.229+1G>A	donor site	dHMN	Gess et al., 2014
	c.14A>G	p.Y5C	dHMN	Gess et al., 2014
HSPB1	c.20C>G	p.P7R	CMT2	Luigetti et al., 2010
	c.45C>A	p.S15R	Peripheral neuropathy	Antoniadi et al., 2015
	c.100G>A	p.G34R	HMSN	Capponi et al., 2011; Muranova et al., 2015
	c.116C>T	p.P39L	dHMN/CMT2	Houlden et al., 2008; Muranova et al., 2015; Yavarna et al., 2015
	c.121G>A	p.E41K	dHMN	Capponi et al., 2011; Muranova et al., 2015
	c.250G>A	p.G84R	CMT2	Manganelli et al., 2014
	c.250G>C	p.G84R	dHMN	James et al., 2008; Fischer et al., 2012; Nefedova et al., 2015
	c.257C>T	p.S86L	dHMN/ALS	Scarlato et al., 2015
	c.295C>A	p.L99M	dHMN/CMT2	Houlden et al., 2008; Nefedova et al., 2015
	c.380G>T	p.R127L	CMT2	Hoyer et al., 2014; Ylikallio et al., 2015
	c.379C>T	p.R127W	dHMN	Evgrafov et al., 2004; Almeida-Souza et al., 2011
	c.404C>G	p.S135C	CMT2	Benedetti et al., 2010; Oberstadt et al., 2016
	c.404C>G	p.S135C	CMT2	Benedetti et al., 2010; Oberstadt et al., 2016
	c.404C>T	p.S135F	CMT2	Evgrafov et al., 2004; Almeida-Souza et al., 2010, 2011
	c.404C>A	p.S135Y	CMT2	Ylikallio et al., 2014
	c.407G>T	p.R136L	dHMN/CMT2	Capponi et al., 2011; Gaeta et al., 2012; Stancanelli et al., 2015
	c.406C>T	p.R136W	CMT2	Evgrafov et al., 2004; Almeida-Souza et al., 2010, 2011
	c.418C>G	p.R140G	dHMN/CMT2	Houlden et al., 2008; Nefedova et al., 2015
	c.421A>C	p.K141Q	dHMN	Ikeda et al., 2009; Nefedova et al., 2013; Maeda et al., 2014
	c.452C>T	p.T151I	dHMN	Evgrafov et al., 2004; Almeida-Souza et al., 2010, 2011
	c.490A>G	p.T164A	CMT2	Lin et al., 2011
	c.523C>T	p.Q175X	CMT2	Rossor et al., 2012b
	c.539C>T	p.T180I	dHMN/CMT2	Luigetti et al., 2010
	c.545C>T	p.P182L	dHMN	Evgrafov et al., 2004; Almeida-Souza et al., 2010, 2011
	c.544C>T	p.P182S	dHMN	Kijima et al., 2005
	c.562C>T	p.R188W	CMT2	Capponi et al., 2011
	c.365-13C>T	acceptor site	CMT2	Benedetti et al., 2010
	c.-217T>C	regulatory	ALS	Dierick et al., 2007
	c.476_477delCT	p.P159RfsX41	Peripheral neuropathy, early onset	Mandich et al., 2010; Capponi et al., 2011
	c.505delA	p.M169CfsX4	CMT	DiVincenzo et al., 2014
	c.171_172insGCGCCCT	p.L58AfsX105	CMT	DiVincenzo et al., 2014
HSPB3	c.21G>T	p.R7S	dHMN	Kolb et al., 2010
HSPB8	c.423G>C)	p.L141N	dHMN/CMT2	Irobi et al., 2004
	c.421A>G	p.L141E	dHMN	Irobi et al., 2004
	c.423G>T	p.L141N	CMT2	Tang B. S. et al., 2005
	c.422A>C	p.L141T	CMT2	Nakhro et al., 2013
	c.151insC	p.P173SfsX43	Distal myopathy/dHMN	Ghaoui et al., 2016

ALS, Amyotrophic lateral sclerosis; CMT2, Charcot-Marie-Tooth disease type 2 or axonal; dHMN, Distal hereditary motor neuropathy; HMSN, hereditary motor and sensory neuropathy.

produces protein aggregates and altered neurofilament transport in the axon (Evgrafov et al., 2004; Ackerley et al., 2006; Zhai et al., 2007). Thus, an increased interaction with tubulin and an enhanced stability of the microtubule network has been observed for some mutants (Almeida-Souza et al., 2011). Moreover, there are severe defects in axon transport in transgenic mice expressing human mutant HSPB1 in neurons due to a decrease in acetylated α-tubulin (d'Ydewalle et al., 2011). As a result, inhibitors of histone deacetylase 6 (HDAC6, a client of HSPB1 that acetylates α-tubulin) have successfully reversed the axonal loss in a mouse model of CMT2F that expresses mutant HSPB1 (d'Ydewalle et al., 2011). HSPB1 is also involved in a variety of human diseases, such as cancer, Alzheimer's disease and heart disease (Sun and MacRae, 2005).

At present, only one family is thought to carry clinical mutations in the ***HSPB3/HSPL27*** gene: a missense mutation c.21G>T (p.R7S) described in two affected sisters who suffer from dHMN (dHMN2C) (**Table 1**; Kolb et al., 2010). The function of HSPB3 is not fully understood, although replacing the positively charged R7 residue with a neutral polar amino acid

would affect its structure and therefore, its proprieties. In contrast to the ubiquitous expression of *HSPB1* and *HSPB8*, *HSPB3* is more tissue specific (heart, brain, skeletal and smooth muscle) and it is expressed strongly in muscle (Sugiyama et al., 2000). HSPB3 interacts with HSPB2 and these two proteins in turn both interact with HSPB8, potentially contributing to maintain myofibril integrity (Fontaine et al., 2005). Finally, HSPB3 and HSPB2 are upregulated in a mouse model for spinal and bulbar muscular atrophy (SBMA), an inherited motoneuron disease (Rusmini et al., 2015).

Mutations in the ***HSPB8/HSP22*** gene were first associated with dHMN (dHMN2A) (Irobi et al., 2004) and later, with CMT2 (CMT2L) (**Table 1**; Tang B. S. et al., 2005). Four mutations have been described and they all affect position K141: c.423G>T/c.423G>C (p.K141N), c.421A>G (p.K141E), and c.422A>C (p.K141T). These mutations are all transmitted in an autosomal dominant fashion (Irobi et al., 2004; Tang B. S. et al., 2005; Nakhro et al., 2013), and this hot-spot residue is located in a hydrophobic strand of the α-crystallin domain. The mutations eliminate the positive charge of the K41 amino acid, which will affect the interactions of HSPB8 with other sHsps like HSPB27, HSPB3, and HSPB2 (Irobi et al., 2004; Fontaine et al., 2006; Kasakov et al., 2007; Nakhro et al., 2013). Mutational screening in a large clinical series revealed additional patients but no novel mutations associated with dHMN or CMT2 (Dierick et al., 2008; Sivera et al., 2013; Fridman et al., 2015). However, two mutations, c.421A>G (p.K141E), and c.151insC (p.P173SfsX43) were recently described in two unrelated families with a new distal neuromyopathy phenotype, expanding the clinical phenotype associated with *HSPB8* (Ghaoui et al., 2016).

HSPB8 is ubiquitously expressed (particularly strongly in the spinal cord, and especially in motor and sensory neurons), and it acts as a chaperone and a regulator of apoptosis (Shemetov et al., 2008). HspB8 acts as a chaperone in association with the co-chaperones Bag3 and Stub1, stimulating chaperone-assisted selective macroautophagy in muscle to maintain the actin cytoskeleton (Arndt et al., 2010). Expression of HSPB8 mutants in cell models promotes the formation of intracellular aggregates and it augments cell death (Benn et al., 2002; Irobi et al., 2004). These protein aggregates are also observed in fibroblasts from patients who carry *HSPB8* mutations, and they are coupled to a decrease in mitochondrial membrane potential and a reduction in cell viability (Irobi et al., 2012; Vicario et al., 2014). Although the pathological mechanisms underlying these conditions remain enigmatic, specific motor neuron degeneration is associated with *HSPB8* mutations (Irobi et al., 2010). In addition, expression of this protein can be induced by estrogen in estrogen receptor-positive breast cancer cells, indicating a role in carcinogenesis, and suggesting the possible involvement of HspB8 in regulating cell proliferation and apoptosis.

Since mutations in these four chaperones, as well as those in other genes, produce a similar pathological phenotype, it would seem obvious that they must share some pathogenic pathways. It has been proposed that most, if not all, of the proteins affected in dHMN/CMT2 are related with the impaired axonal trafficking of cell components (Bucci et al., 2012; Gentil and Cooper, 2012). Considering the activity of all the chaperones described above, it appears that mutations in all these genes could affect the cytoskeleton, either by interacting with relevant proteins (e.g., in the case of the sHsps) or by regulating their specific degradation (e.g., in the case of DNAJB2 and HspB8). Since the cytoskeleton participates in axonal transport, as well as in the dynamics of various organelles and plasma membrane receptors, there are clear potential relationships with other mutations that cause dHMN/CMT2. To date there are no effective treatments for these diseases and therefore, much more research is needed to understand the consequences of each specific mutation that provokes them. However, one potential therapy to be considered, at least in certain cases of these chaperonopathies, could be to overexpress the chaperone to rescue its defective functions. Indeed, the overexpression of HspB8 ameliorates the accumulation of aggregates associated with the p.P182L mutation in HspB1 (Carra et al., 2010), or the effects on its clients, as illustrated by the use of inhibitors of histone deacetylase 6 to treat CMT2F (d'Ydewalle et al., 2011).

AUTHOR CONTRIBUTIONS

Conceptualization: EK, CE; Writing-draft, review and editing: VL, CA, EK, CE; Funding acquisition and supervision: EK, CE.

ACKNOWLEDGMENTS

This work was supported by the Instituto de Salud Carlos III (ISCIII) [Grants no. PI12/000453 and PI15/000187 to CE] and by the MINECO [Grant no. SAF2014-54604-C3-2-R to EK]. CE has a "Miguel Servet" contract funded by the ISCIII and the Centro de Investigación Príncipe Felipe (CIPF) [Grant no. CPII14/00002]. CA is supported by the CIBER de Enfermedades Raras (CIBERER)-ISCIII.

REFERENCES

Ackerley, S., James, P. A., Kalli, A., French, S., Davies, K. E., and Talbot, K. (2006). A mutation in the small heat-shock protein HSPB1 leading to distal hereditary motor neuronopathy disrupts neurofilament assembly and the axonal transport of specific cellular cargoes. *Hum. Mol. Genet.* 15, 347–354. doi: 10.1093/hmg/ddi452

Almeida-Souza, L., Asselbergh, B., d'Ydewalle, C., Moonens, K., Goethals, S., de Winter, V., et al. (2011). Small heat-shock protein HSPB1 mutants stabilize microtubules in Charcot-Marie-Tooth neuropathy. *J. Neurosci.* 31, 15320–15328. doi: 10.1523/JNEUROSCI.3266-11.2011

Almeida-Souza, L., Goethals, S., de Winter, V., Dierick, I., Gallardo, R., Van Durme, J., et al. (2010). Increased monomerization of mutant HSPB1 leads to protein hyperactivity in Charcot-Marie-Tooth neuropathy. *J. Biol. Chem.* 285, 12778–12786. doi: 10.1074/jbc.M109.082644

Antoniadi, T., Buxton, C., Dennis, G., Forrester, N., Smith, D., Lunt, P., et al. (2015). Application of targeted multi-gene panel testing for the diagnosis of inherited peripheral neuropathy provides a high diagnostic yield with unexpected phenotype-genotype variability. *BMC Med. Genet.* 16, 84. doi: 10.1186/s12881-015-0224-8

Arndt, V., Dick, N., Tawo, R., Dreiseidler, M., Wenzel, D., Hesse, M., et al. (2010). Chaperone-assisted selective autophagy is essential for muscle maintenance. *Curr. Biol.* 20, 143–148. doi: 10.1016/j.cub.2009.11.022

Arrigo, A. P. (2013). Human small heat shock proteins: protein interactomes of homo- and hetero-oligomeric complexes: an update. *FEBS Lett.* 587, 1959–1969. doi: 10.1016/j.febslet.2013.05.011

Benedetti, S., Previtali, S. C., Coviello, S., Scarlato, M., Cerri, F., Di Pierri, E., et al. (2010). Analyzing histopathological features of rare Charcot-Marie-Tooth neuropathies to unravel their pathogenesis. *Arch. Neurol.* 67, 1498–1505. doi: 10.1001/archneurol.2010.303

Benn, S. C., Perrelet, D., Kato, A. C., Scholz, J., Decosterd, I., Mannion, R. J., et al. (2002). Hsp27 upregulation and phosphorylation is required for injured sensory and motor neuron survival. *Neuron* 36, 45–56. doi: 10.1016/S0896-6273(02)00941-8

Blumen, S. C., Astord, S., Robin, V., Vignaud, L., Toumi, N., Cieslik, A., et al. (2012). A rare recessive distal hereditary motor neuropathy with HSJ1 chaperone mutation. *Ann. Neurol.* 71, 509–519. doi: 10.1002/ana.22684

Bucci, C., Bakke, O., and Progida, C. (2012). Charcot-Marie-Tooth disease and intracellular traffic. *Prog. Neurobiol.* 99, 191–225. doi: 10.1016/j.pneurobio.2012.03.003

Capponi, S., Geroldi, A., Fossa, P., Grandis, M., Ciotti, P., Gulli, R., et al. (2011). HSPB1 and HSPB8 in inherited neuropathies: study of an Italian cohort of dHMN and CMT2 patients. *J. Peripher. Nerv. Syst.* 16, 287–294. doi: 10.1111/j.1529-8027.2011.00361.x

Carra, S., Boncoraglio, A., Kanon, B., Brunsting, J. F., Minoia, M., Rana, A., et al. (2010). Identification of the Drosophila ortholog of HSPB8: implication of HSPB8 loss of function in protein folding diseases. *J. Biol. Chem.* 285, 37811–37822. doi: 10.1074/jbc.M110.127498

Chen, H. J., Mitchell, J. C., Novoselov, S., Miller, J., Nishimura, A. L., Scotter, E. L., et al. (2016). The heat shock response plays an important role in TDP-43 clearance: evidence for dysfunction in amyotrophic lateral sclerosis. *Brain* 139, 1417–1432. doi: 10.1093/brain/aww028

Chung, K. W., Kim, S. B., Cho, S. Y., Hwang, S. J., Park, S. W., Kang, S. H., et al. (2008). Distal hereditary motor neuropathy in Korean patients with a small heat shock protein 27 mutation. *Exp. Mol. Med.* 40, 304–312. doi: 10.3858/emm.2008.40.3.304

d'Ydewalle, C., Krishnan, J., Chiheb, D. M., Van Damme, P., Irobi, J., Kozikowski, A. P., et al. (2011). HDAC6 inhibitors reverse axonal loss in a mouse model of mutant HSPB1-induced Charcot-Marie-Tooth disease. *Nat. Med.* 17, 968–974. doi: 10.1038/nm.2396

Claeys, K. G., Sozanska, M., Martin, J. J., Lacene, E., Vignaud, L., Stockholm, D., et al. (2010). DNAJB2 expression in normal and diseased human and mouse skeletal muscle. *Am. J. Pathol.* 176, 2901–2910. doi: 10.2353/ajpath.2010.090663

Dierick, I., Baets, J., Irobi, J., Jacobs, A., De Vriendt, E., Deconinck, T., et al. (2008). Relative contribution of mutations in genes for autosomal dominant distal hereditary motor neuropathies: a genotype-phenotype correlation study. *Brain* 131, 1217–1227. doi: 10.1093/brain/awn029

Dierick, I., Irobi, J., Janssens, S., Theuns, J., Lemmens, R., Jacobs, A., et al. (2007). Genetic variant in the HSPB1 promoter region impairs the HSP27 stress response. *Hum. Mutat.* 28, 830. doi: 10.1002/mgg3.106

DiVincenzo, C., Elzinga, C. D., Medeiros, A. C., Karbassi, I., Jones, J. R., Evans, M. C., et al. (2014). The allelic spectrum of Charcot-Marie-Tooth disease in over 17,000 individuals with neuropathy. *Mol. Genet. Genomic Med.* 2, 522–529. doi: 10.1002/mgg3.106

Evgrafov, O. V., Mersiyanova, I., Irobi, J., Van Den Bosch, L., Dierick, I., Leung, C. L., et al. (2004). Mutant small heat-shock protein 27 causes axonal Charcot-Marie-Tooth disease and distal hereditary motor neuropathy. *Nat. Genet.* 36, 602–606. doi: 10.1038/ng1354

Fischer, C., Trajanoski, S., Papic, L., Windpassinger, C., Bernert, G., Freilinger, M., et al. (2012). SNP array-based whole genome homozygosity mapping as the first step to a molecular diagnosis in patients with Charcot-Marie-Tooth disease. *J. Neurol.* 259, 515–523. doi: 10.1007/s00415-011-6213-8

Fontaine, J. M., Sun, X., Benndorf, R., and Welsh, M. J. (2005). Interactions of HSP22 (HSPB8) with HSP20, alphaB-crystallin, and HSPB3. *Biochem. Biophys. Res. Commun.* 337, 1006–1011. doi: 10.1016/j.bbrc.2005.09.148

Fontaine, J. M., Sun, X., Hoppe, A. D., Simon, S., Vicart, P., Welsh, M. J., et al. (2006). Abnormal small heat shock protein interactions involving neuropathy-associated HSP22 (HSPB8) mutants. *FASEB J.* 20, 2168–2170. doi: 10.1096/fj.06-5911fje

Frasquet, M., Chumillas, M. J., Vilchez, J. J., Márquez-Infante, C., Palau, F., Vazquez-Costa, J. F., et al. (2016). Phenotype and natural history of inherited neuropathies caused by HSJ1 c.352+1G>A mutation. *J. Neurol. Neurosurg. Psychiatry* 87, 1265–1268. doi: 10.1136/jnnp-2015-312890

Fridman, V., Bundy, B., Reilly, M. M., Pareyson, D., Bacon, C., Burns, J., et al. (2015). CMT subtypes and disease burden in patients enrolled in the Inherited Neuropathies Consortium natural history study: a cross-sectional analysis. *J. Neurol. Neurosurg. Psychiatr.* 86, 873–878. doi: 10.1136/jnnp-2014-308826

Gaeta, M., Mileto, A., Mazzeo, A., Minutoli, F., Di Leo, R., Settineri, N., et al. (2012). MRI findings, patterns of disease distribution, and muscle fat fraction calculation in five patients with Charcot-Marie-Tooth type 2 F disease. *Skeletal Radiol.* 41, 515–524. doi: 10.1007/s00256-011-1199-y

Gentil, B. J., and Cooper, L. (2012). Molecular basis of axonal dysfunction and traffic impairments in CMT. *Brain Res. Bull.* 88, 444–453. doi: 10.1016/j.brainresbull.2012.05.003

Gess, B., Auer-Grumbach, M., Schirmacher, A., Strom, T., Zitzelsberger, M., Rudnik-Schoneborn, S., et al. (2014). HSJ1-related hereditary neuropathies: novel mutations and extended clinical spectrum. *Neurology* 83, 1726–1732. doi: 10.1212/WNL.0000000000000966

Ghaoui, R., Palmio, J., Brewer, J., Lek, M., Needham, M., Evila, A., et al. (2016). Mutations in HSPB8 causing a new phenotype of distal myopathy and motor neuropathy. *Neurology* 86, 391–398. doi: 10.1212/WNL.0000000000002324

Hageman, J., Rujano, M. A., van Waarde, M. A., Kakkar, V., Dirks, R. P., Govorukhina, N., et al. (2010). A DNAJB chaperone subfamily with HDAC-dependent activities suppresses toxic protein aggregation. *Mol. Cell* 37, 355–369. doi: 10.1016/j.molcel.2010.01.001

Harding, A. E. (1993). *Peripheral Neuropathy*, eds P. J. Dyck, P. K. Thomas, J. W. Griffin, P. A. Low, and J. F. Poduslo Philadelphia, PA: Saunders Company.

Harding, A. E., and Thomas, P. K. (1980). Genetic aspects of hereditary motor and sensory neuropathy (types I and II). *J. Med. Genet.* 17, 329–336. doi: 10.1136/jmg.17.5.329

Hartl, F. U., Bracher, A., and Hayer-Hartl, M. (2011). Molecular chaperones in protein folding and proteostasis. *Nature* 475, 324–332. doi: 10.1038/nature10317

Houlden, H., Laura, M., Wavrant-De Vrieze, F., Blake, J., Wood, N., and Reilly, M. M. (2008). Mutations in the HSP27 (HSPB1) gene cause dominant, recessive, and sporadic distal HMN/CMT type 2. *Neurology* 71, 1660–1668. doi: 10.1212/01.wnl.0000319696.14225.67

Høyer, H., Braathen, G. J., Busk, Ø. L., Holla, Ø. L., Svendsen, M., Hilmarsen, H. T., et al. (2014). Genetic diagnosis of Charcot-Marie-Tooth disease in a population by next-generation sequencing. *Biomed. Res. Int.* 2014:210401. doi: 10.1155/2014/210401

Ikeda, Y., Abe, A., Ishida, C., Takahashi, K., Hayasaka, K., and Yamada, M. (2009). A clinical phenotype of distal hereditary motor neuronopathy type II with a novel HSPB1 mutation. *J. Neurol. Sci.* 277, 9–12. doi: 10.1016/j.jns.2008.09.031

Irobi, J., Almeida-Souza, L., Asselbergh, B., De Winter, V., Goethals, S., Dierick, I., et al. (2010). Mutant HSPB8 causes motor neuron-specific neurite degeneration. *Hum. Mol. Genet.* 19, 3254–3265. doi: 10.1093/hmg/ddq234

Irobi, J., Holmgren, A., De Winter, V., Asselbergh, B., Gettemans, J., Adriaensen, D., et al. (2012). Mutant HSPB8 causes protein aggregates and a reduced mitochondrial membrane potential in dermal fibroblasts from distal hereditary motor neuropathy patients. *Neuromuscul. Disord.* 22, 699–711. doi: 10.1016/j.nmd.2012.04.005

Irobi, J., Van Impe, K., Seeman, P., Jordanova, A., Dierick, I., Verpoorten, N., et al. (2004). Hot-spot residue in small heat-shock protein 22 causes distal motor neuropathy. *Nat. Genet.* 36, 597–601. doi: 10.1038/ng1328

James, P. A., Rankin, J., and Talbot, K. (2008). Asymmetrical late onset motor neuropathy associated with a novel mutation in the small heat shock protein HSPB1 (HSP27). *J. Neurol. Neurosurg. Psychiatr.* 79, 461–463. doi: 10.1136/jnnp.2007.125179

Kakkar, V., Meister-Broekema, M., Minoia, M., Carra, S., and Kampinga, H. H. (2014). Barcoding heat shock proteins to human diseases: looking beyond the heat shock response. *Dis. Model. Mech.* 7, 421–434. doi: 10.1242/dmm.014563

Kasakov, A. S., Bukach, O. V., Seit-Nebi, A. S., Marston, S. B., and Gusev, N. B. (2007). Effect of mutations in the beta5-beta7 loop on the structure and properties of human small heat shock protein HSP22 (HspB8, H11). *FEBS J.* 274, 5628–5642. doi: 10.1111/j.1742-4658.2007.06086.x

Kijima, K., Numakura, C., Goto, T., Takahashi, T., Otagiri, T., Umetsu, K., et al. (2005). Small heat shock protein 27 mutation in a Japanese patient with distal hereditary motor neuropathy. *J. Hum. Genet.* 50, 473–476. doi: 10.1007/s10038-005-0280-6

Kolb, S. J., Snyder, P. J., Poi, E. J., Renard, E. A., Bartlett, A., Gu, S., et al. (2010). Mutant small heat shock protein B3 causes motor

neuropathy: utility of a candidate gene approach. *Neurology* 74, 502–506. doi: 10.1212/WNL.0b013e3181cef84a

Lin, K. P., Soong, B. W., Yang, C. C., Huang, L. W., Chang, M. H., Lee, I. H., et al. (2011). The mutational spectrum in a cohort of Charcot-Marie-Tooth disease type 2 among the Han Chinese in Taiwan. *PLoS ONE* 6:e29393. doi: 10.1371/journal.pone.0029393

Luigetti, M., Fabrizi, G. M., Madia, F., Ferrarini, M., Conte, A., Del Grande, A., et al. (2010). A novel HSPB1 mutation in an Italian patient with CMT2/dHMN phenotype. *J. Neurol. Sci.* 298, 114–117. doi: 10.1016/j.jns.2010.09.008

Lupo, V., Garcia-Garcia, F., Sancho, P., Tello, C., Garcia-Romero, M., Villarreal, L., et al. (2016). Assessment of Targeted Next-Generation Sequencing as a Tool for the Diagnosis of Charcot-Marie-Tooth Disease and Hereditary Motor Neuropathy. *J. Mol. Diagn.* 18, 225–234. doi: 10.1016/j.jmoldx.2015.10.005

Macario, A. J., and Conway de Macario, E. (2007). Chaperonopathies and chaperonotherapy. *FEBS Lett.* 581, 3681–3688. doi: 10.1016/j.febslet.2007.04.030

Maeda, K., Idehara, R., Hashiguchi, A., and Takashima, H. (2014). A family with distal hereditary motor neuropathy and a K141Q mutation of small heat shock protein HSPB1. *Intern. Med.* 53, 1655–1658. doi: 10.2169/internalmedicine.53.2843

Mandich, P., Grandis, M., Varese, A., Geroldi, A., Acquaviva, M., Ciotti, P., et al. (2010). Severe neuropathy after diphtheria-tetanus-pertussis vaccination in a child carrying a novel frame-shift mutation in the small heat-shock protein 27 gene. *J. Child Neurol.* 25, 107–109. doi: 10.1177/0883073809334387

Manganelli, F., Tozza, S., Pisciotta, C., Bellone, E., Iodice, R., Nolano, M., et al. (2014). Charcot-Marie-Tooth disease: frequency of genetic subtypes in a Southern Italy population. *J. Peripher. Nerv. Syst.* 19, 292–298. doi: 10.1111/jns.12092

Muranova, L. K., Weeks, S. D., Strelkov, S. V., and Gusev, N. B. (2015). Characterization of Mutants of Human Small Heat Shock Protein HspB1 Carrying Replacements in the N-Terminal Domain and Associated with Hereditary Motor Neuron Diseases. *PLoS ONE* 10:e0126248. doi: 10.1371/journal.pone.0126248

Murphy, S. M., Laura, M., Fawcett, K., Pandraud, A., Liu, Y. T., Davidson, G. L., et al. (2012). Charcot-Marie-Tooth disease: frequency of genetic subtypes and guidelines for genetic testing. *J. Neurol. Neurosurg. Psychiatr.* 83, 706–710. doi: 10.1136/jnnp-2012-302451

Nakhro, K., Park, J. M., Kim, Y. J., Yoon, B. R., Yoo, J. H., Koo, H., et al. (2013). A novel Lys141Thr mutation in small heat shock protein 22 (HSPB8) gene in Charcot-Marie-Tooth disease type 2L. *Neuromuscul. Disord.* 23, 656–663. doi: 10.1016/j.nmd.2013.05.009

Nefedova, V. V., Datskevich, P. N., Sudnitsyna, M. V., Strelkov, S. V., and Gusev, N. B. (2013). Physico-chemical properties of R140G and K141Q mutants of human small heat shock protein HspB1 associated with hereditary peripheral neuropathies. *Biochimie* 95, 1582–1592. doi: 10.1016/j.biochi.2013.04.014

Nefedova, V. V., Muranova, L. K., Sudnitsyna, M. V., Ryzhavskaya, A. S., and Gusev, N. B. (2015). Small heat shock proteins and distal hereditary neuropathies. *Biochem. Mosc.* 80, 1734–1747. doi: 10.1134/S000629791513009X

Oberstadt, M., Mitter, D., Classen, J., and Baum, P. (2016). Late onset dHMN II caused by c.404C>G mutation in HSPB1 gene. *J. Peripher. Nerv. Syst.* 21, 111–113. doi: 10.1111/jns.12165

Rossor, A. M., Davidson, G. L., Blake, J., Polke, J. M., Murphy, S. M., Houlden, H., et al. (2012b). A novel p.Gln175X [corrected] premature stop mutation in the C-terminal end of HSP27 is a cause of CMT2. *J. Peripher. Nerv. Syst.* 17, 201–205. doi: 10.1111/j.1529-8027.2012.00400.x

Rossor, A. M., Kalmar, B., Greensmith, L., and Reilly, M. M. (2012a). The distal hereditary motor neuropathies. *J. Neurol. Neurosurg. Psychiatr.* 83, 6–14. doi: 10.1136/jnnp-2011-300952

Rusmini, P., Polanco, M. J., Cristofani, R., Cicardi, M. E., Meroni, M., Galbiati, M., et al. (2015). Aberrant autophagic response in the muscle of a knock-in mouse model of spinal and bulbar muscular atrophy. *Sci. Rep.* 5:15174. doi: 10.1038/srep15174

Sanchez, E., Darvish, H., Mesias, R., Taghavi, S., Firouzabadi, S. G., Walker, R. H., et al. (2016). Identification of a large *DNAJB2* deletion in a family with spinal muscular atrophy and parkinsonism. *Hum. Mutat.* 37, 1180–1189. doi: 10.1002/humu.23055

Scarlato, M., Vigano, F., Carrera, P., Previtali, S. C., and Bolino, A. (2015). A novel heat shock protein 27 homozygous mutation: widening of the continuum between MND/dHMN/CMT2. *J. Peripher. Nerv. Syst.* 20, 419–421. doi: 10.1111/jns.12139

Shemetov, A. A., Seit-Nebi, A. S., and Gusev, N. B. (2008). Structure, properties, and functions of the human small heat-shock protein HSP22 (HspB8, H11, E2IG1): a critical review. *J. Neurosci. Res.* 86, 264–269. doi: 10.1002/jnr.21441

Sivera, R., Sevilla, T., Vilchez, J. J., Martinez-Rubio, D., Chumillas, M. J., Vazquez, J. F., et al. (2013). Charcot-Marie-Tooth disease: genetic and clinical spectrum in a Spanish clinical series. *Neurology* 81, 1617–1625. doi: 10.1212/WNL.0b013e3182a9f56a

Smith, H. L., Li, W., and Cheetham, M. E. (2015). Molecular chaperones and neuronal proteostasis. *Semin. Cell Dev. Biol.* 40, 142–152. doi: 10.1016/j.semcdb.2015.03.003

Solla, P., Vannelli, A., Bolino, A., Marrosu, G., Coviello, S., Murru, M. R., et al. (2010). Heat shock protein 27 R127W mutation: evidence of a continuum between axonal Charcot-Marie-Tooth and distal hereditary motor neuropathy. *J. Neurol. Neurosurg. Psychiatr.* 81, 958–962. doi: 10.1136/jnnp.2009.181636

Stancanelli, C., Fabrizi, G. M., Ferrarini, M., Cavallaro, T., Taioli, F., Di Leo, R., et al. (2015). Charcot-Marie-Tooth 2F: phenotypic presentation of the Arg136Leu HSP27 mutation in a multigenerational family. *Neurol. Sci.* 36, 1003–1006. doi: 10.1007/s10072-014-2050-8

Sugiyama, Y., Suzuki, A., Kishikawa, M., Akutsu, R., Hirose, T., Waye, M. M., et al. (2000). Muscle develops a specific form of small heat shock protein complex composed of MKBP/HSPB2 and HSPB3 during myogenic differentiation. *J. Biol. Chem.* 275, 1095–1104. doi: 10.1074/jbc.275.2.1095

Sun, Y., and MacRae, T. H. (2005). The small heat shock proteins and their role in human disease. *FEBS J.* 272, 2613–2627. doi: 10.1111/j.1742-4658.2005.04708.x

Tang, B., Liu, X., Zhao, G., Luo, W., Xia, K., Pan, Q., et al. (2005). Mutation analysis of the small heat shock protein 27 gene in Chinese patients with Charcot-Marie-Tooth disease. *Arch. Neurol.* 62, 1201–1207. doi: 10.1001/archneur.62.8.1201

Tang, B. S., Zhao, G. H., Luo, W., Xia, K., Cai, F., Pan, Q., et al. (2005). Small heat-shock protein 22 mutated in autosomal dominant Charcot-Marie-Tooth disease type 2L. *Hum. Genet.* 116, 222–224. doi: 10.1007/s00439-004-1218-3

Teive, H. A. G., Arruda, W. O., Scola, R. H., Werneck, L. C., and Kok, F. (2015). Distal neuropathy motor neuropathy with HSJ1 chaperone mutation, presenting with peripheral motor neuropathy, associated to Parkinsonism, and cerebellar ataxia: Case Report. *Parkinsonism Relat. Disord.* 22:e154. doi: 10.1016/j.parkreldis.2015.10.361

Vicario, M., Skaper, S. D., and Negro, A. (2014). The small heat shock protein HspB8: role in nervous system physiology and pathology. *CNS Neurol. Disord. Drug Targets* 13, 885–895. doi: 10.2174/1871527313666140711093344

Walker, L. C., Levine, H. III., Mattson, M. P., and Jucker, M. (2006). Inducible proteopathies. *Trends Neurosci.* 29, 438–443. doi: 10.1016/j.tins.2006.06.010

Yavarna, T., Al-Dewik, N., Al-Mureikhi, M., Ali, R., Al-Mesaifri, F., Mahmoud, L., et al. (2015). High diagnostic yield of clinical exome sequencing in Middle Eastern patients with Mendelian disorders. *Hum. Genet.* 134, 967–980. doi: 10.1007/s00439-015-1575-0

Ylikallio, E., Johari, M., Konovalova, S., Moilanen, J. S., Kiuru-Enari, S., Auranen, M., et al. (2014). Targeted next-generation sequencing reveals further genetic heterogeneity in axonal Charcot-Marie-Tooth neuropathy and a mutation in HSPB1. *Eur. J. Hum. Genet.* 22, 522–527. doi: 10.1038/ejhg.2013.190

Ylikallio, E., Konovalova, S., Dhungana, Y., Hilander, T., Junna, N., Partanen, J. V., et al. (2015). Truncated HSPB1 causes axonal neuropathy and impairs tolerance to unfolded protein stress. *BBA Clin* 3, 233–242. doi: 10.1016/j.bbacli.2015.03.002

Zhai, J., Lin, H., Julien, J. P., and Schlaepfer, W. W. (2007). Disruption of neurofilament network with aggregation of light neurofilament protein: a common pathway leading to motor neuron degeneration due to Charcot-Marie-Tooth disease-linked mutations in NFL and HSPB1. *Hum. Mol. Genet.* 16, 3103–3116. doi: 10.1093/hmg/ddm272

Conflict of Interest Statement: The authors declare that the research was conducted in the absence of any commercial or financial relationships that could be construed as a potential conflict of interest.

frontiers in Molecular Biosciences

REVIEW
published: 01 December 2016
doi: 10.3389/fmolb.2016.00079

Mutations in the Human AAA+ Chaperone p97 and Related Diseases

*Wai Kwan Tang and Di Xia **

Laboratory of Cell Biology, Center for Cancer Research, National Cancer Institute, National Institutes of Health, Bethesda, MD, USA

A number of neurodegenerative diseases have been linked to mutations in the human protein p97, an abundant cytosolic AAA+ (ATPase associated with various cellular activities) ATPase, that functions in a large number of cellular pathways. With the assistance of a variety of cofactors and adaptor proteins, p97 couples the energy of ATP hydrolysis to conformational changes that are necessary for its function. Disease-linked mutations, which are found at the interface between two main domains of p97, have been shown to alter the function of the protein, although the pathogenic mutations do not appear to alter the structure of individual subunit of p97 or the formation of the hexameric biological unit. While exactly how pathogenic mutations alter the cellular function of p97 remains unknown, functional, biochemical and structural differences between wild-type and pathogenic mutants of p97 are being identified. Here, we summarize recent progress in the study of p97 pathogenic mutants.

Keywords: VCP/p97, structure and function, mutations, conformational changes, multisystem diseases

OPEN ACCESS

Edited by:
Alberto J. L. Macario, University of Maryland at Baltimore, USA; IEMEST, Italy

Reviewed by:
Leonid Breydo, University of South Florida, USA
Eugene Anatolievich Permyakov, Institute for Instrumentation in Biology of the Russian Academy of Sciences, Russia
Axel Mogk, University of Heidelberg, Germany

***Correspondence:**
Di Xia
xiad@mail.nih.gov

Specialty section:
This article was submitted to Protein Folding, Misfolding and Degradation, a section of the journal Frontiers in Molecular Biosciences

Received: *25 August 2016*
Accepted: *18 November 2016*
Published: *01 December 2016*

Citation:
Tang WK and Xia D (2016) Mutations in the Human AAA+ Chaperone p97 and Related Diseases. Front. Mol. Biosci. 3:79. doi: 10.3389/fmolb.2016.00079

P97 ASSOCIATED DISEASES

Multisystem Proteinopathy (MSP)

MSP1 (OMIM #167320, also called *Inclusion bodies myopathy with Paget's disease of bone and frontotemporal dementia, IBMPFD*) is an autosomal dominant disorder, meaning a single copy of the altered gene from either parent is sufficient to cause the disease. There are also cases of new mutations occurring in individuals with no family history of the disorder. The disease is traced to mutations in the gene that encodes p97, also known as VCP (valosin-containing protein) (Kimonis et al., 2000). MSP1 can affect multiple tissues including muscles, bones, and brain (Benatar et al., 2013; Kim et al., 2013). The first symptom of the disease is often muscle weakness (IBM, inclusion body myopathy), which typically appears late in life when the patient is at the age of 50–60 years old, and is found in more than 90% of cases. Half of the cases develop Paget's disease of the bone (PD), which interferes with the recycling process of new bone tissue replacing old one, causing abnormal bone formation. Bone pain, particularly in the hips and spine, is common. One-third of the cases also involve a brain condition called frontotemporal dementia (FTD). This disorder progressively damages parts of the brain that control reasoning, personality, social skills, speech and language, leading to personality changes, a loss of judgment and inappropriate social behavior. So far, more than 20 missense amino acid substitutions on p97 have been identified in MSP1 patients, all located in the N-terminal and D1 domains of the protein and none is found in the D2 domain (**Figure 1A** and **Table 1**).

Familial Amyotrophic Lateral Sclerosis (FALS)

ALS or Lou Gehrig's disease is a progressive neurodegenerative disease that affects the motor neurons in the brain and spinal cord. When these nerve cells die, the brain loses the ability

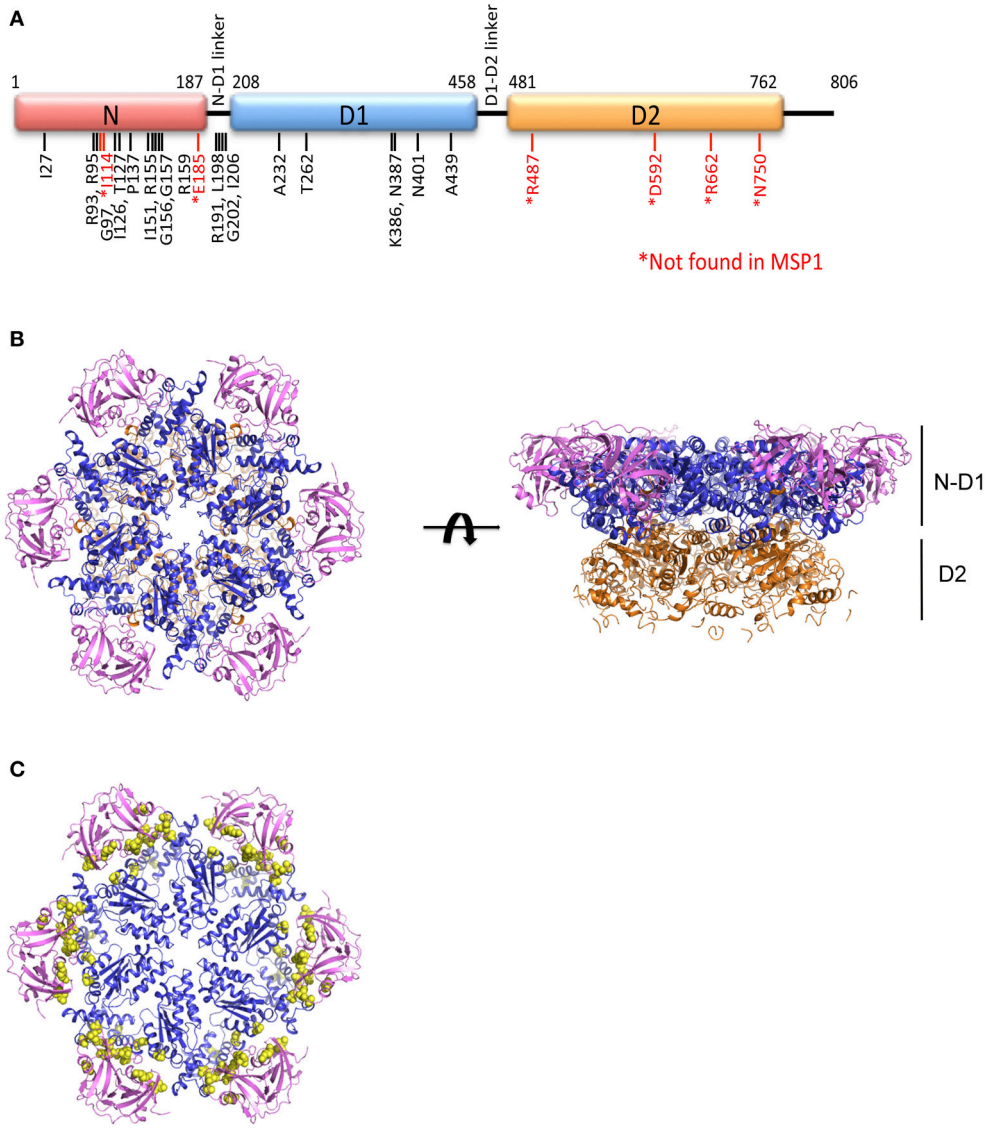

FIGURE 1 | Structure of the AAA ATPase p97. (A) Schematic domain organization of a p97 subunit showing the three structural domains: N-terminal N domain and two ATPase domains D1 and D2, and the positions of pathogenic mutations. **(B)** Ribbon representation of the top and side views of the hexameric structure of ^{FL}p97 (PDB:3CF2, Davies et al., 2008). The N domain is in purple, D1 domain in blue and D2 domain in gold. **(C)** The top view of ^{ND1}p97 structure showing the location of pathogenic mutations. Selected pathogenic mutations (residue I27, R93, I126, P137, R155, R191, L198, I206, A232, T262, N387, N401, A439) are represented as yellow spheres on the ribbon diagram of ^{ND1}p97 with ADP bound (PDB: 1E32, Zhang et al., 2000).

to control muscle movement, causing complete paralysis in late stages of the disease and eventually death. In about 90% of cases, the cause of ALS is sporadic, which means they are not inherited. Pathological hallmarks of ALS are pallor of corticospinal tract due to loss of motor neurons, the presence of ubiquitin-positive inclusions and the deposition of pathological TDP-43 aggregates. The cause of this sporadic ALS is not well understood; it may be due to a combination of environmental and genetic risk factors. About 10% of cases are considered "familial ALS" (FALS, OMIM #613954). In these cases, more than one individual in the family develops ALS and sometimes family members have FTD as well. Mutations in at least 18 genes have been identified in FALS cases, with mutations in the p97 gene contributing <1–2% (**Table 1**) (Johnson et al., 2010; Koppers et al., 2012; Kwok et al., 2015).

Charcot-Marie-Tooth Disease, Type 2Y (CMT2Y)

CMT2Y (OMIM #616687) is an autosomal dominant axonal peripheral neuropathy characterized by distal muscle weakness and atrophy associated with length-dependent sensory loss. The disease CMT is named after the three physicians who first accurately described it in 1886: Jean-Martin Charcot and Pierre Maries in France, and Howard Henry Tooth in England. Its principal features include slowly progressive muscular atrophy,

TABLE 1 | Pathogenic mutations in p97.

	Change in amino acid	Change in gene	Location in protein	Phenotype	References
I27	I27V	79A>G	N domain	IBM, FTD, PDB	Rohrer et al., 2011; Majounie et al., 2012; Weihl et al., 2015
R93	R93C	277C>T	N domain	IBM, PDB, FTD	Guyant-Maréchal et al., 2006; Hübbers et al., 2007
	R93H	278G>A	N domain	HSP	Neveling et al., 2013
R95	R95C	283C>T	N domain	IBM, ALS	Weihl et al., 2015
	R95H	284G>A	N domain	AD	Kaleem et al., 2007
	R95G	283C>G	N domain	IBM, PDB, FTD, ALS	Watts et al., 2004; Kimonis et al., 2008b
G97	G97E	290G>A	N domain	IBM, PDB, FTD	Gu et al., 2012; Jerath et al., 2015
I114	I114V	340A>G	N domain	ALS	Koppers et al., 2012
I126	I126F	376A>T	N domain	IBM, PDB, FTD	Matsubara et al., 2016
T127	T127A	379A>G	N domain	FTD, AD	Shi et al., 2016
P137	P137L	410C>T	N domain	IBM, PDB, FTD	Stojkovic et al., 2009; Palmio et al., 2011
I151	I151V	451A>G	N domain	IBM, ALS	DeJesus-Hernandez et al., 2011; Boland-Freitas et al., 2016
R155	R155S	463C>A	N domain	IBM, PDB, FTD	Stojkovic et al., 2009
	R155L	464G>T	N domain	IBM, PDB, FTD	Kumar et al., 2010
	R155H	464G>A	N domain	IBM, PDB, FTD, ALS	Watts et al., 2004; Hübbers et al., 2007; Kimonis et al., 2008a; Viassolo et al., 2008; Stojkovic et al., 2009; González-Pérez et al., 2012
	R155C	463C>T	N domain	IBM, PDB, FTD, ALS	Watts et al., 2004; Schröder et al., 2005; Guyant-Maréchal et al., 2006; Gidaro et al., 2008; González-Pérez et al., 2012
	R155P	464G>C	N domain	IBM, PDB, FTD	Watts et al., 2004
G156	G156C	466G>C	N domain	ALS	Segawa et al., 2015
	G156S	466G>A	N domain	IBM, PDB, FTD	Komatsu et al., 2013
G157	G157R	469G>C	N domain	IBM, PDB, FTD	Djamshidian et al., 2009
		469G>A	N domain	IBM, PDB, FTD	Stojkovic et al., 2009
M158	M158V	472A>G	N domain	PDB, ALS	Ayaki et al., 2014
R159	R159G	475C>G	N domain	ALS, FTD	Johnson et al., 2010
	R159C	475C>T	N domain	IBM, FTD, PD, ALS	Bersano et al., 2009; Chan et al., 2012; de Bot et al., 2012; González-Pérez et al., 2012
	R159H	476G>A	N domain	IBM, PDB, FTD, ALS	Haubenberger et al., 2005; Stojkovic et al., 2009; van der Zee et al., 2009; Koppers et al., 2012
E185	E185K	553C>T	N domain	CMT2Y	Gonzalez et al., 2014
R191	R191G	571C>G	N-D1 linker	IBM, ALS	González-Pérez et al., 2012
	R191Q	572G>A	N-D1 linker	IBM, PDB, FTD, ALS	Watts et al., 2004; Kimonis et al., 2008b; Stojkovic et al., 2009; Johnson et al., 2010; González-Pérez et al., 2012
L198	L198W	593T>G	N-D1 linker	IBM, PDB, FTD	Watts et al., 2007; Kumar et al., 2010
G202	G202W	604G>T	N-D1 linker	IBM, FTD	Figueroa-Bonaparte et al., 2016
I206	I206F	616A>T	N-D1 linker	IBM, PDB, FTD	Peyer et al., 2013
A232	A232E	695C>A	D1 domain	IBM, PDB	Watts et al., 2004; Kimonis et al., 2008b
T262	T262A	784A>G	D1 domain	IBM, PDB, FTD	Spina et al., 2008
K386	K386E	1158T>C	D1 domain	IBM	Lévesque et al., 2016
N387	N387H	1159A>C	D1 domain	IBM, FTD	Watts et al., 2007
	N387S	1160A>G	D1 domain	IBM, PDB, FTD	Liewluck et al., 2014
	N387T	1160A>C	D1 domain	ALS	Abramzon et al., 2012
N401	N401S	1202A>G	D1 domain	FTD, ALS	Shi et al., 2016
A439	A439S	1315G>T	D1 domain	IBM, PDB	Stojkovic et al., 2009
	A439P	1315G>C	D1 domain	IBM, PDB, FTD	Shi et al., 2012; Kamiyama et al., 2013
	A439G	1316C>G	D1 domain	IBM, FTD	Figueroa-Bonaparte et al., 2016
R487	R487H	1460G>A	D2 domain	FTD, ALS	Hirano et al., 2015
D592	D592N	1774G>A	D2 domain	ALS	Johnson et al., 2010
R662	R662C	1984C>T	D2 domain	ALS	Abramzon et al., 2012
N750	N750S	2249A>G	D2 domain	ALS	Kenna et al., 2013

IBM, inclusion body myopathy; PDB, Paget's disease of bone; FTD, frontotemporal dementia; PD, Parkinson disease; ALS, amyotrophic lateral sclerosis; CMT2Y, Charcot-Marie-Tooth disease.

which initially involves the feet and legs, but does not affect the upper extremities until several years later. CMT is a clinically and genetically heterogeneous disorder and is divided into subtypes based on genetics, pathology, and electrophysiology of the disease (Dyck and Lambert, 1968). The subtype CMT2Y has missense mutations in the p97 gene, which were identified in patients (Gonzalez et al., 2014; Jerath et al., 2015) (**Table 1**). As most patients with CMT2Y do not obtain a genetic diagnosis, the number of cases having mutations in p97 may be higher than expected.

STRUCTURAL AND BIOCHEMICAL DIFFERENCES BETWEEN WILD-TYPE AND PATHOGENIC p97

Structure of p97

P97 is a Type II AAA^+ ATPase (two AAA ATPase domains) and a homo-hexamer with each subunit consisting of three main domains: the N-terminal domain (N domain) followed by two tandem ATPase domains (D1 and D2 domains), which are connected by two short polypeptides (N-D1 and D1-D2 linker). Both the D1 and D2 domains possess all essential sequence elements (Walker A and B motifs) for ATP hydrolysis and share high amino acid sequence identity. The N domains are known for interacting with various cofactors and adaptor proteins. Cofactors of p97 are defined as those proteins that are necessary for p97 function, whereas adaptors are those that target p97 to different cellular locations (Xia et al., 2016). At first glance, a p97 hexamer appears to have two rings of different sizes stacked on top of each other. The crystal structure of full-length wild-type p97 (^{FL}p97) reveals that the two ATPase domains form two concentric rings, called D1 and D2 rings, and the N domains are attached to the periphery of the D1 ring (DeLaBarre and Brunger, 2003) (**Figure 1B**). The hexameric architecture of p97 is maintained by interactions among the D1 domains (Wang et al., 2003), as isolated D2 domains are prone to form heptamers (Davies et al., 2008). This hexameric structure of p97 is very stable and can withstand treatment of up to 6M urea and its assembly does not require the addition of nucleotide (Wang et al., 2003).

More than 20 amino acid mutations have been identified in p97 from MSP1 or IBMPFD patients and these mutations appear to be randomly scattered throughout the sequence of the N and D1 domain of p97 (**Figure 1A**). However, when mapped to the structure of ^{FL}p97, these MSP1 mutations were found exclusively at the interface between the N and D1 domain (**Figure 1C**). None was found at the sites where ATP hydrolysis occurs. Structural studies using X-ray crystallography show the pathogenic mutants retain a hexameric ring structure and share identical overall folding with the wild-type protein (Tang et al., 2010).

Amount of Pre-bound ADP

One important characteristic of p97 related to binding of nucleotides is the presence of pre-bound ADP at the D1 domain, which was hinted at by p97 crystallization experiments in the presence of different types of nucleotides. Crystallographic efforts with wild-type p97 yielded ADP invariably bound to the D1 domain, while various types of nucleotides bound to the D2 domain (Zhang et al., 2000; DeLaBarre and Brunger, 2003), leading to the misconception that the D1 domain was incapable of exchanging for different types of nucleotides. Subsequent experiments led to the realization that the nucleotide state at the D1 domain of p97 is tightly regulated (Davies et al., 2005). Without the addition of any ADP during the course of purification, isolated wild-type p97 was shown to have tightly bound ADP at the D1 domain with at least 3 molecules of ADP per p97 hexamer (DeLaBarre and Brunger, 2003; Briggs et al., 2008; Tang and Xia, 2013). This phenomenon is referred to as the pre-bound ADP at the D1 domain. Apparently, a subset of D1 domains in the hexameric p97 is occupied by ADP, thus preventing saturation of all D1 sites with ATP, which has a higher binding affinity for an empty D1 site (Tang et al., 2010; Tang and Xia, 2013). Thus, structural studies of the conformational change of wild-type p97, especially at low resolution where the nucleotide state is uncertain, should take the feature of the pre-bound ADP into account when interpreting the results.

Compared with wild-type p97, pathogenic mutants have less pre-bound ADP (Tang and Xia, 2013). More importantly, these mutants are not able to tightly regulate the nucleotide state of the D1 domain, as does the wild-type p97. They allow ATP to displace pre-bound ADP. Consequently, a uniform binding of ATP to the D1 sites can be observed (Tang et al., 2010; Tang and Xia, 2013).

Communication among Domains and Subunits

In each biological unit of p97, there are six identical subunits, containing a total of 18 main domains. The proper function of p97 therefore relies on a coordinated interplay among these domains. For instance, the conformation of the N domain has a strong influence over the ATPase activity of p97. Fixing the N domain position by introducing a disulfide bond between the N and the D1 domain reduces p97 ATPase activity (Niwa et al., 2012). The binding of adaptor proteins such as p47 and p37 to the N domain alter the overall ATPase activity of p97 (Meyer et al., 1998; Zhang et al., 2015). On the other hand, the nucleotide states of the D1 domains control the conformations of the N domain of p97 (Tang et al., 2010; Banerjee et al., 2016; Schuller et al., 2016).

The binding of ATP in the D1 domain is required for the activity of the D2 domain, and vice versa (Ye et al., 2003; Nishikori et al., 2011; Tang and Xia, 2013). One of the possible mechanisms of communication between these two ATPase domains is through the D1-D2 linker. This 22-residue linker peptide contains a highly conserved N-terminal half that appears to be a random loop and extends to the vicinity of both the D1 and D2 nucleotide-binding sites, as illustrated in the ^{FL}p97 structures (Davies et al., 2008). The inclusion of the D1-D2 linker to the N-D1 truncate of p97 activates the ATPase activity of the D1 domain (Chou et al., 2014; Tang and Xia, 2016).

Among the three domains of a p97 subunit, the D1 domain seems to play a role consistent with (1) maintaining the hexameric architecture of p97 (Wang et al., 2003), (2) driving the conformational change of the N domain (Tang et al., 2010; Banerjee et al., 2016; Schuller et al., 2016), (3) regulating the

activity of the D2 domain (Tang and Xia, 2013), and (4) communicating with and controlling the nucleotide states of D1 domains of neighboring subunits (Tang and Xia, 2013, 2016; Zhang et al., 2015). All these suggest an intricate communication network centered on the D1 ring of the hexameric p97.

Instead of causing structural changes to the protein, pathogenic p97 mutations appear to alter the function of p97 by perturbing the communication network between domains. Our experiments have shown that while the domain communication within an individual subunit remains undisturbed, communication between neighboring subunits in pathogenic mutants has changed, leading to uncoordinated nucleotide binding among different subunits (Tang et al., 2010; Tang and Xia, 2013). Specifically, the mutations weaken the ADP-binding affinity at the D1 domain and thus relax the tight regulation of the nucleotide states at the D1 domains (Tang and Xia, 2013). As a result, more ATPase domains of mutants are engaged in ATP hydrolysis compared to wild-type p97, giving rise to an apparent more active protein with higher ATPase activity (Halawani et al., 2009; Manno et al., 2010; Tang et al., 2010; Niwa et al., 2012).

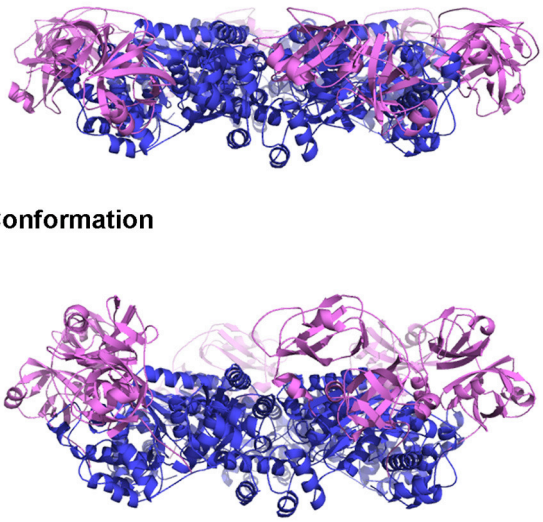

FIGURE 2 | The Up- and Down-conformation of p97 N domain. Ribbon presentation of the structure of the hexameric ^{ND1}p97. The D1 domains are colored in blue and the N domains are in purple.

Nucleotide-Driven Conformational Changes

It is generally believed that p97 functions as a molecular extractor, pulling damaged or unwanted proteins from large molecular or cellular assemblies. It does so by undergoing ATP-dependent conformational changes to generate mechanical forces necessary for substrate extraction (Acharya et al., 1995; Latterich et al., 1995; Rabouille et al., 1995; Xu et al., 2011; Ramanathan and Ye, 2012; Xia et al., 2016). Although exactly how p97 extracts substrate from a large molecular assembly remains unclear, progress has been made in identifying different conformations. Low-resolution cryo-EM studies showed a moderate rotational movement between the D1 and D2 rings in association with changes in the size of the D2 central pore in response to the presence of different nucleotide (Rouiller et al., 2002). However, a similar study by another group suggested a different domain movement (Beuron et al., 2003). The insufficient resolution to determine the exact nucleotide state in each domain of p97 in these studies could be the cause of the inconsistency.

Earlier crystallographic studies showed the D1 domains are always bound with ADP, regardless of the presence of different types of nucleotides in solution, and the N domains are in a conformation that is coplanar with the D1 ring (Zhang et al., 2000; DeLaBarre and Brunger, 2003; Davies et al., 2008). This N domain conformation when the D1 domain is occupied with ADP is termed the Down-conformation (**Figure 2**) (Tang et al., 2010). On the other hand, the nucleotide-binding state in the D2 domains is determined by what is present in solution (either bound ADP, AMP-PNP, or ADP-AlFx). Therefore, these crystallographic data can only reveal the conformational changes associated with the nucleotide state at the D2 domain. The D2 ring undergoes a rotation relative to the D1 ring and size of the D2 central pore changes during ATP cycle, but whether the binding or the hydrolysis of ATP triggers the opening remains controversial (Davies et al., 2005; Pye et al., 2006; Banerjee et al., 2016; Hänzelmann and Schindelin, 2016b; Schuller et al., 2016). It is worth pointing out that, for the same nucleotide state, non-uniform domain conformation is observed in subunits within a crystallographic asymmetric unit, and the magnitude of such a difference is comparable to that observed between different nucleotide states (Davies et al., 2008). It is unclear if the conformational differences observed in various nucleotide states of the D2 domain represent actual changes in solution.

Recently, by genetically modifying some regions in the D2 domain, Hanzelmann and colleagues were able to determine the crystal structure of full-length p97 with both ATPase domains either empty or bound with ATPγS (non-hydrolyzing ATP analog) (Hänzelmann and Schindelin, 2016b). The binding of ATPγS opens the D2 pore and generates a rotational movement between the two concentric rings. However, questions remain concerning the physiological relevance of these observations, as the effect of these mutations on the function of p97 was not characterized.

Pathogenic mutations weaken the ADP binding interactions at D1 sites and alter the regulation imposed among neighboring subunits. Effects of these mutations, though very subtle, are sufficient to make these mutants achieve uniform N domain conformation or loss of asymmetry within the hexamer, which is a property that facilitates crystallographic studies. When ATPγS binds to the D1 sites of the N-D1 fragment of p97, the N domains move to a position above the D1 ring, which is termed the Up-conformation (**Figure 2**) (Tang et al., 2010). Such nucleotide-dependent conformational switch has also been detected for only a subset of subunits in wild-type p97 in solution (Tang et al., 2010). The nucleotide-dependent conformational movement of

the N domain has been confirmed by recent studies of full-length wild-type p97 using single particle cryo-EM (Banerjee et al., 2016; Schuller et al., 2016). Instead of having all six p97 subunits in the Up-conformation in the presence of ATPγS or AMP-PMP, Schuller and colleagues observed a distribution of N domain conformations, either in Up- or Down-conformation within a hexamer (Schuller et al., 2016). By contrast, Benerjee and colleagues only reported a single conformation that N domains of all subunits were in the Up-conformation, despite the very weak EM density for the N domain (Banerjee et al., 2016). More interestingly, crystal structure of the full-length p97 with genetically modified D2 domain showed the N domain remains in the Down-conformation when the D1 domain is bound with ATPγS (Hänzelmann and Schindelin, 2016b). Thus, whether the six nucleotide-binding sites in the D1 ring bind ATP in a concerted manner leading to symmetrical N domain movement or in a sequential/random manner leading to asymmetrical hexamer has yet to come to a consensus. However, the presence of tightly pre-bound ADP in the D1 domains of a subset of p97 subunits may have already suggested a non-uniform nucleotide binding of p97.

A model was proposed to illustrate the regulatory mechanism of ATP binding and hydrolysis in the D1-ring and how it might influence the ATPase activity of the D2 ring (**Figure 3A**) (Tang et al., 2010; Tang and Xia, 2013). In this model, there are four states for a subunit of a wild-type p97 hexamer, each representing one specific nucleotide-binding state. (1) There is an Empty state where no nucleotide is bound at the D1 site; the conformation of the N- domain is unknown (pink sphere). Noticed that for a wild-type p97 hexamer, only a subset of subunits is in the Empty state because of the pre-bound ADP. The N domains for those with pre-bound ADP are in the Down-conformation and are shown as pink sphere labeled with D. (2) When ATP enters the D1 site (ATP state), it is only allowed in the Empty subunits and not allowed in those with pre-bound ADP. The subunits with ATP bound have their N domain adopt the Up-conformation (pink sphere labeled with T), which has been determined from the crystal structure of IBMPFD mutants (Tang et al., 2010). (3) The hydrolysis of ATP to ADP at the D1 domain brings the N domain back to the Down-conformation, which is supported by the crystallographic data from both wild-type p97 and IBMPFD mutants (Zhang et al., 2000; DeLaBarre and Brunger, 2003; Huyton et al., 2003; Tang et al., 2010). (4) Importantly, it was proposed that there are two ADP-bound states existing in equilibrium for a subunit: an ADP-locked and ADP-open state. Both ADP-open and ADP-locked states can coexist for different subunits in a p97 hexamer. The ADP-locked state is inspired by the presence of pre-bound ADP at the D1 site in the wild-type p97, which is difficult to remove (Davies et al., 2005; Briggs et al., 2008; Tang et al., 2010). The ADP-open state represents the situation where ADP has a reduced affinity to the D1 site ready to be exchanged. (5) It was also proposed that the D2 domain of a subunit is permitted to hydrolyze ATP only if its cognate D1 domain is occupied by ATP.

A major difference between the wild-type and mutant p97 was proposed to be the regulation of the inter-conversion or the equilibration between the ADP-open and ADP-locked state (**Figure 3B**). In the wild type, the equilibration favors the ADP-locked state, whereas in the mutant, it prefers the ADP-open state. This means, in the case of a wild-type p97 hexamer, that ATP can only get into a subset of D1 domains, driving corresponding N domains to the Up-conformation. This non-uniform nucleotide-binding state in the wild-type p97 in the presence of ATP generates an asymmetry in the N domain conformation in a hexameric p97. In p97 mutants, the equilibration between ADP-locked and ADP-open states is shifted toward the latter. As a result,

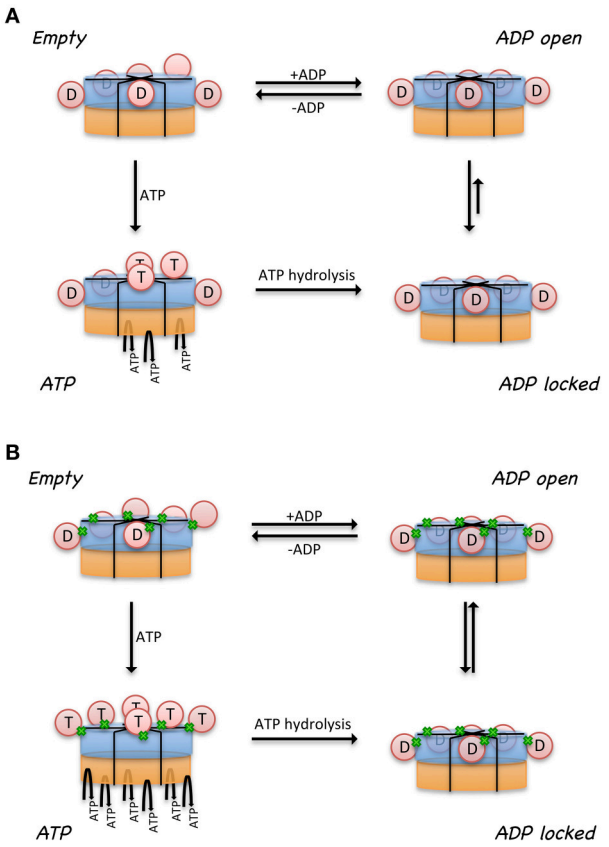

FIGURE 3 | Model proposed for the relationship between control of N domain conformation and ATPase activity in p97. Cartoon representation of a hexameric p97 shows the D1 domains in blue, D2 domains in orange, and the N domains in pink circle. N domains that are labeled with the letter "D" are in the Down-conformation and their corresponding D1 domains are occupied by ADP. N domains that are labeled with the letter "T" are in the Up-conformation and their corresponding D1 domains are occupied with ATP. Only those subunits that have their D1 domains occupied by ATP are capable of hydrolyzing ATP in their D2 domains. The conformation of the N domains is not determined when their corresponding D1 domains are empty (No label in the N domain). Proposed nucleotide binding and hydrolysis cycle for **(A)** the wild-type p97 and for **(B)** mutant p97. Mutations are represented by the green dots at the interface between N and D1 domains. Empty state indicates a state in the absence of added ATP or ADP. The ATP state is the presence of added ATP. The ADP-locked state refers to a subset of subunits where ADP in the D1 domain is very tightly bound, whereas the ADP-open state refers to a subset of subunits where ADP molecules in the D1 domains are able to exchange nucleotides with those in solution. The ADP-locked and ADP-open states are in equilibrium in solution.

a uniform nucleotide-binding state at the D1 domains and a synchronized N domain movement can be reached in the presence of a sufficiently high concentration of ATP, forming symmetrical hexamers. More importantly, this model implies that the function of p97 requires an asymmetry in the D1 nucleotide-binding state in a hexameric ring. We should also point out that a consequence of this model is that the p97 mutants are higher in ATPase activity, because there are more ATP molecules occupying the D1 sites, which is required for ATP hydrolysis in the D2 domain (Tang and Xia, 2013).

Although the role of the conformational changes observed in p97 during the ATP cycle in relation to its physiological function remains unclear, the opening and closing of the D2 pore as well as the up-and-down swinging motion of the N domain have consistently been observed. As experimental evidence increasingly points to a role played by p97 in extracting protein substrates from its interacting partners, the coordinated up-and-down motion of the N domain at the D1 ring and the opening and closing of the D2 ring within the hexamer during the ATP hydrolysis could conceivably generate a pulling force to extract protein substrates from various organelles. Taking ERAD as an example, p97 is recruited to the ER membrane via interaction between the N domain and adaptor proteins. The swinging movement of the N domain would create a pulling force to extract the protein substrates from the ER membrane. Conceivably, the generation of this pulling force requires a highly sophisticated coordination among the subunits of p97. As shown from biochemical and structural studies, individual subunits of pathogenic mutants fail to communicate, resulting in uniform movement of the N domain. This un-coordinated conformational change in pathogenic p97 may be why mutants fail to process protein substrates effectively, thus leading to accumulation of protein inclusions.

Interacting with Protein Partners

Over 30 different cofactor/adaptor proteins have been identified; they interact mostly with the N domain but in some cases the C-terminal tail of p97. These proteins either function as adaptors that recruit p97 to a specific subcellular compartment or substrate, or serve as cofactors that help in substrate processing. They are found in many different subcellular structures such as mitochondria, endoplasmic reticulum membrane, nuclear membrane, and Golgi body. Hence, their bindings lead p97 to function in different cellular pathways.

Several common binding-domains or motifs, such as the UBX domain, the PUB-domain, and the VCP-interacting motif (VIM), have been found to interact with p97. Despite differences in structures among these binding motifs, most of them bind to the N domain at the interface between the two subdomains, as shown from crystal structures of these binary complexes (**Figure 4**). This observation provides an explanation for the mutually exclusive binding pattern observed biochemically among various p97-interacting proteins (Meyer et al., 2000; Rumpf and Jentsch, 2006). Intriguingly, while all six binding interfaces on the N domains of a hexameric p97 are available, crystal structures of

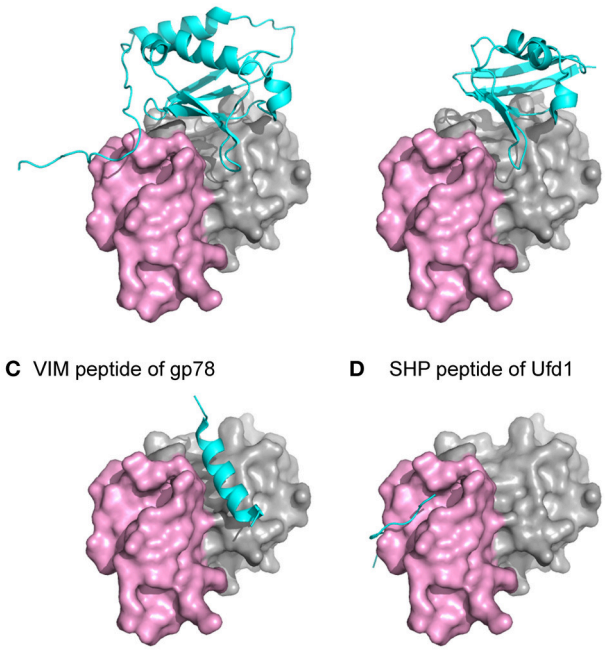

FIGURE 4 | Structures of p97 in complex with interacting proteins. The N domain of p97 is shown as a surface representation with the two subdomains, double ψ-barrel and β-barrel, in gray and violet, respectively. Individual domains or peptides from different p97-interacting proteins are shown as a cyan cartoon. All the structures were superposed with the N domain of p97 and presented in the same orientation. **(A)** PDB:1S3S (Dreveny et al., 2004). **(B)** PDB:4KDI (Kim et al., 2014). **(C)** PDB:3TIW (Hänzelmann and Schindelin, 2011). **(D)** PDB:5C1B (Hänzelmann and Schindelin, 2016a).

the complexes showed the binding stoichiometry is not more than 3 molecules of adaptor proteins to 1 ^{FL}p97 hexamer (Dreveny et al., 2004; Hänzelmann and Schindelin, 2016a). Consistently, binding studies using the isothermal calorimetry (ITC) technique showed a similar effect (Hänzelmann et al., 2011). Indeed, the sharing of the same binding interface and the substoichiometric binding of the interacting protein to p97 led to the hierarchical binding model for p97 to fulfill specific cellular functions (Hänzelmann et al., 2011; Meyer et al., 2012).

The impact of pathogenic mutations on the interactions between p97 and adaptor proteins has been investigated. So far, there is no structural data in the literature that demonstrate the difference in adaptor protein binding between wild-type and mutant p97. Using isolated ^{FL}p97, it was shown biochemically that cofactors p37 and p47 regulate ATPase activity of p97 in a concentration-dependent manner. By contrast, mutant p97 lost this regulation although it still interacts with the cofactors (Zhang et al., 2015). Results derived from cell-based experiments from different groups are not always consistent (Fernández-Sáiz and Buchberger, 2010; Manno et al., 2010). For example, in one study, isolated mutant p97 exhibited the same binding as wild-type p97 toward the adaptor proteins p47, Ufd1-Npl4, and E4B, the human UFD-2 homolog. However, mutants in the

same study showed impaired binding to ubiquitin ligase E4B in the presence of Ufd1-Npl4. *In vivo* pull-down experiments using HEK293 cells showed reduced binding toward the E4B and enhanced binding toward ataxin 3, thus resembling the accumulation of mutant ataxin 3 on p97 in spinocerebellar ataxia type 3 (Fernández-Sáiz and Buchberger, 2010). In another study, however, similar *in vivo* pull-down were carried out showing enhanced binding of the Ufd1-Npl4 pair by IBMPFD mutants but not for p47 (Manno et al., 2010). An increased amount of cofactor pair Ufd1-Npl4 was detected in association with mutant p97 (Fernández-Sáiz and Buchberger, 2010; Manno et al., 2010). However, no significant difference was found in the binding of the same adaptor to either wild-type or pathogenic mutants when using isolated protein for pull-down assays (Hübbers et al., 2007; Fernández-Sáiz and Buchberger, 2010). This inconsistency may be due to the difference in the N domain conformation, which depends on the nucleotide state at the D1 domain of p97. Such an effect can be demonstrated by the seven-fold decrease in the binding affinity of SVIP to pathogenic p97 in the presence of ATPγS (Hänzelmann et al., 2011). So far, two nucleotide-dependent conformations (the Up- and Down-conformation) of the N domain have been observed in p97. In both cases, the binding interface for adaptor proteins is available but orients differently. In the Up-conformation, the binding interface faces outward to the side of the hexameric ring, while in Down-conformation, the binding interface faces down toward the D2 ring. As the sizes and shapes of adaptor proteins vary, it is conceivable that the binding of some adaptor proteins will be hindered by spatial restrictions caused by different N domain conformations.

FUNCTIONAL DEFECTS IN PATHOGENIC p97

The diverse biological roles played by p97 in various cellular activities, such as membrane fusion, DNA repair, and protein homeostasis, have been reported and extensively reviewed (Dantuma and Hoppe, 2012; Meyer et al., 2012; Yamanaka et al., 2012; Franz et al., 2014; Meyer and Weihl, 2014; Xia et al., 2016). These important functional roles are reflected by the sequence conservation of the protein and indicate that mutations in p97 would have severe functional consequences. Despite embryonic lethality in p97 knock-out mice (Müller et al., 2007) and accelerated MSP1 pathology in homozygote p97 mutant mice (Nalbandian et al., 2012), pathogenic mutations in p97 seems well tolerated and affect only a subset of its functions, as there is no evidence of developmental abnormalities in affected individuals (Kimonis et al., 2008b). This is consistent with the fact that MSP1 is a late-onset disease and clinical pathology of MSP1 seems to point to a defective function in maintaining protein homeostasis.

Pathological features in MSP1 patient samples include rimmed vacuoles found in muscle tissues that stain positive for p97 and ubiquitin (Watts et al., 2004) and nuclear inclusions in neurons, which also stained positive for p97 and polyubiquitin in brain tissues (Kimonis and Watts, 2005; Schröder et al., 2005). This common pathologic feature found in MSP1 affected tissues suggests a defective function of pathogenic p97 mutants in protein degradation/trafficking pathways. Similar phenotypes can be reproduced in *in vitro* cultured cells, either transfected with disease-associated p97 mutants (Weihl et al., 2006; Janiesch et al., 2007) or derived from patient tissues (Ritz et al., 2011). Moreover, studies using various animal models further strengthen the linkage between mutations in p97 and MSP1. Transgenic mice bearing a p97 mutation (R155H or A232E) display dominant-negative phenotypes similar to MSP1 patients (Weihl et al., 2007; Custer et al., 2010); mutant p97 (R155H) knock-in mice display progressive muscle weakness and other MSP1-like symptoms (Badadani et al., 2010).

One of the best studied cellular functions of p97 is endoplasmic reticulum-associated degradation (ERAD) (Meyer et al., 2012). Protein substrates in the ER are labeled with polyubiquitin chains, recognized, and subsequently retrotranslocated by p97 across the ER membrane to the cytosol, where they are degraded by the proteasome. Failure to clear these polyubiquitinated protein substrates leads to ER stress. It has been shown that MSP1 mutants have impaired ERAD, leading to accumulation of ERAD substrates (Weihl et al., 2006; Erzurumlu et al., 2013).

Another characteristic that sets pathogenic mutants apart from wild-type p97 is their failure to form a ternary complex with ubiquitylated CAV1 (Ritz et al., 2011). CAV1 (caveolin-1) is a main constituent of caveolae, small invaginations on the plasma membrane. The degradation of CAV1 through the endocytic pathway requires mono-ubiquitin modification (Haglund et al., 2003; Parton and Simons, 2007). During maturation, CAV1 first forms SDS-resistant oligomers that associate to form larger assemblies in a cholesterol-dependent manner during exit from the Golgi apparatus. P97 binds to a mono-ubiquitylated cargo substrate, CAV1, on endosomes and is critical for its transport to endolysosomes. Blocking p97 binding of CAV1 with MSP1-associated mutations or its protein segregase activity with the Walker B motif mutation or the DBeQ inhibitor leads to accumulation of CAV1 at the limiting membrane of late endosomes (Ritz et al., 2011).

Besides ubiquitin, TAR DNA-binding protein-43 (TDP-43) is also found in protein inclusions in MSP1 affected tissues (Neumann et al., 2007; Weihl et al., 2008). TDP-43, the major pathological protein in ALS and FTD (Neumann et al., 2006), is primarily localized in the nucleus (Wang et al., 2001) and was suggested to play a role in transcription repression and other cellular processes (reviews please see Wang et al., 2008; Buratti and Baralle, 2009). Although how TDP-43 gets into the protein inclusions in tissue samples of MSP1 patients is unknown, it is believed that TDP-43 is a substrate for either proteasome or autophagic degradation (Caccamo et al., 2009; Wang et al., 2010), hence suggesting a role of p97 in autophagy, a degradation process involving the lysosomal machinery. The role of p97 in autophagy has been demonstrated in both mammalian and yeast cells, in which p97 has been found essential for the maturation of autophagosomes (Tresse et al., 2010). MSP1 mutants have also been observed to accumulate autophagosome markers p62 and LC3-II (Ju et al., 2009; Vesa et al., 2009; Tresse et al., 2010).

CONCLUSIONS AND PERSPECTIVE

Since the recognition of the linkage between MSP1 disease and the AAA protein p97 in 2001 (Kovach et al., 2001), there has been a steady increase in the number of pathogenic mutations being identified and increasing number of diseases associated with these mutations in p97. The association of the mutations with the disease calls for a clear understanding of the exact molecular function and its underlying mechanism of p97. Through comparative studies between wild type and mutants and using an array of genetic, biochemical, and structural methodologies, these mutants added a new dimension to our understanding on the structure and function of p97. Despite the progress made, a few fundamental mechanistic questions regarding the action of p97 remain unclear and require further engagement of the research community. First, what is the physiological significance of the conformational changes in p97? To answer this question, an *in vitro* system needs to be established to reconstruct the process identified *in vivo* for p97, which would allow us to investigate the role of p97 in a well-controlled manner and to pinpoint the steps in the reaction coordinates, which are affected by mutations. Secondly, studies are required to further identify properties of p97 that are affected by mutations, such as binding of adaptor/cofactor proteins. Finally, mutations in p97 can cause different diseases. How do cellular factors influence the ultimate clinical outcomes in patients? As a late-onset disease, individuals with p97 mutations can live a normal life for a long time without symptoms. Identifying the factors that delay the onset of the diseases and understanding how they interact with p97 can have a significant impact on those who are predisposed to the disease. The path to address these questions seems unlikely to be straight forward, as pathogenic mutations only manifest their effects in a subtle way and p97 involves in many cellular pathways. Nevertheless, optimism is warranted, given the progresses made in the past, that this path will lead us to the solutions to these unsolved issues.

ETHICS STATEMENT

The authors declare no competing financial interests.

AUTHOR CONTRIBUTIONS

All authors listed, have made substantial, direct and intellectual contribution to the work, and approved it for publication.

ACKNOWLEDGMENTS

We thank George Leiman for editorial assistance during the preparation of this manuscript. This research was supported by the Intramural Research Program of the National Cancer Institute.

REFERENCES

Abramzon, Y., Johnson, J. O., Scholz, S. W., Taylor, J. P., Brunetti, M., Calvo, A., et al. (2012). Valosin-containing protein (VCP) mutations in sporadic amyotrophic lateral sclerosis. *Neurobiol. Aging* 33, 2231.e2231–2231.e2236. doi: 10.1016/j.neurobiolaging.2012.04.005

Acharya, U., Jacobs, R., Peters, J. M., Watson, N., Farquhar, M. G., and Malhotra, V. (1995). The formation of Golgi stacks from vesiculated Golgi membranes requires two distinct fusion events. *Cell* 82, 895–904. doi: 10.1016/0092-8674(95)90269-4

Ayaki, T., Ito, H., Fukushima, H., Inoue, T., Kondo, T., Ikemoto, A., et al. (2014). Immunoreactivity of valosin-containing protein in sporadic amyotrophic lateral sclerosis and in a case of its novel mutant. *Acta Neuropathol. Commun.* 2, 172. doi: 10.1186/s40478-014-0172-0

Badadani, M., Nalbandian, A., Watts, G. D., Vesa, J., Kitazawa, M., Su, H., et al. (2010). VCP associated inclusion body myopathy and paget disease of bone knock-in mouse model exhibits tissue pathology typical of human disease. *PLoS ONE* 5:e13183. doi: 10.1371/journal.pone.0013183

Banerjee, S., Bartesaghi, A., Merk, A., Rao, P., Bulfer, S. L., Yan, Y., et al. (2016). 2.3 A resolution cryo-EM structure of human p97 and mechanism of allosteric inhibition. *Science* 351, 871–875. doi: 10.1126/science.aad7974

Benatar, M., Wuu, J., Fernandez, C., Weihl, C. C., Katzen, H., Steele, J., et al. (2013). Motor neuron involvement in multisystem proteinopathy: implications for ALS. *Neurology* 80, 1874–1880. doi: 10.1212/WNL.0b013e3182929fc3

Bersano, A., Del Bo, R., Lamperti, C., Ghezzi, S., Fagiolari, G., Fortunato, F., et al. (2009). Inclusion body myopathy and frontotemporal dementia caused by a novel VCP mutation. *Neurobiol. Aging* 30, 752–758. doi: 10.1016/j.neurobiolaging.2007.08.009

Beuron, F., Flynn, T. C., Ma, J., Kondo, H., Zhang, X., and Freemont, P. S. (2003). Motions and negative cooperativity between p97 domains revealed by cryo-electron microscopy and quantised elastic deformational model. *J. Mol. Biol.* 327, 619–629. doi: 10.1016/S0022-2836(03)00178-5

Boland-Freitas, R., Graham, J., Davis, M., Geevasinga, N., Vucic, S., and Ng, K. (2016). Late onset distal myopathy of the upper limbs due to p.Ile151Val mutation in VCP. *Muscle Nerve.* 54, 165–166. doi: 10.1002/mus.25073

Briggs, L. C., Baldwin, G. S., Miyata, N., Kondo, H., Zhang, X., and Freemont, P. S. (2008). Analysis of nucleotide binding to P97 reveals the properties of a tandem AAA hexameric ATPase. *J. Biol. Chem.* 283, 13745–13752. doi: 10.1074/jbc.M709632200

Buratti, E., and Baralle, F. E. (2009). The molecular links between TDP-43 dysfunction and neurodegeneration. *Adv. Genet.* 66, 1–34. doi: 10.1016/s0065-2660(09)66001-6

Caccamo, A., Majumder, S., Deng, J. J., Bai, Y., Thornton, F. B., and Oddo, S. (2009). Rapamycin rescues TDP-43 mislocalization and the associated low molecular mass neurofilament instability. *J. Biol. Chem.* 284, 27416–27424. doi: 10.1074/jbc.M109.031278

Chan, N., Le, C., Shieh, P., Mozaffar, T., Khare, M., Bronstein, J., et al. (2012). Valosin-containing protein mutation and Parkinson's disease. *Parkinsonism Relat. Disord.* 18, 107–109. doi: 10.1016/j.parkreldis.2011.07.006

Chou, T. F., Bulfer, S. L., Weihl, C. C., Li, K., Lis, L. G., Walters, M. A., et al. (2014). Specific inhibition of p97/VCP ATPase and kinetic analysis demonstrate interaction between D1 and D2 ATPase domains. *J. Mol. Biol.* 426, 2886–2899. doi: 10.1016/j.jmb.2014.05.022

Custer, S. K., Neumann, M., Lu, H., Wright, A. C., and Taylor, J. P. (2010). Transgenic mice expressing mutant forms VCP/p97 recapitulate the full spectrum of IBMPFD including degeneration in muscle, brain and bone. *Hum. Mol. Genet.* 19, 1741–1755. doi: 10.1093/hmg/ddq050

Dantuma, N. P., and Hoppe, T. (2012). Growing sphere of influence: Cdc48/p97 orchestrates ubiquitin-dependent extraction from chromatin. *Trends Cell Biol.* 22, 483–491. doi: 10.1016/j.tcb.2012.06.003

Davies, J. M., Brunger, A. T., and Weis, W. I. (2008). Improved structures of full-length p97, an AAA ATPase: implications for mechanisms of nucleotide-dependent conformational change. *Structure* 16, 715–726. doi: 10.1016/j.str.2008.02.010

Davies, J. M., Tsuruta, H., May, A. P., and Weis, W. I. (2005). Conformational changes of p97 during nucleotide hydrolysis determined by small-angle X-Ray scattering. *Structure* 13, 183–195. doi: 10.1016/j.str.2004.11.014

de Bot, S. T., Schelhaas, H. J., Kamsteeg, E. J., and van de Warrenburg, B. P. (2012). Hereditary spastic paraplegia caused by a mutation in the VCP gene. *Brain* 135:e223; author reply e224. doi: 10.1093/brain/aws201

DeJesus-Hernandez, M., Desaro, P., Johnston, A., Ross, O. A., Wszolek, Z. K., Ertekin-Taner, N., et al. (2011). Novel p.Ile151Val mutation in VCP in a patient of African American descent with sporadic ALS. *Neurology* 77, 1102–1103. doi: 10.1212/WNL.0b013e31822e563c

DeLaBarre, B., and Brunger, A. T. (2003). Complete structure of p97/valosin-containing protein reveals communication between nucleotide domains. *Nat. Struct. Biol.* 10, 856–863. doi: 10.1038/nsb972

Djamshidian, A., Schaefer, J., Haubenberger, D., Stogmann, E., Zimprich, F., Auff, E., et al. (2009). A novel mutation in the VCP gene (G157R) in a German family with inclusion-body myopathy with Paget disease of bone and frontotemporal dementia. *Muscle Nerve* 39, 389–391. doi: 10.1002/mus.21225

Dreveny, I., Kondo, H., Uchiyama, K., Shaw, A., Zhang, X., and Freemont, P. S. (2004). Structural basis of the interaction between the AAA ATPase p97/VCP and its adaptor protein p47. *EMBO J.* 23, 1030–1039. doi: 10.1038/sj.emboj.7600139

Dyck, P. J., and Lambert, E. H. (1968). Lower motor and primary sensory neuron diseases with peroneal muscular atrophy. II. Neurologic, genetic, and electrophysiologic findings in various neuronal degenerations. *Arch. Neurol.* 18, 619–625. doi: 10.1001/archneur.1968.00470360041003

Erzurumlu, Y., Kose, F. A., Gozen, O., Gozuacik, D., Toth, E. A., and Ballar, P. (2013). A unique IBMPFD-related P97/VCP mutation with differential binding pattern and subcellular localization. *Int. J. Biochem. Cell Biol.* doi: 10.1016/j.biocel.2013.01.006

Fernández-Sáiz, V., and Buchberger, A. (2010). Imbalances in p97 co-factor interactions in human proteinopathy. *EMBO Rep.* 11, 479–485. doi: 10.1038/embor.2010.49

Figueroa-Bonaparte, S., Hudson, J., Barresi, R., Polvikoski, T., Williams, T., Töpf, A., et al. (2016). Mutational spectrum and phenotypic variability of VCP-related neurological disease in the UK. *J. Neurol. Neurosurg. Psychiatry* 87, 680–681. doi: 10.1136/jnnp-2015-310362

Franz, A., Ackermann, L., and Hoppe, T. (2014). Create and preserve: proteostasis in development and aging is governed by Cdc48/p97/VCP. *Biochim. Biophys. Acta* 1843, 205–215. doi: 10.1016/j.bbamcr.2013.03.031

Gidaro, T., Modoni, A., Sabatelli, M., Tasca, G., Broccolini, A., and Mirabella, M. (2008). An Italian family with inclusion-body myopathy and frontotemporal dementia due to mutation in the VCP gene. *Muscle Nerve* 37, 111–114. doi: 10.1002/mus.20890

Gonzalez, M. A., Feely, S. M., Speziani, F., Strickland, A. V., Danzi, M., Bacon, C., et al. (2014). A novel mutation in VCP causes Charcot-Marie-Tooth Type 2 disease. *Brain* 137, 2897–2902. doi: 10.1093/brain/awu224

González-Pérez, P., Cirulli, E. T., Drory, V. E., Dabby, R., Nisipeanu, P., Carasso, R. L., et al. (2012). Novel mutation in VCP gene causes atypical amyotrophic lateral sclerosis. *Neurology* 79, 2201–2208. doi: 10.1212/WNL.0b013e318275963b

Gu, J. M., Ke, Y. H., Yue, H., Liu, Y. J., Zhang, Z., Zhang, H., et al. (2012). A novel VCP mutation as the cause of atypical IBMPFD in a Chinese family. *Bone* 52, 9–16. doi: 10.1016/j.bone.2012.09.012

Guyant-Maréchal, L., Laquerriere, A., Duyckaèrts, C., Dumanchin, C., Bou, J., Dugny, F., et al. (2006). Valosin-containing protein gene mutations: clinical and neuropathologic features. *Neurology* 67, 644–651. doi: 10.1212/01.wnl.0000225184.14578.d3

Haglund, K., Di Fiore, P. P., and Dikic, I. (2003). Distinct monoubiquitin signals in receptor endocytosis. *Trends Biochem. Sci.* 28, 598–603. doi: 10.1016/j.tibs.2003.09.005

Halawani, D., LeBlanc, A. C., Rouiller, I., Michnick, S. W., Servant, M. J., and Latterich, M. (2009). Hereditary inclusion body myopathy-linked p97/VCP mutations in the NH2 domain and the D1 ring modulate p97/VCP ATPase activity and D2 ring conformation. *Mol. Cell. Biol.* 29, 4484–4494. doi: 10.1128/MCB.00252-09

Hänzelmann, P., and Schindelin, H. (2011). The structural and functional basis of the p97/valosin-containing protein (VCP)-interacting motif (VIM): mutually exclusive binding of cofactors to the N-terminal domain of p97. *J. Biol. Chem.* 286, 38679–38690. doi: 10.1074/jbc.M111.274506

Hänzelmann, P., and Schindelin, H. (2016a). Characterization of an additional binding surface on the p97 N-terminal domain involved in bipartite cofactor interactions. *Structure* 24, 140–147. doi: 10.1016/j.str.2015.10.027

Hänzelmann, P., and Schindelin, H. (2016b). Structural basis of ATP hydrolysis and intersubunit signaling in the AAA+ ATPase p97. *Structure* 24, 127–139. doi: 10.1016/j.str.2015.10.026

Hänzelmann, P., Buchberger, A., and Schindelin, H. (2011). Hierarchical binding of cofactors to the AAA ATPase p97. *Structure* 19, 833–843. doi: 10.1016/j.str.2011.03.018

Haubenberger, D., Bittner, R. E., Rauch-Shorny, S., Zimprich, F., Mannhalter, C., Wagner, L., et al. (2005). Inclusion body myopathy and Paget disease is linked to a novel mutation in the VCP gene. *Neurology* 65, 1304–1305. doi: 10.1212/01.wnl.0000180407.15369.92

Hirano, M., Nakamura, Y., Saigoh, K., Sakamoto, H., Ueno, S., Isono, C., et al. (2015). VCP gene analyses in Japanese patients with sporadic amyotrophic lateral sclerosis identify a new mutation. *Neurobiol. Aging 36*, 1604.e1601–1606.e1601. doi: 10.1016/j.neurobiolaging.2014.10.012

Hübbers, C. U., Clemen, C. S., Kesper, K., Böddrich, A., Hofmann, A., Kämäräinen, O., et al. (2007). Pathological consequences of VCP mutations on human striated muscle. *Brain* 130, 381–393. doi: 10.1093/brain/awl238

Huyton, T., Pye, V. E., Briggs, L. C., Flynn, T. C., Beuron, F., Kondo, H., et al. (2003). The crystal structure of murine p97/VCP at 3.6A. *J. Struct. Biol.* 144, 337–348. doi: 10.1016/j.jsb.2003.10.007

Janiesch, P. C., Kim, J., Mouysset, J., Barikbin, R., Lochmüller, H., Cassata, G., et al. (2007). The ubiquitin-selective chaperone CDC-48/p97 links myosin assembly to human myopathy. *Nat. Cell Biol.* 9, 379–390. doi: 10.1038/ncb1554

Jerath, N. U., Crockett, C. D., Moore, S. A., Shy, M. E., Weihl, C. C., Chou, T. F., et al. (2015). Rare manifestation of a c.290 C>T, p.Gly97Glu VCP mutation. *Case Rep. Genet.* 2015:239167. doi: 10.1155/2015/239167

Johnson, J. O., Mandrioli, J., Benatar, M., Abramzon, Y., Van Deerlin, V. M., Trojanowski, J. Q., et al. (2010). Exome sequencing reveals VCP mutations as a cause of familial ALS. *Neuron* 68, 857–864. doi: 10.1016/j.neuron.2010.11.036

Ju, J. S., Fuentealba, R. A., Miller, S. E., Jackson, E., Piwnica-Worms, D., Baloh, R. H., et al. (2009). Valosin-containing protein (VCP) is required for autophagy and is disrupted in VCP disease. *J. Cell Biol.* 187, 875–888. doi: 10.1083/jcb.200908115

Kaleem, M., Zhao, A., Hamshere, M., and Myers, A. J. (2007). Identification of a novel valosin-containing protein polymorphism in late-onset Alzheimer's disease. *Neurodegener. Dis.* 4, 376–381. doi: 10.1159/000105158

Kamiyama, T., Sengoku, R., Sasaki, M., Hayashi, Y., Nishino, I., Mochio, S., et al. (2013). [An advanced case of myopathy and dementia with a new mutation in the valosin-containing protein gene]. *Rinsho Shinkeigaku* 53, 465–469. doi: 10.5692/clinicalneurol.53.465

Kenna, K. P., McLaughlin, R. L., Byrne, S., Elamin, M., Heverin, M., Kenny, E. M., et al. (2013). Delineating the genetic heterogeneity of ALS using targeted high-throughput sequencing. *J. Med. Genet.* 50, 776–783. doi: 10.1136/jmedgenet-2013-101795

Kim, H. J., Kim, N. C., Wang, Y. D., Scarborough, E. A., Moore, J., Diaz, Z., et al. (2013). Mutations in prion-like domains in hnRNPA2B1 and hnRNPA1 cause multisystem proteinopathy and ALS. *Nature* 495, 467–473. doi: 10.1038/nature11922

Kim, S. J., Cho, J., Song, E. J., Kim, S. J., Kim, H. M., Lee, K. E., et al. (2014). Structural basis for ovarian tumor domain-containing protein 1 (OTU1) binding to p97/valosin-containing protein (VCP). *J. Biol. Chem.* 289, 12264–12274. doi: 10.1074/jbc.M113.523936

Kimonis, V. E., Fulchiero, E., Vesa, J., and Watts, G. (2008a). VCP disease associated with myopathy, Paget disease of bone and frontotemporal dementia: review of a unique disorder. *Biochim. Biophys. Acta* 1782, 744–748. doi: 10.1016/j.bbadis.2008.09.003

Kimonis, V. E., Kovach, M. J., Waggoner, B., Leal, S., Salam, A., Rimer, L., et al. (2000). Clinical and molecular studies in a unique family with autosomal dominant limb-girdle muscular dystrophy and Paget disease of bone. *Genet. Med.* 2, 232–241. doi: 10.1097/00125817-200007000-00006

Kimonis, V. E., Mehta, S. G., Fulchiero, E. C., Thomasova, D., Pasquali, M., Boycott, K., et al. (2008b). Clinical studies in familial VCP myopathy associated

with Paget disease of bone and frontotemporal dementia. *Am. J. Med. Genet. A* 146A, 745–757. doi: 10.1002/ajmg.a.31862

Kimonis, V. E., and Watts, G. D. (2005). Autosomal dominant inclusion body myopathy, Paget disease of bone, and frontotemporal dementia. *Alzheimer Dis. Assoc. Disord.* 19(Suppl. 1), S44–S47. doi: 10.1097/01.wad.0000183081.76820.5a

Komatsu, J., Iwasa, K., Yanase, D., and Yamada, M. (2013). Inclusion body myopathy with Paget disease of bone and frontotemporal dementia associated with a novel G156S mutation in the VCP gene. *Muscle Nerve.* 48, 995–996. doi: 10.1002/mus.23960

Koppers, M., van Blitterswijk, M. M., Vlam, L., Rowicka, P. A., van Vught, P. W., Groen, E. J., et al. (2012). VCP mutations in familial and sporadic amyotrophic lateral sclerosis. *Neurobiol. Aging* 33, 837.e7–837.e13. doi: 10.1016/j.neurobiolaging.2011.10.006

Kovach, M. J., Waggoner, B., Leal, S. M., Gelber, D., Khardori, R., Levenstien, M. A., et al. (2001). Clinical delineation and localization to chromosome 9p13.3-p12 of a unique dominant disorder in four families: hereditary inclusion body myopathy, Paget disease of bone, and frontotemporal dementia. *Mol. Genet. Metab.* 74, 458–475. doi: 10.1006/mgme.2001.3256

Kumar, K. R., Needham, M., Mina, K., Davis, M., Brewer, J., Staples, C., et al. (2010). Two Australian families with inclusion-body myopathy, Paget's disease of bone and frontotemporal dementia: novel clinical and genetic findings. *Neuromuscul. Disord.* 20, 330–334. doi: 10.1016/j.nmd.2010.03.002

Kwok, C. T., Wang, H. Y., Morris, A. G., Smith, B., Shaw, C., and de Belleroche, J. (2015). VCP mutations are not a major cause of familial amyotrophic lateral sclerosis in the UK. *J. Neurol. Sci.* 349, 209–213. doi: 10.1016/j.jns.2015.01.021

Latterich, M., Fröhlich, K. U., and Schekman, R. (1995). Membrane fusion and the cell cycle: Cdc48p participates in the fusion of ER membranes. *Cell* 82, 885–893. doi: 10.1016/0092-8674(95)90268-6

Lévesque, S., Auray-Blais, C., Gravel, E., Boutin, M., Dempsey-Nunez, L., Jacques, P. E., et al. (2016). Diagnosis of late-onset Pompe disease and other muscle disorders by next-generation sequencing. *Orphanet J. Rare Dis.* 11, 8. doi: 10.1186/s13023-016-0390-6

Liewluck, T., Milone, M., Mauermann, M. L., Castro-Couch, M., Cerhan, J. H., and Murthy, N. S. (2014). A novel VCP mutation underlies scapuloperoneal muscular dystrophy and dropped head syndrome featuring lobulated fibers. *Muscle Nerve* 50, 295–299. doi: 10.1002/mus.24290

Majounie, E., Traynor, B. J., Chiò, A., Restagno, G., Mandrioli, J., Benatar, M., et al. (2012). Mutational analysis of the VCP gene in Parkinson's disease. *Neurobiol. Aging* 33, 209.e201–209.202. doi: 10.1016/j.neurobiolaging.2011.07.011

Manno, A., Noguchi, M., Fukushi, J., Motohashi, Y., and Kakizuka, A. (2010). Enhanced ATPase activities as a primary defect of mutant valosin-containing proteins that cause inclusion body myopathy associated with Paget disease of bone and frontotemporal dementia. *Genes Cells* 15, 911–922. doi: 10.1111/j.1365-2443.2010.01428.x

Matsubara, S., Shimizu, T., Komori, T., Mori-Yoshimura, M., Minami, N., and Hayashi, Y. K. (2016). Nuclear inclusions mimicking poly(A)-binding protein nuclear 1 inclusions in a case of inclusion body myopathy associated with Paget disease of bone and frontotemporal dementia with a novel mutation in the valosin-containing protein gene. *Neuromuscul. Disord.* 26, 436–440. doi: 10.1016/j.nmd.2016.05.001

Meyer, H., Bug, M., and Bremer, S. (2012). Emerging functions of the VCP/p97 AAA-ATPase in the ubiquitin system. *Nat. Cell Biol.* 14, 117–123. doi: 10.1038/ncb2407

Meyer, H., and Weihl, C. C. (2014). The VCP/p97 system at a glance: connecting cellular function to disease pathogenesis. *J. Cell Sci.* 127, 3877–3883. doi: 10.1242/jcs.093831

Meyer, H. H., Kondo, H., and Warren, G. (1998). The p47 co-factor regulates the ATPase activity of the membrane fusion protein, p97. *FEBS Lett.* 437, 255–257. doi: 10.1016/S0014-5793(98)01232-0

Meyer, H. H., Shorter, J. G., Seemann, J., Pappin, D., and Warren, G. (2000). A complex of mammalian ufd1 and npl4 links the AAA-ATPase, p97, to ubiquitin and nuclear transport pathways. *EMBO J.* 19, 2181–2192. doi: 10.1093/emboj/19.10.2181

Müller, J. M., Deinhardt, K., Rosewell, I., Warren, G., and Shima, D. T. (2007). Targeted deletion of p97 (VCP/CDC48) in mouse results in early embryonic lethality. *Biochem. Biophys. Res. Commun.* 354, 459–465. doi: 10.1016/j.bbrc.2006.12.206

Nalbandian, A., Llewellyn, K. J., Kitazawa, M., Yin, H. Z., Badadani, M., Khanlou, N., et al. (2012). The homozygote VCP(R155H/R155H) mouse model exhibits accelerated human VCP-associated disease pathology. *PLoS ONE* 7:e46308. doi: 10.1371/journal.pone.0046308

Neumann, M., Mackenzie, I. R., Cairns, N. J., Boyer, P. J., Markesbery, W. R., Smith, C. D., et al. (2007). TDP-43 in the ubiquitin pathology of frontotemporal dementia with VCP gene mutations. *J. Neuropathol. Exp. Neurol.* 66, 152–157. doi: 10.1097/nen.0b013e31803020b9

Neumann, M., Sampathu, D. M., Kwong, L. K., Truax, A. C., Micsenyi, M. C., Chou, T. T., et al. (2006). Ubiquitinated TDP-43 in frontotemporal lobar degeneration and amyotrophic lateral sclerosis. *Science* 314, 130–133. doi: 10.1126/science.1134108

Neveling, K., Feenstra, I., Gilissen, C., Hoefsloot, L. H., Kamsteeg, E. J., Mensenkamp, A. R., et al. (2013). A *post-hoc* comparison of the utility of sanger sequencing and exome sequencing for the diagnosis of heterogeneous diseases. *Hum. Mutat.* 34, 1721–1726. doi: 10.1002/humu.22450

Nishikori, S., Esaki, M., Yamanaka, K., Sugimoto, S., and Ogura, T. (2011). Positive cooperativity of the p97 AAA ATPase is critical for essential functions. *J. Biol. Chem.* 286, 15815–15820. doi: 10.1074/jbc.M110.201400

Niwa, H., Ewens, C. A., Tsang, C., Yeung, H. O., Zhang, X., and Freemont, P. S. (2012). The role of the N-domain in the ATPase activity of the mammalian AAA ATPase p97/VCP. *J. Biol. Chem.* 287, 8561–8570. doi: 10.1074/jbc.M111.302778

Palmio, J., Sandell, S., Suominen, T., Penttilä, S., Raheem, O., Hackman, P., et al. (2011). Distinct distal myopathy phenotype caused by VCP gene mutation in a Finnish family. *Neuromuscul. Disord.* 21, 551–555. doi: 10.1016/j.nmd.2011.05.008

Parton, R. G., and Simons, K. (2007). The multiple faces of caveolae. *Nat. Rev. Mol. Cell Biol.* 8, 185–194. doi: 10.1038/nrm2122

Peyer, A. K., Kinter, J., Hench, J., Frank, S., Fuhr, P., Thomann, S., et al. (2013). Novel valosin containing protein mutation in a Swiss family with hereditary inclusion body myopathy and dementia. *Neuromuscul. Disord.* 23, 149–154. doi: 10.1016/j.nmd.2012.09.009

Pye, V. E., Dreveny, I., Briggs, L. C., Sands, C., Beuron, F., Zhang, X., et al. (2006). Going through the motions: the ATPase cycle of p97. *J. Struct. Biol.* 156, 12–28. doi: 10.1016/j.jsb.2006.03.003

Rabouille, C., Levine, T. P., Peters, J. M., and Warren, G. (1995). An, N. S.F-like ATPase, p97, and, N. S.F mediate cisternal regrowth from mitotic Golgi fragments. *Cell* 82, 905–914. doi: 10.1016/0092-8674(95)90270-8

Ramanathan, H. N., and Ye, Y. (2012). The p97 ATPase associates with EEA1 to regulate the size of early endosomes. *Cell Res.* 22, 346–359. doi: 10.1038/cr.2011.80

Ritz, D., Vuk, M., Kirchner, P., Bug, M., Schütz, S., Hayer, A., et al. (2011). Endolysosomal sorting of ubiquitylated caveolin-1 is regulated by VCP and UBXD1 and impaired by VCP disease mutations. *Nat. Cell Biol.* 13, 1116–1123. doi: 10.1038/ncb2301

Rohrer, J. D., Warren, J. D., Reiman, D., Uphill, J., Beck, J., Collinge, J., et al. (2011). A novel exon 2 I27V VCP variant is associated with dissimilar clinical syndromes. *J. Neurol.* 258, 1494–1496. doi: 10.1007/s00415-011-5966-4

Rouiller, I., DeLaBarre, B., May, A. P., Weis, W. I., Brunger, A. T., Milligan, R. A., et al. (2002). Conformational changes of the multifunction p97 AAA ATPase during its ATPase cycle. *Nat. Struct. Biol.* 9, 950–957. doi: 10.1038/nsb872

Rumpf, S., and Jentsch, S. (2006). Functional division of substrate processing cofactors of the ubiquitin-selective Cdc48 chaperone. *Mol. Cell* 21, 261–269. doi: 10.1016/j.molcel.2005.12.014

Schröder, R., Watts, G. D., Mehta, S. G., Evert, B. O., Broich, P., Fliessbach, K., et al. (2005). Mutant valosin-containing protein causes a novel type of frontotemporal dementia. *Ann. Neurol.* 57, 457–461. doi: 10.1002/ana.20407

Schuller, J. M., Beck, F., Lössl, P., Heck, A. J., and Förster, F. (2016). Nucleotide-dependent conformational changes of the AAA+ ATPase p97 revisited. *FEBS Lett.* 590, 595–604. doi: 10.1002/1873-3468.12091

Segawa, M., Hoshi, A., Naruse, H., Kuroda, M., Bujo, H., and Ugawa, Y. (2015). [A patient with familial amyotrophic lateral sclerosis associated with a new valosin-containing protein (VCP) gene mutation]. *Rinsho Shinkeigaku* 55, 914–920. doi: 10.5692/clinicalneurol.cn-000765

Shi, Z., Hayashi, Y. K., Mitsuhashi, S., Goto, K., Kaneda, D., Choi, Y. C., et al. (2012). Characterization of the Asian myopathy patients with VCP mutations. *Eur. J. Neurol.* 19, 501–509. doi: 10.1111/j.1468-1331.2011.03575.x

Shi, Z., Liu, S., Xiang, L., Wang, Y., Liu, M., Liu, S., et al. (2016). Frontotemporal dementia-related gene mutations in clinical dementia patients from a Chinese population. *J. Hum. Genet.* doi: 10.1038/jhg.2016.92. [Epub ahead of print].

Spina, S., Van Laar, A. D., Murrell, J. R., de Courten-Myers, G., Hamilton, R. L., Farlow, M. R., et al. (2008). Frontotemporal dementia associated with a Valosin-Containing Protein mutation: report of three families. *FASEB J.* 22, 58.4.

Stojkovic, T., Hammouda el, H., Richard, P., López de Munain, A., Ruiz-Martinez, J., Gonzalez, P. C., et al. (2009). Clinical outcome in 19 French and Spanish patients with valosin-containing protein myopathy associated with Paget's disease of bone and frontotemporal dementia. *Neuromuscul. Disord.* 19, 316–323. doi: 10.1016/j.nmd.2009.02.012

Tang, W. K., and Xia, D. (2013). Altered intersubunit communication is the molecular basis for functional defects of pathogenic p97 mutants. *J. Biol. Chem.* 288, 36624–36635. doi: 10.1074/jbc.M113.488924

Tang, W. K., and Xia, D. (2016). Role of the D1-D2 linker of human VCP/p97 in the asymmetry and ATPase activity of the D1-domain. *Sci. Rep.* 6:20037. doi: 10.1038/srep20037

Tang, W. K., Li, D., Li, C. C., Esser, L., Dai, R., Guo, L., et al. (2010). A novel ATP-dependent conformation in p97 N-D1 fragment revealed by crystal structures of disease-related mutants. *EMBO J.* 29, 2217–2229. doi: 10.1038/emboj.2010.104

Tresse, E., Salomons, F. A., Vesa, J., Bott, L. C., Kimonis, V., Yao, T. P., et al. (2010). VCP/p97 is essential for maturation of ubiquitin-containing autophagosomes and this function is impaired by mutations that cause IBMPFD. *Autophagy* 6, 217–227. doi: 10.4161/auto.6.2.11014

van der Zee, J., Pirici, D., Van Langenhove, T., Engelborghs, S., Vandenberghe, R., Hoffmann, M., et al. (2009). Clinical heterogeneity in 3 unrelated families linked to VCP p.Arg159His. *Neurology* 73, 626–632. doi: 10.1212/WNL.0b013e3181b389d9

Vesa, J., Su, H., Watts, G. D., Krause, S., Walter, M. C., Martin, B., et al. (2009). Valosin containing protein associated inclusion body myopathy: abnormal vacuolization, autophagy and cell fusion in myoblasts. *Neuromuscul. Disord.* 19, 766–772. doi: 10.1016/j.nmd.2009.08.003

Viassolo, V., Previtali, S. C., Schiatti, E., Magnani, G., Minetti, C., Zara, F., et al. (2008). Inclusion body myopathy, Paget's disease of the bone and frontotemporal dementia: recurrence of the VCP R155H mutation in an Italian family and implications for genetic counselling. *Clin. Genet.* 74, 54–60. doi: 10.1111/j.1399-0004.2008.00984.x

Wang, I. F., Wu, L. S., and Shen, C. K. (2008). TDP-43: an emerging new player in neurodegenerative diseases. *Trends Mol. Med.* 14, 479–485. doi: 10.1016/j.molmed.2008.09.001

Wang, J., Song, J. J., Seong, I. S., Franklin, M. C., Kamtekar, S., Eom, S. H., et al. (2001). Nucleotide-dependent conformational changes in a protease-associated ATPase HsIU. *Structure* 9, 1107–1116. doi: 10.1016/S0969-2126(01)00670-0

Wang, Q., Song, C., and Li, C. C. (2003). Hexamerization of p97-VCP is promoted by ATP binding to the D1 domain and required for ATPase and biological activities. *Biochem. Biophys. Res. Commun.* 300, 253–260. doi: 10.1016/S0006-291X(02)02840-1

Wang, X., Fan, H., Ying, Z., Li, B., Wang, H., and Wang, G. (2010). Degradation of TDP-43 and its pathogenic form by autophagy and the ubiquitin-proteasome system. *Neurosci. Lett.* 469, 112–116. doi: 10.1016/j.neulet.2009.11.055

Watts, G. D., Thomasova, D., Ramdeen, S. K., Fulchiero, E. C., Mehta, S. G., Drachman, D. A., et al. (2007). Novel VCP mutations in inclusion body myopathy associated with Paget disease of bone and frontotemporal dementia. *Clin. Genet.* 72, 420–426. doi: 10.1111/j.1399-0004.2007.00887.x

Watts, G. D., Wymer, J., Kovach, M. J., Mehta, S. G., Mumm, S., Darvish, D., et al. (2004). Inclusion body myopathy associated with Paget disease of bone and frontotemporal dementia is caused by mutant valosin-containing protein. *Nat. Genet.* 36, 377–381. doi: 10.1038/ng1332

Weihl, C. C., Baloh, R. H., Lee, Y., Chou, T. F., Pittman, S. K., Lopate, G., et al. (2015). Targeted sequencing and identification of genetic variants in sporadic inclusion body myositis. *Neuromuscul. Disord.* 25, 289–296. doi: 10.1016/j.nmd.2014.12.009

Weihl, C. C., Dalal, S., Pestronk, A., and Hanson, P. I. (2006). Inclusion body myopathy-associated mutations in p97/VCP impair endoplasmic reticulum-associated degradation. *Hum. Mol. Genet.* 15, 189–199. doi: 10.1093/hmg/ddi426

Weihl, C. C., Miller, S. E., Hanson, P. I., and Pestronk, A. (2007). Transgenic expression of inclusion body myopathy associated mutant p97/VCP causes weakness and ubiquitinated protein inclusions in mice. *Hum. Mol. Genet.* 16, 919–928. doi: 10.1093/hmg/ddm037

Weihl, C. C., Temiz, P., Miller, S. E., Watts, G., Smith, C., Forman, M., et al. (2008). TDP-43 accumulation in inclusion body myopathy muscle suggests a common pathogenic mechanism with frontotemporal dementia. *J. Neurol. Neurosurg. Psychiatry* 79, 1186–1189. doi: 10.1136/jnnp.2007.131334

Xia, D., Tang, W. K., and Ye, Y. (2016). Structure and function of the AAA+ ATPase p97/Cdc48p. *Gene* 583, 64–77. doi: 10.1016/j.gene.2016.02.042

Xu, S., Peng, G., Wang, Y., Fang, S., and Karbowski, M. (2011). The AAA-ATPase p97 is essential for outer mitochondrial membrane protein turnover. *Mol. Biol. Cell* 22, 291–300. doi: 10.1091/mbc.E10-09-0748

Yamanaka, K., Sasagawa, Y., and Ogura, T. (2012). Recent advances in p97/VCP/Cdc48 cellular functions. *Biochim. Biophys. Acta* 1823, 130–137. doi: 10.1016/j.bbamcr.2011.07.001

Ye, Y., Meyer, H. H., and Rapoport, T. A. (2003). Function of the p97-Ufd1-Npl4 complex in retrotranslocation from the ER to the cytosol: dual recognition of nonubiquitinated polypeptide segments and polyubiquitin chains. *J. Cell Biol.* 162, 71–84. doi: 10.1083/jcb.200302169

Zhang, X., Gui, L., Zhang, X., Bulfer, S. L., Sanghez, V., Wong, D. E., et al. (2015). Altered cofactor regulation with disease-associated p97/VCP mutations. *Proc. Natl. Acad. Sci. U.S.A.* 112, E1705–E1714. doi: 10.1073/pnas.1418820112

Zhang, X., Shaw, A., Bates, P. A., Newman, R. H., Gowen, B., Orlova, E., et al. (2000). Structure of the AAA ATPase p97. *Mol. Cell* 6, 1473–1484. doi: 10.1016/S1097-2765(00)00143-X

Conflict of Interest Statement: The authors declare that the research was conducted in the absence of any commercial or financial relationships that could be construed as a potential conflict of interest.

frontiers in Molecular Biosciences

ORIGINAL RESEARCH
published: 07 October 2016
doi: 10.3389/fmolb.2016.00065

Effects of a Mutation in the *HSPE1* Gene Encoding the Mitochondrial Co-chaperonin HSP10 and Its Potential Association with a Neurological and Developmental Disorder

Anne S. Bie[1]†, Paula Fernandez-Guerra[1], Rune I. D. Birkler[1], Shahar Nisemblat[2], Dita Pelnena[1], Xinping Lu[2], Joshua L. Deignan[3], Hane Lee[3], Naghmeh Dorrani[3,4], Thomas J. Corydon[5], Johan Palmfeldt[1], Liga Bivina[6], Abdussalam Azem[2], Kristin Herman[6] and Peter Bross[1]**

[1] Research Unit for Molecular Medicine, Aarhus University and Aarhus University Hospital, Aarhus, Denmark, [2] Department of Biochemistry & Molecular Biology, Tel Aviv University, Tel Aviv, Israel, [3] Department of Pathology and Laboratory Medicine, David Geffen School of Medicine at University of California, Los Angeles, Los Angeles, CA, USA, [4] Department of Pediatrics, David Geffen School of Medicine at University of California, Los Angeles, Los Angeles, CA, USA, [5] Department of Biomedicine, Aarhus University, Aarhus, Denmark, [6] Division of Genomic Medicine, Department of Pediatrics, UC Davis Health System, Sacramento, CA, USA

We here report molecular investigations of a missense mutation in the *HSPE1* gene encoding the HSP10 subunit of the HSP60/ HSP10 chaperonin complex that assists protein folding in the mitochondrial matrix. The mutation was identified in an infant who came to clinical attention due to infantile spasms at 3 months of age. Clinical exome sequencing revealed heterozygosity for a *HSPE1* NM_002157.2:c.217C>T *de novo* mutation causing replacement of leucine with phenylalanine at position 73 of the HSP10 protein. This variation has never been observed in public exome sequencing databases or the literature. To evaluate whether the mutation may be disease-associated we investigated its effects by *in vitro* and *ex vivo* studies. Our *in vitro* studies indicated that the purified mutant protein was functional, yet its thermal stability, spontaneous refolding propensity, and resistance to proteolytic treatment were profoundly impaired. Mass spectrometric analysis of patient fibroblasts revealed barely detectable levels of HSP10-p.Leu73Phe protein resulting in an almost 2-fold decrease of the ratio of HSP10 to HSP60 subunits. Amounts of the mitochondrial superoxide dismutase SOD2, a protein whose folding is known to strongly depend on the HSP60/HSP10 complex, were decreased to approximately 20% in patient fibroblasts in spite of unchanged SOD2 transcript levels. As a likely consequence, mitochondrial superoxide levels were increased about 2-fold. Although, we cannot exclude other causative or contributing factors, our experimental data support the notion that the HSP10-p.Leu73Phe mutation could be the cause or a strong contributing factor for the disorder in the described patient.

Keywords: protein folding, molecular chaperones, mitochondrial proteins, neurological disorders, *De novo* mutations, oxidative stress

OPEN ACCESS

Edited by:
Alberto J. L. Macario, University of Maryland, Baltimore, USA

Reviewed by:
Johannes Herrmann, Kaiserslautern University of Technology, Germany
Ophry Pines, Hebrew University of Jerusalem, Israel

***Correspondence:**
Anne S. Bie
anne.sigaard.bie@regionh.dk
Peter Bross
peter.bross@clin.au.dk

†Present Address:
Anne S. Bie, Neurogenetics Research Laboratory, Department of Neurology, Danish Dementia Research Centre, University of Copenhagen, Rigshospitalet, Copenhagen, Denmark

Specialty section:
This article was submitted to Protein Folding<comma> Misfolding and Degradation, a section of the journal Frontiers in Molecular Biosciences

Received: *26 July 2016*
Accepted: *21 September 2016*
Published: *07 October 2016*

Citation:
Bie AS, Fernandez-Guerra P, Birkler RID, Nisemblat S, Pelnena D, Lu X, Deignan JL, Lee H, Dorrani N, Corydon TJ, Palmfeldt J, Bivina L, Azem A, Herman K and Bross P (2016) Effects of a Mutation in the HSPE1 Gene Encoding the Mitochondrial Co-chaperonin HSP10 and Its Potential Association with a Neurological and Developmental Disorder. Front. Mol. Biosci. 3:65. doi: 10.3389/fmolb.2016.00065

INTRODUCTION

Heat shock protein 10 (HSP10) and heat shock protein 60 (HSP60) are the constituents of the HSP60/HSP10 chaperonin complex that assists folding of proteins in the mitochondrial matrix space (Cheng et al., 1989; Hartman et al., 1992). Chaperonins including the most thoroughly investigated *Escherichia coli* GroEL/GroES complex constitute a subfamily of the molecular chaperones characterized by the extraordinary architecture of these complexes that provides an inner cavity for folding of proteins (Horwich and Fenton, 2009; Hayer-Hartl et al., 2016). The HSP60 subunits are organized in a double-barrel structure that is built by two heptameric rings of 60 kDa subunits stacked back-to-back (Nisemblat et al., 2015). The inner cavity of the barrel initially binds unfolded proteins to the inner wall. Subsequent binding of a heptamer of HSP10 subunits puts a "lid" on the cavity. Binding of ATP molecules to the HSP60 subunits results in conformational changes of the HSP60/HSP10 complex (Saibil et al., 2013). Finally, timed ATP hydrolysis triggering additional conformational changes of the complex leads to dissociation of the HSP10 lid and discharge of the enclosed protein. One or several rounds of this process facilitate folding of interacting proteins. *In vitro* refolding studies have shown that under non-permissive conditions (i.e., spontaneous folding is minimal) the presence of HSP10 is strictly essential for efficient folding of model substrate proteins (Schmidt et al., 1994).

Together with other chaperones and proteases, the HSP60/HSP10 complex forms the protein quality control (PQC) system in the mitochondrial matrix and its expression is regulated by the mitochondrial unfolded protein response and the heat-shock responses (Aldridge et al., 2007). PQC systems, also known as proteostasis networks (Balch et al., 2008), consist of molecular chaperones and proteases that collectively maintain the functional proteome by, on one hand assisting protein folding and on the other hand removing misfolded proteins, thus promoting folding to the native state and minimizing deleterious effects of misfolded proteins. PQC systems play a decisive role in many diseases including protein aggregation diseases like Alzheimer's and Parkinson's disease as well as protein misfolding diseases like phenylketonuria and medium-chain acyl-CoA dehydrogenase deficiency (Gregersen et al., 2006; Chen et al., 2011).

The mitochondrial matrix proteome is estimated to consist of at least 500 proteins (Rhee et al., 2013) that maintain mitochondrial ATP production, the energy fuel of cells. Furthermore, a plethora of other synthetic and important catalytic and regulatory functions (Raimundo, 2014) takes place in the mitochondrial matrix, which is the most protein-dense compartment in the cell.

The human HSP10 protein is encoded by the *HSPE1* gene that is located in a head to head arrangement with the *HSPD1* gene encoding HSP60. Both genes are transcribed under control of a bidirectional promoter localized between the genes (Ryan et al., 1997). The head to head arrangement of the *HSPD1* and *HSPE1* genes appears to secure transcription of both chaperonin genes at a fixed ratio and it is conserved from *Caenorhabditis elegans* to humans. Organization of the *E. coli groEL* and *groES* genes in an operon under control of a common promoter likewise has the same purpose (Ryan et al., 1997).

The neurological disorders hereditary spastic paraplegia SPG13 (Hansen et al., 2002) and MitCHAP-60 disease (Magen et al., 2008) are caused by missense mutations in the *HSPD1* gene (reviewed in Bross and Fernandez-Guerra, 2016). Hereditary spastic paraplegia SPG13 (OMIM #605280) is a late onset, autosomal dominantly inherited disorder that primarily affects motor neurons with the longest axons in the spinal cord. In contrast, the autosomal recessively inherited MitCHAP-60 disease (OMIM #612233) is linked to a much more severe fatal neurodegenerative disorder of early onset causing death within the first two decades of life and associated with highly pronounced cerebral hypomyelination. Investigations of the purified mutant HSP60 proteins associated with both diseases have indicated that these HSP60 mutant proteins are apparently normally incorporated into HSP60 ring complexes, but display reduced ATP hydrolysis activity and impaired refolding activity (Bross et al., 2008; Parnas et al., 2009).

In vivo studies in mice have shown that knock-out of both alleles of the *Hspd1* gene is embryonally lethal (Christensen et al., 2010). However, mice heterozygous for the knock-out allele recapitulate features of hereditary spastic paraplegia with late onset motoneuron disorder (Magnoni et al., 2013). These mice display swollen mitochondria in spinal cord, deficient complex III activity in spinal cord and brain cortex as well as increased protein carbonylation in these tissues suggesting increased ROS production (Magnoni et al., 2014). Importantly, complex III deficiency was found to be associated with decreased levels of the complex III subunit UQCRC1 and increased ROS levels appear to be due to impaired folding and increased turnover of the matrix superoxide dismutase SOD2. This suggested that HSP60 haploinsufficiency caused impaired folding of certain mitochondrial proteins thus leading to a variety of impaired functions. The different phenotypes caused by the different *HSPD1* mutant alleles and inheritance modes suggests that different types and degrees of disturbances of this system cause distinct phenotypic manifestations. The study of these genetic diseases is thus a unique opportunity to enlighten these basic mechanisms in humans and for pinpointing modes how to target these mechanisms for the treatment of diseases.

In the present study we investigated a patient with a history of infantile spasms, hypotonia, developmental delay, a slightly enlarged liver, macrocephaly, and mild non-specific dysmorphic features. Clinical exome sequencing revealed heterozygosity for a *de novo* point mutation in the *HSPE1* gene triggering studies of possible effects of the mutation at protein level and at cellular level in patient fibroblasts. As potentially disease-causing mutations in the *HSPE1* gene so-far only have been observed in this single patient, we cannot fully exclude other genetic and/or environmental causes, However, our results show that the investigated mutation causes malfunction of the HSP60/HSP10 complex. Taken together with the knowledge on diseases caused

Abbreviations: CSF, cerebrospinal fluid; PQC, protein quality control; SRM, selected reaction monitoring.

by mutations in the gene encoding the HSP60 subunit we make the case for a mutation disease relationship.

MATERIALS AND METHODS

Clinical Patient Analysis

The patient, a male infant, came to clinical attention due to infantile spasms at 3 months of age. Subsequent clinical investigations revealed hypotonia, developmental delay, a slightly enlarged liver, macrocephaly, and some mild nonspecific dysmorphic features. For more detailed description of the clinical picture see *Extended clinical patient information* in Appendix. Metabolic analysis on plasma, urine and cerebrospinal fluid (CSF) showed an unusual urine amino acid profile that did not fit a pattern of known metabolic disorders. Data on compounds that deviated from the control range in at least one analysis are shown in **Table 1**. It was characteristic for the metabolite analyses that values varied between repeated analyses suggesting that environmental factors and conditions may influence the metabolic profiles. Plasma amino acids and urine organic acids were overall normal. Urine dicarboxylic acids were slightly increased in two out of three analyses, which could indicate a fatty acid oxidation disorder. However, a plasma acyl-carnitine profile that had been determined prior to the first biochemical lab tests at age 6 months, showed no abnormalities.

Interestingly, the pyridoxal 5′-phosphate concentration in CSF was just below the reference interval and defective pyridoxine metabolism has been shown to cause seizures (Mills et al., 2006; Plecko et al., 2007). Furthermore, gamma aminobutyrate was elevated in urine, which could indicate GABA transaminase deficiency. GABA transaminase is dependent on pyridoxal 5′-phosphate and hence also related to the seizure symptoms. Imaging of the patient's brain was carried out with and without contrast (not shown), but no significant interval changes were detected, nor were there any mass effect, infarct, hemorrhage, demyelination or hydrocephalus. Because of mild hepatosplenomegaly noted at one point, lysosomal enzyme screening was carried out but results were inconspicuous.

Chromosomal microarray analysis showed a *de novo* 0.146 Mb deletion at 17q23.3 and a 0.316 Mb gain at 17q25.1 that was maternally inherited. The deletion involved a single gene, TANC2, which is most expressed in the adult brain and has very low expression in the fetal brain. It has not been associated with a known disorder to date. A review of the genes involved in the duplication did not show any genes that were suspected to be associated with the clinical features of this patient.

TABLE 1 | Selected metabolite data.

	Compound	[mmol/mmol creatine]	Control range	
			Low	High
Urine organic acids	3OH-Buturic	25/4/0	0	10
	Glutaric	6/3/2	0	5
	Acetoacetic	11/3/2	0	2
	Suberic	12/7/7	0	7
	OH-Dicanedioic	7/5/5	0	2
	Methylmalonic	2/6/5	0	5
	Octanoic	0/9/7	0	2
	Pyrovic	7/18/23	0	22
Urine amino acids	Gamma-aminobutyrate	143/71/107	0	11.9
	Hydroxy-lysine	5018/2273/1937	1.1	11
	Alpha-aminoadipic	212/64/202	5.1	30.3
	Beta-alanine	510/115/473	0	33.6
	Taurine	897/319/647	617	428.7
	Glutamine	181/173/151	75.8	176.7
	Halfcysteine	74/111/227	15.4	160.6
	Lysine	33/23/101	21.4	96.2
	Compound	**μmol/L**	**Control range**	
			Low	**High**
Cerebrospinal fluid	Pyridoxal 5-Phosphate	22	23	64
	Free sialic acid	28	2	22
	Total sialic acid	60	8	50

Urine organic acids and urine amino acid concentrations were measured as mmol/mol creatinine. Values from 3 measurements are given separated by "/." Organic acids and amino acids concentrations in cerebrospinal fluid were measured as μmol/L. Only compounds that differed from control samples in at least one measurement are shown.

Cell Culturing

The patient fibroblast line was derived from a skin biopsy. Informed consent from the parents was obtained at the time of the skin biopsy and documented in the patient's medical record. Information included that the primary research focus would be to study the effect of the variant on the function of *HSPE1* and the potential impact it would have on the patient's clinical phenotype. Written informed consent from the family was also obtained. The investigation was performed in accordance with regulations set by the Danish National Committee on Health Research Ethics. Patient skin fibroblasts and three anonymized age-matched control fibroblasts were cultured according to standard procedures. In brief, fibroblasts were maintained in Dulbecco's modified Eagles media (DMEM), supplemented with 10% (v/v) fetal bovine serum, 29 mg/mL of L-glutamine (Leo Pharmaceutical), and 1% penicillin/streptomycin (Leo Pharmaceutical) at 37°C and 5% CO_2. Fibroblasts were negative for *Mycoplasma sp.* and tests were performed routinely (PromoKine, Heidelberg, Germany)

DNA and RNA Purification

High molecular weight genomic DNA was isolated from whole blood by QIAcube (QIAGEN) according to manufacturer's protocol at UCLA Molecular Diagnostics Laboratories. RNA was isolated from fibroblast pellets by Trizol (Life Technologies) according to manufacturer's description. Quality and amounts of the DNA and RNA preparations was measured by NanoDrop Spectrophotometer (Thermo Scientific), Qubit (ThermoFisher Scientific), and agarose gel electrophoresis.

DNA Sequencing

Clinical exome sequencing and data analysis was performed at the UCLA Clinical Genomics Center on the patient and both

parents (i.e., Trio-CES) following the CLIA (Clinical Laboratory Improvement Amendments) and CAP (College of American Pathologists) validated protocols (Lee et al., 2014). Briefly, exome capture was performed using the Agilent SureSelect Human All Exon 50 Mb kit (Agilent technologies) and HiSeq2000 (Illumina) as 50 bp paired end run. In the patient, total 13,377,501,340 bases of sequence were generated and uniquely aligned to the human reference genome, generating a mean depth of coverage of 150x per base within the RefSeq protein coding bases of the human genome with 94% of the bases covered at greater than 9 reads. Parental samples were sequenced at similar depth of coverage (mother: 159X; father: 152X). The *HSPE1* de novo variant was confirmed by Sanger sequencing at the UCLA Orphan Disease Testing Center (ODTC) in the trio.

Sanger sequencing of fibroblast genomic DNA and PCR products from cDNA derived from fibroblast RNA was performed using Big Dye® Terminator v.1.1 Cycle Sequencing Kit (Life Technologies, USA) and analysis with the Genetic Analyzer 3500 Dx (Life Technologies, USA). Sequence data were evaluated with Gensearch software (PhenoSystems, Belgium).

Selected Reaction Monitoring (SRM)

Fibroblasts were lysed in 100 mM ammonium bicarbonate and 1 M urea with ultrasonication (Branson Sonifier 250, Branson Ultrasonics Corp) at output control 3 and 30 % duty cycle for three cycles of five pulses, with 1 min on ice between each cycle. Lysates were centrifuged at 13,000 *g* for 30 min at 4°C. Protein concentration of the soluble fraction was measured by Bradford Protein assay (Bio-Rad) and 30 μg were used for SRM analysis. Relative quantification of peptides was carried out using a modified version of the SRM assay described in Fernández-Guerra et al. (2014). In brief all targeted proteins were monitored by detection of 2–5 tryptic peptides. Defined amounts of heavy labeled synthetic peptide analogs were spiked into the samples and used for relative quantification. The summed fragment ion peak areas for each peptide were normalized to the signal responses from the corresponding spiked heavy-labeled peptide standards. The means of the ratios for each peptide measured in control fibroblasts were set to 100% and the means for the patient fibroblast samples were expressed as the percentage of these. Samples from 3 independently grown control fibroblasts and 3 parallel cultures of patient fibroblasts were analyzed.

cDNA Analysis and PCR

cDNA was synthesized from 1 μg of RNA using the iScript™ cDNA Synthesis Kit (BioRad). Subsequent qRT-PCR analysis was performed using TaqMan gene expression assays for *HSPE1, HSPD1, SOD2,* and *ACADM* and analyzed on ABI StepOne plus (Applied Biosystems) essentially as described in Hansen et al. (2008). Relative transcript levels were calculated using the standard curve method.

For sequencing of the mutation site on genomic DNA, a fragment was amplified with primers situated in intron 2 and the 3′-UTR of exon 4 of the *HSPE1* gene, respectively. For sequencing of the mutation site in cDNA derived from patient or control fibroblasts isolated RNA was amplified using primers in exon 2 and the coding region of exon 4. For primer sequences see **Supplementary Table S1**. Correct size of PCR products was analyzed by agarose gel electrophoresis.

In vitro Synthesis and Mitochondrial Import Assay

In vitro transcription/translation and subsequent import into mitochondria was performed as described in Bross et al. (2003) with minor modifications. Briefly, cDNA sequences for wild type *HSPE1* and *HSPE1_* c.217C>T in pcDNA3.1 plasmids (Eurofins) were used to produce HSP10-p.wt and HSP10-p.Leu73Phe protein by *in vitro* transcription/translation in rabbit reticulocyte lysate systems (TNT T7 kit, Promega) in the presence of [^{35}S]-methionine as recommended by the supplier. Mitochondria were isolated from fresh mouse liver. Import mixtures were incubated at 37°C and aliquots were removed immediately after addition of the labeled HSP10 and after 15, 30, and 60 min. Fractions of the soluble proteins from mitochondrial lysates were analyzed by SDS PAGE (Criterion TGX gel, Any kDa, Biorad). Gels were stained with Coomassie, dried, exposed to phosphor imaging screens overnight and radiolabeled proteins were visualized by phosphor imaging (Typhoon, GE Healthcare).

Cloning, Mutagenesis and Purification of HSP10-Leu73Phe Protein

Human HSP10 cDNA (GenBank accession no. P61604) was inserted into the pET22b(+) expression plasmid (Novagen) using NdeI and XhoI restriction sites. A stop codon was inserted at the end of the cDNA sequence to generate a construct that does not contain a C-terminus His-tag. The Leu73Phe mutation was inserted into the HSP10 gene by site-directed mutagenesis according to the protocol of Stratagene, using the primers mHSP10L73F_F and m HSP10L73F_R (for primer sequences see **Supplementary Table S1**).

HSP10 was expressed as described in Parnas et al. (2009) and purified as follows: the cell pellet was resuspended (1:10 w/v) in a buffer containing 20 mM Tris-HCl pH 7.7, 5 mM MgSO4, 1 mM DTT, 1500 units DNase. Cells were homogenized and passed through a microfluidizer. Immediately after lysis, PMSF (0.5 mM) and 1 μg/ml of each of the following protease inhibitors (Sigma) were added: Pepstatin, Chymostatin, Antipain, Leupeptin, and Aprotinin. Debris was removed by centrifugation for 30 min at 35,000 *g*. The supernatant was loaded onto a RESOURCE Q column (GH Healthcare) equilibrated with buffer A (20 mM Tris-HCl pH 7.7, 0.1 mM EDTA, and 1 mM DTT). Unbound proteins were collected from the column and dialyzed over night against buffer B (20 mM MES pH 6.6 and 0.1 mM EDTA). The protein was then loaded on a SOURCE-S column (GH Healthcare) equilibrated with buffer B. Bound proteins were eluted from the column with a linear gradient of 0–500 mM NaCl (in buffer B). HSP10-enriched fractions were collected and concentrated. The protein was then loaded on a Superdex 200 prep grade gel-filtration column (Pharmacia) equilibrated with buffer C (50 mM Tris-HCl pH 7.7 and 100 mM NaCl). Fractions containing heptameric HSP10 were concentrated to approximately 40 mg/ml and flash-frozen in liquid nitrogen for storage. All stages were carried out at 4°C.

Analysis of tryptic peptides by a nano Liquid-Chromatography system (Ultimate 3000, Dionex) coupled to a mass spectrometer (Q Exactive, Thermo Fisher Scientific) through an EASY-Spray nano-electrospray ion source (Thermo Scientific) confirmed high purity.

Malate Dehydrogenase (MDH) Refolding Assay

Refolding of HCl-denatured MDH was carried out as previously described by Bonshtien et al. (2009).

Thermal Unfolding/Refolding Kinetics

Temperature-dependent denaturation/renaturation experiments were performed using a ChirascanTM CD (CircularDichroism) spectrometer as described by Vitlin Gruber et al. (2013).

Limited Proteolysis Assay

Purified HSP10-p.wt or HSP-p.Leu73Phe protein at 0.1 mg/ml in 100 mM Tris-HCl (pH 7.8) was incubated at 37°C. Trypsin was added to a final concentration of 0.01 mg/ml (molar ratio HSP10:trypsin 10:1). Samples were taken immediately before and 2, 10, 25, 60, and 120 min after addition of trypsin. Samples were quenched by addition of SDS PAGE sample buffer and incubation at 95°C for 2 min. As control, series without addition of trypsin were performed. Samples were subjected to SDS PAGE and proteins stained with Coomassie.

For analysis of the content of HSP10 bands from SDS PAGE, Coomassie–stained bands were excised and peptides extracted as described (Edhager et al., 2014). Peptides were analyzed using a nano Liquid-Chromatography system (Ultimate 3000, Dionex) coupled to a mass spectrometer (Q Exactive, Thermo Fisher Scientific) through an EASY-Spray nano-electrospray ion source (Thermo Scientific).

Image Cytometry and Bioenergetics Measurements

All cytometric fluorescent measurements were performed using the NC-3000 image cytometer (Chemometec) as described in Fernandez-Guerra et al. (2016). Mitochondrial oxygen consumption rate profiling assays of cultured fibroblasts were performed using a Seahorse XF^{e}96 extracellular flux analyzer and the Mito Stress test kit (Seahorse Bioscience) as recommended by the supplier with the following modifications: 15,000 cells per well were seeded 24 h before analysis and FCCP was added at 1 μM final concentration. Oxygen consumption rate (OCR) was normalized to total protein amount measured in each well after the analysis using the Bradford Protein assay (Bio-Rad).

Mitochondrial Morphology

The mitochondrial morphology of fibroblast from the patient and healthy individuals was analyzed using Mitotracker Green FM (Molecular Probes, Life Technologies). Fibroblasts from the patient and healthy individuals were seeded at 50% confluence in 6-well plates (Nunc, Roskilde, Denmark) 24 h before the analysis. The fibroblasts were stained with 100 nM Mitotracker Green (Molecular probes) for 30 min at 37°C. Pictures were obtained with the EVOS FLoid Cell Imaging Station (Life Technologies) with the standard green channel of the instrument (482/18 nm excitation and 532/59 nm emission). The image was adjusted for contrast with the software of the instrument; no further processing of the image was done.

RESULTS

Clinical Exome Sequencing Reveals a *De novo* Mutation in the *HSPE1* Gene Encoding the HSP10 Subunit of the Mitochondrial HSP60/HSP10 Chaperonin Complex

As clinical and metabolic investigations of the patient did not reveal the causative factor of the symptoms (for information on the patient see Materials and Methods *Clinical patient analysis* and Appendix "*Extended clinical patient information*"), whole exome sequencing on the patient and the parents was performed as the next step. No relevant mutations were found in a list of 758 genes (**Supplementary Table S2**) annotated with keywords relevant for the disease phenotype. However, further analysis of the exome sequencing data revealed a *de novo* heterozygous missense variation, c.217C>T [p.Leu73Phe], in the *HSPE1* gene encoding the mitochondrial co-chaperonin HSP10 that forms part of the HSP60/ HSPSP10 chaperonin complex. Presence in the patient and absence in the parents was confirmed by Sanger sequencing. The detected variation has to our knowledge never before been reported in the literature or publicly accessible genetic databases and the *HSPE1* gene has not previously been associated with a human disorder. Variation in the third position of the CTC codon for the mutated leucine-73 of the *HSPE1* gene (to T or G) resulting in codons that also specify leucine has been observed as documented by the Exome Aggregation Consortium (ExAC; Cambridge, MA; accessed December 2015). Investigation of the HSP10 mutation *in silico* using the prediction tool PolyPhen2 predicted the mutation to be "possibly damaging," with a score of 0.954 on a scale from 0 to 1. Similarly, the SIFT prediction tool (Ng and Henikoff, 2001) predicted the mutation to be "damaging."

Inspection of the crystal structure of the HSP60/HSP10 complex (**Figure 1**) showed that the mutated leucine-73 is located distantly from the mobile loop region that mediates interaction with HSP60 and the mutation is thus not expected to directly affect this interaction. Leucine-73 is facing the hydrophobic core made by the beta-sheets building the HSP10 main body (**Figure 1**). When we examined leucine-73 solvent accessibility using the PISA program (Krissinel and Henrick, 2007) we noticed that the average accessible surface area (ASA) of this residue is only 1.36 Å^2 indicating that it is tightly packed. The neighboring Leu72 for instance has an average ASA of 53.3 Å^2, while Leu97 that is positioned between HSP10 subunits has an ASA of more than 120 Å^2.

In vitro Studies of the Mutation Effect

To explore the effects of the mutation on structural and functional properties of the co-chaperonin, we performed *in vitro* studies on purified HSP10-p.Leu73Phe protein following

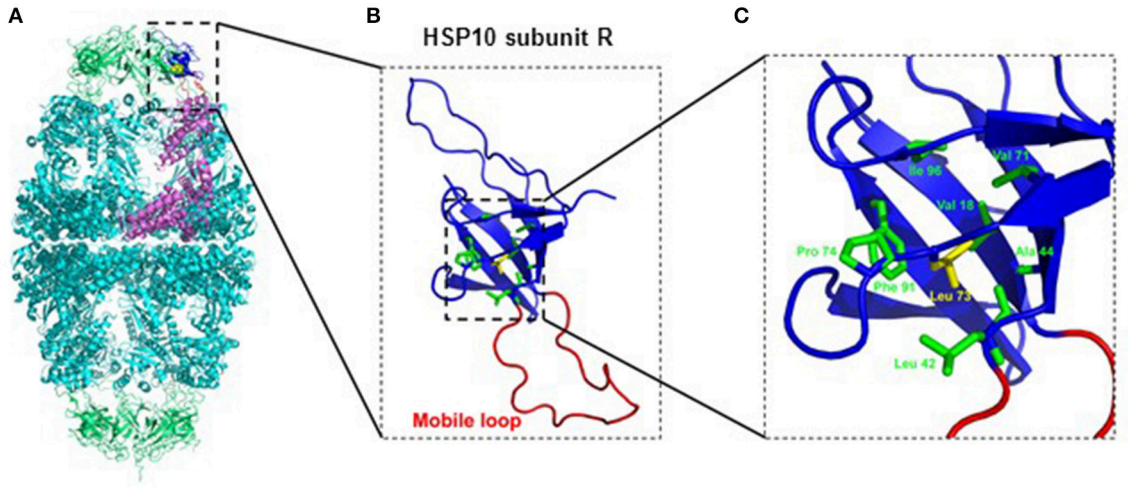

FIGURE 1 | Position of Leucine-73 in the HSP60/HSP10 complex structure. (A) HSP60-HSP10 symmetric football complex shown in cartoon representation. HSP60 subunits are in cyan and HSP10 subunits are in green. One HSP60 subunit (subunit D) and its interacting HSP10 subunit (subunit R) are emphasized (purple and blue respectively). The mobile loop of subunit R is in red. Leucine-73 residue is depicted in yellow with space filling representation. **(B)** Enlarged view of the boxed area in **(A)** displaying HSP10's subunit R. Color scheme as in **(A)**. Leucine-73 and its interacting residues at the hydrophobic core of HSP10 (green) are presented as sticks. **(C)** Enlarged view of the boxed hydrophobic core of HSP10 from figure **(B)**. Leucine-73 and its interacting residues are labeled. Leucine-73 is facing the hydrophobic core made by the beta-sheets building HSP10 main body. In addition, analysis of Leucine-73 interactions in all HSP10 subunits using the PISA and PIC servers (Krissinel and Henrick, 2007; Tina et al., 2007) showed that Leucine-73 is tightly packed in the core of the HSP10 molecule. It has an average accessible surface area of only 1.36 $Å^2$, while it interacts with the following residues of the core: Val18, Leu42, Ala44, Val71, Pro74, Phe91, and Ile96. Illustrations were generated using the PyMOL program (The PyMOL Molecular Graphics System, version 1.5.0.4; Schrödinger, LLC; available at www.pymol.org), with PDB ID: 4PJ1.

recombinant expression in bacteria. We analyzed the function of HSP10-p.Leu73Phe *in vitro* by testing its ability to assist HSP60 in refolding of malate dehydrogenase (MDH). MDH was denatured and diluted into a solution with HSP60 to allow its binding to the chaperonin. Then ATP and different concentrations of either HSP10-p.wt (**Figure 2A**) or HSP10-p.Leu73Phe (**Figure 2B**) were added to let the folding reaction proceed. Surprisingly, the results showed that the HSP10-p.Leu73Phe protein was fully active and even had a tendency to display slightly faster kinetics in assisting MDH refolding. However, when comparing the different HSP10 concentrations, we noticed that the reaction with HSP10-p.wt was already saturated at 2.5 μM HSP10 protein whereas HSP10-p.Leu73Phe had to be present at 5 μM to saturate the reaction (**Figures 2A,B**).

We then investigated the thermal stability of the HSP10-pLeu73Phe protein *in vitro*. Thermal unfolding and refolding of mutant and wild type HSP10 proteins was monitored by CD spectroscopy. **Figure 2C** shows a representative experiment. The HSP10-p.Leu73Phe protein unfolds with a Tm of only 59°C compared to HSP10-p.wt that displays a Tm of approximately 73°C (**Figure 2C**; stippled lines). A 14° difference between the Tm's of wild type and mutant HSP10 would result in a reduction of the free energy of unfolding of approximately 3 kcal (Greenfield, 2006). Considering that the free energy difference between the unfolded and folded conformations of proteins is in the range of 5–20 kcal (Pace, 1990), we conclude that the conformational stability of the HSP10 mutant protein is significantly decreased.

We also examined the reverse reaction of refolding wild type and mutant HSP10 by gradually decreasing the temperature from 90° to 25°C. Both proteins spontaneously refold upon decreasing the temperature (**Figure 2C**; solid lines). The Tm of refolding of both the wild type and mutant HSP10 has shifted to lower temperatures compared to their respective Tm for unfolding. Interestingly the HSP10-p.Leu73Phe protein regained a lower level of refolding at 25°C (approximately 80%) compared to HSP10-p.wt (approximately 95%). Altogether, these results suggest that the Leu73Phe mutation negatively affects the conformational stability of the HSP10 protein and impairs its spontaneous refolding.

Decreased conformational stability should render the HSP10-p.Leu73Phe protein more vulnerable to proteolytic attack. To test this we performed a limited proteolysis experiment of the HSP10-p.Leu73Phe protein at physiological temperature and pH. Purified wild type and mutant HSP10 were incubated at 37°C and pH 7.8 with trypsin for different time periods. Both the wild type and the mutant HSP10 proteins were trimmed to a shorter core fragment (HSP10∗) shortly after addition of trypsin (**Figure 2D**). The core fragment band of HSP10-p.wt was largely stable to further attack by trypsin for up to 2 h whereas the HSP10-p.Leu73Phe core fragment band was continuously degraded resulting in strongly reduced levels already after 1 h and absence of the band after 2 h incubation (**Figures 2D,E**). This suggests that the core fragment is much more susceptible to proteolytic degradation when it carries a phenylalanine at the mutation site than when it carries the wild type leucine.

To elucidate which part of HSP10 was lacking in the trimmed core fragments, we performed mass spectrometric analysis of the excised full-length and core HSP10 bands (**Supplementary Figure S1**). Both the full-length and the core

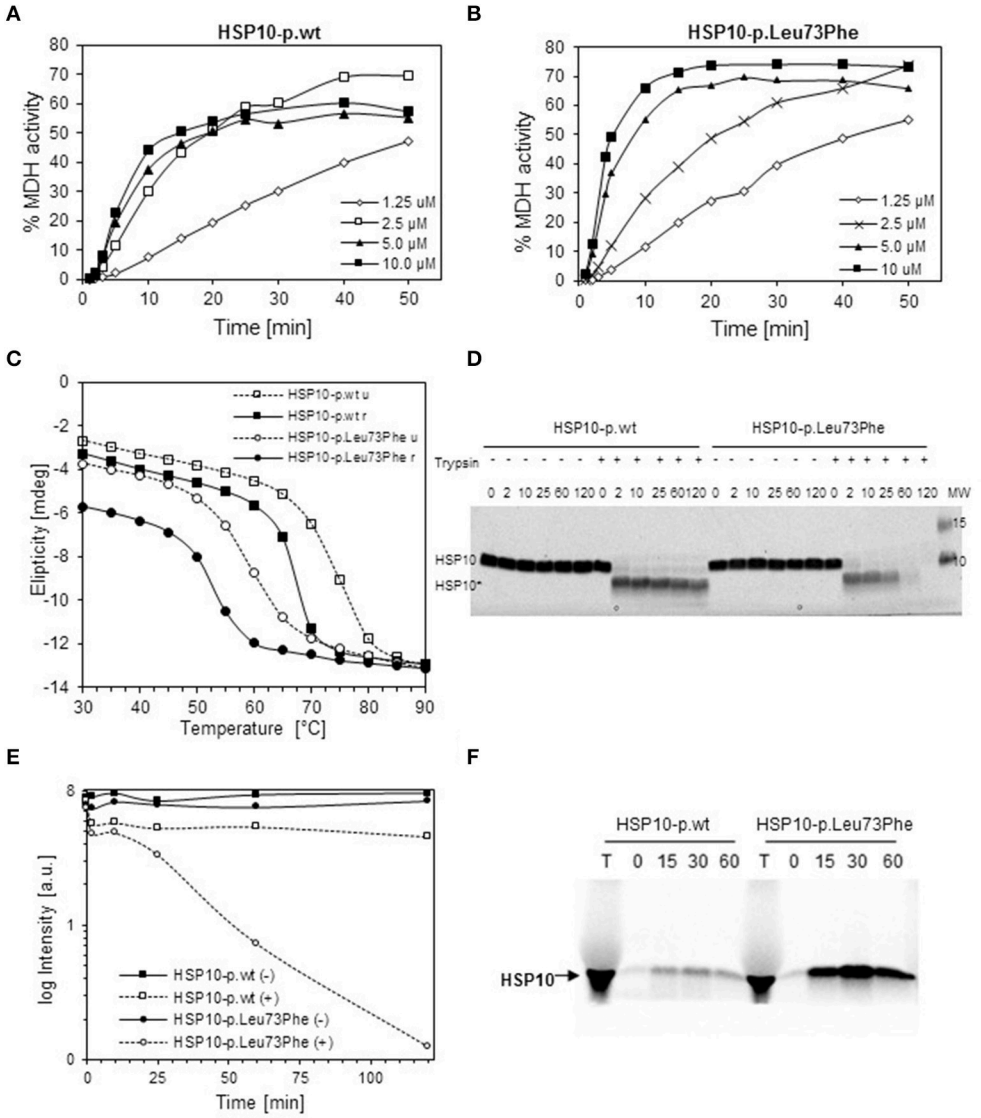

FIGURE 2 | *In vitro* properties of recombinantly produced HSP10-p.Leu73Phe. (A,B) Refolding kinetics of denatured MDH. HCl-denatured MDH (0.33 mM) was refolded at 30°C with HSP60 (10 µM), ATP (1 mMol/L) and the indicated concentrations of wild type **(A)** or p.Leu73Phe mutant **(B)** HSP10. Refolding is expressed as the percentage of MDH activity before denaturation. **(C)** Thermal unfolding/refolding kinetics of wild type and p.Leu73Phe mutant HSP10. Folding status was monitored by following the circular dichroism signal at 222 nm. 0.3 mg/ml HSP10-p.wt or HSP10-p.Leu73Phe in buffer containing 50 mM Tris-HCl pH 7.7 and 100 mM NaCl were analyzed. The experiments were carried out by varying the temperature from 25 to 90°C (stippled lines; u = unfolding) and back to 25°C (solid lines; r = refolding). Ellipticity was measured with 2°C intervals, 180 s setting time and 120 s time per point. **(D)** Limited proteolysis of HSP10 proteins with trypsin. HSP10-p.wt and HSP10-Leu73Phe at 0.1 µg/ml in 100 mM Tris-HCl (pH 7.8) were incubated at 37°C with or without addition of trypsin at a stoichiometric ratio of 1:10 (trypsin: HSP10). Proteolysis was stopped with addition of SDS PAGE sample buffer at the time points indicated and proteins were separated by SDS PAGE and stained with Coomassie. The positions of full-length HSP10 and HSP10 core fragment are indicated. **(E)** Quantification of the band-intensities from the Coomassie-stained gel shown in **(D)**. **(F)** Import kinetics of wild type and p.Leu73Phe mutant HSP10 into isolated mouse liver mitochondria. The HSP10 proteins were synthesized and radioactively labeled using a reticulocyte lysate system programmed by plasmids carrying the respective cDNAs as described in Materials and Methods. Translated proteins were added to freshly isolated mouse liver mitochondria and incubated at 37°C. Aliquots were taken at the time points indicated, and mitochondria were trypsin-treated and reisolated. Aliquots were run on SDS PAGE followed by phosphorimaging. T: aliquot from the *in vitro* translation reaction.

bands from wild type and mutant HSP10 showed robust MS signals for the peptides comprising amino acids 41–54 and 71–80 (peptide containing the mutation site). However, the peptide comprising amino acids 9–15 (FLPLFDR) was clearly present in the full-length band yet strongly decreased in the core bands, suggesting that low amounts of trypsin trim off N-terminal parts in both the wild type and the mutant HSP10 protein.

To rule out the possibility that the mutation impairs import of mutant HSP10 protein, we compared import of the *in vitro* labeled HSP10 wild type and mutant proteins into isolated

mouse liver mitochondria. Aliquots were taken at the time points indicated and imported proteins were analyzed by SDS PAGE and phosphorimaging after reisolation of the mitochondria. **Figure 2F** shows the band pattern from a representative experiment. To our surprise the HSP10-p.Leu73Phe protein was clearly imported more efficiently than the wild type HSP10 protein. Adding the HSP10 proteins to the import mixture in unfolded conformation after precipitation and resuspension in denaturant resulted qualitatively in the same picture (data not shown).

The Effects of the HSP10 Mutation in Patient Fibroblasts

To evaluate the consequences of the conformational destabilization of HSP10 by the p.Leu73Phe mutation *in vivo* we turned to a cellular model system. A fibroblast culture was established from a skin biopsy of the patient. We first confirmed heterozygosity of the *HSPE1:* c.217C>T mutation by Sanger sequencing of genomic DNA isolated from the fibroblasts (**Figure 3A**). To elucidate whether the c.217C>T mutation affects transcript levels we isolated RNA from the fibroblast culture. Sequencing of the PCR product amplified from the reverse transcribed RNA (**Figure 3B**) showed a very similar tracing pattern around the mutation site as sequencing of the PCR product amplified from genomic DNA from the patient (**Figure 3A**). The peaks for both the C and the T at position 217 had comparable heights in Sanger sequencing of both genomic DNA and cDNA suggesting that roughly half of the *HSPE1* transcripts in the patient fibroblasts carried the mutation. The primers used for amplification of the cDNA were localized in exons 2 and 4, respectively, surrounding the mutation site in exon 3. The sequence reads of the junctions between exons 2 and 3 and between exons 3 and 4 were as expected indicating that splicing was unaffected by the mutation. qRT-PCR analysis of HSP10 and HSP60 transcript levels showed no significant differences between patient and control fibroblasts (**Supplementary Figure S1**). Taken together, this is consistent with the notion that the *HSPE1*:c.217C>T mutation does not significantly affect transcript levels or splicing.

To detect and quantitate the steady state levels of the HSP10-p.Leu73Phe protein in fibroblasts of the patient we applied a targeted mass spectrometric approach known as selected reaction monitoring (SRM) using heavy-labeled synthetic peptides as internal standards. Very small amounts of mutant HSP10-p.Leu73Phe protein were present in fibroblasts from the patient. Identification of this peptide was based on its fragmentation pattern that was the same as that of the heavy labeled synthetic peptide that had been spiked into the sample (**Figure 3C**). No corresponding peptide with such a pattern was detectable in control fibroblasts (data not shown). This indicated that small amounts of mutant HSP10-p.Leu73Phe protein were present in fibroblasts from the patient.

We then quantitated the total amounts of wild type and mutant HSP10 protein in patient and control fibroblasts using two peptides present in both the wild type and the HSP10-p.Leu73Phe protein (peptides 1 and 2 in **Figure 3D**). SRM analysis showed that the amounts of the HSP10 peptides 1 and 2 in the patient fibroblasts were decreased to approximately 50% as compared to the controls (**Figure 3E**). Measurement of the wild type peptide spanning the mutation site (peptide 3) showed only slightly lower relative amounts than peptides 1 and 2 (approximately 40% compared to approximately 50% for peptides 1 and 2) in the patient fibroblasts compared to the control fibroblasts. Taken together, our data strongly suggests that the majority of the HSP10 protein present in patient fibroblasts represents wild type HSP10 protein expressed from the wild type allele.

We have previously observed decreased SOD2 protein levels due to misfolding and degradation of SOD2 protein followed by increased oxidative protein damage (protein carbonylation) in a mouse model for hereditary spastic paraplegia due to HSP60 haplosufficiency (Magnoni et al., 2013). As our present investigations had shown half levels of HSP10 protein in fibroblasts from our patient, we speculated that this might also affect SOD2 protein amounts and superoxide levels. Again using SRM mass spectrometry with heavy labeled peptides as standards, we quantified SOD2 in cell lysates from patient and control fibroblasts. In parallel we quantified the complex partner HSP60, the fatty acid oxidation enzyme medium-chain acyl-CoA dehydrogenase (MCAD) that previously had been shown to interact with the HSP60/HSP10 complex (Saijo et al., 1994; Saijo and Tanaka, 1995) and the mitochondrial outer membrane protein VDAC, which was not expected to interact with the HSP60/HSP10 complex. We found comparable protein levels for HSP60, MCAD, and VDAC in patient and control fibroblasts (**Figure 4A**). However, the protein level of SOD2 was reduced to approximately 20% in the patient fibroblasts compared to controls. RT-qPCR analysis showed that SOD2 mRNA transcript levels, like those for the HSP60 and MCAD mRNAs, were similar in the fibroblasts from patient and controls (**Supplementary Figure S2**). Hence, decreased SOD2 protein levels were not due to decreased SOD2 transcript levels.

Decreased SOD2 protein levels would be expected to result in increased superoxide levels in the mitochondrial matrix. Indeed, when measuring mitochondrial superoxide with the fluorescent probe MitoSOX we observed an approximately 2-fold increase in average MitoSOX fluorescence intensity in the patient fibroblasts compared to control fibroblasts (**Figure 4B**). In an attempt to identify further functions that may be affected we also evaluated a number of cellular and mitochondria-related phenotypes of the patient fibroblasts. Fluorescence microscopic analysis of mitochondria labeled with Mitotracker green revealed no morphological differences between patient and control fibroblasts (**Supplementary Figure S3**). Furthermore, no significant differences between patient and control fibroblasts were observed in assays for cellular viability (**Supplementary Figure S4A**), overall oxidation state measured as the level of reduced thiols (**Supplementary Figure S4B**), and mitochondrial membrane potential (**Supplementary Figure S4C**). We finally analyzed OCR as a measure for mitochondrial respiratory chain activity using a Seahorse extracellular flux analyzer. No significant differences in basal OCR, reserve capacity, and ATP-linked

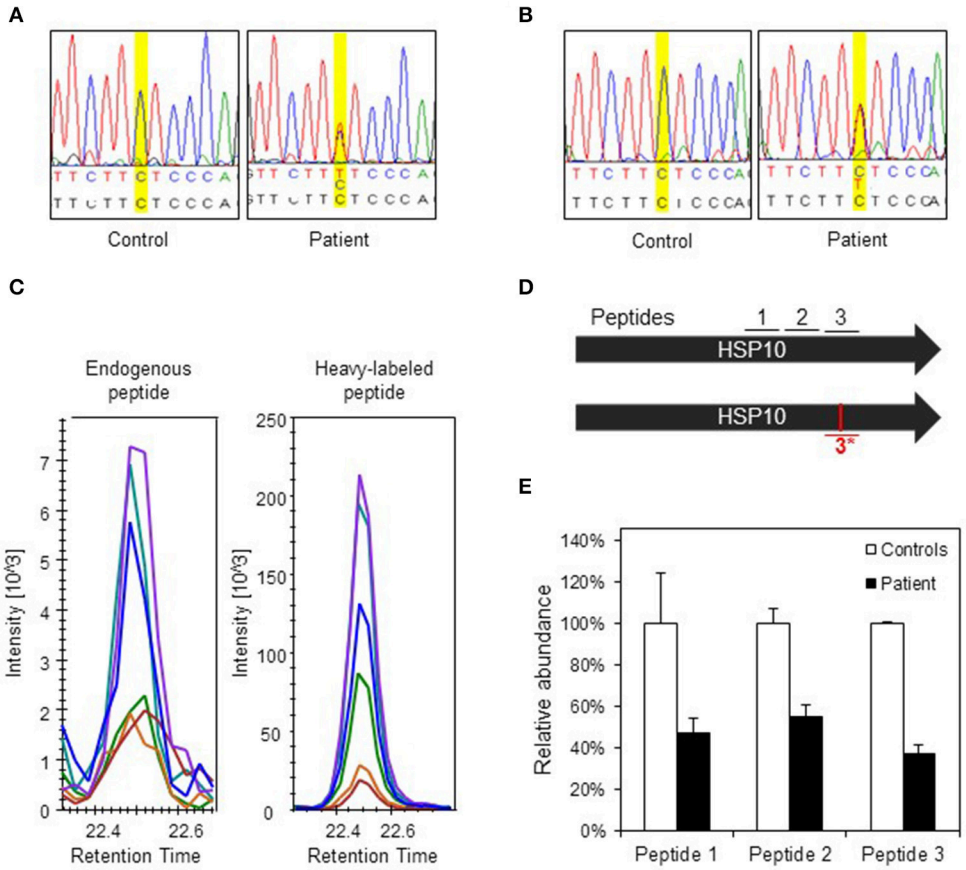

FIGURE 3 | Analysis of DNA, RNA, and protein in patient fibroblasts. (A) Confirmation of c.217 C > T mutation in patient fibroblasts. A fragment spanning the mutation site was amplified by PCR and analyzed by Sanger sequencing. Yellow highlighting indicates position c.217 and bases are indicated below: top line depicts bases found by sequencing, lower line shows reference sequence. **(B)** Sequencing of transcripts. Total RNA was isolated from control and patient fibroblast and used for cDNA synthesis followed by PCR amplification of a fragment comprising the mutation site. PCR fragments were analyzed by Sanger sequencing. **(C)** Detection of the mutant peptide in patient fibroblasts by SRM-MS. The fragmentation patterns for the analyzed peptide fragments for the mutant peptide (#3*) detected in fibroblasts from the patient (left panel) and the heavy-labeled peptide that was spiked into the sample (right panel) are shown. The graphs show the peaks for the different fragment ions in corresponding colors. **(D)** Peptides used for SRM analysis. Bars show the two HSP10 alleles of the patient with position of the peptides and the mutation site. Peptides #1 and #2 are common to wild type and p.Leu73Phe HSP10 and the peptides spanning the mutation site (#3 wild type and #3*, mutant) are depicted. **(E)** Quantification of HSP10 in patient and control fibroblasts. The two peptides common to both wild type and p.Leu73Phe HSP10 (#1 and #2) and the peptide with wild type sequence spanning the mutation site (#3) were quantitated by SRM analysis as described in Materials and Methods. The mean of the quantitated amounts of the three peptides measured in three different control fibroblast cultures were set to 100% and the mean amounts measured in three patient cell cultures grown in parallel were expressed as percentage of these. Error bars denote standard deviation of the mean.

respiration (**Supplementary Figure S4D**) as well as basal extracellular acidification rate (data not shown) between patient and control fibroblasts were observed. This suggests that HSP10 deficiency did not have a major effect on mitochondrial respiratory chain activity and balance between mitochondrial respiration and anaerobic glycolysis.

DISCUSSION

Exome sequencing of the patient with infantile spasms and developmental delay described here detected heterozygosity for a *de novo* mutation in the *HSPE1* gene and chromosomal microarray analysis detected a *de novo* deletion affecting the *TANC2* gene. Expression levels of the TANC gene family genes *TANC1* and *TANC2* have been indicated to regulate the density of dendritic spines and excitatory synapses (Han et al., 2010) and diagnostic exome sequencing identified a *de novo* TANC1 missense variation in one patient with severe intellectual disability (de Ligt et al., 2012). Both the HSP10 missense mutation and the loss of one *TANC2* allele may potentially be disease-associated. Because the *HSPE1* gene encoding the small subunit of the mitochondrial HSP60/HSP10 chaperonin complex is essential for cell function and mutations in its complex partner HSP60 have been associated with neurological diseases, we have in the present study focused on investigating the effects of the HSP10-p.Leu73Phe mutation.

The odds for accidentally finding a *de novo* mutation in a specific gene are small. Data from exome sequencing predict on average one *de novo* missense mutation per exome per

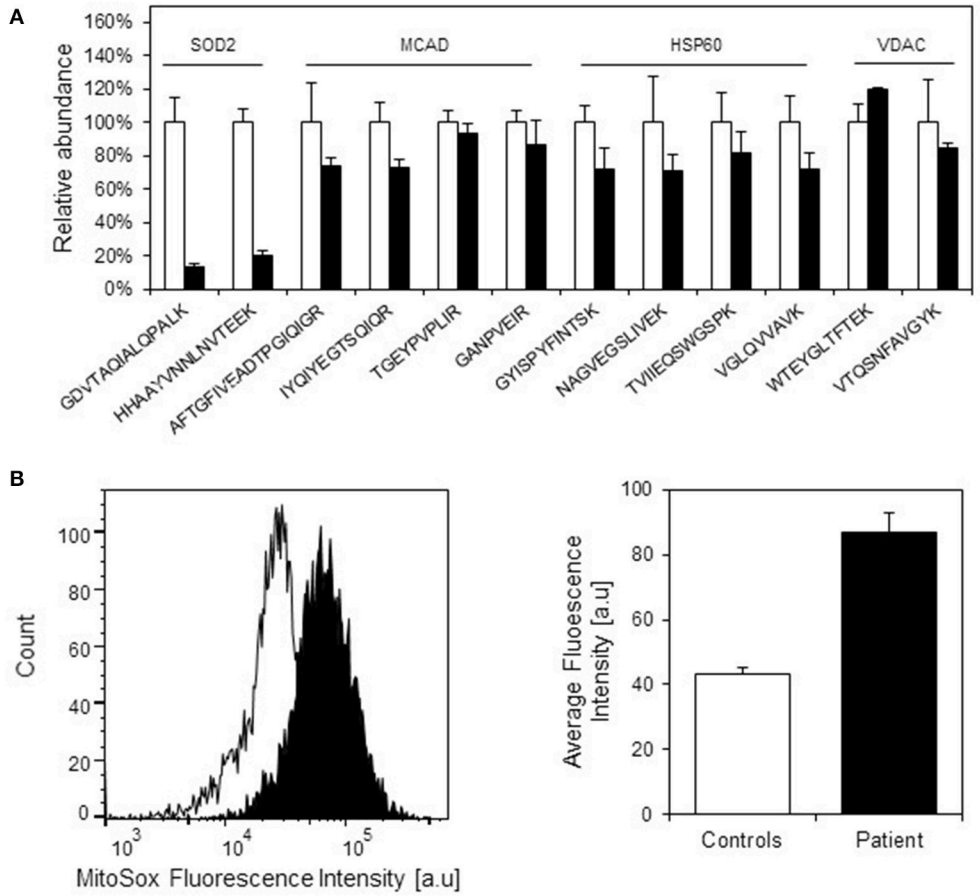

FIGURE 4 | Protein levels of selected mitochondrial proteins in patient and control fibroblasts. (A) Levels of peptides for HSP60, MCAD, VDAC, and SOD2 were measured by SRM-MS. The quantitated amounts of all peptides measured in three different control fibroblast (open bars) were set to 100% and the amounts measured in three parallel grown patient fibroblast cultures (filled bars) were expressed as percent fraction of these. Error bars denote standard deviation of the mean. T-testing showed that the levels of the SOD2 peptides were significantly decreased ($p < 0.05$) in patient fibroblasts, while the peptides for MCAD, HSP60, and VDAC were not significantly different in patient compared to control fibroblasts. **(B)** Mitochondrial superoxide levels. Superoxide levels were determined using the fluorescent superoxide reporter MitoSOX. The left graph shows the histogram from one analysis; open peak: control, closed peak: patient. The right graph shows average mean fluorescence intensities measured from three independent cultivations and analyses of control fibroblasts and parallel cultivations of the patient fibroblast. Error bars represent SEM for the three respective replicates.

generation (Veltman and Brunner, 2012; Alkuraya, 2016). Given this number, the length of the HSP10 coding region with 306 bases, the total human exome length with approximately 3.10^7 bases, and the world population at currently approximately 7.5×10^6 people, one can statistically expect 27 currently living individuals carrying a *de novo* mutation in the *HSPE1* exome. A considerable fraction of these would be synonymous, so only a handful of individuals will have missense or premature stop codon variations in the *HSPE1* gene.

Inspection of the mutation site in the structure of the human HSP60/HSP10 complex showed that leucine-73 of HSP10 is not localized in the domain that interacts with HSP60 subunits in the complex. Rather, it is situated in the central part of the HSP10 structure, tightly packed by residues within the same HSP10 subunit. The phenylalanine that replaces leucine in the mutant protein can apparently be accommodated in the structure, but, because it is more bulky, it requires rearrangements. Such rearrangements of the domain are expected to impair folding and stability. Our *in vitro* analysis of recombinant HSP10-p.Leu73Phe protein showed that although this protein could be recombinantly expressed and purified in a fully functional form, its thermal stability was indeed profoundly decreased and its spontaneous refolding after denaturation was impaired. Although, the decreased melting temperature of the HSP10-p.Leu73Phe protein determined under *in vitro* conditions was well above 37°C, we show that the mutant HSP10 protein displays increased susceptibility to proteolytic attack at 37°C and physiological pH.

Our observation that posttranslational import of the HSP10-p.Leu73Phe protein into isolated mitochondria was more efficient than import of the wild type HSP10 protein was surprising. However, it has been shown for some other proteins

that mutations destabilizing the conformational structure of precursor proteins in the cytosol enhances their post-translational import into mitochondria (Vestweber and Schatz, 1988). Protein import through the mitochondrial outer and inner membrane as well as degradation by the ATP dependent proteases Lon and ClpXP in the mitochondrial matrix require previous unfolding of the transported/degraded polypeptide (Lee et al., 2001; Prakash and Matouschek, 2004; Maurizi and Stan, 2013). Thus, what at first sight appears to be counterintuitive, likely reflects that the decreased conformational stability renders the mutant HSP10 protein both more prone to be transported through the mitochondrial import system and more prone to degradation by mitochondrial proteases. In line with this, the steady state levels of the HSP10-p.Leu73Phe protein in the patient fibroblasts were much lower than those of the HSP10-p.wt protein. Because transcript levels of the mutant allele appeared unchanged and—given its position in the transcript—because an effect of the mutation on translation is unlikely, this suggested that the decreased level of the HSP10-p.Leu73Phe protein is due to higher susceptibility to proteolytic degradation.

Given the measured decreased Hsp10 to HSP60 protein ratio, we wondered what effects this could potentially have? The genes encoding HSP60 and HSP10, respectively, of eukaryotes from *C. elegans* to humans are organized in a head-to-head arrangement with a common bidirectional promoter (Ryan et al., 1997; Bross et al., 2013). Furthermore, in bacteria the corresponding genes encoding the large and small chaperonin subunits are typically organized in an operon under control of a common promoter (Lund, 2009). These architectures may provide transcription of both chaperonin genes at a fixed ratio suggesting that this ratio is crucial for correct function of chaperonin complexes. It has indeed been shown that the kinetics of *in vitro* refolding of malate dehydrogenase by the HSP60/HSP10 complex depended on the HSP10 to HSP60 ratio (Levy-Rimler et al., 2001). Maximum refolding rate was obtained at approximately 2:1 HSP10: HSP60 molar ratio and clearly lower refolding was observed at a ratio of to 1:1. Levy-Rimler et al. also presented evidence that HSP10 stabilizes the double-ring conformation of human HSP60. Thus, the observed almost 2-fold decrease of the HSP10/HSP60 ratio would be expected to compromise the function and capacity of the HSP60/HSP10 complex to assist folding and result in significant impairment of folding of those proteins that are most dependent on folding assistance by the HSP60/HSP10 complex.

We have previously shown that folding of SOD2, the superoxide dismutase in the mitochondrial matrix, was dramatically compromised in mice that express half levels of HSP60 due to heterozygosity for a knock-out allele of the murine *Hspd1* gene (Magnoni et al., 2014). Furthermore, we could demonstrate physical interaction of SOD2 with the HSP60/HSP10 complex. As expected, our analyses of the patient fibroblasts studied here showed that SOD2 protein levels were significantly decreased. Decreased SOD2 protein levels were not caused by decreased *SOD2* transcript levels as shown by qRT-PCR analysis. This is consistent with the notion that SOD2 is one of the proteins in the mitochondrial matrix, which particularly depend on the HSP60/HSP10 complex to acquire its native state. The native state of the SOD2 enzyme is a homotetramer with a manganese atom in the active site of all four subunits (Borgstahl et al., 1992). Decreasing either component of the HSP60/HSP10 complex appears to impair SOD2 protein folding and entail degradation of SOD2 folding intermediates. Recombinant expression experiments in *E. coli* have shown that yield, metal content and activity of human SOD2 were increased when the bacterial HSP60/HSP10 homolog GroEL/GroES was co-overexpressed (Hunter and Hunter, 2013). Assistance by the HSP60/HSP10 chaperonin complex for folding and concomitant metal incorporation may be a particularly crucial step that it is impaired when the capacity of HSP10/HSP60 complex is limiting.

No monogenic human disease caused by mutations in the *SOD2* gene has been described yet. A series of knockout mouse models for the *Sod2* gene have been investigated mostly in context with research of the mitochondrial free radical theory of aging (Barja, 2013). Knock-out of both *Sod2* alleles leads to lethality within 18 days of birth in different strain backgrounds (reviewed in Marecki et al., 2014). Mice with only one *Sod2*-knock-out allele that express half levels of the SOD2 protein had normal life-span and no overt phenotype, but displayed increased oxidative damage as well as increased apoptosis tendency (Strassburger et al., 2005; Wenzel et al., 2008). The SOD2 levels we measured in the patient fibroblasts were less than 50% of controls suggesting more severe consequences than those modeled in the heterozygous SOD2 knockout mice. Damage caused by high levels of reactive oxygen species is especially critical for neuronal tissue that only to very limited extent can be regenerated. A consequence of decreased SOD2 activity would be increased superoxide levels in the mitochondrial matrix and we indeed measured a significant increase in matrix superoxide using the mitochondrial matrix fluorescence reporter MitoSOX. This may advocate that increased superoxide levels represent one of the disease-associated molecular phenotypes in the current case.

The question remains whether increased superoxide levels are the only major effect of the HSP10 mutation in the patient cells investigated in our study. The observation of intermittently increased levels of various disease marker metabolites related to mitochondrial enzyme deficiencies in the patient suggests that the SOD2 deficiency is probably only one of several consequences of the skewed HSP10/HSP60 ratio. Our further analysis of the patient fibroblasts for general mitochondrial factors like mitochondrial membrane potential, cellular redox status and mitochondrial respiratory chain activity showed no significant differences compared to controls suggesting that potential additional effects on these parameters are subtle or not manifesting in fibroblasts.

We also analyzed whether the levels of medium-chain acyl-CoA dehydrogenase (MCAD) were affected in the patient cells. MCAD is an enzyme involved in mitochondrial fatty acid oxidation that has previously been shown to interact with the

HSP60/HSP10 complex (Yokota et al., 1992; Saijo et al., 1994). Yet, our investigations showed similar MCAD protein levels in the patient and control fibroblasts, suggesting that folding of this interactor is less affected by the decreased HSP10 levels. The interactors of the homologous bacterial GroEL/GroES complex have been characterized and distinguished into classes depending on the length of the time period they interact (Ewalt et al., 1997). Among approximately 250 interactors a core set of about 85 proteins was shown to be highly dependent on folding assistance by the chaperonin complex (Kerner et al., 2005). Such an inventory of interactors and validation of their dependence on the function of the HSP60/HSP10 complex would be helpful for pinpointing further candidates, but is still lacking for the mammalian HSP60/HSP10 complex.

In conclusion, as we did not investigate potential effects of the deletion of parts of the *TANC2* gene, we can currently not exclude that it is disease associated. However, based on the results from a battery of *in vitro* and *ex vivo* studies, we make the case that heterozygosity for the HSP10-p.Leu76Phe *de novo* missense mutation potentially could be responsible for the neurological and developmental disorder of the patient reported here.

AUTHOR CONTRIBUTIONS

AB, PB, AA, PF, KH, JP, and TC designed the experimental setup. KH, LB, have performed the clinical analysis of the patient. JD, HL, ND performed the clinical exome sequencing, chromosome microarray analysis and interpretation of these data. AB, SN, XL, PF, DP, RB, JP, and PB performed the experimental work. All authors were involved in writing the first draft and finalizing the manuscript.

ACKNOWLEDGMENTS

We thank UCLA Clinical Genomics Center Genomic Data Board for reviewing the CES data. We thank prof. Wolfgang Voos, University of Bonn, Germany, for advice for the mitochondrial import assay. We gratefully acknowledge the collaboration with the family of the patient that first made this study possible. This work was supported by grants from the Ludvig and Sara Elsass Foundation (to PB; J.-nrs.: 3993 and 4756), Aarhus University HEALTH graduate school (to AB), and the Eva & Henry Frænkels Mindefond (to PB). The mass spectrometers were funded by the John and Birthe Meyer Foundation (Research Unit for Molecular Medicine). The work at the laboratory of Azem is supported by the DFG trilateral project (Reference number SCHO 754/5-1).

SUPPLEMENTARY MATERIAL

The Supplementary Material for this article can be found online at: http://journal.frontiersin.org/article/10.3389/fmolb.2016.00065

Supplementary Figure S1 | Mass spectrometric analysis of HSP10 full-length and core bands. (A) Full-length and core bands from a limited proteolysis experiment like the one shown in **Figure 2D** were excised and prepared for mass spectrometry (LC-MS/MS). Elution profiles for detected peptides are shown in **(A)**. The arrows point to peptides that are highlighted in the corresponding colors in **(B)**. Green arrow: amino acids 41–54 (VLQATVVAVGSGSK), magenta arrows: amino acids 71–80 (VL-x-PEYGGTK with Leu (wt) or Phe (mutant), respectively, at the "x"-position), blue arrow: amino acids 9–15 (FLPLFDR). **(B)** HSP10 subunit R in schematic representation. Position of lysine and arginine residues are highlighted in yellow, the mutated leucine-73 residue is shown as sticks in red and the amino (N) and carboxy-terminal (C) positions are depicted. The representation was made with Discovery Studio Visualizer v.4.5 (Biovia) using PDB coordinates for the human HSP60/HSP10 complex (4PJ1).

Supplementary Figure S2 | RT-qPCR quantitation of transcript levels. RNA purified from patient and three individual control fibroblasts was reverse transcribed into cDNA and subjected to quantitative analysis with qPCR TaqMan assays. Error bars represent standard error of mean for biological triplicates. Filled bars: Patient, open bars: mean from three pooled controls. *P*-values were obtained with student's *t*-test and showed no significant differences.

Supplementary Figure S3 | Mitochondrial morphology. Fibroblasts from the patient and a healthy control individual were seeded at 50% confluence in 6-well plates 24 h before the analysis. The fibroblasts were stained with 100 nM Mitotracker Green for 30 min at 37°C. Pictures were obtained with the EVOS FLoid Cell Imaging Station as described in materials and methods. Two representative pictures each of the control (left panel) and the patient (right panel) fibroblasts are shown.

Supplementary Figure S4 | Cellular viability, thiol redox status, mitochondrial membrane potential, and mitochondrial oxygen consumption profiling. (A) Cellular viability measured as the percentage of viable cells. **(B)** Cellular thiol redox status measured as intensity of the Vita-Bright 48 (V.B-48) fluorescent dye. V.B-48 becomes fluorescent when it reacts with reduced thiols which are used to quench molecules that are damaging to the cell, such as free radicals, and are used as a measurement for general cellular oxidative/reduced status. **(C)** The mitochondrial membrane potential measured as the red/green ratio of the fluorescent dye JC-1. An assay control (control cells treated with the uncoupler CCCP) is also shown. **(D)** Mitochondrial oxygen consumption rate profiling. Oxygen consumption rate (OCR) of patient and control fibroblasts in dependence of addition of modulators [1: oligomycin (inhibitor of complex V); 2: FCCP (uncoupler); 3: antimycin A and rotenone (inhibitors of complex I and III, respectively)] was measured using the Mito Stress test-kit and the Seahorse XF^e96 extracellular flux analyzer. Samples from 3 different control fibroblasts and 3 independently grown cultures of the patient fibroblasts were analyzed. OCR was normalized to total protein amount quantified by the Bradford assay.

Supplementary Table S1 | Oligonucleotide primer sequences.

Supplementary Table S2 | Genes investigated in exome sequencing.

REFERENCES

Aldridge, J. E., Horibe, T., and Hoogenraad, N. J. (2007). Discovery of genes activated by the mitochondrial unfolded protein response (mtUPR) and cognate promoter elements. *PLoS ONE* 2:e874. doi: 10.1371/journal.pone.0000874

Alkuraya, F. S. (2016). Discovery of mutations for Mendelian disorders. *Hum. Genet.* 135, 615–623. doi: 10.1007/s00439-016-1664-8

Balch, W. E., Morimoto, R. I., Dillin, A., and Kelly, J. W. (2008). Adapting proteostasis for disease intervention. *Science* 319, 916–919. doi: 10.1126/science.1141448

Barja, G. (2013). Updating the mitochondrial free radical theory of aging: an integrated view, key aspects, and confounding concepts. *Antioxid Redox Signal* 19, 1420–1445. doi: 10.1089/ars.2012.5148

Bonshtien, A. L., Parnas, A., Sharkia, R., Niv, A., Mizrahi, I., Azem, A., et al. (2009). Differential effects of co-chaperonin homologs on cpn60 oligomers. *Cell Stress Chaperones* 14, 509–519. doi: 10.1007/s12192-009-0104-2

Borgstahl, G. E., Parge, H. E., Hickey, M. J., Beyer, W. F. Jr., Hallewell, R. A., and Tainer, J. A. (1992). The structure of human mitochondrial manganese superoxide dismutase reveals a novel tetrameric interface of two 4-helix bundles. *Cell* 71, 107–118.

Bross, P., and Fernandez-Guerra, P. (2016). Disease-associated mutations in the HSPD1 gene encoding the large subunit of the mitochondrial HSP60/HSP10 chaperonin complex. *Front. Mol. Biosci.* 3:49. doi: 10.3389/fmolb.2016.00049

Bross, P., Magnoni, R., and Sigaard Bie, A. (2013). Molecular chaperone disorders: defective Hsp60 in neurodegeneration. *Curr. Top. Med. Chem.* 12, 2491–2503. doi: 10.2174/1568026611212220005

Bross, P., Naundrup, S., Hansen, J., Nielsen, M. N., Christensen, J. H., Kruhoffer, M., et al. (2008). The HSP60-(P.val98ile) mutation associated with hereditary spastic paraplegia SPG13 compromises chaperonin function both *in vitro* and *in vivo*. *J. Biol.Chem.* 283, 15694–15700. doi: 10.1074/jbc.M800548200

Bross, P., Winter, V., Pedersen, C. B., and Gregersen, N. (2003). "Investigation of folding and degradation of in vitro synthesized mutant proteins in mitochondria," in *Protein Misfolding and Disease - Principles and Protocols,* Vol. 232, eds P. Bross and N. Gregersen (Totowa, NJ: Humana Press), 285–294.

Chen, B., Retzlaff, M., Roos, T., and Frydman, J. (2011). Cellular strategies of protein quality control. *Cold Spring Harb. Perspect. Biol.* 3:a004374. doi: 10.1101/cshperspect.a004374

Cheng, M. Y., Hartl, F. U., Martin, J., Pollock, R. A., Kalousek, F., Neupert, W., et al. (1989). Mitochondrial heat-shock protein hsp60 is essential for assembly of proteins imported into yeast mitochondria. *Nature* 337, 620–625.

Christensen, J. H., Nielsen, M. N., Hansen, J., Fuchtbauer, A., Fuchtbauer, E. M., West, M., et al. (2010). Inactivation of the hereditary spastic paraplegia-associated Hspd1 gene encoding the Hsp60 chaperone results in early embryonic lethality in mice. *Cell Stress Chaperones* 15, 851–863. doi: 10.1007/s12192-010-0194-x

de Ligt, J., Willemsen, M. H., van Bon, B. W., Kleefstra, T., Yntema, H. G., Kroes, T., et al. (2012). Diagnostic exome sequencing in persons with severe intellectual disability. *N. Engl. J. Med.* 367, 1921–1929. doi: 10.1056/NEJMoa1206524

Edhager, A. V., Stenbroen, V., Nielsen, N. S., Bross, P., Olsen, R. K., Gregersen, N., et al. (2014). Proteomic investigation of cultivated fibroblasts from patients with mitochondrial short-chain acyl-CoA dehydrogenase deficiency. *Mol. Genet. Metab.* 111, 360–368. doi: 10.1016/j.ymgme.2014.01.007

Ewalt, K. L., Hendrick, J. P., Houry, W. A., and Hartl, F. U. (1997). *In vivo* observation of polypeptide flux through the bacterial chaperonin system. *Cell* 90, 491–500.

Fernández-Guerra, P., Birkler, R. I. D., Merinero, B., Ugarte, M., Gregersen, N., Rodríguez-Pombo, P., et al. (2014). Selected reaction monitoring as an effective method for reliable quantification of disease-associated proteins in maple syrup urine disease. *Mol. Genet. Genomic Med.* 2, 383–392. doi: 10.1002/mgg3.88

Fernandez-Guerra, P., Lund, M., Corydon, T. J., Cornelius, N., Gregersen, N., Palmfeldt, J., et al. (2016). Application of an image cytometry protocol for cellular and mitochondrial phenotyping on fibroblasts from patients with inherited disorders. *JIMD Rep.* 27, 17–26. doi: 10.1007/8904_2015_494

Greenfield, N. J. (2006). Using circular dichroism collected as a function of temperature to determine the thermodynamics of protein unfolding and binding interactions. *Nat. Protoc.* 1, 2527–2535. doi: 10.1038/nprot.2006.204

Gregersen, N., Bross, P., Vang, S., and Christensen, J. H. (2006). Protein misfolding and human disease. *Annu. Rev. Genomics Hum. Genet.* 7, 103–124. doi: 10.1146/annurev.genom.7.080505.115737

Han, S., Nam, J., Li, Y., Kim, S., Cho, S. H., Cho, Y. S., et al. (2010). Regulation of dendritic spines, spatial memory, and embryonic development by the TANC family of PSD-95-interacting proteins. *J. Neurosci.* 30, 15102–15112. doi: 10.1523/jneurosci.3128-10.2010

Hansen, J., Corydon, T. J., Palmfeldt, J., Durr, A., Fontaine, B., Nielsen, M. N., et al. (2008). Decreased expression of the mitochondrial matrix proteases Lon and ClpP in cells from a patient with hereditary spastic paraplegia (SPG13). *Neuroscience* 153, 474. doi: 10.1016/j.neuroscience.2008.01.070

Hansen, J. J., Dürr, A., Cournu-Rebeix, I., Georgopoulos, C., Ang, D., Nielsen, M. N., et al. (2002). Hereditary spastic paraplegia SPG13 is associated with a mutation in the gene encoding the Mitochondrial Chaperonin Hsp60. *Am. J. Hum. Genet.* 70, 1328–1332. doi: 10.1086/339935

Hartman, D. J., Hoogenraad, N. J., Condron, R., and Hoj, P. B. (1992). Identification of a mammalian 10-kDa heat shock protein, a mitochondrial chaperonin 10 homologue essential for assisted folding of trimeric ornithine transcarbamoylase *in vitro*. *Proc. Natl. Acad. Sci. U.S.A.* 89, 3394–3398.

Hayer-Hartl, M., Bracher, A., and Hartl, F. U. (2016). The GroEL-GroES chaperonin machine: a nano-cage for protein folding. *Trends Biochem. Sci.* 41, 62–76. doi: 10.1016/j.tibs.2015.07.009

Horwich, A. L., and Fenton, W. A. (2009). Chaperonin-mediated protein folding: using a central cavity to kinetically assist polypeptide chain folding. *Q. Rev. Biophys.* 42, 83–116. doi: 10.1017/s0033583509004764

Hunter, G. J., and Hunter, T. (2013). GroESL protects superoxide dismutase (SOD)- Deficient cells against oxidative stress and is a chaperone for SOD. *Health* 5, 1719–1729. doi: 10.4236/health.2013.510232

Kerner, M. J., Naylor, D. J., Ishihama, Y., Maier, T., Chang, H. C., Stines, A. P., et al. (2005). Proteome-wide analysis of chaperonin-dependent protein folding in *Escherichia coli*. *Cell* 122, 209–220. doi: 10.1016/j.cell.2005.05.028

Krissinel, E., and Henrick, K. (2007). Inference of macromolecular assemblies from crystalline state. *J. Mol. Biol.* 372, 774–797. doi: 10.1016/j.jmb.2007.05.022

Lee, C., Schwartz, M. P., Prakash, S., Iwakura, M., and Matouschek, A. (2001). ATP-dependent proteases degrade their substrates by processively unraveling them from the degradation signal. *Mol. Cell* 7, 627–637. doi: 10.1016/S1097-2765(01)00209-X

Lee, H., Deignan, J. L., Dorrani, N., Strom, S. P., Kantarci, S., Quintero-Rivera, F., et al. (2014). Clinical exome sequencing for genetic identification of rare Mendelian disorders. *JAMA* 312, 1880–1887. doi: 10.1001/jama.2014.14604

Levy-Rimler, G., Viitanen, P., Weiss, C., Sharkia, R., Greenberg, A., Niv, A., et al. (2001). The effect of nucleotides and mitochondrial chaperonin 10 on the structure and chaperone activity of mitochondrial chaperonin 60. *Eur. J. Biochem.* 268, 3465–3472. doi: 10.1046/j.1432-1327.2001.02243.x

Lund, P. A. (2009). Multiple chaperonins in bacteria–why so many? *FEMS Microbiol. Rev.* 33, 785–800. doi: 10.1111/j.1574-6976.2009.00178.x

Magen, D., Georgopoulos, C., Bross, P., Ang, D., Segev, Y., Goldsher, D., et al. (2008). Mitochondrial hsp60 chaperonopathy causes an autosomal-recessive neurodegenerative disorder linked to brain hypomyelination and leukodystrophy. *Am. J. Hum. Genet.* 83, 30–42. doi: 10.1016/j.ajhg.2008.05.016

Magnoni, R., Palmfeldt, J., Christensen, J. H., Sand, M., Maltecca, F., Corydon, T. J., et al. (2013). Late onset motoneuron disorder caused by mitochondrial Hsp60 chaperone deficiency in mice. *Neurobiol. Dis.* 54, 12–23. doi: 10.1016/j.nbd.2013.02.012

Magnoni, R., Palmfeldt, J., Hansen, J., Christensen, J. H., Corydon, T. J., and Bross, P. (2014). The Hsp60 folding machinery is crucial for manganese superoxide dismutase folding and function. *Free Radic. Res.* 48, 168–179. doi: 10.3109/10715762.2013.858147

Marecki, J. C., Parajuli, N., Crow, J. P., and MacMillan-Crow, L. A. (2014). The use of the Cre/loxP system to study oxidative stress in tissue-specific manganese superoxide dismutase knockout models. *Antioxid Redox Signal* 20, 1655–1670. doi: 10.1089/ars.2013.5293

Maurizi, M. R., and Stan, G. (2013). ClpX shifts into high gear to unfold stable proteins. *Cell* 155, 502–504. doi: 10.1016/j.cell.2013.10.007

Mills, P. B., Struys, E., Jakobs, C., Plecko, B., Baxter, P., Baumgartner, M., et al. (2006). Mutations in antiquitin in individuals with pyridoxine-dependent seizures. *Nat. Med.* 12, 307–309. doi: 10.1038/nm1366

Ng, P. C., and Henikoff, S. (2001). Predicting deleterious amino acid substitutions. *Genome Res.* 11, 863–874. doi: 10.1101/gr.176601

Nisemblat, S., Yaniv, O., Parnas, A., Frolow, F., and Azem, A. (2015). Crystal structure of the human mitochondrial chaperonin symmetrical football complex. *Proc. Natl. Acad. Sci. U.S.A.* 112, 6044–6049. doi: 10.1073/pnas.1411718112

Pace, C. N. (1990). Measuring and increasing protein stability. *Trends Biotechnol.* 8, 93–98.

Parnas, A., Nadler, M., Nisemblat, S., Horovitz, A., Mandel, H., and Azem, A. (2009). The MitCHAP-60 disease is due to entropic destabilization of the human mitochondrial Hsp60 oligomer. *J. Biol. Chem.* 284, 28198–28203. doi: 10.1074/jbc.M109.031997

Plecko, B., Paul, K., Paschke, E., Stoeckler-Ipsiroglu, S., Struys, E., Jakobs, C., et al. (2007). Biochemical and molecular characterization of 18 patients with pyridoxine-dependent epilepsy and mutations of the antiquitin (ALDH7A1) gene. *Hum. Mutat.* 28, 19–26. doi: 10.1002/humu.20433

Prakash, S., and Matouschek, A. (2004). Protein unfolding in the cell. *Trends Biochem. Sci.* 29, 593–600. doi: 10.1016/j.tibs.2004.09.011

Raimundo, N. (2014). Mitochondrial pathology: stress signals from the energy factory. *Trends Mol. Med.* 20, 282–292. doi: 10.1016/j.molmed.2014.01.005

Rhee, H. W., Zou, P., Udeshi, N. D., Martell, J. D., Mootha, V. K., Carr, S. A., et al. (2013). Proteomic mapping of mitochondria in living cells

via spatially restricted enzymatic tagging. *Science* 339, 1328–1331. doi: 10.1126/science.1230593

Ryan, M. T., Herd, S. M., Sberna, G., Samuel, M. M., Hoogenraad, N. J., and Hoj, P. B. (1997). The genes encoding mammalian chaperonin 60 and chaperonin 10 are linked head-to-head and share a bidirectional promoter. *Gene* 196, 9–17.

Saibil, H. R., Fenton, W. A., Clare, D. K., and Horwich, A. L. (2013). Structure and allostery of the chaperonin GroEL. *J. Mol. Biol.* 425, 1476–1487. doi: 10.1016/j.jmb.2012.11.028

Saijo, T., and Tanaka, K. (1995). Isoalloxazine ring of FAD is required for the formation of the core in the Hsp60-assisted folding of medium chain Acyl-CoA dehydrogenase subunit into the assembly competent conformation in mitochondria. *J. Biol. Chem.* 270, 1899–1907.

Saijo, T., Welch, W. J., and Tanaka, K. (1994). Intramitochondrial folding and assembly of medium-chain acyl-CoA dehydrogenase (MCAD) - Demonstration of impaired transfer of K304E-variant MCAD from its complex with Hsp60 to the native tetramer. *J. Biol. Chem.* 269, 4401–4408.

Schmidt, M., Buchner, J., Todd, M. J., Lorimer, G. H., and Viitanen, P. V. (1994). On the role of Groes in the Chaperonin-assisted folding reaction - three case studies. *J. Biol. Chem.* 269, 10304–10311.

Strassburger, M., Bloch, W., Sulyok, S., Schuller, J., Keist, A. F., Schmidt, A., et al. (2005). Heterozygous deficiency of manganese superoxide dismutase results in severe lipid peroxidation and spontaneous apoptosis in murine myocardium *in vivo*. *Free Radic. Biol. Med.* 38, 1458–1470. doi: 10.1016/j.freeradbiomed.2005.02.009

Tina, K. G., Bhadra, R., and Srinivasan, N. (2007). PIC: protein interactions calculator. *Nucleic Acids Res.* 35, W473–W476. doi: 10.1093/nar/gkm423

Veltman, J. A., and Brunner, H. G. (2012). *De novo* mutations in human genetic disease. *Nat. Rev. Genet.* 13, 565–575. doi: 10.1038/nrg3241

Vestweber, D., and Schatz, G. (1988). Point mutations destabilizing a precursor protein enhance its post-translational import into mitochondria. *Embo J.* 7, 1147–1151.

Vitlin Gruber, A., Nisemblat, S., Zizelski, G., Parnas, A., Dzikowski, R., Azem, A., et al. (2013). *P. falciparum* cpn20 Is a Bona Fide Co-Chaperonin that can replace GroES in *E. coli*. *PLoS ONE* 8:e53909. doi: 10.1371/journal.pone.0053909

Wenzel, P., Schuhmacher, S., Kienhofer, J., Muller, J., Hortmann, M., Oelze, M., et al. (2008). Manganese superoxide dismutase and aldehyde dehydrogenase deficiency increase mitochondrial oxidative stress and aggravate age-dependent vascular dysfunction. *Cardiovasc. Res.* 80, 280–289. doi: 10.1093/cvr/cvn182

Yokota, I., Saijo, T., Vockley, J., and Tanaka, K. (1992). Impaired tetramer assembly of variant medium-chain acyl-coenzyme A dehydrogenase with a glutamate or aspartate substitution for lysine 304 causing instability of the protein. *J. Biol. Chem.* 267, 26004–26010.

Conflict of Interest Statement: The authors declare that the research was conducted in the absence of any commercial or financial relationships that could be construed as a potential conflict of interest.

APPENDIX

Extended Clinical Patient Information

The patient presented at 3 months of age with spastic movements. An EEG diagnosed infantile spasms. A brain MRI did not show any abnormalities. At the age of 3, he was diagnosed with myoclonic and tonic epilepsy. He came to the attention of medical genetics at 7 months of age. Developmental milestones were globally delayed. He rolled over at 7 months, sat at 16 months, and walked at 3½years. At 17 months he said only a single word. At the age of 4, he is still largely nonverbal. He was found to have intermittent exotropia and cortical visual impairment on ophthalmologic examination. Mild hepatomegaly and slightly course features were noted by neurology, prompting the lysosomal screening. These were not appreciated by genetics. Aside from mild macrocephaly and a thin upper lip, the patient did not demonstrate dysmorphic features on examination by genetics.

frontiers in Molecular Biosciences

REVIEW
published: 30 September 2016
doi: 10.3389/fmolb.2016.00063

DNAJB6 Myopathies: Focused Review on an Emerging and Expanding Group of Myopathies

*Alessandra Ruggieri, Simona Saredi, Simona Zanotti, Maria Barbara Pasanisi, Lorenzo Maggi and Marina Mora **

Neuromuscular Diseases and Neuroimmunology Unit, Fondazione IRCCS Istituto Neurologico Carlo Besta, Milan, Italy

OPEN ACCESS

Edited by:
Alberto J. L. Macario, University of Maryland at Baltimore, USA; IEMEST, Italy

Reviewed by:
Harm Kampinga, University Medical Center Groningen, Netherlands
Conrad C. Weihl, Washington University in St. Louis, USA

***Correspondence:**
Marina Mora
marina.mora@istituto-besta.it

Specialty section:
This article was submitted to Protein Folding, Misfolding and Degradation, a section of the journal Frontiers in Molecular Biosciences

Received: *27 May 2016*
Accepted: *20 September 2016*
Published: *30 September 2016*

Citation:
Ruggieri A, Saredi S, Zanotti S, Pasanisi MB, Maggi L and Mora M (2016) DNAJB6 Myopathies: Focused Review on an Emerging and Expanding Group of Myopathies. Front. Mol. Biosci. 3:63. doi: 10.3389/fmolb.2016.00063

Mutations in the *DNAJB6* gene have been associated with the autosomal dominant limb girdle muscular dystrophy type 1D (LGMD1D), a disorder characterized by abnormal protein aggregates and rimmed vacuoles in muscle fibers. DNAJB6 is a ubiquitously expressed Hsp40 co-chaperone characterized by a J domain that specifies Hsp70 functions in the cellular environment. DNAJB6 is also a potent inhibitor of expanded polyglutamine (polyQ) aggregation preventing aggregate toxicity in cells. In *DNAJB6*-mutated patients this anti-aggregation property is significantly reduced, albeit not completely lost. To elucidate the pathogenetic mechanisms underlying the DNAJB6-related myopathy, animal models have been created showing that, indeed, conditional muscular expression of a DNAJB6 mutant in the mouse causes a LGMD1D myofibrillary muscle tissue phenotype. Both mutations and phenotypes reported until recently were rather homogeneous, being exclusively missense mutations of a few amino acids of the protein G/F domain, and with a phenotype characterized by adult-onset slowly progressive muscular dystrophy predominantly affecting proximal muscles. Lately, several novel mutations and new phenotypes of DNAJB6 have been described. These mutations once more affect the G/F domain of DNAJB6 with missense changes and a splice site mutation; and the phenotypes include childhood onset and distal involvement of muscles, or childhood-onset LGMD1D with loss of ambulation in early adulthood and respiratory involvement. Thus, the spectrum of *DNAJB6*-related phenotypes is widening. Although our knowledge about the role of DNAJB6 in the pathogenesis of muscle diseases has made great progression, several questions remain unsolved, including why a ubiquitous protein affects only, or predominantly, skeletal muscle; why only the G/F domain is involved; and what is the possible role of the DNAJB6a isoform. Clarification of these issues will provide clues to implement possible therapeutic strategies for DNAJB6-related myopathies.

Keywords: DNAJB6, chaperone, LGMD1D, distal myopathy, autophagy, protein aggregation, vacuolar myopathy

INTRODUCTION

The first description of what it was, at that time, defined as "an unusual form of muscular dystrophy" dates back to 1969, when Schneiderman et al. (1969) described a four generation family affected by a late onset dominant muscular dystrophy form, predominantly affecting proximal limb muscles. Neither the genetic cause of this dystrophy nor the locus were at that point clarified.

A step forward on the identification of the causative gene for this form of limb girdle muscular dystrophy (LGMD), now named LGMD1D, was taken by Speer et al. (1999) who provided evidence of linkage to the 7q locus. In this study Speer and colleagues gathered five families based on the presence, in the affected members, of progressive proximal lower limb muscle weakness with or without proximal upper limb involvement, increased creatine kinase (CK) levels, absent ankle deep tendon reflexes, and no features suggestive of any other known myopathy, by muscle histology and electron microscopy. Genome wide linkage excluded three of the five families establishing evidence for linkage to 7q for the remaining two, previously described by Schneiderman et al. (1969) and Speer et al. (1995). Two recombination events in both families allowed the authors to better define the region in an interval of 9 cM comprised between markers D7S2546 and D7S2423.

Few years passed by before new LGMD1D families were reported in 2010 (Sandell et al., 2010). One year later, Hackman et al. (2011) collected four informative new Finnish families leading the way to the identification of the genetic cause of LGMD1D. The presence of informative recombination in two unaffected members of two of these families allowed reducing the 7q region to 3.4 Mb, containing 12 known genes, and at least 14 hypothetical genes or pseudogenes. Subsequently, a candidate gene sequencing approach let Sarparanta et al. (2012) to identify the LGMD1D causative gene.

With the discovery of novel mutations in the *DNAJB6* gene, the spectrum of related phenotypes, in terms of age of onset, severity and group of muscles involved, is widening.

In the present review we will focus our attention on the pathological effects of mutations affecting the DNAJB6 chaperone protein, and on the clinical and histopathological features of the DNAJB6-related myopathies.

MOLECULAR ASPECTS OF DNAJB6

Cells, at each stage of their life, depend on the essential support of proteins as building blocks and to carry out all cellular functions. Proteins have a proper three-dimensional conformation, which, as demonstrated by *in vitro* experiments (Anfinsen, 1973), depends on the amino acid sequence and can be achieved spontaneously according to the global minimum of free energy. However, the experimental conditions required for a proper *in vitro* folding are very restrictive and not applicable to the crowded cellular environment where hydrophobic effects will make harder to control the folding. Moreover, this process is challenged by various stress conditions, some, such as the increase in protein synthesis during cell cycle progression, constitutive; others, such as environmental or pathophysiological stresses (e.g., temperature increase or tissue injury and repair), sporadic. Therefore, in order to prevent the formation of toxic protein aggregates, the cell requires an active and dynamic system able to control proper protein folding and clearance of the misfolded and damaged proteins.

Molecular chaperones are part of this dynamic system that helps maintaining cellular protein homeostasis through their ability to interact among themselves and with specific partners, thus influencing conformation and function of a wide range of different substrates such as p53 and other transcription factors, including steroid receptors, as well as proteins that unfold and aggregate in neurodegenerative diseases (polylglutamine androgen receptor, huntingtin, α-synuclein, tau) and a variety of protein kinases (Morimoto, 2008; Pratt et al., 2015). They are named heat shock proteins (HSPs) and grouped into families according to their molecular weight: Hsp100, Hsp90, Hsp70, Hsp60, Hsp40, and sHsp (small heat-shock protein). The Hsp70 chaperones are involved in a plethora of processes including folding of newly synthesized proteins, transport of proteins across membranes, refolding of misfolded and aggregated proteins, and control of regulatory protein activity (Bukau et al., 2006). Hsp70 chaperones have a 40 kD N-terminal ATPase domain and a 25 kDa C-terminal peptide-binding domain (PBD), and cycle between ATP- and ADP-bound conformation. In the ATP form, the bond between client polypeptides (newly synthesized or misfolded proteins) and the PBD of Hsp70, is weak.

The chaperone-client polypeptide interaction is stabilized by the intervention of co-chaperone proteins belonging to the DnaJ family (Hsp40). The DNAJ co-chaperones associate with the client proteins presenting them to the Hsp70 chaperone, thus leading to the formation of a trimeric complex. Co-chaperone plus substrate stimulate the Hsp70 dependent hydrolysis of ATP to ADP with consequent conformational change of the Hsp70 protein that increases its affinity for the substrate and triggers the separation of the DnaJ co-chaperone. The release of the client protein is then achieved by the dissociation of ADP, stimulated by nucleotide exchange factors (NEFs), allowing the Hsp70 chaperone to be ready for a new cycle (Laufen et al., 1999; Kampinga and Craig, 2010; **Figure 1**).

DNAJ/Hsp40 co-chaperones are a diverse and large group of proteins characterized by the presence of a 70 amino acid sequence, the J domain, as common signature. The J domain stimulates the Hsp70 ATPase activity and contains a conserved tripeptide sequence (histidine, proline and aspartic acid, HPD) critical for its function. The Hsp40 family is divided into three subtypes according to their structure (**Figure 2**). The type I, or A, is closely related to the *E. coli* DnaJ and comprises the J domain at the N-terminus, a glycine/phenylalanine (G/F)-rich domain, a cysteine-rich region, and a C-terminal region that recognizes and binds to the substrate. The direct function of the G/F domain is not clear. A likely one is that the G/F domain participates in the recognition and modulation of particular substrates, thus acting on the specification of Hsp70 function (Fan et al., 2003). The DNAJ type II or B, has similar structure to type A, but lacks the cysteine-rich domain. The type III, or C, contains, as conserved

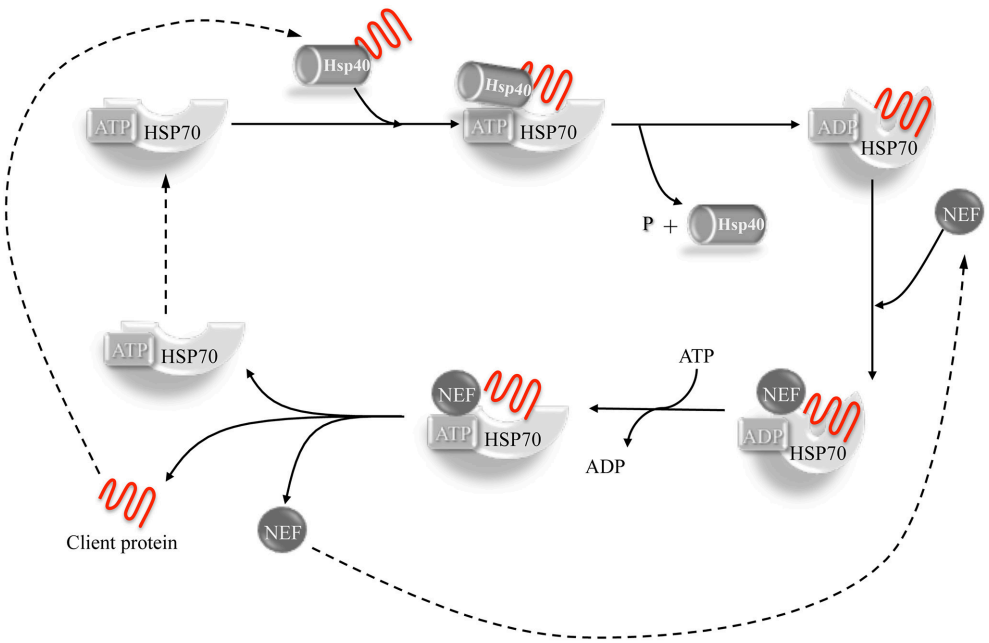

FIGURE 1 | The Hsp40-Hsp70 cycle. Hsp40 co-chaperone forms complexes with unfolded or non- native proteins delivering them to Hsp70. The interaction between Hsp40 and the ATP-bound Hsp70 takes place through the J-domain. The client protein transiently interacts with the Hsp70 and the interaction is stabilized by a conformational change in Hsp70 caused by the hydrolysis of ATP which, in turn, is stimulated by both Hsp40 and client protein. Hsp40 is then released. A nucleotide exchange factor (NEF) then binds Hsp70 (having more affinity for the ADP-bound form compared to the ATP form), stimulating the dissociation of ADP through a conformational change in Hsp70. An ATP molecule is bound again to Hsp70 because of its higher cellular concentration, causing the release of the client protein. The system is then ready for a new cycle (Kampinga and Craig, 2010).

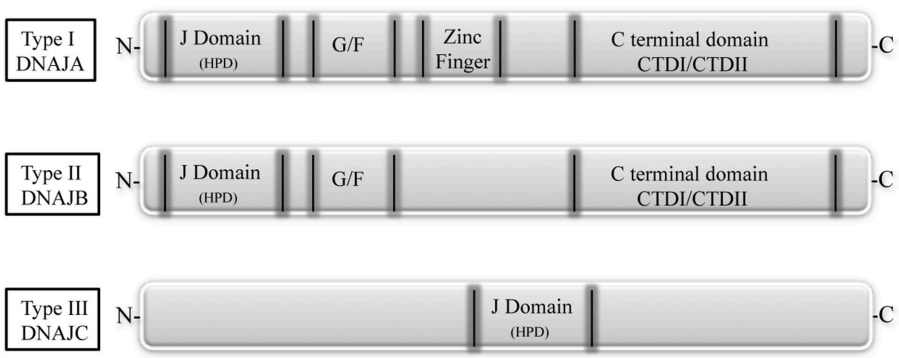

FIGURE 2 | The DNAJ protein family. Based on their structure, DNAJs are divided into three subtypes. Type I, or A, has an N-terminal J domain (with a conserved histidine, proline, and aspartic acid tripeptide), followed by a glycine/phenylalanine-rich domain (G/F), by a zinc finger region rich in cysteine, and by a C-terminal domain, responsible for client binding and presenting two barrel domains, CTDI and CDTII. Type II, or B, is similar to type I, but lacks the zinc finger region. Type III, or C, has only the conserved J domain which is variably located in the protein (Fan et al., 2003).

region, only the J domain, which can be localized anywhere in the protein (Li et al., 2009; Kampinga and Craig, 2010).

Even though it has been demonstrated that the J domain alone is capable of stimulating the ATPase activity of Hsp70, the presence of a functional Hsp70 PBD is required to allow the formation of a complex between the unfolded protein and Hsp70 (Fan et al., 2003). DNAJ proteins, promote multiple functions of Hsp70 by binding and delivering a variety of non-native clients. Some DNAJ chaperones are involved in the correct folding of the newly synthesized proteins (DNAJA1 and DNAJB1), some have a role in delivering misfolded proteins to the nucleus for proteasomal degradation (DNAJB1), some (DNAJB9, DNAJC10, DNAJB11) intervene in the endoplasmic-reticulum-associated protein degradation (ERAD) pathway, recognizing misfolded proteins that are consequently ubiquitinylated and degraded (Park et al., 2013; Dekker et al., 2015).

A distinctive characteristic of DNAJB6 and DNAJB8 is their capability to act as powerful inhibitors of misfolded poly-Q protein aggregation, which is dependent on and occurs through direct interaction with the C-terminus SSF-SST serine-rich region (Hageman et al., 2010; Gillis et al., 2013). The purified DNAJB6 protein is able to inhibit the formation of pathogenic polyQ aggregates at a substoichiometric molar ratio and independently from the presence of Hsp70 and ATP (Månsson et al., 2014). Unlike in purified protein, in living systems there is need for interaction between DNAJB6 and Hsp70 in those situations in which the DNAJB6 anti-aggregation capability is somehow limited (Kakkar et al., 2016).

This thorough study by Kampinga's group also demonstrated that the most efficient anti-aggregation activity is dependent on an array of 18 hydroxyl groups in the S/T-rich region of DNAJB6. Additional evidence of DNAJB6 anti-aggregation property comes from demonstration that overexpression of the human DNAJB6b in yeast could directly prevent [URE3] prion formation and block the propagation and spontaneous formation of Ure2 amyloid fibers (Reidy et al., 2016). This further proof indicating DNAJB6 as anti-aggregant acting on structurally different types of amyloids, makes DNAJB6 an attractive therapeutic target in amyloid storage disorders.

In general, because of their involvement in the diverse tasks of protein homeostasis control, DNAJ proteins are also clinically relevant disease targets. In fact, mutations leading to disease have been found in seven distinct DNAJ proteins, comprising DNAJB2, DNAJB6, DNAJC5, DNAJC6, DNAJC13, DNAJC19, and DNAJC29 (Koutras and Braun, 2014).

The present review will focus on mutations affecting the chaperone DNAJB6 (**Figure 3**), causing limb-girdle muscular dystrophy type 1D (LGMD1D) and, as shown by recent reports, other forms of myopathy affecting distal muscles. DNAJB6 is ubiquitously expressed as two isoforms with distinct cellular localizations: The longer DNAJB6a localizes to the nucleus and the shorter DNAJB6b localizes to both the cytoplasm and the nucleus.

In the thorough work of Udd's group (Sarparanta et al., 2012), the molecular mechanisms explaining the dominant form of LGMD1D affecting Finnish, American, and Italian patients sharing the common 7q36 locus, were investigated. These authors showed that, in muscle tissue, DNAJB6 protein is primarily localized at the Z-disks, and that in LGMD1D patients a Z-disk myofibrillar disintegration was visible with accumulation of DNAJB6 and its known ligands MLF1 (myeloid leukemia factor 1), HSPA8 and KRT18 (keratin 18). With the use of morpholino (MO) in *in vivo* experiments on zebrafish, they were able to demonstrate loss of muscle integrity caused by the silencing of *dnajb6b* (the unique ortholog of the human gene), impairment visible already at 2 days post fertilization in injected embryos. Expression of the human wild-type DNAJB6 could rescue the phenotype thus demonstrating that loss of DNAJB6 was the direct cause of muscle defects. Furthermore, to investigate the effects of specific mutations on the a and b isoforms, human mutated transcripts generated for both isoforms were injected into zebrafish embryos showing that only the b isoform recapitulates the muscular phenotype observed with the dnajb6 splice blocking morpholino. Moreover, Sarparanta and coll. showed that the molar ratio of mutant to wild-type *DNAJB6* mRNA is crucial: An equimolar injection of mutant and wild type *DNAJB6* messenger will increase the severity of the phenotype, suggesting a dominant effect. An excess of mutant over wild-type is lethal for embryos, while the opposite allows a progressively increasing rescue. Using a filter trap assay, the mutant proteins were shown to have reduced anti-aggregation properties of polyglutamine-containing huntingtin (pEGFP/HD-120Q), compared to wild-type DNAJB6 protein, confirming data previously found by Hageman et al. (2010). The reported mutations, although not affecting the S/T-rich region proven to be responsible for the anti-aggregation activity (Kakkar et al., 2016), might indirectly alter this property—e.g., modifying the protein conformation and impairing the interaction with different clients—thus causing protein accumulation in patient's muscles and variability of clinical severity.

Because of the Z-disk localization and the interaction of DNAJB6 with HSPA8, one of the components of the chaperone-assisted selective autophagy (CASA) complex (Izawa et al., 2000; Arndt et al., 2010), the authors investigated the possible link between DNAJB6 and CASA. By co-immunoprecipitation and proximity ligation assay, the authors showed interaction of DNAJB6 with the components of the CASA complex BAG3 (a protein found to be mutated in myofibrillar myopathy type 6), HSPB8 and STUB1, but none of the interactions appeared to be affected by the p.Phe93Leu DNAJB6 mutation. The authors concluded that the myofibrillary muscle tissue phenotype of LGMD1D patients could be due to an inefficient maintenance of the sarcomeric structure or an increased accumulation of misfolded sarcomeric proteins caused by the impairment of the CASA system, although experimental evidence of a direct role of DNAJB6 in the CASA machinery has yet to be provided.

Another important work investigating the effects of the LGMD1D mutations, by Stein et al. (2014), exploited the yeast ortholog Hsp40 Sis1, creating a Sis1-DNAJB6 protein chimera in which the G/F domain of DNAJB6 was substituted to that of Sis1. With the use of the prion strains of [*RNQ*+] and [*PSI*+], Stein and coworkers, showed that, compared to the wild type chimera, in the LGMD1D mutant chimera the ability to process the protein aggregate conformers was impaired. They also investigated these findings in a mammalian system by monitoring TDP-43 aggregate formation in HeLa cells upon heat-shock and during recovery. TDP-43 contains a C-terminal prion-like domain (Fuentealba et al., 2010) and forms aggregates in skeletal muscle of *DNAJB6*-mutated patients (Harms et al., 2012). In Hela cells expressing TDP-43 and DNAJB6 mutations and in primary patients' fibroblasts, TDP-43 aggregates persisted after heat-shock and recovery, but not in Hela cells expressing DNAJB6-wild type and in control fibroblasts, thus confirming previous suggestion that TDP-43 is a client protein of DNAJB6 (Udan-Johns et al., 2014). These authors proposed that a different degree of selectivity for substrate conformers would be conferred to the co-chaperone protein by the G/F domain: Different mutations in this domain would disrupt the substrate selectivity differentially, thus providing an explanation for the diverse clinical presentations of *DNAJB6*-related myopathies.

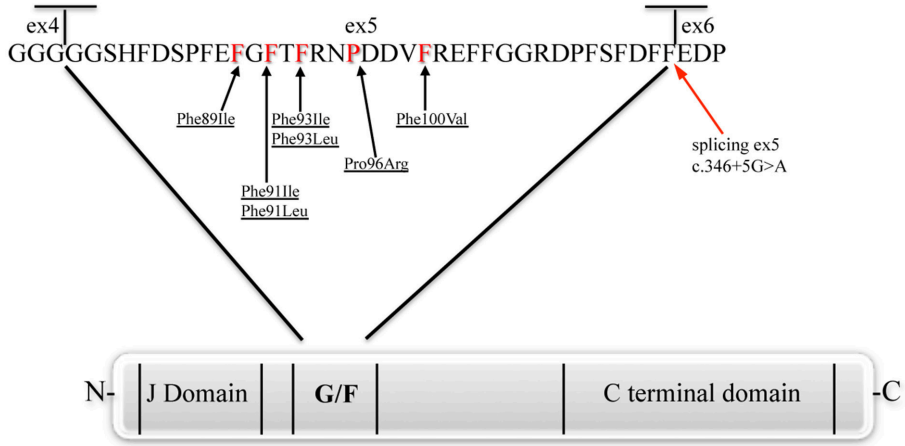

FIGURE 3 | The DNAJB6 protein. The J, G/F and C-terminal domains, and position of the amino acid and splicing mutations are represented (Fan et al., 2003; Sato et al., 2013; Ruggieri et al., 2015).

ANIMAL MODELS

In addition to the zebrafish utilized by the Udd's group (Sarparanta et al., 2012) to demonstrate that *DNAJB6* was the gene responsible for LGMD1D, very recently the *Drosophila melanogaster* has been used to establish a mechanistic link between the human genes *DNAJB6* and *hnRNPA2B1* (causing multi system proteinopathy and autosomal dominant familial amyotrophic lateral sclerosis) (Li et al., 2016). These authors generated transgenic *Drosophila* lines either carrying mutations in *Hrb98DE* (the fly homolog of *hnRNPA2B1*) or in *MRJ* (the fly homolog of human *DNAJB6*), in amino acids corresponding to those mutated in LGDM1D patients. They demonstrated that the cytoplasmic aggregation and mislocalization of the mutant Hrb98DE and hnRNPA2B1 proteins, was rescued by co-expressing the wild-type *MRJ* but not the disease-associated *MRJ* mutant. In addition, partial reduction of the endogenous *MRJ* levels, obtained using a classical loss of function line, caused great increase in cytoplasmic aggregation of the mutant Hrb98DE. Finally, the authors showed that an intact G/F domain is indispensable for controlling the formation of mutation-dependent Hrb98DE or hnRNPA2 cytoplasmic aggregates.

The first study of *DNAJB6* homolog gene in mouse was published in 1999 (Hunter et al., 1999). These authors identified, by gene trap screen, the *Mrj* (mammalian relative of DnaJ) gene and characterized its expression during mouse development, showing that *Mrj* is expressed throughout the trophoblast lineage with higher levels in the trophoblast giant cells of the placenta. The homozygous *Mrj* mutants were lethal because of a failure in chorioallantoic fusion at embryonic day 8.5. Eight years later Watson et al. (2007) demonstrated that absence of a functional Mrj protein in trophoblast cells, causes the deposition of keratin aggregates that disrupt cell function and organization, leading to defects in chorioallantoic fusion.

A mouse model for the study of DNAJB6-related myopathy has recently been established by Bengoechea et al. (2015). These authors generated, under the muscle creatine kinase (MCK) promoter, four different transgenic animals, for both the long and short *DNAJB6a* and *DNAJB6b* isoforms: Two wild-type and two with the most common human mutation F93L. The authors observed that the DNAJB6b-F93L protein levels were higher than those of the wild type protein, and showed that this was due to a slower degradation rate of the mutant protein compared to the wild-type. Bengoechea and coworkers also demonstrated that only the DNAJB6b-F93L mutant construct was able to induce some of the pathological features of the LGMD1D phenotype, such as muscle weakness, myofibrillar disorganization, desmin accumulation, autophagic vacuoles, and aggregation of RNA binding proteins (hnRNAPA1 and hnRNAPA2/B1). Electron microscopy highlighted myofibrillar disorganization, mitochondrial alteration and presence of autophagic vacuoles. Immunostaning showed desmin, keratin 8 and 18 accumulation in muscle fibers, and aggregation of RNA binding proteins (hnRNAPA1 and hnRNAPA2/B1).

Another recent interesting mouse model, by Kakkar et al. (2016) overexpressing the human DNAJB6 protein under control of a brain-specific nestin promoter, although not directly related to muscle diseases, shows the potential of DNAJB6 as therapeutic target in protein aggregate disorders. This mouse was crossed with the R6/2 polyQ mice (HTT), model for Huntington disease. The double transgenic mice HTT/DNAJB6 had a significant reduction of inclusions in the brain only and a better rotarod test performance, when compared to the HTT mice. Since the overexpression of DNAJB6 protein in brain did not show secondary effects in these animals, the authors speculate that DNAJB6 could be a valid therapeutic target in polyQ disorders.

CLINICAL FEATURES OF DNAJB6-RELATED MYOPATHIES

Clinical features are summarized in **Table 1** and histopathological aspects are represented in **Figure 4**.

TABLE 1 | Clinical and molecular findings in DNAJB6-related families.

DNAJB6 mutation	References	Family ID	Ethnicity	Age of onset	Prevalent weakness distribution	EMG	Serum CK	Muscle pathology	Cardiac involvement	Loss of ambulation	Respiratory failure	Bulbar weakness
c.265T>A p.Phe89Ile	Sarparanta et al., 2012	DUK1047	Caucasian American	20–55	P > D; LL > UL	Myopathic	Normal −10 x	Myopathic, RV, MA	No	na	No	No
c.265T>A p.Phe89Ile	Sarparanta et al., 2012	DUK1701	Caucasian American	14–55	P > D; LL = UL	Myopathic	Normal −3.5 x	Myopathic, not reassessed	No	Yes	No	Yes (3 of 15 patients)
c.265T>A p.Phe89Ile	Suarez-Cedeno et al., 2014	n.d.	Native American/ Scottish	<10–adult	P > D; LL = UL; Ax	Myopathic	Normal	RV, intracellular congophilic inclusions	No	Yes (a 50 years old pt with childhood onset)	No	No
c.265T>A p.Phe89Ile	Couthouis et al., 2014	n.d.	Caucasian American	8–18	P > D; LL > UL	na	P1: 181 U/L P2: 3000 U/L	Rimmed vacuoles	No	Yes (the 56 years old proband)	Dyspnea and sleep-disorder breathing	No
c.271T>A p.Phe91Ile	Palmio et al., 2015	Family A	Finnish	6–13	P > D; LL > UL; Ax	Myopathic	Normal −2 x	Myopathic, RV	No	Yes (at age 27 years)	Severe	Yes
c.271T>A p.Phe91Ile	Ruggieri et al., 2015	1s	Italian	16	P > D; LL = UL	Myopathic	Normal	Dystrophic, RV	No	Yes	Mild, non-Progressive	No
c.271T>C p.Phe91Leu	Palmio et al., 2015	B	British	12	P = D; LL > UL; Ax	na	Normal	na, RV	No	Yes	Severe	Yes
c.271T >C p.Phe91Leu	Nam et al., 2015	Family 1	Korean	8–11	P > D; LL > UL	Myopathic	83–245 U/L	Myopathic, RV	Prolonged QT, RBBB, 1st AV block	Yes (a female pt in her 20s)	Mild	Yes
c.273C>G p.Phe91Leu	Ruggieri et al., 2015	2s	Italian	11	P = D; LL = UL	Myopathic	1.2 x	Dystrophic, RV	No	Yes	Nocturnal and daily non-invasive ventilation, cough mechanical assistance	Yes
c.277T>A p.Phe93Ile	Sato et al., 2013	FA	Japanese	30s	P > D; LL > UL	Myopathic	268–1044 U/L	Myopathic, RV	CRBBB in FA-1	No	No	No
c.277T>C p.Phe93Leu	Harms et al., 2012	Family 1	Caucasian	30s	P > D; LL > UL	Myopathic	2–5 x	RV, intracellular congophili cinclusions	No	No (wheelchair use for community mobility 20 years from onset)	No	No
c.277T>C p.Phe93Leu	Sarparanta et al., 2012	IT2	Italian	30–55	P > D; LL > UL	Myopathic	Normal −8 x	Myopathic, RV, MA	No	na	No	No
c.279C>A p.Phe93Leu	Sarparanta et al., 2012	IT1	Italian	20–50	P > D; LL = UL	Myopathic	2 x	Myopathic, RV	No	na	No	No

(Continued)

TABLE 1 | Continued

DNAJB6 mutation	References	Family ID	Ethnicity	Age of onset	Prevalent weakness distribution	EMG	Serum CK	Muscle pathology	Cardiac involvement	Loss of ambulation	Respiratory failure	Bulbar weakness
c.279C>G p.Phe93Leu	Sarparanta et al., 2012	FF1	Finnish	20–60	P > D; LL > UL	Myopathic	Normal −3 x	Myopathic, RV, MA	No	Yes (a 80 years old patient)	No	Yes (1 of 10 pts)
c.279C>G p.Phe93Leu	Sarparanta et al., 2012	FF2	Finnish	45–50	P > D; LL > UL	Myopathic	2–3 x	Myopathic, RV, MA	No	No	No	No
c.279C>G p.Phe93Leu	Sarparanta et al., 2012	FF3	Finnish	38	P > D; LL > UL	Myopathic	3 x	Myopathic, RV, MA	No	No	No	Yes
c.279C>G p.Phe93Leu	Sarparanta et al., 2012	FF4	Finnish	28–40	P > D; LL > UL	Myopathic	Normal −8 x	Myopathic, RV, MA	No	No	No	No
c.279C>G p.Phe93Leu	Sarparanta et al., 2012	FF5	Finnish	40	P > D; LL > UL	Myopathic	Normal	Myopathic, RV, MA	No	No	No	Yes
c.279C>G p.Phe93Leu	Sato et al., 2013	FB	Japanese	25	P > D; LL > UL	na	696 U/L	Myopathic, RV	No	No	No	No
c.279C>G p.Phe93Leu	Sato et al., 2013	FC	Japanese	50s	P > D; LL > UL	na	523 U/L	Myopathic, RV	No	No	No	No
c.279C>G p.Phe93Leu	Sato et al., 2013	FD	Japanese	37–57	P > D; LL > UL	Myopathic	165–251 U/L	Myopathic, RV	No	Yes (a 75 years old patient)	No	No
c.279C>G p. Phe93Leu	Yabe et al., 2014	FD	Japanese	57	P > D; LL > UL	Myopathic	93 U/L	Myopathic, RV	No	Yes	No	No
c.279C>G p.Phe93Leu	Ruggieri et al., 2015	3s	Italian	45	P > D; LL > UL	Myopathic	1.5 x	Myopathic, RV	No	No	No	No
c.287C>G p.Pro96Arg	Harms et al., 2012	Family 2	African American	18–35	D > P; LL = UL	Myopathic	278–339 U/L	na	No	Yes (within 20–30 years from onset)	No	No
c.298T>G p.Phe100Val	Ruggieri et al., 2015	Family 1	Italian	10–50	P = D; LL > UL	Myopathic	1.5–4 x	Dystrophic, RV	No	Yes	Dyspnea	Yes (4 of 5 pts)
c.346+5G>A splicing	Ruggieri et al., 2015	4s	Italian	6	D > P; LL > UL	Myopathic	1.1 x	Dystrophic, RV	No	Yes	Mild	No

Pt, patient; na, not available; RV, rimmed vacuoles; MA, myofibrillar accumulations; CRBBB, complete right bundle-branch block; RBBB, right bundle branch block; 1st AV block, first degree atrioventricular block; Ax, axial muscles.

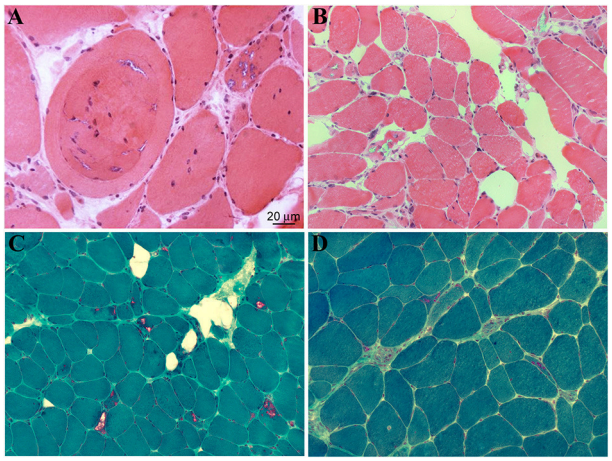

FIGURE 4 | Histopathological features of muscle biopsies from DNAJB6-mutated patients. H&E **(A,B)** and Gomori trichrome stains **(C,D)** reveal several autophagic vacuoles, visible either in subsarcolemmal regions or centrally located, internalized myonuclei as well as variability in fiber sizes (Ruggieri et al., 2015).

In the first description of the "unusual form of muscular dystrophy" in the paper by Schneiderman et al. (1969), clinical symptoms presented since the third decade of life, manifesting as difficulty in climbing stairs, subsequently followed by proximal upper limb muscles weakness. No bulbar or facial muscle involvement were reported. Disease progression was slow over the years, with only two patients in their seventies being bedridden. Electromyography was normal, as normal were mental abilities. Light microscopy of deltoid muscle biopsies of clinically affected subjects, showed marked variation in fiber size, numerous vacuolated fibers, and slight increase in connective tissue and fat. At the electron microscopy some of the myofibers presented foci of degenerated myofibrils at the center and in the subsarcolemmal regions, which were replaced by granular or vacuoles containing myelin-like bodies, dense lysosomal-like structure, and dilated vesicles.

Subsequent linkage studies on Schneiderman's patients and additional American and Finnish families by several groups (Speer et al., 1995, 1999; Sandell et al., 2010; Hackman et al., 2011) allowed the identification of a common haplotype on 7q36, a region of 3.4 Mb, containing 12 known genes. All the patients were characterized by late onset progressive proximal lower limb muscle weakness with or without proximal upper limb involvement, increased CK levels, absent ankle deep tendon reflexes, and no features suggestive of any other known myopathy. Histology of different lower limb muscles (vastus lateralis, medial gastrocnemius, or soleus) displayed myopathic and dystrophic features, rimmed vacuoles and protein aggregates.

Sequencing of the candidate genes among the 12 present in the linked region, allowed Sarparanta et al. (2012) to identify the genetic cause of LGMD1D in the *DNAJB6* gene. The changes were all point mutations, notably c.279C>G (p.Phe93Leu) in the Finnish families, c.267T>A (p.Phe89Ile) in the American families, and c.279C>A and c.277T>C (p.Phe93Leu) in further Italian families. Interestingly, all the reported mutations were in the exon 5 of the gene, encoding the G/F domain.

The association of these clinical features with mutations in the *DNAJB6* gene and the use of new sequencing technologies allowed the identification of novel mutations in more LGMD1D patients. By exome sequencing in patients that presented with dominant or sporadic myopathy and that were genetically unresolved, Harms et al. (2012) identified *DNAJB6* mutations in two new families, in particular a c.277T>C (p.Phe93Leu) and a c.287C>G (p.Pro96Arg) change. Of the two mutated families though, one Caucasian presented weakness in the limb-girdle muscles, while the second, of African American origin, had predominant lower limb distal weakness, which had never been reported before. The number of published mutations and ethnicity increased with the description of four additional Japanese families by Sato et al. (2013) and two further cases with childhood onset and lower limb proximal muscle weakness described by Suarez-Cedeno et al. (2014) and Couthouis et al. (2014).

Of note, one Japanese patient carrying the Phe93Leu mutation was detailed (Yabe et al., 2014) as having developed fronto-temporal dementia (FTD). His cognitive impairment worsened with age and the patient died at 76 years of age. The immunoreactivity of DNAJB6 in the frontal cortex was greatly reduced as compared with other forms of dementia, but was normal in the thalamus. In the fronto-temporal cortex ubiquitin-positive aggregates were also present. No mutations in any of the known FTD genes were revealed. Based on altered LC3 and p62 immunostaining of the frontal lobe of this patient, the authors suggested a possible impairment of the autophagy pathway such as seen in patients with *VCP* gene mutations. Considering that this suggestion is solely based on histological findings, further investigation to prove its accuracy will be necessary, as stated by the authors themselves.

More recently, the widening of the phenotypic spectrum of *DNAJB6*-related myopathies was confirmed and a tentative genotype-phenotype correlation was hypothesized. In the work by Ruggieri et al. (2015), the authors redefined the genetic locus and some clinical features of a previously reported family with "autosomal dominant vacuolar neuromyopathy" (Servidei et al., 1999). By whole exome sequencing, a novel missense mutation in the *DNAJB6* gene, a c.298T>G (p.Phe100Val), was identified in this family. Again, this mutation affects a conserved amino acid of the G/F domain. Moreover, four sporadic cases were reported, one with a known transition c.279C>G (p.Phe93Leu) and three with novel mutations of the G/F domain: Two missense, c.271T>A (p.Phe91Ile), and c.273C>G (p.Phe91Leu), and one, c.346+5 G>A, leading to an alternative splicing event causing the skipping of exon 5. Clinically the two patients carrying the different mutations of Phe91 had a severe childhood-onset limb-girdle myopathy. The patients with the Phe100Val mutation had distal-onset myopathy, unique early bulbar involvement, and a gender-modified wide age-of-onset range. The patient with the splicing defect that entirely eliminates DNAJB6's G/F domain (ΔG/F),

had severe distal childhood-onset myopathy. Muscle imaging revealed that muscles previously considered uninvolved in DNAJB6-myopathy, e.g., lateral gastrocnemii, were affected in patients with new mutations. The authors observed that the mutations affecting the amino acid in the more C-terminal part of the G/F domain (Pro96 and Phe100 in this) as well as the mutation causing skipping of the entire G/F domain were correlating with a more distal phenotype compared to the more N-terminal amino acids (Phe89, Phe91, and Phe93). Furthermore, they highlighted the fact that there seems to be a range of severity correlating with the different *DNAJB6* mutations so far reported, even though more cases are necessary to confirm this hypothesis. In particular, from most severe to least severe LGMD1D phenotype, the mutations are as follow: ΔG/F and Phe91 mutations, Phe100Val, Pro96Arg, and Phe89 mutations and Phe93 mutations.

This genotype-phenotype correlation was once more confirmed by Palmio et al. (2015), reporting a Finnish family and a sporadic British female case with a severe form of LGMD1D with childhood onset, rapidly progressing to loss of walking ability within the end of the third decade, contractures and respiratory failure. The patients carried mutations of the Phe91 amino acid, respectively c.271T>A (p.Phe91Ile) and c.271T>C (p.Phe91Leu). Likewise, the severe phenotype associated to the Phe91Leu was observed by Nam et al. (2015) in a Korean LGMD1D family with childhood onset and fast progression of the symptoms as well as involvement of respiratory and bulbar muscles.

It is intriguing to note that the correlation between genotype and clinical presentation can be seen as well with the use of imaging techniques. In fact, muscle imaging has shown that the pattern of muscle involvement appears to be more variable than previously thought and somewhat different according to the mutated amino acid. Indeed, in 2013 Sandell et al. (2013), published the first analysis of muscle MRI or CT features in 23 Finnish and Italian *DNAJB6* mutated patients. All the patients carried mutations affecting the Phe93 amino acid. The pattern and timing of engagement of the imaged muscles were consistent among all the patients and considered pathognomonic for LGMD1D: At the early stages of the disease the more affected muscles were soleus, adductor magnus, semimembranosus, and biceps femoris, then the medial gastrocnemius and adductor longus, and finally also the vasti muscles of the quadriceps resulted to be compromised. The muscles that were affected only in a very late stage of the disorder were lateral gastrocnemius, rectus femoris, sartorius, gracilis, and the anterolateral muscles of the lower legs. However, it was later on shown that this pattern of involvement was slightly different in patients with the Phe91, Phe100, and ΔG/F changes (Nam et al., 2015; Palmio et al., 2015; Ruggieri et al., 2015). In patients with these mutations, the recti, sartorii, gracilis, and anterolateral muscles were relatively spared, but the lateral gastrocnemii were greatly compromised already in relatively early stages of the disease.

CONCLUSIONS

With the discovery of novel mutations in the *DNAJB6* gene, the spectrum of related phenotypes, in terms of age of onset, severity and group of muscles involved, is expanding. The number and type of mutations (all but one missense) so far appears limited, involving a few amino acids of the G/F domain.

Although our knowledge of the role of DNAJB6 in the pathogenesis of muscle diseases has made great progression, several questions remain unsolved:

(1) DNAJB6 is a ubiquitous protein. Therefore, why do *DNAJB6* mutations affect mainly skeletal muscle and rarely the central nervous system (as known so far), and why has no cardiac involvement been reported in these patients? Possible explanations include the selective expression of a DNAJB6 client protein in skeletal muscle, the interaction of DNAJB6 with the CASA system particularly with BAG3 (already known to cause a myofibrillar myopathy), or a functional redundancy of DNAJ family members in all tissues except skeletal muscle.
(2) Why are only mutations of the G/F domain implicated? Are any other regions of the protein more flexible and therefore more adaptable to variations, or are mutations in other regions lethal? In this context, the animal models could be useful in preclinical studies addressed to better understand the physio-pathological mechanisms involved in DNAJB6-related myopathies.
(3) Is there a function for the DNAJB6a isoform in muscle? It is known that it reduces malignancy in several forms of cancer by acting on AKT and β catenin pathways (Yu et al., 2015). Could this be related to a possible role of DNAJB6a in fine-tuning of critical cellular signaling also in muscle?

The clarification of these issues and of the molecular mechanisms driven by DNAJB6 protein will provide the knowledge for implementing therapeutic strategies for patients with DNAJB6-related myopathies, as well as for patients with neurodegenerative diseases caused by toxic protein aggregation.

AUTHOR CONTRIBUTIONS

MM and AR conceived the review focus, conducted literature review, summarized, and finalized the manuscript. AR, SS, and SZ reviewed literature, wrote first draft, and finalized the manuscript. BP and LM revised and finalized the clinical part of the manuscript. All authors approved final version of manuscript.

FUNDING

This work was supported by Institutional funds from the Italian Ministry of Health.

REFERENCES

Anfinsen, C. B. (1973). Principles that govern the folding of protein chains. *Science* 181, 223–230.

Arndt, V., Dick, N., Tawo, R., Dreiseidler, M., Wenzel, D., Hesse, M., et al. (2010). Chaperone-assisted selective autophagy is essential for muscle maintenance. *Curr. Biol.* 20, 143–148. doi: 10.1016/j.cub.2009.11.022

Bengoechea, R., Pittman, S. K., Tuck, E. P., True, H. L., and Weihl, C. C. (2015). Myofibrillar disruption and RNA-binding protein aggregation in a mouse model of limb-girdle muscular dystrophy 1D. *Hum. Mol. Genet.* 24, 6588–6602. doi: 10.1093/hmg/ddv363

Bukau, B., Weissman, J., and Horwich, A. (2006). Molecular chaperones and protein quality control. *Cell* 125, 443–451. doi: 10.1016/j.cell.2006.04.014

Couthouis, J., Raphael, A. R., Siskind, C., Findlay, A. R., Buenrostro, J. D., Greenleaf, W. J., et al. (2014). Exome sequencing identifies a DNAJB6 mutation in a family with dominantly-inherited limb-girdle muscular dystrophy. *Neuromuscul. Disord.* 24, 431–435. doi: 10.1016/j.nmd.2014.01.014

Dekker, S. L., Kampinga, H. H., and Bergink, S. (2015). DNAJs: more than substrate delivery to HSPA. *Front. Mol. Biosci.* 2:35. doi: 10.3389/fmolb.2015.00035

Fan, C. Y., Lee, S., and Cyr, D. M. (2003). Mechanisms for regulation of Hsp70 function by Hsp40. *Cell Stress Chaperones* 8, 309–316.

Fuentealba, R. A., Udan, M., Bell, S., Wegorzewska, I., Shao, J., Diamond, M. I., et al. (2010). Interaction with polyglutamine aggregates reveals a Q/N-rich domain in TDP-43. *J. Biol. Chem.* 285, 26304–26314. doi: 10.1074/jbc.M110.125039

Gillis, J., Schipper-Krom, S., Juenemann, K., Gruber, A., Coolen, S., van den Nieuwendijk, R., et al. (2013). The DNAJB6 and DNAJB8 protein chaperones prevent intracellular aggregation of polyglutamine peptides. *J. Biol. Chem.* 288, 17225–17237. doi: 10.1074/jbc.M112.421685

Hackman, P., Sandell, S., Sarparanta, J., Luque, H., Huovinen, S., Palmio, J., et al. (2011). Four new Finnish families with LGMD1D; refinement of the clinical phenotype and the linked 7q36 locus. *Neuromuscul. Disord.* 21, 338–344. doi: 10.1016/j.nmd.2011.02.008

Hageman, J., Rujano, M. A., van Waarde, M. A., Kakkar, V., Dirks, R. P., Govorukhina, N., et al. (2010). A DNAJB chaperone subfamily with HDAC-dependent activities suppresses toxic protein aggregation. *Mol. Cell* 37, 355–369. doi: 10.1016/j.molcel.2010.01.001

Harms, M. B., Sommerville, R. B., Allred, P., Bell, S., Ma, D., Cooper, P., et al. (2012). Exome sequencing reveals DNAJB6 mutations in dominantly-inherited myopathy. *Ann. Neurol.* 71, 407–416. doi: 10.1002/ana.22683

Hunter, P. J., Swanson, B. J., Haendel, M. A., Lyons, G. E., and Cross, J. C. (1999). Mrj encodes a DnaJ-related co-chaperone that is essential for murine placental development. *Development* 126, 1247–1258.

Izawa, I., Nishizawa, M., Ohtakara, K., Ohtsuka, K., Inada, H., and Inagaki, M. (2000). Identification of Mrj, a DnaJ/Hsp40 family protein, as a keratin 8/18 filament regulatory protein. *J. Biol. Chem.* 275, 34521–34527. doi: 10.1074/jbc.M003492200

Kakkar, V., Månsson, C., de Mattos, E. P., Bergink, S., van der Zwaag, M., van Waarde, M. A., et al. (2016). The S/T-rich motif in the DNAJB6 chaperone delays polyglutamine aggregation and the onset of disease in a mouse model. *Mol. Cell* 62, 272–283. doi: 10.1016/j.molcel.2016.03.017

Kampinga, H. H., and Craig, E. A. (2010).The Hsp70 chaperone machinery: J proteins as drivers of functional specificity. *Nat. Rev. Mol. Cell Biol.* 11, 579–592. doi: 10.1038/nrm2941

Koutras, C., and Braun, J. E. (2014). J protein mutations and resulting proteostasis collapse. *Front. Cell. Neurosci.* 8:191. doi: 10.3389/fncel.2014.00191

Laufen, T., Mayer, M. P., Beisel, C., Klostermeier, D., Mogk, A., Reinstein, J., et al. (1999). Mechanism of regulation of hsp70 chaperones by DnaJ cochaperones. *Proc. Natl. Acad. Sci. U.S.A.* 96, 5452–5457.

Li, J., Qian, X., and Sha, B. (2009). Heat shock protein 40: structural studies and their functional implications. *Protein Pept. Lett.* 16, 606–612. doi: 10.2174/092986609788490159

Li, S., Zhang, P., Freibaum, B. D., Kim, N. C., Kolaitis, R. M., Molliex, A., et al. (2016). Genetic interaction of hnRNPA2B1 and DNAJB6 in a Drosophila model of multisystem proteinopathy. *Hum. Mol. Genet.* 25, 936–950. doi: 10.1093/hmg/ddv627

Månsson, C., Kakkar, V., Monsellier, E., Sourigues, Y., Härmark, J., Kampinga, H. H., et al. (2014). DNAJB6 is a peptide-binding chaperone which can suppress amyloid fibrillation of polyglutamine peptides at substoichiometric molar ratios. *Cell Stress Chaperones* 19, 227–239. doi: 10.1007/s12192-013-0448-5

Morimoto, R. I. (2008). Proteotoxic stress and inducible chaperone networks in neurodegenerative disease and aging. *Genes Dev.* 22, 1427–1438. doi: 10.1101/gad.1657108

Nam, T. S., Li, W., Heo, S. H., Lee, K. H., Cho, A., Shin, J. H., et al. (2015). A novel mutation in DNAJB6, p.(Phe91Leu), in childhood-onset LGMD1D with a severe phenotype. *Neuromuscul. Disord.* 25, 843–851. doi: 10.1016/j.nmd.2015.08.002

Palmio, J., Jonson, P. H., Evilä, A., Auranen, M., Straub, V., Bushby, K., et al. (2015). Novel mutations in DNAJB6 gene cause a very severe early-onset limb-girdle muscular dystrophy 1D disease. *Neuromuscul. Disord.* 25, 835–842. doi: 10.1016/j.nmd.2015.07.014

Park, S. H., Kukushkin, Y., Gupta, R., Chen, T., Konagai, A., Hipp, M. S., et al. (2013). PolyQ proteins interfere with nuclear degradation of cytosolic proteins by sequestering the Sis1p chaperone. *Cell* 154, 134–145. doi: 10.1016/j.cell.2013.06.003

Pratt, W. B., Gestwicki, J. E., Osawa, Y., and Lieberman, A. P. (2015). Targeting Hsp90/Hsp70-based protein quality control for treatment of adult onset neurodegenerative diseases. *Annu. Rev. Pharmacol. Toxicol.* 55, 353–371. doi: 10.1146/annurev-pharmtox-010814-124332

Reidy, M., Sharma, R., Roberts, B. L., and Masison, D. C. (2016). Human J-protein DnaJB6b cures a subset of *Saccharomyces cerevisiae* prions and selectively blocks assembly of structurally related amyloids. *J. Biol. Chem.* 291, 4035–4047. doi: 10.1074/jbc.M115.700393

Ruggieri, A., Brancati, F., Zanotti, S., Maggi, L., Pasanisi, M. B., Saredi, S., et al. (2015). Complete loss of the DNAJB6 G/F domain and novel missense mutations cause distal-onset DNAJB6 myopathy. *Acta Neuropathol. Commun.* 3:44. doi: 10.1186/s40478-015-0224-0

Sandell, S., Huovinen, S., Sarparanta, J., Luque, H., Raheem, O., Haapasalo, H., et al. (2010). The enigma of 7q36 linked autosomal dominant limb girdle muscular dystrophy. *J. Neurol. Neurosurg. Psychiatry* 81, 834–839. doi: 10.1136/jnnp.2009.192351

Sandell, S. M., Mahjneh, I., Palmio, J., Tasca, G., Ricci, E., and Udd, B. A. (2013). 'Pathognomonic' muscle imaging findings in DNAJB6 mutated LGMD1D. *Eur. J. Neurol.* 20, 1553–1559. doi: 10.1111/ene.12239

Sarparanta, J., Jonson, P. H., Golzio, C., Sandell, S., Luque, H., Screen, M., et al. (2012). Mutations affecting the cytoplasmic functions of the co-chaperone DNAJB6 cause limb-girdle muscular dystrophy. *Nat. Genet.* 44, 450–455, S1–S2. doi: 10.1038/ng.1103

Sato, T., Hayashi, Y. K., Oya, Y., Kondo, T., Sugie, K., Kaneda, D., et al. (2013). DNAJB6 myopathy in an Asian cohort and cytoplasmic/nuclear inclusions. *Neuromuscul. Disord.* 23, 269–276. doi: 10.1016/j.nmd.2012.12.010

Schneiderman, L. J., Sampson, W. I., Schoene, W. C., and Haydon, G. B. (1969). Genetic studies of a family with two unusual autosomal dominant conditions: muscular dystrophy and Pelger-Huet anomaly. Clinical, pathologic and linkage considerations. *Am. J. Med.* 46, 380–393.

Servidei, S., Capon, F., Spinazzola, A., Mirabella, M., Semprini, S., de Rosa, G., et al. (1999). A distinctive autosomal dominant vacuolar neuromyopathy linked to 19p13. *Neurology* 53, 830–837.

Speer, M. C., Gilchrist, J. M., Chutkow, J. G., McMichael, R., Westbrook, C. A., Stajich, J. M., et al. (1995). Evidence for locus heterogeneity in autosomal dominant limb-girdle muscular dystrophy. *Am. J. Hum. Genet.* 57, 1371–1376.

Speer, M. C., Vance, J. M., Grubber, J. M., Lennon Graham, F., Stajich, J. M., Viles, K. D., et al. (1999). Identification of a new autosomal dominant limb-girdle muscular dystrophy locus on chromosome 7. *Am. J. Hum. Genet.* 64, 556–562.

Stein, K. C., Bengoechea, R., Harms, M. B., Weihl, C. C., and True, H. L. (2014). Myopathy-causing mutations in an Hsp40 chaperone disrupt processing of specific client conformers. *J. Biol. Chem.* 289, 21120–21130. doi: 10.1074/jbc.M114.572461

Suarez-Cedeno, G., Winder, T., and Milone, M. (2014). DNAJB6 myopathy: a vacuolar myopathy with childhood onset. *Muscle Nerve* 49, 607–610. doi: 10.1002/mus.24106

Udan-Johns, M., Bengoechea, R., Bell, S., Shao, J., Diamond, M. I., True, H. L., et al. (2014). Prion-like nuclear aggregation of TDP-43 during heat shock is regulated by Hsp40/70 chaperones. *Hum. Mol. Genet.* 23, 157–170. doi: 10.1093/hmg/ddt408

Watson, E. D., Geary-Joo, C., Hughes, M., and Cross, J. C. (2007). The Mrj co-chaperone mediates keratin turnover and prevents the formation of toxic inclusion bodies in trophoblast cells of the placenta. *Development* 134, 1809–1817. doi: 10.1242/dev.02843

Yabe, I., Tanino, M., Yaguchi, H., Takiyama, A., Cai, H., Kanno, H., et al. (2014). Pathology of frontotemporal dementia with limb girdle muscular dystrophy caused by a DNAJB6 mutation. *Clin. Neurol. Neurosurg.* 127, 10–12. doi: 10.1016/j.clineuro.2014.09.013

Yu, V. Z., Wong, V. C., Dai, W., Ko, J. M., Lam, A. K., Chan, K. W., et al. (2015). Nuclear localization of DNAJB6 is associated with survival of patients with esophageal cancer and reduces AKT signaling and proliferation of cancer cells. *Gastroenterology* 149, 1825.e5–1836.e5. doi: 10.1053/j.gastro.2015.08.025

Conflict of Interest Statement: The authors declare that the research was conducted in the absence of any commercial or financial relationships that could be construed as a potential conflict of interest.

frontiers in Molecular Biosciences

MINI REVIEW
published: 12 September 2016
doi: 10.3389/fmolb.2016.00053

Melusin Promotes a Protective Signal Transduction Cascade in Stressed Hearts

Matteo Sorge and Mara Brancaccio *

Department of Molecular Biotechnology and Health Sciences, University of Torino, Torino, Italy

Melusin is a chaperone protein selectively expressed in heart and skeletal muscles. Melusin expression levels correlate with cardiac function in pre-clinical models and in human patients with aortic stenosis. Indeed, previous studies in several animal models indicated that Melusin plays a broad cardioprotective role in different pathological conditions. Chaperone proteins, besides playing a role in protein folding, are also able to facilitate supramolecular complex formation and conformational changes due to activation/deactivation of signaling molecules. This role sets chaperone proteins as crucial regulators of intracellular signal transduction pathways. In particular Melusin activates AKT and ERK1/2 signaling, protects cardiomyocytes from apoptosis and induces a compensatory hypertrophic response in several pathological conditions. Therefore, selective delivery of the Melusin gene in heart via cardiotropic adenoviral associated virus serotype 9 (AAV9), may represent a new promising gene-therapy approach for different cardiac pathologies.

Keywords: chaperone, Melusin, intracellular signaling, apoptosis, ERK 1/2, AKT, HSP90, heart failure

OPEN ACCESS

Edited by:
Alberto J. L. Macario, University of Maryland at Baltimore, USA; Institute of Marine and Environmental Technology, USA; Istituto Euro-Mediterraneo di Scienza e Tecnologia, Italy

Reviewed by:
Chrisostomos Prodromou, University of Sussex, UK
Eileen M. Lafer, University of Texas Health Science Center at San Antonio, USA

***Correspondence:**
Mara Brancaccio
mara.brancaccio@unito.it

Specialty section:
This article was submitted to Protein Folding, Misfolding and Degradation, a section of the journal Frontiers in Molecular Biosciences

Received: *17 June 2016*
Accepted: *29 August 2016*
Published: *12 September 2016*

Citation:
Sorge M and Brancaccio M (2016) Melusin Promotes a Protective Signal Transduction Cascade in Stressed Hearts. Front. Mol. Biosci. 3:53. doi: 10.3389/fmolb.2016.00053

ROLE OF CHAPERONES AND CO-CHAPERONES IN THE STRESSED HEART

Proteins are synthesized as linear amino acid chains that must fold in a specific three-dimensional structure and maintain their functional conformation to carry out their biological functions (Balchin et al., 2016). However, the preservation of a particular fold depends on different factors, including temperature, pH, protein-protein interactions, post-translational modifications, mechanical stretch, etc. Moreover, in several cases, proteins need to change conformation to accomplish their functions. For instance, extracellular ligands, by binding to membrane receptors, are able to trigger a cascade of conformational changes in cytoplasmic signal transduction proteins. During structural switches, proteins pass through metastable intermediates exposing hydrophobic amino acid residues, potentially causing toxic protein aggregates. Cells evolved an organized chaperone system to cope with misfolding of native proteins and assist physiological protein conformational changes and unfolding emergencies.

The highly specialized sarcomeric structures in cardiomyocytes consist of a number of proteins bound to each other in a very regulated fashion, creating a dense protein matrix. Mechanical overload is sensed by membrane receptors connecting the extracellular matrix to the intracellular cytoskeleton, like integrins (Brancaccio et al., 2006). Growing evidence indicates that excessive mechanical stretch, such as the ones induced by hypertension, aortic stenosis, myocardial

infarction, etc., induces protein misfolding (Willis and Patterson, 2010; Tarone and Brancaccio, 2014; McLendon and Robbins, 2015; Parry et al., 2015). Moreover, mechanical stretch and humoral factors released in response to excessive workload activate signal transduction pathways (Tarone and Lembo, 2003) that need to be assisted by chaperones to properly sustain cell survival and induce cardiomyocyte hypertrophic growth. Unfolded proteins, by exposing hydrophobic amino acid stretches, are prone to form insoluble toxic aggregates in cardiomyocytes, potentially contributing to cell death (Del Monte and Agnetti, 2014; Parry et al., 2015). Accordingly, patients suffering from hypertrophic cardiomyopathy and idiopathic dilated cardiomyopathy accumulate misfolded proteins in the heart (Parry et al., 2015).

Chaperone proteins are characterized by different molecular weight, subcellular localization and enzymatic activity. In response to stressful conditions, chaperone expression is induced in cardiomyocytes to cope with the unfolding emergency. However, if stress conditions persist, chaperone activity becomes insufficient for protecting cells form proteotoxicity, and pathological remodeling takes place (Del Monte and Agnetti, 2014). Several chaperones have been described to build a compensatory response in the stressed heart in a cooperative manner (Willis and Patterson, 2010; Tarone and Brancaccio, 2014). HSP90 is one of the most important molecular chaperones, acting as a dynamic dimer that switches through multiple conformations. Co-chaperones regulate HSP90 ATPase activity, interact with further components of the machinery and drive substrate binding (Li et al., 2012; Verma et al., 2016). HSP90 interacts with a variety of substrates also called "HSP90 client proteins" among them transcription factors, signaling molecules, apoptosis regulators, and cytoskeletal components (http://www.picard.ch/downloads/downloads.htm), controlling their activity and degradation. It is thus conceivable that Hsp90 plays multiple important roles in sustaining heart function upon stress adaptation, by inducing protein refolding, directing unfolded proteins to proteasome degradation, and assisting conformational changes in signal transduction molecules (Ficker et al., 2003; Kupatt et al., 2004; Tarone and Brancaccio, 2014; Parry et al., 2015).

A second class of chaperones, the small heat shock proteins (sHsps) family, is devoid of ATPase activity and characterized by an α-crystallin domain responsible for their oligomerization. The association between sHsp oligomers and client proteins is required for their anti-aggregation activity (Vos et al., 2011; Bakthisaran et al., 2015; Haslbeck and Vierling, 2015). sHsps show anti-apoptotic activity, inhibit misfolded protein aggregation, mediate protein refolding in cooperation with Hsp90, and regulate signal transduction pathways (Vos et al., 2008, 2011; Bakthisaran et al., 2015). Growing experimental evidence indicates a role for this class of chaperones in sustaining heart function in stress conditions (Willis and Patterson, 2010; Tarone and Brancaccio, 2014; Parry et al., 2015). For instance, αB-crystallin protects the heart from ischemia/reperfusion injury and, when overexpressed, it attenuates cardiac hypertrophy caused by pressure overload. Moreover, missense mutations in the αB-crystallin coding gene cause a desmin related cardiomyopathy (Boelens, 2014; Anbarasu and Sivakumar, 2016). Hsp27, another chaperone expressed in the heart, protects from ischemia/reperfusion damage when overexpressed (Christians et al., 2012). Hsp20 also displays a well-documented cardioprotective activity by enhancing cardiomyocyte survival and improving heart contractility in different models of heart failure (Fan and Kranias, 2011; Martin et al., 2014).

In this review we will focus on the cardioprotective role of the muscle specific chaperone protein Melusin, showing both Hsp90 co-chaperone function and typical features of sHsps.

MELUSIN STRUCTURE AND CHAPERONE FUNCTION

Melusin is a chaperone protein, encoded by the *ITGB1BP2* gene, expressed selectively in heart and skeletal muscles. Melusin has been identified as an interactor of the cytoplasmic region of β1 integrin (Brancaccio et al., 1999), a membrane receptor that connects the intracellular cytoskeleton with the extracellular matrix, allowing muscle cells to respond to mechanical stimuli (Brancaccio et al., 2006). This chaperone protein shows a highly conserved structure in vertebrates, consisting of two Cysteine and Histidine-Rich Domains (CHORDS), a CS domain, shared by CHORD proteins and by the co-chaperone protein Sgt1 (Shirasu et al., 1999), and a C-terminal Ca^{2+}-binding domain, enriched in aspartic and glutamic acid residues (Brancaccio et al., 1999). CHORD I-II domains in the amino-terminal region of Melusin are 60-amino acid zinc-binding domains, highly conserved during evolution and able to mediate the binding of Melusin to HSP90 (Hahn, 2005; Sbroggiò et al., 2008; Hong et al., 2013). Moreover, the CS domain, structurally similar to α-crystallin and p23 chaperone proteins (Garcia-Ranea et al., 2002), has also been described as an HSP90 binding module (Lee et al., 2004; Zhang et al., 2010). Melusin, through its CHORD domains, directly binds the ATPase domain of HSP90 (Sbroggiò et al., 2008) preferentially in its ADP-bound state (Gano and Simon, 2010; Zhang et al., 2010; Hong et al., 2013). In addition, the binding of Ca^{2+} to the C-terminal domain of Melusin enhances its interaction with HSP90 (Hong et al., 2013). This is particularly relevant considering the crucial role of Ca^{2+} ions in muscle contraction and the link between heart failure and Ca^{2+} cycling dysfunction in cardiomyocytes (Marks, 2013). Interestingly, Melusin inhibits denatured protein aggregation *in vitro* in a dose dependent manner, showing a potential intrinsic chaperone activity (Sbroggiò et al., 2008), and displays the ability to oligomerize (Hong et al., 2013), a feature correlated with increased chaperone activity in small heat shock proteins (Garrido et al., 2012; Bakthisaran et al., 2015; Haslbeck and Vierling, 2015). These are relevant functions considering the accumulation of toxic misfolded proteins occurring during cardiomyopathy (Willis and Patterson, 2013; Del Monte and Agnetti, 2014; Tarone and Brancaccio, 2014). However, it is noteworthy that the ability of Melusin to act as a chaperone is based only on *in vitro* experiments and further evidences are required to confirm this property *in vivo*.

MELUSIN CARDIOPROTECTIVE ROLE IN ANIMAL MODELS OF CARDIOMYOPATHY

The protective role of Melusin in the heart is strictly related to the cardiac response to stress stimuli. Upon mechanical stretch, the heart activates a compensatory hypertrophic response, causing an increase in the thickness of the left ventricle wall that preserves contractility. However, if the stimulus becomes chronic, the heart undergoes a pathological evolution from adaptive hypertrophy to dilated cardiomyopathy with loss of contractile function, known as "maladaptive remodeling."

In a mouse model subjected to cardiac mechanical stretch via surgical aortic banding, mimicking human pathologies such as chronic aortic stenosis, left ventricle outflow obstruction, or systemic hypertension, Melusin expression levels increase in left ventricles in the first week of pressure overload, during the induction of the compensatory hypertrophic response (De Acetis et al., 2005; Sbroggiò et al., 2008). However, Melusin expression decreases when chamber dilation and loss of contractility ensues (De Acetis et al., 2005). Notably, this correlation between Melusin expression levels and cardiac response to stress has been reported also in a dog model of volume overload (Donker et al., 2007). Another pathological condition characterized by maladaptive remodeling in humans is the myocardial infarction (Heusch et al., 2014). The occlusion of coronary arteries induces an ischemic insult to the cardiac tissue in which the damaged area is replaced by a non-contractile connective scar and the healthy portion undergoes hypertrophy because of increased hemodynamic stress. In a rat model of myocardial infarction obtained by permanent coronary ligation, analysis at different time points after the ischemic injury revealed a direct correlation between Melusin expression and the rates of left ventricle systolic pressure and fractional shortening (Gu et al., 2012).

To investigate the specific role of Melusin in protecting myocardium from adverse remodeling *in vivo*, Melusin-*null* mice (Brancaccio et al., 2003) and transgenic mice overexpressing Melusin in cardiomyocytes (De Acetis et al., 2005) have been generated. Melusin-*null* mice are healthy and fertile under normal conditions and they do not display obvious defects in striated muscle development and structure. These mice show normal myocardial parameters (Brancaccio et al., 2003), indicating that Melusin is not crucial for cardiac development and basal physiological functions. However, the cardioprotective role of Melusin becomes evident under mechanical stress conditions. Whereas wild-type mice activate a compensatory hypertrophic response after 4 weeks following aortic stenosis, Melusin-*null* mice fail to activate this program and rapidly develop a dilated cardiomyopathy with left ventricle dilation, chamber wall thinning, and impaired contractility (Brancaccio et al., 2003).

The importance of Melusin in the cardiac response to mechanical stretch has been further confirmed by analyzing Melusin overexpressing mice. In basal conditions, these mice show a mild cardiomyocyte hypertrophy without alteration of contractile function (De Acetis et al., 2005). Instead, upon pressure overload conditions, Melusin overexpression effectively protects mouse myocardium by sustaining the compensatory hypertrophic response and healthy contractile function even after 12 weeks of aortic banding, when wild-type mice have already developed a dilated cardiomyopathy and heart failure (De Acetis et al., 2005).

During maladaptive remodeling of the heart, cardiomyocyte loss, inflammation, deposition of fibrotic tissue, and reduction of capillary density typically occur. Notably, Melusin overexpression protects cardiomyocytes from apoptotic death, reduces inflammation and stromal tissue deposition and stimulates capillary growth (De Acetis et al., 2005; **Figure 1**).

In mice overexpressing Melusin in which myocardial infarction is induced by permanent left descending coronary ligation, Melusin ensures a double protective role. In the early phase, it reduces the inflammatory response and protects against cardiac rupture; in long term recovery it prevents the heart from dilated degeneration by improving cardiomyocyte survival (Unsold et al., 2014).

Upon acute coronary occlusion, the duration of the ischemia determines the extent of cardiac damage. In clinical practice, acute myocardial infarction is treated with angioplasty or thrombolysis to induce a prompt coronary re-opening. However, sudden re-oxygenation determines the so-called "reperfusion injury," characterized by the production of reactive oxygen species, calcium overload, and the opening of the mitochondrial permeability transition pore, which all cause cardiomyocyte death and subsequent inflammation, thereby worsening the initial ischemic damage (Yellon and Hausenloy, 2007; Perrelli et al., 2011). The ischemia-reperfusion injury is well-reproduced in isolated perfused hearts with the Langendorff technique. In this model, Melusin overexpression significantly reduces the infarct size area and cardiomyocyte cell death, thus protecting the heart from ischemia-reperfusion injury (Penna et al., 2014).

MELUSIN IN HUMAN CARDIOMYOPATHIES

A link between Melusin expression and cardiac functional parameters has also been observed in humans. In a cohort

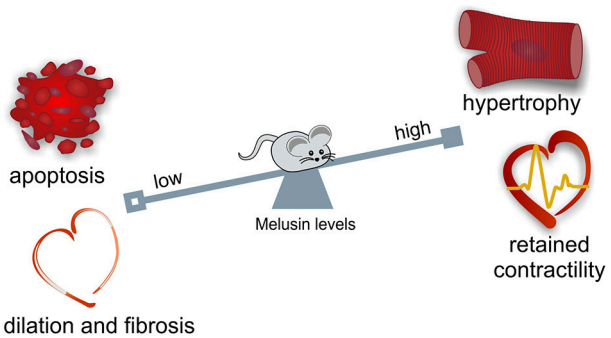

FIGURE 1 | Melusin cardioprotective role in the heart. Melusin protects the heart from "maladaptive remodeling" during mechanical stress. Melusin potentiates the compensatory hypertrophic response of the heart preserving its contractile function. Melusin also prevents cardiac dilation and fibrosis deposition and protects cardiomyocytes from apoptotic death.

of 17 patients with aortic stenosis evolved to severe heart failure, Melusin expression positively correlates with left ventricle ejection fraction (Brokat et al., 2007). A genetic screening for Melusin mutations in cardiomyopathic patients, performed by three independent laboratories, have revealed two missense mutations, a His13Tyr mutation in the CHORD I domain in a family with hypertrophic cardiomyopathy (Palumbo et al., 2009), and an Ala313Gly mutation in the carboxy terminal region linking the CS domain to the acidic domain in a family with dilated cardiomyopathy (Ruppert et al., 2013) but their segregation in the family members not always correlates with the onset of cardiomyopathy, making their causative significance unclear. Furthermore, structural analysis on the Melusin homolog in plants suggests that His13Tyr mutation does not disrupt the interaction with Hsp90 and that Ala313Gly mutation is distant from known CS domain interaction sites (Zhang et al., 2010). Another silent mutation, an intronic duplication and some polymorphisms has also been found in a study of population screening comparing cardiopathic and healthy subjects (Palumbo et al., 2009). However, all these analyses led to the consideration that Melusin gene (*ITGB1BP2*) mutations are very rare within the population, with no significant relevance in the epidemiology of cardiomyopathy. On the other hand, pre-clinical studies indicate that the regulation of Melusin expression may play a key role in improving the ability of the myocardium to cope with different stressors.

MELUSIN CARDIOPROTECTIVE SIGNAL TRANSDUCTION

Mechanical stress induces in the heart the activation of specific signal transduction pathways and the release of neurohumoral mediators acting on cardiomyocytes, fibroblasts and endothelial cells, regulating the heart's response to stress. The balance between these signals may direct the overall cardiac response to a compensatory or to a maladaptive remodeling (Tarone and Lembo, 2003). Extensive data indicate that the activation of the MAPK and AKT signal transduction pathways in cardiomyocytes promotes cell survival and compensatory hypertrophic growth, protecting the heart from dilation and failure (Selvetella et al., 2004; Baines and Molkentin, 2005; Tarone et al., 2013). Molecular analysis of the myocardial signaling pathways, indicate that Melusin interacts with several signaling molecules, including the Focal Adhesion Kinase (FAK), the MAPK scaffold protein IQGAP1, the mitogen activated protein kinases c-Raf, MEK1/2, and ERK1/2 (Sbroggiò et al., 2011a) and the phosphoinositide 3-kinases (PI3Ks), which in turn activate AKT (Waardenberg et al., 2011). We demonstrated a role for the Focal adhesion kinase in activating Melusin-bound ERK1/2 in response to mechanical stretch (Sbroggiò et al., 2011a). The Melusin binding protein IQGAP1 is a scaffold protein able to bind c-Raf, MEK1/2, and ERK1/2 and to facilitate their sequential phosphorylation. Accordingly, IQGAP1 is essential for the activation of the MAPK pathway in response to Melusin overexpression and pressure overload *in vivo* (Sbroggiò et al., 2011a,b).

These data suggest that Melusin, along with Hsp90, mediates the assembly of a signalosome organized on the scaffold protein IQGAP1 to activate and integrate beneficial ERK1/2 signaling (Tarone et al., 2013) with the AKT pathway (**Figure 2**). In accordance, a role for Hsp90 in promoting and maintaining the assembly of protein complexes has been previously described (Makhnevych and Houry, 2012).

Melusin, indeed, potentiates ERK1/2 and AKT phosphorylation in transgenic mice subjected to transverse aortic constriction, preventing the evolution to dilated cardiomyopathy (Brancaccio et al., 2003; De Acetis et al., 2005). In the model of myocardial infarction due to permanent coronary ligation, Melusin overexpression significantly enhances ERK1/2 phosphorylation at the myocardial infarct border zone, where mechanical stretch is higher, reducing the extent of the damage (Unsold et al., 2014). Furthermore, the activation of the reperfusion injury salvage kinase (RISK) pathway, composed by the PI3K/AKT and the ERK1/2 pathways, has been shown to protect cardiomyocytes during the reperfusion phase (Hausenloy and Yellon, 2004). This pathway is required for Melusin protective role in the ischemia/reperfusion model, since their pharmacological inhibition abrogates Melusin protection (Penna et al., 2014). Notably, in the pathological heart, when Melusin expression is decreased, also the ERK1/2 and AKT compensatory pathways are downregulated, allowing the establishment of detrimental signaling that further impact on heart function (De Acetis et al., 2005).

CONCLUSION AND THERAPEUTIC PERSPECTIVES

Melusin is a chaperone protein selectively expressed in cardiac and skeletal muscles, indicating a tissue specific function for this protein. Accordingly, its expression is upregulated in response to mechanical overload in the heart during the hypertrophic phase (De Acetis et al., 2005; Sbroggiò et al., 2008). Melusin protective activity in these conditions has been widely demonstrated in a number of preclinical models (Brancaccio et al., 2003; De Acetis et al., 2005; Penna et al., 2014; Unsold et al., 2014) and associated with its ability to build a supramolecular complex activating ERK1/2 and AKT beneficial pathways in cardiomyocytes (Sbroggiò et al., 2011a,b). In this view, increasing Melusin expression in the heart may represent a new therapeutic approach in cardiomyopathic patients. To date, adeno-associated viruses (AVVs) are the most promising viral vectors for gene therapy, also approved by FDA for human clinical trials. AAVs ensure a stable and efficient transgene expression even in non-proliferating cells and, once in the human body, do not induce a significant immune response or insertional mutagenesis risk (Ponnazhagan et al., 1997; Chirmule et al., 1999). In particular adenoviral associated virus serotype 9 (AAV9) is able to direct transgene expression in cardiomyocytes, representing a promising vector for gene therapy in cardiac diseases. In our laboratory, an AAV9 virus carrying human Melusin cDNA, able to induce Melusin expression selectively in the heart is currently

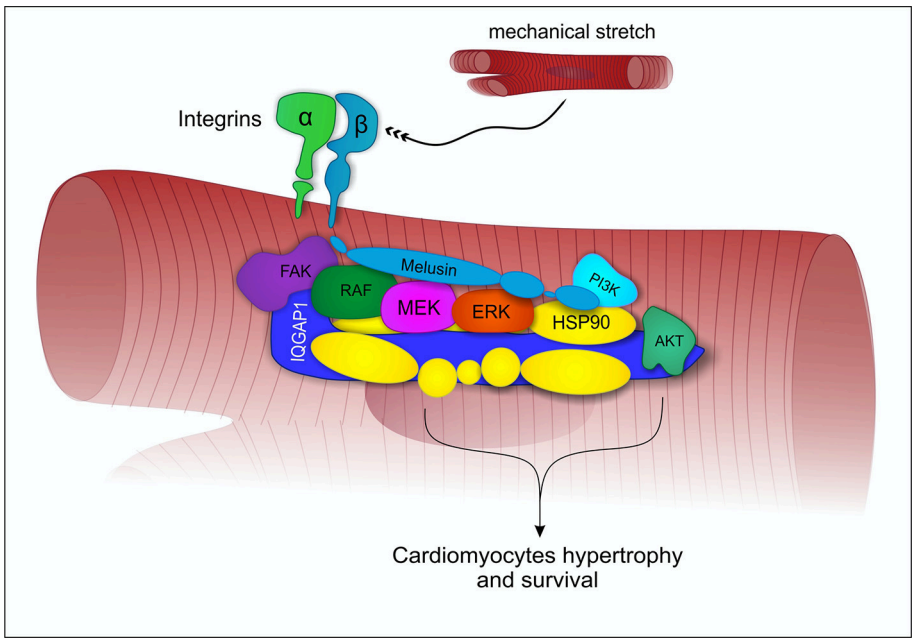

FIGURE 2 | Melusin-dependent activation of ERK1/2 and AKT under mechanical stress. Under mechanical stretch condition, Melusin binds to the cytoplasmic domain of β1-integrin and interacts with IQGAP1, leading to the activation of ERK1/2 and AKT cardioprotective pathways.

under investigation for its ability to counteract cardiomyopathy in different mouse models.

AUTHOR CONTRIBUTIONS

MS wrote the manuscript and drew the figures. MB wrote the manuscript.

ACKNOWLEDGMENTS

We dedicate this manuscript to the memory of Prof. Guido Tarone. We thank Sara Cabodi and Enzo Calautti for comments on the manuscript. This work was supported by funding from Telethon grant GGP12047 to MB.

REFERENCES

Anbarasu, K., and Sivakumar, J. (2016). Multidimensional significance of crystallin protein-protein interactions and their implications in various human diseases. *Biochim. Biophys. Acta* 1860(1 Pt B), 222–233. doi: 10.1016/j.bbagen.2015.09.005

Baines, C. P., and Molkentin, J. D. (2005). STRESS signaling pathways that modulate cardiac myocyte apoptosis. *J. Mol. Cell. Cardiol.* 38, 47–62. doi: 10.1016/j.yjmcc.2004.11.004

Bakthisaran, R., Tangirala, R., and Rao Ch, M. (2015). Small heat shock proteins: role in cellular functions and pathology. *Biochim. Biophys. Acta* 1854, 291–319. doi: 10.1016/j.bbapap.2014.12.019

Balchin, D., Hayer-Hartl, M., and Hartl, F. U. (2016). *In vivo* aspects of protein folding and quality control. *Science* 353:aac4354. doi: 10.1126/science.aac4354

Boelens, W. C. (2014). Cell biological roles of alphaB-crystallin. *Prog. Biophys. Mol. Biol.* 115, 3–10. doi: 10.1016/j.pbiomolbio.2014.02.005

Brancaccio, M., Fratta, L., Notte, A., Hirsch, E., Poulet, R., Guazzone, S., et al. (2003). Melusin, a muscle-specific integrin beta1-interacting protein, is required to prevent cardiac failure in response to chronic pressure overload. *Nat. Med.* 9, 68–75. doi: 10.1038/nm805

Brancaccio, M., Guazzone, S., Menini, N., Sibona, E., Hirsch, E., De Andrea, M., et al. (1999). Melusin is a new muscle-specific interactor for beta(1) integrin cytoplasmic domain. *J. Biol. Chem.* 274, 29282–29288. doi: 10.1074/jbc.274.41.29282

Brancaccio, M., Hirsch, E., Notte, A., Selvetella, G., Lembo, G., and Tarone, G. (2006). Integrin signalling: the tug-of-war in heart hypertrophy. *Cardiovasc. Res.* 70, 422–433. doi: 10.1016/j.cardiores.2005.12.015

Brokat, S., Thomas, J., Herda, L. R., Knosalla, C., Pregla, R., Brancaccio, M., et al. (2007). Altered melusin expression in the hearts of aortic stenosis patients. *Eur. J. Heart Fail.* 9, 568–573. doi: 10.1016/j.ejheart.2007.02.009

Chirmule, N., Propert, K., Magosin, S., Qian, Y., Qian, R., and Wilson, J. (1999). Immune responses to adenovirus and adeno-associated virus in humans. *Gene Ther.* 6, 1574–1583. doi: 10.1038/sj.gt.3300994

Christians, E. S., Ishiwata, T., and Benjamin, I. J. (2012). Small heat shock proteins in redox metabolism: implications for cardiovascular diseases. *Int. J. Biochem. Cell Biol.* 44, 1632–1645. doi: 10.1016/j.biocel.2012.06.006

De Acetis, M., Notte, A., Accornero, F., Selvetella, G., Brancaccio, M., Vecchione, C., et al. (2005). Cardiac overexpression of melusin protects from dilated cardiomyopathy due to long-standing pressure overload. *Circ. Res.* 96, 1087–1094. doi: 10.1161/01.RES.0000168028.36081.e0

Del Monte, F., and Agnetti, G. (2014). Protein post-translational modifications and misfolding: new concepts in heart failure. *Proteomics Clin. Appl.* 8, 534–542. doi: 10.1002/prca.201400037

Donker, D. W., Maessen, J. G., Verheyen, F., Ramaekers, F. C., Spätjens, R. L., Kuijpers, H., et al. (2007). Impact of acute and enduring volume overload on mechanotransduction and cytoskeletal integrity of canine left ventricular myocardium. *Am. J. Physiol. Heart Circ. Physiol.* 292, H2324–H2332. doi: 10.1152/ajpheart.00392.2006

Fan, G. C., and Kranias, E. G. (2011). Small heat shock protein 20 (HspB6) in cardiac hypertrophy and failure. *J. Mol. Cell. Cardiol.* 51, 574–577. doi: 10.1016/j.yjmcc.2010.09.013

Ficker, E., Dennis, A. T., Wang, L., and Brown, A. M. (2003). Role of the cytosolic chaperones Hsp70 and Hsp90 in maturation of the cardiac potassium channel HERG. *Circ. Res.* 92, e87–e100. doi: 10.1161/01.RES.0000079028.31393.15

Gano, J. J., and Simon, J. A. (2010). A proteomic investigation of ligand-dependent HSP90 complexes reveals CHORDC1 as a novel ADP-dependent HSP90-interacting protein. *Mol. Cell. Proteomics* 9, 255–270. doi: 10.1074/mcp.M900261-MCP200

Garcia-Ranea, J. A., Mirey, G., Camonis, J., and Valencia, A. (2002). p23 and HSP20/alpha-crystallin proteins define a conserved sequence domain present in other eukaryotic protein families. *FEBS Lett.* 529, 162–167. doi: 10.1016/S0014-5793(02)03321-5

Garrido, C., Paul, C., Seigneuric, R., and Kampinga, H. H. (2012). The small heat shock proteins family: the long forgotten chaperones. *Int. J. Biochem. Cell Biol.* 44, 1588–1592. doi: 10.1016/j.biocel.2012.02.022

Gu, R., Zheng, D., Bai, J., Xie, J., Dai, Q., and Xu, B. (2012). Altered melusin pathways involved in cardiac remodeling following acute myocardial infarction. *Cardiovasc. Pathol.* 21, 105–111. doi: 10.1016/j.carpath.2011.03.002

Hahn, J. S. (2005). Regulation of Nod1 by Hsp90 chaperone complex. *FEBS Lett.* 579, 4513–4519. doi: 10.1016/j.febslet.2005.07.024

Haslbeck, M., and Vierling, E. (2015). A first line of stress defense: small heat shock proteins and their function in protein homeostasis. *J. Mol. Biol.* 427, 1537–1548. doi: 10.1016/j.jmb.2015.02.002

Hausenloy, D. J., and Yellon, D. M. (2004). New directions for protecting the heart against ischaemia-reperfusion injury: targeting the Reperfusion Injury Salvage Kinase (RISK)-pathway. *Cardiovasc. Res.* 61, 448–460. doi: 10.1016/j.cardiores.2003.09.024

Heusch, G., Libby, P., Gersh, B., Yellon, D., Bohm, M., Lopaschuk, G., et al. (2014). Cardiovascular remodelling in coronary artery disease and heart failure. *Lancet* 383, 1933–1943. doi: 10.1016/S0140-6736(14)60107-0

Hong, T. J., Kim, S., Wi, A. R., Lee, P., Kang, M., Jeong, J. H., et al. (2013). Dynamic nucleotide-dependent interactions of cysteine- and histidine-rich domain (CHORD)-containing Hsp90 cochaperones Chp-1 and melusin with cochaperones PP5 and Sgt1. *J. Biol. Chem.* 288, 215–222. doi: 10.1074/jbc.M112.398636

Kupatt, C., Dessy, C., Hinkel, R., Raake, P., Daneau, G., Bouzin, C., et al. (2004). Heat shock protein 90 transfection reduces ischemia-reperfusion-induced myocardial dysfunction via reciprocal endothelial NO synthase serine 1177 phosphorylation and threonine 495 dephosphorylation. *Arterioscler. Thromb. Vasc. Biol.* 24, 1435–1441. doi: 10.1161/01.ATV.0000134300.87476.d1

Lee, Y. T., Jacob, J., Michowski, W., Nowotny, M., Kuznicki, J., and Chazin, W. J. (2004). Human Sgt1 binds HSP90 through the CHORD-Sgt1 domain and not the tetratricopeptide repeat domain. *J. Biol. Chem.* 279, 16511–16517. doi: 10.1074/jbc.M400215200

Li, J., Soroka, J., and Buchner, J. (2012). The Hsp90 chaperone machinery: conformational dynamics and regulation by co-chaperones. *Biochim. Biophys. Acta* 1823, 624–635. doi: 10.1016/j.bbamcr.2011.09.003

Makhnevych, T., and Houry, W. A. (2012). The role of Hsp90 in protein complex assembly. *Biochim. Biophys. Acta* 1823, 674–682. doi: 10.1016/j.bbamcr.2011.09.001

Marks, A. R. (2013). Calcium cycling proteins and heart failure: mechanisms and therapeutics. *J. Clin. Invest.* 123, 46–52. doi: 10.1172/JCI62834

Martin, T. P., Currie, S., and Baillie, G. S. (2014). The cardioprotective role of small heat-shock protein 20. *Biochem. Soc. Trans.* 42, 270–273. doi: 10.1042/BST20130272

McLendon, P. M., and Robbins, J. (2015). Proteotoxicity and cardiac dysfunction. *Circ. Res.* 116, 1863–1882. doi: 10.1161/CIRCRESAHA.116.305372

Palumbo, V., Segat, L., Padovan, L., Amoroso, A., Trimarco, B., Izzo, R., et al. (2009). Melusin gene (ITGB1BP2) nucleotide variations study in hypertensive and cardiopathic patients. *BMC Med. Genet.* 10:140. doi: 10.1186/1471-2350-10-140

Parry, T. L., Melehani, J. H., Ranek, M. J., and Willis, M. S. (2015). Functional amyloid signaling via the inflammasome, necrosome, and signalosome: new therapeutic targets in heart failure. *Front. Cardiovasc. Med.* 2:25. doi: 10.3389/fcvm.2015.00025

Penna, C., Brancaccio, M., Tullio, F., Rubinetto, C., Perrelli, M. G., Angotti, C., et al. (2014). Overexpression of the muscle-specific protein, melusin, protects from cardiac ischemia/reperfusion injury. *Basic Res. Cardiol.* 109:418. doi: 10.1007/s00395-014-0418-9

Perrelli, M. G., Pagliaro, P., and Penna, C. (2011). Ischemia/reperfusion injury and cardioprotective mechanisms: role of mitochondria and reactive oxygen species. *World J. Cardiol.* 3, 186–200. doi: 10.4330/wjc.v3.i6.186

Ponnazhagan, S., Erikson, D., Kearns, W. G., Zhou, S. Z., Nahreini, P., Wang, X. S., et al. (1997). Lack of site-specific integration of the recombinant adeno-associated virus 2 genomes in human cells. *Hum. Gene Ther.* 8, 275–284. doi: 10.1089/hum.1997.8.3-275

Ruppert, V., Meyer, T., Richter, A., Maisch, B., and Pankuweit, S. (2013). Identification of a missense mutation in the melusin-encoding ITGB1BP2 gene in a patient with dilated cardiomyopathy. *Gene* 512, 206–210. doi: 10.1016/j.gene.2012.10.055

Sbroggiò, M., Ferretti, R., Percivalle, E., Gutkowska, M., Zylicz, A., Michowski, W., et al. (2008). The mammalian CHORD-containing protein melusin is a stress response protein interacting with Hsp90 and Sgt1. *FEBS Lett.* 582, 1788–1794. doi: 10.1016/j.febslet.2008.04.058

Sbroggiò, M., Bertero, A., Velasco, S., Fusella, F., De Blasio, E., Bahou, W. F., et al. (2011a). ERK1/2 activation in heart is controlled by melusin, focal adhesion kinase and the scaffold protein IQGAP1. *J. Cell Sci.* 124(Pt 20), 3515–3524. doi: 10.1242/jcs.091140

Sbroggiò, M., Carnevale, D., Bertero, A., Cifelli, G., De Blasio, E., Mascio, G., et al. (2011b). IQGAP1 regulates ERK1/2 and AKT signalling in the heart and sustains functional remodelling upon pressure overload. *Cardiovasc. Res.* 91, 456–464. doi: 10.1093/cvr/cvr103

Selvetella, G., Hirsch, E., Notte, A., Tarone, G., and Lembo, G. (2004). Adaptive and maladaptive hypertrophic pathways: points of convergence and divergence. *Cardiovasc. Res.* 63, 373–380. doi: 10.1016/j.cardiores.2004.04.031

Shirasu, K., Lahaye, T., Tan, M. W., Zhou, F., Azevedo, C., and Schulze-Lefert, P. (1999). A novel class of eukaryotic zinc-binding proteins is required for disease resistance signaling in barley and development in *C. elegans*. *Cell* 99, 355–366. doi: 10.1016/S0092-8674(00)81522-6

Tarone, G., and Brancaccio, M. (2014). Keep your heart in shape: molecular chaperone networks for treating heart disease. *Cardiovasc. Res.* 102, 346–361. doi: 10.1093/cvr/cvu049

Tarone, G., and Lembo, G. (2003). Molecular interplay between mechanical and humoral signalling in cardiac hypertrophy. *Trends Mol. Med.* 9, 376–382. doi: 10.1016/S1471-4914(03)00164-3

Tarone, G., Sbroggiò, M., and Brancaccio, M. (2013). Key role of ERK1/2 molecular scaffolds in heart pathology. *Cell. Mol. Life Sci.* 70, 4047–4054. doi: 10.1007/s00018-013-1321-5

Unsöld, B., Kaul, A., Sbroggiò, M., Schubert, C., Regitz-Zagrosek, V., Brancaccio, M., et al. (2014). Melusin protects from cardiac rupture and improves functional remodelling after myocardial infarction. *Cardiovasc. Res.* 101, 97–107. doi: 10.1093/cvr/cvt235

Verma, S., Goyal, S., Jamal, S., Singh, A., and Grover, A. (2016). Hsp90: friends, clients and natural foes. *Biochimie* 127, 227–240. doi: 10.1016/j.biochi.2016.05.018

Vos, M. J., Hageman, J., Carra, S., and Kampinga, H. H. (2008). Structural and functional diversities between members of the human HSPB, HSPH, HSPA, and DNAJ chaperone families. *Biochemistry* 47, 7001–7011. doi: 10.1021/bi800639z

Vos, M. J., Zijlstra, M. P., Carra, S., Sibon, O. C., and Kampinga, H. H. (2011). Small heat shock proteins, protein degradation and protein aggregation diseases. *Autophagy* 7, 101–103. doi: 10.4161/auto.7.1.13935

Waardenberg, A. J., Bernardo, B. C., Ng, D. C., Shepherd, P. R., Cemerlang, N., Sbroggiò, M., et al. (2011). Phosphoinositide 3-kinase (PI3K(p110alpha)) directly regulates key components of the Z-disc and cardiac structure. *J. Biol. Chem.* 286, 30837–30846. doi: 10.1074/jbc.M111.271684

Willis, M. S., and Patterson, C. (2010). Hold me tight: role of the heat shock protein family of chaperones in cardiac disease. *Circulation* 122, 1740–1751. doi: 10.1161/CIRCULATIONAHA.110.942250

Willis, M. S., and Patterson, C. (2013). Proteotoxicity and cardiac dysfunction–Alzheimer's disease of the heart? *N. Engl. J. Med.* 368, 455–464. doi: 10.1056/NEJMra1106180

Yellon, D. M., and Hausenloy, D. J. (2007). Myocardial reperfusion injury. *N. Engl. J. Med.* 357, 1121–1135. doi: 10.1056/NEJMra071667

Zhang, M., Kadota, Y., Prodromou, C., Shirasu, K., and Pearl, L. H. (2010). Structural basis for assembly of Hsp90-Sgt1-CHORD protein complexes: implications for chaperoning of NLR innate immunity receptors. *Mol. Cell* 39, 269–281. doi: 10.1016/j.molcel.2010.05.010

Conflict of Interest Statement: The authors declare that the research was conducted in the absence of any commercial or financial relationships that could be construed as a potential conflict of interest.

frontiers in Molecular Biosciences

MINI REVIEW
published: 31 August 2016
doi: 10.3389/fmolb.2016.00049

Disease-Associated Mutations in the *HSPD1* Gene Encoding the Large Subunit of the Mitochondrial HSP60/HSP10 Chaperonin Complex

*Peter Bross * and Paula Fernandez-Guerra*

Research Unit for Molecular Medicine, Department of Molecular Medicine, Aarhus University and Aarhus University Hospital, Aarhus, Denmark

Heat shock protein 60 (HSP60) forms together with heat shock protein 10 (HSP10) double-barrel chaperonin complexes that are essential for folding to the native state of proteins in the mitochondrial matrix space. Two extremely rare monogenic disorders have been described that are caused by missense mutations in the *HSPD1* gene that encodes the HSP60 subunit of the HSP60/HSP10 chaperonin complex. Investigations of the molecular mechanisms underlying these disorders have revealed that different degrees of reduced HSP60 function produce distinct neurological phenotypes. While mutations with deleterious or strong dominant negative effects are not compatible with life, *HSPD1* gene variations found in the human population impair HSP60 function and depending on the mechanism and degree of HSP60 dys- and mal-function cause different phenotypes. We here summarize the knowledge on the effects of disturbances of the function of the HSP60/HSP10 chaperonin complex by disease-associated mutations.

Keywords: HSP60, chaperonin, neurological disease, protein folding problem, mitochondria, gene variation

OPEN ACCESS

Edited by:
Alberto J. L. Macario, University of Maryland at Baltimore, USA

Reviewed by:
Carlos H. Ramos, State University of Campinas, Brazil
Konstantin K. Turoverov, Institute of Cytology (RAS), Russia

****Correspondence:***
Peter Bross
peter.bross@clin.au.dk

Specialty section:
This article was submitted to Protein Folding, Misfolding and Degradation, a section of the journal Frontiers in Molecular Biosciences

Received: *15 July 2016*
Accepted: *22 August 2016*
Published: *31 August 2016*

Citation:
Bross P and Fernandez-Guerra P (2016) Disease-Associated Mutations in the HSPD1 Gene Encoding the Large Subunit of the Mitochondrial HSP60/HSP10 Chaperonin Complex. Front. Mol. Biosci. 3:49. doi: 10.3389/fmolb.2016.00049

INTRODUCTION

The type I chaperonins, a subclass of the molecular chaperone family of proteins, assist folding of proteins in the bacterial cytosol, the mitochondrial matrix space, and the chloroplast stroma. Like its bacterial and chloroplast homologs the mitochondrial HSP60/HSP10 complex is composed of two seven-meric rings of the large subunit (HSP60) stacked back to back (Nisemblat et al., 2015; **Figure 1A**). The HSP60 ring structures enclose an inner cavity that is sealed by lids formed by seven-meric rings of the small subunit (HSP10). With the exception of a few endosymbionts, homologs of these proteins are abundantly expressed in mitochondria, chloroplasts and bacteria. The functional folding cycle of the mammalian HSP60/HSP10 complex (Nielsen and Cowan, 1998; Levy-Rimler et al., 2001, 2002) has to a large degree been elucidated in analogy to detailed studies of the homologous GroEL/GroES complex of *E. coli* bacteria (Horwich, 2013; Hayer-Hartl et al., 2015). Cycles including binding of proteins undergoing folding to the HSP60 rings, their encapsulation by association of HSP10 rings and dissociation of both the HSP10 ring and the enclosed protein are orchestrated by ATP binding, hydrolysis and release of ADP by the HSP60 subunits. These cycles promote folding of proteins to the native state, but not every cycle results in successful folding. Some proteins may require several rounds. Knock-out experiments have shown that the genes encoding homologs of the HSP60/HSP10 complex are essential in organisms from bacteria to mice (Cheng et al., 1989; Fayet et al., 1989; Perezgasga et al., 1999; Christensen et al., 2010). In humans

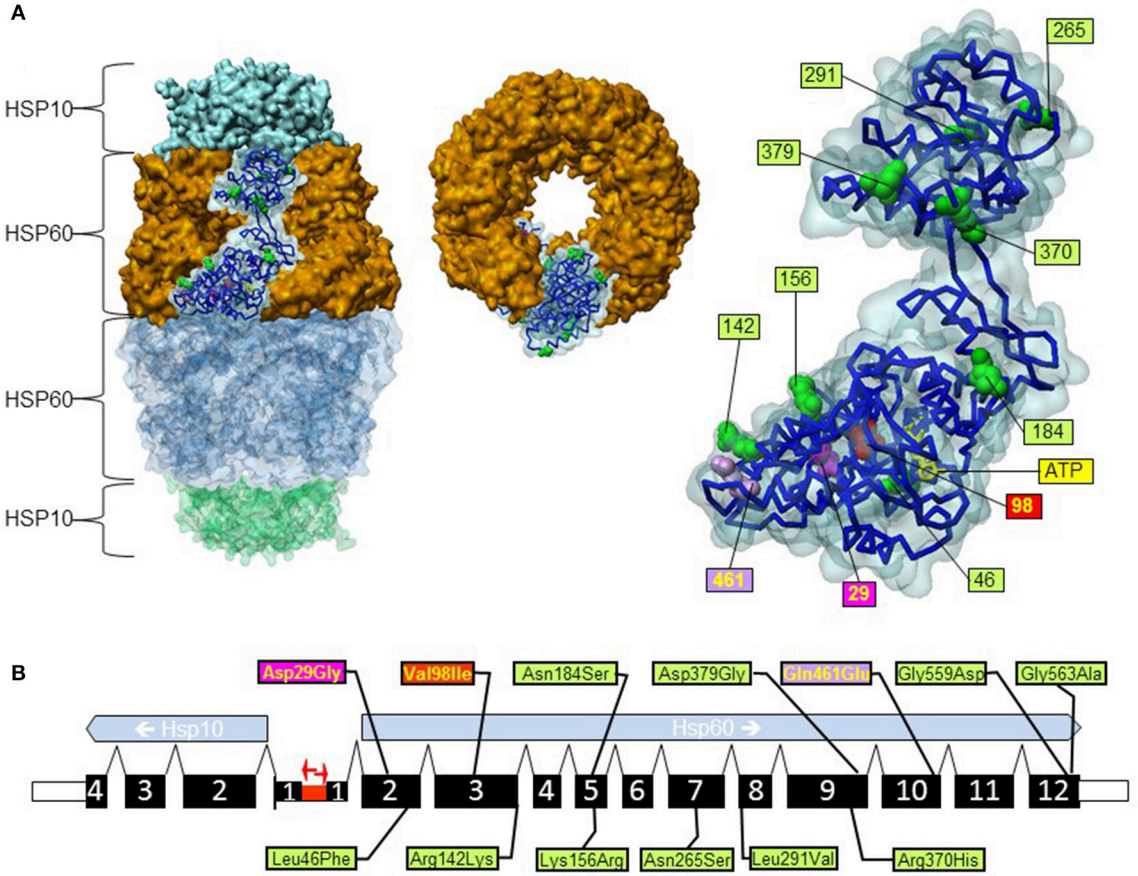

FIGURE 1 | Position of gene variations in the *HSPD1* gene and the HSP60 protein structure. (A) Structure of the HSP60/HSP10 complex and position of mutations. 3d structure representations were created based on PDB coordinates 4pj1 (Nisemblat et al., 2015) using the software Discovery Studio 4.5.0.15071 (Biovia). Left: surface representation of the structure of the HSP60/HSP10 complex; HSP60 and HSP10 rings are indicated. The surface representation of one subunit of the upper HSP60 ring is shown transparent and the carbon backbone and space filling representation of amino acid positions where missense variations have been found are shown. Middle: upside view of the upper HSP60 ring. Right: enlarged view of the highlighted subunit from the complex shown on the left with numbering of positions with missense variations. The mutations p.Gly559Asp and p.Gly563Ala are not shown because the C-terminal part of the HSP60 protein is not contained in the crystal structure. The bound ATP molecule is shown as yellow sticks. **(B)** Exon structure of the human *HSPD1 and HSPE1* genes encoding HSP60 and HSP10. The two genes are situated in a head to head configuration on chromosome 2 with a common bidirectional promoter (red arrows). Exons are numbered and their coding parts are given as broad bars. Positions of missense variations are shown; color coding is in relation to disease-association (see text).

only few gene variations altering the amino acid sequence of HSP60 and HSP10 have been described (**Table 1**). However, very rare disease-associated missense mutations in HSP60 have been associated with a dominant form of hereditary spastic paraplegia (HSP; Hansen et al., 2002) and a recessively inherited white matter disorder called MitCHAP60 disease (Magen et al., 2008). In another article published under this research topic we describe the first potentially disease associated mutation in HSP10 that has been identified in a patient with a neurological and developmental disorder (Bie et al., submitted).

AMINO ACID SEQUENCE VARIATIONS IN HSP60

The genomic structure for the human *HSPD1* and *HSPE1* genes encoding the proteins HSP60 and HSP10, respectively, has been characterized experimentally (Hansen et al., 2003). The *HSPD1* and *HSPE1* genes are localized at chromosome locus 2q33.1 in a head to head arrangement with a bidirectional common promoter (**Figure 1**). Such a head to head arrangement is evolutionary conserved from *C. elegans* to humans (Bross, 2015). The two genes comprise ∼17 kb and consist of 12 and 4 exons, respectively (**Figure 1B**). The first exon of Hsp60 is non-coding and the first exon of Hsp10 contains only the first codon (Hansen et al., 2003). At present there are two amino acid variations in HSP60 known for which a clear disease-association has been established: the HSP60-p.Val98Ile mutation associated with a dominantly inherited form of HSP (SPG13; OMIM #605280; Hansen et al., 2002) and the HSP60-p.Asp29Gly mutation causing a recessively inherited white matter disease called MitCHAP60 disease (OMIM #612233; Magen et al., 2008). Besides these two, a number of other variations have been described (**Figure 1** and **Table 1**; Hansen et al., 2002, 2007; Bross

TABLE 1 | Missense variations in the *HSPD1* gene encoding HSP60.

Variation	Disease association	Growth in genetic complementation assay	ExAC allele count	PolyPhen-2 prediction[#]	References
p.Asp29Gly	MitCHAP60	Slow, temperature-sensitive	0	benign	Magen et al., 2008
p.Leu46Phe		Not tested	29	possibly damaging	ExAC
p.Val98Ile	SPG13	No growth	0	possibly damaging	Hansen et al., 2002
p.Arg142Lys		Not tested	56	benign	ExAC
p.Lys156Arg		Not tested	17	benign	ExAC
p.Asn184Ser		Unaffected	61	benign	Hansen et al., 2002
p.Asn265Ser		Not tested	23	possibly damaging	ExAC
p.Leu291Val		Not tested	12	probably damaging	ExAC
p.Arg370His		Not tested	13	benign	ExAC
p.Asp379Gly		Unaffected	0	benign	Bross et al., 2007
p.Gln461Glu	SPG13*	Impaired	0	probably damaging	Hansen et al., 2007
p.Gly559Asp		Unaffected	0	possibly damaging	Bross et al., 2007
p.Gly563Ala		Unaffected	1904	probably damaging	Bross et al., 2007

Missense variations recorded in the literature and/or in the ExAC consortium database with ≥10 alleles are shown. The basis for scoring growth in the genetic complementation assay is explained in Section Functional analysis in vivo. Prediction of possible impact of amino acid substitutions was performed using the PolyPhen-2 webserver (Adzhubei et al., 2010).
[#]PolyPhen-2 has three prediction output options, from the highest probability score for being damaging to the lowest: "probably damaging," "possibly damaging" and "benign." The asterisk denotes that the variation/disease relationship for the p.Gln461Glu variation is not fully established. For further details see text.

et al., 2007). The Exome Aggregation Consortium webserver (ExAC; Cambridge, MA (URL: http://exac.broadinstitute.org) [June, 2016 accessed]) lists 95 missense variations for the protein product of the canonical *HSPD1* transcript. This website provides high quality exome sequencing data from more than 60,000 unrelated adults without severe pediatric disease. Of the 95 *HSPD1* missense variations 60 have only been seen in one single allele and only 9 have been observed in more than 10 of the ∼120,000 alleles recorded (**Table 1**).

FUNCTIONAL ANALYSES OF HSP60 VARIANT PROTEINS

Table 1 lists both the *HSPD1* missense variations described in the literature and those present in ≥10 alleles in the ExAC Consortium Website. The functional consequences for some of these variations have been investigated previously and the results are summarized in this review.

In vitro Analyses of Disease-Associated HSP60 Variant Proteins

Expression in *E. coli* had indicated that the two disease-associated variant proteins HSP60-p.Val98Ile and HSP60-p.Asp29Gly displayed similar stability as wild type HSP60 suggesting that the amino acid replacements caused functional impairment (Hansen et al., 2002; Magen et al., 2008). Indeed, the purified HSP60-p.Val98Ile protein assembled into native ring complexes in the same way and with similar efficiency as the wild type HSP60 protein but displayed a reduced ATPase hydrolysis rate and a severely decreased *in vitro* refolding activity with malate dehydrogenase as substrate (Bross et al., 2008). The ATPase function and refolding activity of the purified HSP60-p.Asp29Gly variant protein associated with MitCHAP60 disease was found decreased in a similar way (Parnas et al., 2009). This study also indicated impaired stability of HSP60-p.Asp29Gly oligomers causing their disassembly at low protein concentrations.

Functional Analysis *In vivo*

A sophisticated genetic complementation assay for analyzing the function of variants of the human HSP60/HSP10 chaperonin complex has been developed in the lab of Costa Georgopoulos (Richardson et al., 2001). This assay is based on knocking out the chromosomal *groESgroEL* operon and testing whether cell viability and growth properties can be maintained by providing the bacterial cells with a plasmid encoding the chaperonin gene variants to be investigated. Knock-out cells are not viable, but providing the cells with plasmids with cDNAs encoding the wild type human HSP60 and HSP10 genes maintains cell viability demonstrating that the human HSP60/HSP10 complex can functionally replace the bacterial GroEL/GroES complex (Richardson et al., 2001).

Seven human HSP60 missense variants have so-far been investigated using this functional assay (**Table 1**). These studies showed that the SPG13-associated mutant HSP60-p.Val98Ile was unable to functionally replace the bacterial chaperonin. However, cells expressing the HSP60-p.Asp29Gly variant displayed slow and temperature-sensitive growth. Cells with the HSP60-p.Gln461Glu variation found in a sporadic spastic paraplegia patient also displayed impaired growth. The four other HSP60 variants studied: p.Asn184Ser, p.Asp379Gly, p.Gly559Asp, and p.Gly563Ala, behaved like wild type HSP60 in the genetic complementation assay suggesting that they have no significant effect.

Bioinformatics prediction of the effects of the variations using the PolyPhen-2 tool (Adzhubei et al., 2010) predicts damaging effects for the HSP60-p.Val98Ile and HSP60-Gln461Glu variations, but benign for the HSP60-p.Asp29Gly for which a clear disease relationship has been established. PolyPhen-2 also

predicts "damaging" for the two carboxy-terminal variations and four of the six missense variants found in more than 10 alleles in the ExAC dataset. Given the discrepancy between experimental and prediction results this prediction results must be taken with caution. Inspection of the position of the variations in the crystal structure of the HSP60/HSP10 complex (Nisemblat et al., 2015) shows that the variations with an established disease-association (HSP60-p.Asp29Gly and HSP60-p.Val98Ile) are localized in the core of the equatorial domain of the HSP60 protein, whereas most of the other variation sites are localized on the surface of HSP60 subunits (**Figure 1A**).

The SPG13-associated mutation HSP60-p.Val98Ile is dominantly inherited, i.e., the patient cells express both a wild type and a mutant allele and these two variant proteins are likely on equal terms incorporated into HSP60 ring structures resulting in heteromeric rings with stochastically distributed content of the two variants. To test whether incorporation of mutant HSP60-p.Val98Ile subunits together with wild type HSP60 subunits into HSP60 ring complexes would cause a dominant negative effect, the complementation assay was further engineered. *E. coli* cells with the deletion of the endogenous *groESgroEL* operon and containing a plasmid with an IPTG-inducible operons comprising HSP10 and wild type HSP60 were transformed with a second plasmid comprising an arabinose-inducible operon with the respective mutant HSP60 variant and HSP10 (Bross et al., 2008). There was no effect on growth in cells expressing both wild type HSP60 and HSP60-p.Val98Ile. As a control, expression of an artificially constructed ATPase-deficient HSP60 variant together with wild type HSP60 blocked growth. These experiments strongly indicated that the HSP60-p.Val98Ile mutation exerts no significant dominant negative effect on co-expressed wild type HSP60 protein.

CLINICAL PHENOTYPES OF SPG13 AND MITCHAP60 DISEASE

Notwithstanding the rarity, studies of the very large index family that led to the discovery of the association of the HSP60-p.Val98Ile mutation with HSP has given a firm basis for the mutation/disease relationship (Hansen et al., 2002). SPG13 is dominantly inherited with a pure spastic paraplegia phenotype with high penetrance (Fontaine et al., 2000). Hereditary spastic paraplegia is a complex disease both genetically and clinically with mutations in more than 60 different genes established as causal and with all inheritance modes (Kumar et al., 2015; Tesson et al., 2015; Di Fabio et al., 2016). The characteristic spastic gait has given the acronym SPG and subsequent numerals distinguish the different genetic forms of HSP. Spastic gait and spasticity in the lower limbs are also observed as a side phenotype in many other neurological diseases. The disease is only classified as HSP if the paraplegia is the major clinical characteristic. Clinical analysis of the 10 MitChap60 patients homozygous for the HSP60-p.Asp29Gly mutation revealed also spastic paraplegia in all them (Magen et al., 2008). However, this "side-phenotype" was overshadowed by the much more severe presentation characterized by early-onset, profound cerebral involvement and lethality of these patients. A number of other SPG genes are also disease genes in other neurological diseases illustrating that maintaining the classical distinctions becomes more and more difficult (Tesson et al., 2015). Rather, the phenotype in a given patient depends on multiple factors, like the mutated gene, the nature of the mutation and its location in the protein, the zygosity of the mutation, and influences of modifier variants and the environment.

POTENTIAL DISEASE-ASSOCIATION OF OTHER MISSENSE VARIATIONS IN HSP60

In spite of widely spread genetic screening, so far only one single additional spastic paraplegia patient heterozygous for another mutation in HSP60 (HSP60-p.Gln461Glu) has been reported (Hansen et al., 2007). The causative nature of this mutation is uncertain because two siblings carrying this mutation were asymptomatic. However, as the genetic complementation test showed a mild functional impairment (See Section Functional analysis *in vivo*), this variation may be disease-associated with reduced penetrance. The most frequently observed amino acid variation in HSP60, HSP60-p.Gly563Ala, has been found in homozygous form in one sporadic Danish spastic paraplegia patient (Svenstrup et al., 2009). Frequency analysis of this polymorphisms in Danish controls showed an allele frequency of 1.3% and similar allele frequencies were observed in all ethnic groups in the ExAC database. In addition, the number of homozygotes in the ExAC database is consistent with Hardy Weinberg distribution and the genetic complementation assay did not indicate impaired function of the HSP60-p.Gly563Ala protein. Taken together this suggests that this variation has no significant effect on function (Bross et al., 2007).

CELLULAR AND MOUSE MODELS FOR HSP60 DEFICIENCY

Effects of expressing the SPG13- and MitCHap60-associated mutant proteins on mitochondrial morphology have been assessed in Cos-7 cells transfected with cDNAs encoding the disease-associated mutant proteins (Miyamoto et al., 2015, 2016). Cos-7 cells expressing either the mutant variants HSP60-p.Asp29Gly, HSP60-p.Val98Ile or HSP60-p.Gln461Glu displayed increased mitochondrial fission and decreased mitochondrial membrane potential whereas Cos-7 cells transfected with wild type HSP60 cDNA did not. This indicates that the studied mutant proteins interfere with the function of the endogenous wild type protein.

ShRNA-mediated knock-down of HSP60 in human HEK293 cells decreased the steady state levels of the mitochondrial medium-chain acyl-CoA dehydrogenase (Corydon et al., 2005), an enzyme whose subunits transiently interact with HSP60 before assembling into functional tetramers (Yokota et al., 1992; Saijo et al., 1994). Folding of ectopically expressed mitochondria-targeted green fluorescence protein (GFP) was decreased both in HEK293 cells in which HSP60 was knocked

down and in HEK293 expressing a dominant negative ATPase-deficient HSP60 variant (Corydon et al., 2005; Bie et al., 2011). Furthermore, a series of assays of HSP60 knock-down in the mouse hypothalamic cell line N25/2 revealed decreases in mitochondrial respiration, levels of respiratory chain subunits, mitochondrial DNA levels and an increase in mitochondrial volume and mitochondrial superoxide (Kleinridders et al., 2013). These cellular models can be used for further studies elucidating the multiple effects of deficiency of the HSP60/HSP10 chaperonin complex.

Knock-out of both HSP60-encoding alleles in mice is not compatible with life. Such embryos died early during development (Christensen et al., 2010). However, mice which are heterozygous for one HSP60 knock-out allele, and which express half levels of HSP60 protein, developed normally and were borne in the expected Hardy-Weinberg frequency. More thorough long-term analysis of these mice revealed a late onset and slowly progressive deficit in motor functions recapitulating features of HSP SPG13 in humans (Magnoni et al., 2013). The phenotype was accompanied by morphological changes of mitochondria in spinal cord axons. Furthermore, decreased ATP synthesis was observed in mitochondria isolated from brain cortex and spinal cord. The respiratory chain defect could be narrowed down to impaired activity of respiratory chain complex III. Proteomic analysis of mitochondria from mutant mouse tissues consistently revealed decreased levels of the UQCRC1 subunit of complex III in these tissues. As UQCRC1 transcript levels were even increased and an effect on translation is improbable, this suggested that deficiency of the HSP60/HSP10 chaperonin complex resulted in impaired folding of the UQCRC1 protein entailing premature degradation of the UQCRC1 protein. Based on the same criteria and supported by direct interaction with HSP60, the manganese-dependent superoxide dismutase SOD2 was identified as another protein that is highly dependent on appropriate HSP60/HSP10 chaperone complex function (Magnoni et al., 2014).

Proteins like UQCRC1 or SOD2 thus appear to depend more than others proteins on folding assistance by the HSP60/HSP10 complex. For *E. coli* 85 proteins that display obligate dependence on folding assistance by the bacterial chaperonin complex have been characterized (Kerner et al., 2005). Identification of those proteins whose folding obligatorily requires the human HSP60/HSP0 complex is still lacking. Such knowledge would be very helpful to identify further mitochondrial functions affected by deficiencies of the HSP60/HSP10 complex.

PERSPECTIVES

Different mutations in HSP60 or its partner protein HSP10 lead to distinct phenotypes of neurological disorders with a clear mitochondrial dysfunction pattern. These diseases are very rare as deleterious effects of mutations in these essential genes are not compatible with normal embryonal development (Christensen et al., 2010). The broader use of exome sequencing will likely reveal more cases also including *de novo* mutations in the *HSPD1* and *HSPE1* genes in sporadic diseases. Clinical geneticists should therefore be aware of this and it will be important to collect the knowledge of these rare cases to be able study genotype/phenotype relationships and to assess the disease-causing nature of variations.

Besides being affected by mutations, the activity and function of the HSP60/HSP10 complex can also be regulated by its expression levels. The regulation of the transcription levels of both proteins occurs via different elements in the bidirectional promoter. SP1 elements provide robust house-keeping levels of expression and on top of that heat-shock elements, mitochondrial unfolding protein response elements, and STAT3 elements further modulate expression adapting it to specific situations (Zhao et al., 2002; Hansen et al., 2003; Horibe and Hoogenraad, 2007; Kim and Lee, 2007; Kim et al., 2007; Kleinridders et al., 2013). One study also shows that Hsp60 mRNA is a direct target of miR-1 and miR-206 in cardiomyocytes (Shan et al., 2010).

Indeed, dysregulation of HSP60 expression in hypothalamus has been implicated with type 2 diabetes mellitus (Kleinridders et al., 2013) and changes in chaperonin expression and activity have been observed in several diseases such as cardiomyopathies, autoimmune disorders, and cancer (Cappello et al., 2014).

Finally, posttranslational modifications of the HSP60/HSP10 complex may regulate the activity of the complex. Like other molecular chaperones HSP60 is a highly modified protein with a long list of PTMs recorded in the UniProt database (Consortium, 2015): phosphorylation, acetylation, succinylation, malonylation, nitrosylation, sumoylation, ubiquitination, N-glycosylation, and O-GlcNAcylation. Acetylation of the co-chaperonin HSP10 has been indicated to affect activity of the chaperonin complex (Lu et al., 2014). One of the HSP60 missense variations shown in **Table 1**, Lysine-156, has been described before as modified by acetylation both in the human acute myeloid leukemia cell line MV4-11 (Choudhary et al., 2009) and in mouse liver HSP60 (Rardin et al., 2013). The p.Lys156Arg missense variation is classified as benign by the bioinformatics tools due to conservation of the positive charge, but elimination of this acetylation site may affect regulation of HSP60 function. Regulation of the activity of the HSP60/HSP10 complex at different levels may thus be a crucial hub for development of mitochondrial dysfunction, a hallmark in many disease processes.

AUTHOR CONTRIBUTIONS

PF and PB have both contributed to writing the draft and producing the final version.

ACKNOWLEDGMENTS

The research of PB has been supported by the Ludvig and Sara Elsass Foundation. The authors would like to thank the Exome Aggregation Consortium and the groups that provided exome variant data for comparison. A full list of contributing groups can be found at http://exac.broadinstitute.org/about.

REFERENCES

Adzhubei, I. A., Schmidt, S., Peshkin, L., Ramensky, V. E., Gerasimova, A., Bork, P., et al. (2010). A method and server for predicting damaging missense mutations. *Nat. Methods* 7, 248–249. doi: 10.1038/nmeth0410-248

Bie, A. S., Palmfeldt, J., Hansen, J., Christensen, R., Gregersen, N., Corydon, T. J., et al. (2011). A cell model to study different degrees of Hsp60 deficiency in HEK293 cells. *Cell Stress Chaperones* 16, 633–640. doi: 10.1007/s12192-011-0275-5

Bross, P. (2015). *The Hsp60 Chaperonin*. Cham: Springer International Publishing.

Bross, P., Li, Z., Hansen, J., Hansen, J. J., Nielsen, M. N., Corydon, T. J., et al. (2007). Single-nucleotide variations in the genes encoding the mitochondrial Hsp60/Hsp10 chaperone system and their disease-causing potential. *J. Hum. Genet.* 52, 56–65. doi: 10.1007/s10038-006-0080-7

Bross, P., Naundrup, S., Hansen, J., Nielsen, M. N., Christensen, J. H., Kruhoffer, M., et al. (2008). The HSP60-(P.val98ile) mutation associated with hereditary spastic paraplegia SPG13 compromises chaperonin function both *in vitro* and *in vivo*. *J. Biol. Chem.* 283, 15694–15700. doi: 10.1074/jbc.M800548200

Cappello, F., Marino Gammazza, A., Palumbo Piccionello, A., Campanella, C., Pace, A., Conway de Macario, E., et al. (2014). Hsp60 chaperonopathies and chaperonotherapy: targets and agents. *Expert Opin. Ther. Targets* 18, 185–208. doi: 10.1517/14728222.2014.856417

Cheng, M. Y., Hartl, F. U., Martin, J., Pollock, R. A., Kalousek, F., Neupert, W., et al. (1989). Mitochondrial heat-shock protein hsp60 is essential for assembly of proteins imported into yeast mitochondria. *Nature* 337, 620–625.

Choudhary, C., Kumar, C., Gnad, F., Nielsen, M. L., Rehman, M., Walther, T. C., et al. (2009). Lysine acetylation targets protein complexes and co-regulates major cellular functions. *Science* 325, 834–840. doi: 10.1126/science.1175371

Christensen, J. H., Nielsen, M. N., Hansen, J., Füchtbauer, A., Füchtbauer, E. M., West, M., et al. (2010). Inactivation of the hereditary spastic paraplegia-associated Hspd1 gene encoding the Hsp60 chaperone results in early embryonic lethality in mice. *Cell Stress Chaperones* 15, 851–863. doi: 10.1007/s12192-010-0194-x

Consortium, T. U. (2015). UniProt: a hub for protein information. *Nucleic Acids Res.* 43, D204–D212. doi: 10.1093/nar/gku989

Corydon, T. J., Hansen, J., Bross, P., and Jensen, T. G. (2005). Down-regulation of Hsp60 expression by RNAi impairs folding of medium-chain acyl-CoA dehydogenase wild-type and disease-associated proteins. *Mol. Genet. Metab.* 85, 260–270. doi: 10.1016/j.ymgme.2005.04.003

Di Fabio, R., Storti, E., Tessa, A., Pierelli, F., Morani, F., and Santorelli, F. M. (2016). Hereditary spastic paraplegia: pathology, genetics and therapeutic prospects. *Expert Opin. Orphan Drugs* 4, 429–442. doi: 10.1517/21678707.2016.1153964

Fayet, O., Ziegelhoffer, T., and Georgopoulos, C. (1989). The groES and groEL heat shock gene products of *Escherichia coli* are essential for bacterial growth at all temperatures. *J. Bacteriol.* 171, 1379–1385.

Fontaine, B., Davoine, C. S., Dürr, A., Paternotte, C., Feki, I., Weissenbach, J., et al. (2000). A new locus for autosomal dominant pure spastic paraplegia, on chromosome 2q24-q34. *Am. J. Hum. Genet.* 66, 702–707. doi: 10.1086/302776

Hansen, J. J., Bross, P., Westergaard, M., Nielsen, M. N., Eiberg, H., Børglum, A. D., et al. (2003). Genomic structure of the human mitochondrial chaperonin genes: *HSP60* and *HSP10* are localised head to head on chromosome 2 separated by a bidirectional promoter. *Hum. Genet.* 112, 71–77. doi: 10.1007/s00439-002-0837-9

Hansen, J. J., Dürr, A., Cournu-Rebeix, I., Georgopoulos, C., Ang, D., Nielsen, M. N., et al. (2002). Hereditary spastic paraplegia SPG13 is associated with a mutation in the gene encoding the mitochondrial chaperonin Hsp60. *Am. J. Hum. Genet.* 70, 1328–1332. doi: 10.1086/339935

Hansen, J., Svenstrup, K., Ang, D., Nielsen, M. N., Christensen, J. H., Gregersen, N., et al. (2007). A novel mutation in the HSPD1 gene in a patient with hereditary spastic paraplegia. *J. Neurol.* 254, 897–900. doi: 10.1007/s00415-006-0470-y

Hayer-Hartl, M., Bracher, A., and Hartl, F. U. (2015). The GroEL-GroES chaperonin machine: a nano-cage for protein folding. *Trends Biochem. Sci.* 441, 62–76. doi: 10.1016/j.tibs.2015.07.009

Horibe, T., and Hoogenraad, N. J. (2007). The chop gene contains an element for the positive regulation of the mitochondrial unfolded protein response. *PLoS ONE* 2:e835. doi: 10.1371/journal.pone.0000835

Horwich, A. L. (2013). Chaperonin-mediated protein folding. *J. Biol. Chem.* 288, 23622–23632. doi: 10.1074/jbc.X113.497321

Kerner, M. J., Naylor, D. J., Ishihama, Y., Maier, T., Chang, H. C., Stines, A. P., et al. (2005). Proteome-wide analysis of chaperonin-dependent protein folding in *Escherichia coli*. *Cell* 122, 209–220. doi: 10.1016/j.cell.2005.05.028

Kim, S. W., Kim, J. B., Kim, J. H., and Lee, J. K. (2007). Interferon-gamma-induced expressions of heat shock protein 60 and heat shock protein 10 in C6 astroglioma cells: identification of the signal transducers and activators of transcription 3-binding site in bidirectional promoter. *Neuroreport* 18, 385–389. doi: 10.1097/WNR.0b013e32801299cc

Kim, S. W., and Lee, J. K. (2007). NO-induced downregulation of HSP10 and HSP60 expression in the postischemic brain. *J. Neurosci. Res.* 85, 1252–1259. doi: 10.1002/jnr.21236

Kleinridders, A., Lauritzen, H. P., Ussar, S., Christensen, J. H., Mori, M. A., Bross, P., et al. (2013). Leptin regulation of Hsp60 impacts hypothalamic insulin signaling. *J. Clin. Invest.* 123, 4667–4680. doi: 10.1172/JCI67615

Kumar, K. R., Blair, N. F., and Sue, C. M. (2015). An update on the hereditary spastic paraplegias: new genes and new disease models. *Mov. Disord. Clin. Pract.* 2, 213–223. doi: 10.1002/mdc3.12184

Levy-Rimler, G., Bell, R. E., Ben-Tal, N., and Azem, A. (2002). Type I chaperonins: not all are created equal. *FEBS Lett.* 529, 1. doi: 10.1016/S0014-5793(02)03178-2

Levy-Rimler, G., Viitanen, P., Weiss, C., Sharkia, R., Greenberg, A., Niv, A., et al. (2001). The effect of nucleotides and mitochondrial chaperonin 10 on the structure and chaperone activity of mitochondrial chaperonin 60. *Eur. J. Biochem.* 268, 3465–3472. doi: 10.1046/j.1432-1327.2001.02243.x

Lu, Z., Chen, Y., Aponte, A. M., Battaglia, V., Gucek, M., and Sack, M. N. (2014). Prolonged fasting identifies heat shock protein 10 as a sirtuin 3 substrate: elucidating a new mechanism linking mitochondrial protein acetylation to fatty acid oxidation enzyme folding and function. *J. Biol. Chem.* 290, 2466–2476. doi: 10.1074/jbc.M114.606228

Magen, D., Georgopoulos, C., Bross, P., Ang, D., Segev, Y., Goldsher, D., et al. (2008). Mitochondrial hsp60 chaperonopathy causes an autosomal-recessive neurodegenerative disorder linked to brain hypomyelination and leukodystrophy. *Am. J. Hum. Genet.* 83, 30–42. doi: 10.1016/j.ajhg.2008.05.016

Magnoni, R., Palmfeldt, J., Christensen, J. H., Sand, M., Maltecca, F., Corydon, T. J., et al. (2013). Late onset motoneuron disorder caused by mitochondrial Hsp60 chaperone deficiency in mice. *Neurobiol. Dis.* 54, 12–23. doi: 10.1016/j.nbd.2013.02.012

Magnoni, R., Palmfeldt, J., Hansen, J., Christensen, J. H., Corydon, T. J., and Bross, P. (2014). The Hsp60 folding machinery is crucial for manganese superoxide dismutase folding and function. *Free Radic. Res.* 48, 168–179. doi: 10.3109/10715762.2013.858147

Miyamoto, Y., Eguchi, T., Kawahara, K., Hasegawa, N., Nakamura, K., Funakoshi-Tago, M., et al. (2015). Hypomyelinating leukodystrophy-associated missense mutation in HSPD1 blunts mitochondrial dynamics. *Biochem. Biophys. Res. Commun.* 462, 275–281. doi: 10.1016/j.bbrc.2015.04.132

Miyamoto, Y., Megumi, F.-T., Hasegawa, N., Eguchi, T., Tanoue, A., Tamura, H., et al. (2016). Data supporting mitochondrial morphological changes by SPG13-associated HSPD1 mutants. *Data Brief* 6, 482–488. doi: 10.1016/j.dib.2015.12.038

Nielsen, K. L., and Cowan, N. J. (1998). A single ring is sufficient for productive chaperonin-mediated folding *in vivo*. *Mol. Cell* 2, 93–99. doi: 10.1016/S1097-2765(00)80117-3

Nisemblat, S., Yaniv, O., Parnas, A., Frolow, F., and Azem, A. (2015). Crystal structure of the human mitochondrial chaperonin symmetrical football complex. *Proc. Natl. Acad. Sci. U.S.A.* 112, 6044–6049. doi: 10.1073/pnas.1411718112

Parnas, A., Nadler, M., Nisemblat, S., Horovitz, A., Mandel, H., and Azem, A. (2009). The MitCHAP-60 disease is due to entropic destabilization of the human mitochondrial Hsp60 oligomer. *J. Biol. Chem.* 284, 28198–28203. doi: 10.1074/jbc.M109.031997

Perezgasga, L., Segovia, L., and Zurita, M. (1999). Molecular characterization of the 5′ control region and of two lethal alleles affecting the hsp60 gene in *Drosophila* melanogaster. *FEBS Lett.* 456, 269–273. doi: 10.1016/S0014-5793(99)00963-1

Rardin, M. J., Newman, J. C., Held, J. M., Cusack, M. P., Sorensen, D. J., Li, B., et al. (2013). Label-free quantitative proteomics of the lysine acetylome in mitochondria identifies substrates of SIRT3 in metabolic pathways. *Proc. Natl. Acad. Sci. U.S.A.* 110, 6601–6606. doi: 10.1073/pnas.1302961110

Richardson, A., Schwager, F., Landry, S. J., and Georgopoulos, C. (2001). The importance of a mobile loop in regulating chaperonin/ co-chaperonin interaction: humans versus *Escherichia coli*. *J. Biol. Chem.* 276, 4981–4987. doi: 10.1074/jbc.M008628200

Saijo, T., Welch, W. J., and Tanaka, K. (1994). Intramitochondrial folding and assembly of medium-chain acyl-CoA dehydrogenase (MCAD) - Demonstration of impaired transfer of K304E-variant MCAD from its complex with Hsp60 to the native tetramer. *J. Biol. Chem.* 269, 4401–4408.

Shan, Z. X., Lin, Q. X., Deng, C. Y., Zhu, J. N., Mai, L. P., Liu, J. L., et al. (2010). miR-1/miR-206 regulate Hsp60 expression contributing to glucose-mediated apoptosis in cardiomyocytes. *FEBS Lett.* 584, 3592–3600. doi: 10.1016/j.febslet.2010.07.027

Svenstrup, K., Bross, P., Koefoed, P., Hjermind, L. E., Eiberg, H., Born, A. P., et al. (2009). Sequence variants in SPAST, SPG3A and HSPD1 in hereditary spastic paraplegia. *J. Neurol. Sci.* 284, 90–95. doi: 10.1016/j.jns.2009.04.024

Tesson, C., Koht, J., and Stevanin, G. (2015). Delving into the complexity of hereditary spastic paraplegias: how unexpected phenotypes and inheritance modes are revolutionizing their nosology. *Hum. Genet.* 134, 511–538. doi: 10.1007/s00439-015-1536-7

Yokota, I., Saijo, T., Vockley, J., and Tanaka, K. (1992). Impaired tetramer assembly of variant medium-chain acyl-coenzyme A dehydrogenase with a glutamate or aspartate substitution for lysine 304 causing instability of the protein. *J. Biol. Chem.* 267, 26004–26010.

Zhao, Q., Wang, J., Levichkin, I. V., Stasinopoulos, S., Ryan, M. T., and Hoogenraad, N. J. (2002). A mitochondrial specific stress response in mammalian cells. *EMBO J.* 21, 4411–4419. doi: 10.1093/emboj/cdf445

Conflict of Interest Statement: The authors declare that the research was conducted in the absence of any commercial or financial relationships that could be construed as a potential conflict of interest.

frontiers in Molecular Biosciences

ORIGINAL RESEARCH
published: 09 August 2016
doi: 10.3389/fmolb.2016.00040

Screening of Drugs Inhibiting *In vitro* Oligomerization of Cu/Zn-Superoxide Dismutase with a Mutation Causing Amyotrophic Lateral Sclerosis

*Itsuki Anzai[1], Keisuke Toichi[1], Eiichi Tokuda[1], Atsushi Mukaiyama[2,3], Shuji Akiyama[2,3] and Yoshiaki Furukawa[1]**

[1] Laboratory for Mechanistic Chemistry of Biomolecules, Department of Chemistry, Keio University, Yokohama, Japan, [2] Research Center of Integrative Molecular Systems, Institute for Molecular Science, Okazaki, Japan, [3] Department of Functional Molecular Science, SOKENDAI (The Graduate University for Advanced Studies), Okazaki, Japan

OPEN ACCESS

Edited by:
Alberto J. L. Macario, University of Maryland at Baltimore, USA; Institute of Marine and Environmental Technology, USA; Istituto Euro-Mediterraneo di Scienza e Tecnologia, Italy

Reviewed by:
Leonid Breydo, University of South Florida, USA
Antonio Trovato, University of Padua, Italy

***Correspondence:**
Yoshiaki Furukawa
furukawa@chem.keio.ac.jp

Specialty section:
This article was submitted to Protein Folding, Misfolding and Degradation, a section of the journal Frontiers in Molecular Biosciences

Received: 21 June 2016
Accepted: 27 July 2016
Published: 09 August 2016

Citation:
Anzai I, Toichi K, Tokuda E, Mukaiyama A, Akiyama S and Furukawa Y (2016) Screening of Drugs Inhibiting In vitro Oligomerization of Cu/Zn-Superoxide Dismutase with a Mutation Causing Amyotrophic Lateral Sclerosis. Front. Mol. Biosci. 3:40. doi: 10.3389/fmolb.2016.00040

Dominant mutations in Cu/Zn-superoxide dismutase (*SOD1*) gene have been shown to cause a familial form of amyotrophic lateral sclerosis (*SOD1*-ALS). A major pathological hallmark of this disease is abnormal accumulation of mutant SOD1 oligomers in the affected spinal motor neurons. While no effective therapeutics for *SOD1*-ALS is currently available, SOD1 oligomerization will be a good target for developing cures of this disease. Recently, we have reproduced the formation of SOD1 oligomers abnormally cross-linked *via* disulfide bonds in a test tube. Using our *in vitro* model of SOD1 oligomerization, therefore, we screened 640 FDA-approved drugs for inhibiting the oligomerization of SOD1 proteins, and three effective classes of chemical compounds were identified. Those hit compounds will provide valuable information on the chemical structures for developing a novel drug candidate suppressing the abnormal oligomerization of mutant SOD1 and possibly curing the disease.

Keywords: Cu/Zn-superoxide dismutase, amyotrophic lateral sclerosis, protein misfolding, protein aggregation, drug screening

INTRODUCTION

Amyotrophic lateral sclerosis (ALS) is a fatal neurodegenerative disease characterized by the progressive loss of motor neurons, leading to muscle atrophy and total paralysis. While increasing numbers of causative genes for a familial form of ALS have been identified, ~90% of the ALS cases are sporadic, and the pathomechanism still remains largely unknown (Andersen and Al-Chalabi, 2011; Renton et al., 2014). Also, no clinically approved drug is available for ALS except Riluzole, which can extend the median survival by only a few months (Genc and Ozdinler, 2014); therefore, a great need for new ALS therapeutics is obvious. Despite this, it remains obscure what triggers sporadic ALS, hampering the identification of molecular target(s) for the development of drugs to ameliorate and eventually prevent this devastating disease.

As mentioned, several genes responsible for a familial form of ALS cases have been identified (Abel et al., 2012), among which mutations in Cu/Zn-superoxide dismutase (*SOD1*) gene are the most common cause (about 20%) of familial ALS cases (*SOD1*-ALS; Rosen et al., 1993). A pathological hallmark observed in *SOD1*-ALS cases is abnormal accumulation of mutant SOD1 proteins in the affected motor neurons as inclusions (Bruijn et al., 1998). Furthermore, *in vivo*

as well as *in vitro* experiments have shown that pathogenic mutations trigger the misfolding of SOD1 proteins and then lead to the formation of insoluble SOD1 oligomers/aggregates (reviewed in Furukawa, 2012). Misfolding of SOD1 proteins is thus one of the promising targets to develop therapeutics of *SOD1*-ALS cases.

SOD1 is an antioxidant enzyme detoxifying superoxide radicals and becomes enzymatically active by binding copper and zinc ions and forming a highly conserved intramolecular disulfide bond (McCord and Fridovich, 1969; Furukawa et al., 2004). Given that these post-translational processes are known to stabilize the native conformation of SOD1 proteins, pathogenic mutations are considered to decrease the conformational stability of SOD1 by compromising binding of the metal ions and/or formation of the disulfide bond (Furukawa and O'Halloran, 2005; Rodriguez et al., 2005). Regardless of the presence or absence of metal binding and/or disulfide formation, furthermore, most of pathogenic mutations are shown to decrease structural stability of SOD1 proteins (Furukawa and O'Halloran, 2005; Rodriguez et al., 2005); therefore, the decrease in the structural stability of SOD1 is considered to trigger the misfolding into a toxic conformer(s). It is thus well expected that misfolding of SOD1 into oligomers and aggregates can be suppressed by stabilizing the native conformation of SOD1.

A native form of SOD1 is a homodimer, and the mutation-induced monomerization of SOD1 has been suggested to trigger the aggregation (Rakhit et al., 2004). Actually, introduction of a disulfide bond between the SOD1 subunits by either genetic engineering (Ray et al., 2004) or chemical cross-linkers (Auclair et al., 2010) has been shown to forcedly stabilize the SOD1 dimeric structure. The coordination of a metallo-complex, cisplatin, at the dimer interface was also shown to be effective to suppressing the SOD1 oligomerization in the cultured cells as well as in a test tube (Banci et al., 2012). To more reversibly stabilize the natively dimeric SOD1 conformation, small drugs that can bind at the dimer interface were identified by extensive *in silico* screening of ∼1.5 million compounds (Ray et al., 2005; Nowak et al., 2010). These drugs were found to protect A4V-mutant SOD1 from chemical unfolding induced by guanidine hydrochloride (Gdn) and also significantly slow the aggregation (Ray et al., 2005; Nowak et al., 2010). The binding site of those drugs in SOD1, however, needs to be experimentally confirmed in more detail; actually, some of the drugs were shown to bind at the alternative site other than the dimer interface (Antonyuk et al., 2010; Wright et al., 2013). Further studies will also be required to confirm the reproducibility on the stabilizing effects of those drugs on SOD1 (Wright et al., 2013), and *in vivo* efficacy of those dimer-stabilizing drugs remains to be tested. To identify drugs that can reduce the intracellular aggregation of mutant SOD1, moreover, high throughput screening of ∼50,000 small molecules has been performed in the cultured cells expressing mutant SOD1 fused with a fluorescent protein, GFP (Benmohamed et al., 2011). Aggregation properties of SOD1 proteins have, however, been reported to be affected by the fusion with a GFP tag (Stevens et al., 2010). While efforts have been made to stabilize mutant SOD1 in a drug-based approach, no drugs are promising for animal and clinical trials, and we hence still need to explore and test more numbers of potent inhibitors for aggregation/oligomerization of mutant SOD1 proteins.

Here, we have performed screening of FDA-approved drugs in our experimental setup reproducing SOD1 oligomerization *in vitro* and identified drugs that can suppress the formation of insoluble SOD1 oligomers. Previously, we have shown that pathogenic SOD1 proteins form SDS-resistant oligomers crosslinked *via* disulfide bonds in the spinal cords of symptomatic ALS-model mice expressing mutant SOD1 (Furukawa et al., 2006). We also recently reported that formation of disulfide-crosslinked oligomers was reproduced in a test tube by incubation of metal-deficient (apo) SOD1 with the disulfide bond (apo-SOD1$^{S\text{-}S}$) in the presence of a denaturant (Toichi et al., 2013). The hit compounds in a library of FDA-approved drugs efficiently suppressed the formation of insoluble SOD1 oligomers crosslinked *via* disulfide bonds. The structural/chemical information on those compounds will hence be useful to design a pharmaceutical drug for *SOD1*-ALS with aggregation-inhibiting properties.

MATERIALS AND METHODS

Preparation of Proteins

Expression and purification of SOD1 with G37R mutation were performed as described previously (Furukawa et al., 2016). Briefly, SOD1(G37R) was expressed in *E. coli* SHuffle^{TM} (New England BioLabs) as a fusion protein with an N-terminal 6x His tag and was purified with Ni^{2+}-affinity chromatography using HisTrap HP column (1 mL, GE Healthcare). The purified proteins were dialyzed against 50 mM sodium acetate, 100 mM NaCl, and 10 mM EDTA at pH 4.0, which removed metal ions bound to the His-tagged SOD1(G37R). After proteolytic cleavage of the His tag with thrombin, the demetallated and untagged SOD1(G37R) was further purified with gel-filtration chromatography using Cosmosil 5Diol-300-II column (nacalai tesque). Presence of the intramolecular disulfide bond in SOD1 was confirmed based upon its distinct electrophoretic mobility in non-reducing SDS-PAGE (Toichi et al., 2013). HTT^{EX1}(42Q) were prepared as described previously (Mitomi et al., 2012). Concentrations of SOD1 and HTT^{EX1}(42Q) proteins were spectroscopically determined from the absorbance at 280 nm in the presence of 6 M guanidine hydrochloride (Gdn) by using 5625 and 42,860 $cm^{-1}M^{-1}$ as an extinction coefficient, respectively.

Screening of Drugs Inhibiting the SOD1 Oligomerization

To examine effects of drugs on the abnormal oligomerization of SOD1 *in vitro*, apo-SOD1(G37R)$^{S\text{-}S}$ (20 μM, 150 μL) in a buffer at pH 7.4 containing 100 mM Na-Pi, 100 mM NaCl and 5 mM EDTA (NNE buffer) with 1 M Gdn was first prepared in each well of a 96-well-plate. Then, 1.5 μL of a 2.0 g/L stock solution of drugs in DMSO was added to the protein sample solution in a well of the plate (the final concentration of drugs tested was 20 μg/mL). In this study, we have examined 640 drugs in the FDA approved drug library (#BML-2841J-0100, Japanese version, Enzo Life Science). The oligomerization reaction was started by

shaking the samples with a POM ball (3/32 inch, SANPLATEC) in a plate shaker (MBR-022UP, TAITEC) at 1200 rpm, 37°C and monitored by the increase of solution turbidity (absorbance increase at 350 nm). After 12 h of agitation, the samples were collected and ultracentrifuged at 110,000 $\times g$ for 15 min. to obtain soluble supernatant and insoluble pellet separately. After removing Gdn in the soluble supernatant with PAGE Clean Up Kit (nacalai tesque), the proteins in both fractions were analyzed by non-reducing SDS-PAGE.

Electrophoresis

To protect free thiols from aberrant oxidation during electrophoresis, proteins were reacted with a thiol-specific modifier, iodoacetamide (IA); the samples were first dissolved in a buffer at pH 8.0 containing 100 mM Na-Pi, 2% SDS, and 100 mM IA and then incubated at 37°C for an hour. Followed by the addition of an SDS-PAGE sample buffer without any reductants, the protein samples were boiled at 100°C for 5 min. and then loaded on a 12.5% resolving polyacrylamide gel with a 5% stacking gel. After electrophoresis, the protein bands on a gel were visualized by Coomassie Brilliant Blue.

Differential Scanning Calorimetry

Effects of drugs on the thermal stability of SOD1 were examined by differential scanning calorimetry (DSC) using MicroCal VP-DSC (GE Healthcare). Apo-SOD1(G37R)$^{S\text{-}S}$ (0.3 g/L; *ca.* 20 μM) in the NNE buffer with or without a drug (20 μg/mL) was first degassed using ThermoVac (GE Healthcare) at 20°C for 5 min., and then the thermograms were obtained by increasing temperature from 15° to 75°C at a scan rate of 1.0°C/min. Baselines were collected by using the NNE buffer containing corresponding drugs and DMSO. The thermograms of protein samples were corrected with the baselines and then normalized by protein concentrations.

MALDI-TOF Mass Spectrometry

To map the disulfide bond in SOD1, the limited proteolysis followed by the peptide mapping was performed. As described, apo-SOD1(G37R)$^{S\text{-}S}$ was agitated in the presence of 1 M Gdn for 2 h at 37°C, and a soluble fraction of the sample was collected by ultracentrifugation at 110,000 $\times g$ for 15 min. Proteins in the soluble fraction were first precipitated using PAGE Clean Up Kit and then redissolved in the NNE buffer containing 100 mM IA and 6 M Gdn. After incubation at 37°C for an hour, by which free thiolate groups were alkylated and thus protected, the buffer was exchanged to 100 mM Na-Pi at pH 8.0 by using a Zeba™ Spin Desalting Column (Thermo). SOD1 proteins (48 μg) collected by the spin column were treated with 0.24 μg of porcine pancreas trypsin in a sequencing grade (Wako) and incubated at 37°C for 16 h. After addition of 0.1% trifluoroacetic acid and 6 M Gdn, the trypsinized samples were desalted with ZipTip C18 (Millipore) and then spotted on a MALDI target plate with human ACTH (18–39) (*m*/*z*, 2466.6; Wako) and bovine pancreas insulin (*m*/*z*, 5734.5; nacalai tesque) as internal standards and with α-cyano-4-hydroxycinnamic acid (Wako) as a matrix. Spectra were obtained using Ultraflex™ (Bruker Daltonics) in linear mode, and mass peaks were assigned using MS Bridge (University of California, San Francisco, CA).

RESULTS AND DISCUSSION

Oligomerization of Mutant SOD1 in the Destabilizing Conditions

It has been reported that agitation of apo-SOD1$^{S\text{-}S}$ forms insoluble aggregates in the presence of 1 M Gdn (Chattopadhyay et al., 2008; Toichi et al., 2013). As shown in **Figure 1A**, we confirmed the increase of solution turbidity by agitation of 20 μM apo-SOD1$^{S\text{-}S}$ with a pathogenic mutation, G37R [apo-SOD1(G37R)$^{S\text{-}S}$], at 37°C, indicating the formation of insoluble aggregates. In contrast, the agitation of apo-SOD1(G37R)$^{S\text{-}S}$ in the absence of Gdn did not result in the formation of insoluble aggregates (**Figure 1A**). To further confirm the insolubilization of apo-SOD1(G37R)$^{S\text{-}S}$ by its agitation in the presence of 1 M Gdn at 37°C, the samples were fractionated into soluble supernatant and insoluble pellets by ultracentrifugation and analyzed by non-reducing SDS-PAGE (**Figure 1B**). Increase in the solution turbidity was confirmed to associate with the formation of insoluble SOD1 oligomers that were sensitive to the reducing reagent, dithiothreitol (DTT; **Figure 1C**). Namely, in the current reaction conditions, apo-SOD1(G37R)$^{S\text{-}S}$ was converted to the insoluble SOD1 oligomers crosslinked *via* disulfide bonds (S-S oligomers).

We also noted that, before the formation of S-S oligomers, the electrophoretic mobility of SOD1 under the denatured condition (i.e., in SDS-PAGE) became slightly retarded and blurred (compare the bands in the soluble fractions at 240 vs. 0 min. in **Figure 1B**). Treatment of the samples with DTT again collapsed those distinct SOD1 bands into a single band corresponding to the disulfide-reduced SOD1 (SOD1^{SH}; **Figure 1C**). Consistent with our previous findings (Toichi et al., 2013), these results indicate that the disulfide shuffling occurs first within a SOD1 molecule and then between the molecules to form the insoluble S-S oligomers. Given that accumulation of the insoluble S-S oligomers is known as a pathological hallmark observed in the spinal cords of the affected mice expressing mutant human SOD1 proteins (Deng et al., 2006; Furukawa et al., 2006), we attempted to seek small molecules that can inhibit the formation of insoluble S-S oligomers.

Screening of Drugs for the Activity to Suppress the Oligomerization of Mutant SOD1

To facilitate the transfer of possible drug candidates to the clinical trials, we chose a library of 640 drugs, which have been already approved by the U.S. Food and Drug Administration (FDA). Twenty micrometer of apo-SOD1(G37R)$^{S\text{-}S}$ in the NNE buffer containing 1 M Gdn were mixed with a drug in the final concentration of 20 μg/mL and shaken at 1200 rpm, 37°C. While, in the absence of any drugs, the solution turbidity (absorbance at 350 nm) of apo-SOD1(G37R)$^{S\text{-}S}$ was around 0.2 at 500 min after agitation (**Figure 1A**), drugs showing the turbidity of $<$0.02 at 500 min after agitation were chosen in this

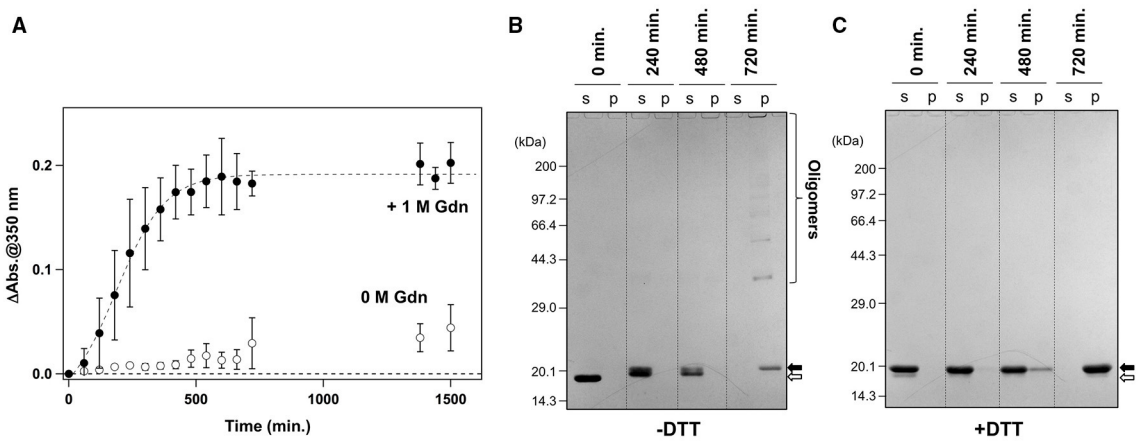

FIGURE 1 | Formation of insoluble apo-SOD1(G37R)$^{S-S}$ oligomers by structural destabilization. (A) Formation kinetics of insoluble aggregates from 20 μM apo-SOD1(G37R)$^{S-S}$ was monitored by the increase of solution turbidity (absorbance at 350 nm) in the absence (open circles) and presence (filled circles) of 1 M Gdn. Experiments were repeated more than three times to estimate error bars (standard deviation). **(B,C)** During the aggregation of apo-SOD1(G37R)$^{S-S}$ shown in **(A)**, aliquots were taken from the sample solution at the indicated time, fractionated into soluble supernatant (s), and insoluble pellet (p) by ultracentrifugation and then analyzed by **(B)** non-reducing SDS-PAGE and **(C)** reducing SDS-PAGE after treatment of the samples with DTT. The bands corresponding to SOD1 proteins with and without the canonical disulfide bond are indicated by open and filled arrows, respectively.

study as "hit" compounds probably suppressing the formation of insoluble SOD1 aggregates. In the library of FDA-approved drugs, six compounds were found to almost completely suppress the increase of solution turbidities: simvastatin (**Figure 2A**), lovastatin (**Figure 2B**), mevastatin (**Figure 2C**), miltefosine (**Figure 2E**), alfacalcidol (**Figure 3A**), calcidiol (**Figure 3B**), and calcitriol (**Figure 3C**). Inhibitory effects of these drugs on the formation of insoluble aggregates were also confirmed in the final concentration of 10 μg/mL (data not shown). Based upon the chemical structure, those hit compounds can be categorized into three groups as follows.

The first group contains simvastatin, lovastatin, and mevastatin, all of which are cholesterol-lowering agents by inhibiting the rate-limiting enzyme, HMG-CoA reductase, in cholesterol biosynthesis with quite similar chemical structures composed of hexahydronaphthalene, heptanoic acid lactone, and butanoate groups (**Figures 2A–C**). In the absence of any drugs, apo-SOD1(G37R)$^{S-S}$ formed insoluble S-S oligomers with no SOD1 proteins in the soluble fraction (**Figure 4**, no drugs), resulting in the increase of solution turbidity. By addition of those three statins, all SOD1 proteins remained soluble (**Figure 4**), corroborating the suppression of turbidity increase. Notably, the library of FDA-approved drugs tested in this study contains another statin with the similar structure, pravastatin lactone, which was, however, found to have no effects on the turbidity increase of the apo-SOD1(G37R)$^{S-S}$ sample (**Figure 2D**) and show reduced ability to suppress the formation of insoluble S-S oligomers (**Figure 4**). Other statins in the library (nystatin, cilastatin, cerivastatin, and fluvastatin), which have quite distinct chemical structures from e.g., simvastatin, were also tested but exhibited no effects on the SOD1 aggregation *in vitro* (data not shown). Further investigation will be required to describe *in vitro* efficacy of those statins as an inhibitor for SOD1 aggregation, but lovastatin and pravastatin lactone differ in only one structural respect: a substituent in the hexahydronaphthalene group is a methyl group in lovastatin but a hydroxyl group in pravastatin lactone (**Figures 2B,D**). Hydrophobicity in the hexahydronaphthalene group would hence be necessary for inhibition of the SOD1 oligomerization (*vide infra*).

The second group includes alfacalcidol, calcidiol, and calcitriol (**Figures 3A–C**), all of which are derivatives of vitamin D. Actually, calciferol (vitamin D_2) and cholecalciferol (vitamin D_3) were not included in the FDA-approved drug library used in this study but effectively suppressed the increase of the solution turbidity in the apo-SOD1(G37R)$^{S-S}$ sample (**Figures 3E,F**). The drug library in this study has another vitamin D derivative, calcipotriol, which was, however, ineffective to the suppression of the solution turbidity increase in the apo-SOD1(G37R)$^{S-S}$ sample (**Figure 3D**). Furthermore, SOD1 proteins were confirmed to remain soluble without any insoluble SOD1 aggregates/oligomers by adding either one of vitamin D derivatives examined here except calcipotriol (**Figure 4**). While no obvious correlation was confirmed between the chemical structures and the efficacy to suppress the formation of insoluble SOD1 oligomers, it is interesting to note that the water solubility of calcipotriol is presumably higher than those of the other vitamin D derivatives. More precisely, as summarized in **Table 1**, the water solubility of the vitamin D derivatives that are effective to the inhibition of SOD1 aggregation ranges from 0.00038 g/L (1.0 μM, cholecalciferol) to 0.0067 g/L (16 μM, calcitriol); in contrast, calcipotriol is expected to have 0.014 g/L (33 μM) of the water solubility. Actually, the water solubility of pravastatin lactone (0.024 g/L, 59 μM), which was unable to suppress the turbidity increase (**Figure 2D**), is comparable to that of calcipotriol and is

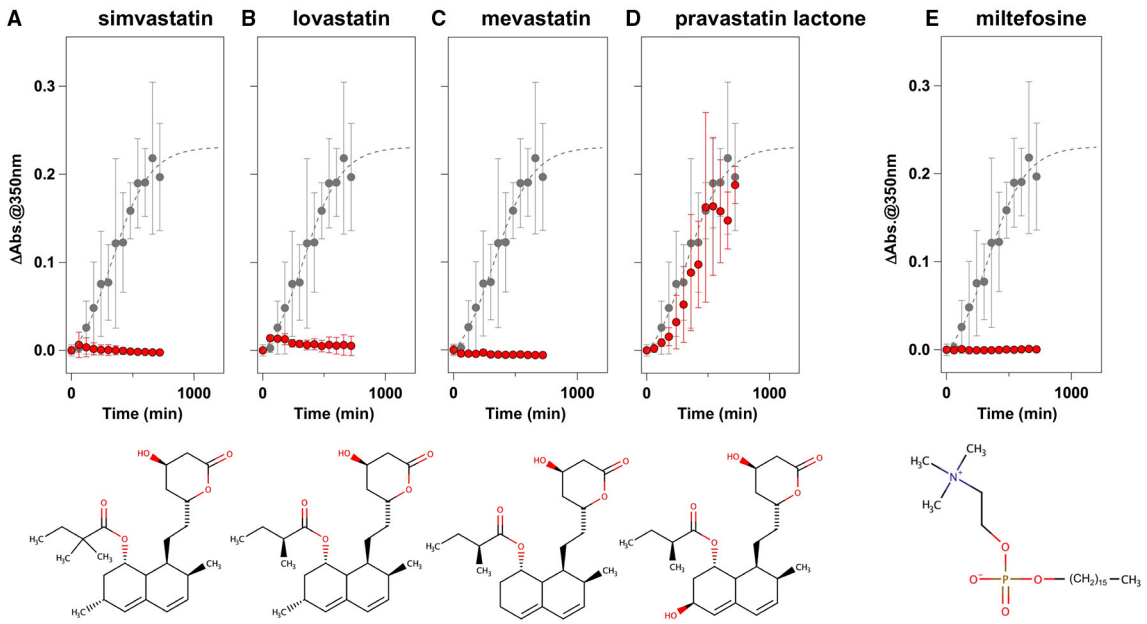

FIGURE 2 | Statins and miltefosine as potent inhibitors for the formation of insoluble apo-SOD1(G37R)$^{S\text{-}S}$ aggregates. (A–E) The turbidity increase of 20 μM apo-SOD1(G37R)$^{S\text{-}S}$ in the presence of 1 M Gdn is shown in the presence of the following compounds (red filled circles): **(A)** simvastatin, **(B)** lovastatin, **(C)** mevastatin, **(D)** pravastatin lactone, and **(E)** miltefosine. In each panel, the aggregation kinetics without any drugs was shown as gray filled circles. The kinetics was monitored by changes in the solution turbidity (the absorbance at 350 nm), and the final concentration of drugs added was 20 μg/mL. Experiments were repeated more than three times to estimate error bars (standard deviation). Structures of the chemical compounds were also shown below the panels.

significantly higher than those of the other statins that can inhibit the SOD1 aggregation (0.00077–0.0048 g/L; **Table 1**). Collectively, therefore, the hydrophobicity of the drugs would be an important factor to modulate the efficacy for inhibiting the oligomerization of SOD1. We further speculate that apo-SOD1(G37R)$^{S\text{-}S}$ exposes its hydrophobic interior upon structural destabilization and thereby forms abnormal oligomers. The drugs with significant hydrophobicity might hence inhibit such abnormal oligomerization by interacting with the hydrophobic interior of SOD1.

Miltefosine, a phospholipid antimicrobial drug, belongs to the last group of our hit compounds (**Figure 2E**). In the presence of miltefosine, the turbidity increase of apo-SOD1(G37R)$^{S\text{-}S}$ was almost completely suppressed (**Figure 2E**), and no insoluble SOD1 oligomers were detected (**Figure 4**). The water solubility of miltefosine has been calculated as a very limited value (0.00022 g/L, 0.5 μM, **Table 1**). Actually, however, miltefosine (Cayman Chemical No. 63280) was soluble in water (2.5 g/L) probably by forming micelles because of its hydrophobic alkane chain with hydrophilic phosphate and amine groups. We thus suppose that the hydrophobic part of miltefosine plays a role in the interaction with misfolded SOD1 and the inhibition of abnormal oligomerization.

Specificity of the Drugs to Suppress Protein Aggregation/Oligomerization

Not all drugs with significant hydrophobicity (or limited water solubility) were potent against inhibition of SOD1 oligomerization; for example, cerivastatin and fluvastatin have comparable water solubility (*ca.* 4×10^{-3} g/L) to that of simvastatin and mevastatin but did not affect the aggregation kinetics of apo-SOD1(G37R)$^{S\text{-}S}$ (data not shown). Accordingly, the chemical structures of our hit compounds will have specific interactions with apo-SOD1(G37R)$^{S\text{-}S}$ to inhibit the formation of insoluble oligomers.

In addition to the formation of S-S oligomers, we have previously shown that reduction of the disulfide bond in apo-SOD1 triggers the formation of insoluble aggregates with amyloid-like fibrillar morphologies (Furukawa et al., 2008). As shown in **Figure 5A** (no drugs), the disulfide-reduced form of apo-SOD1 with G37R mutation [apo-SOD1(G37R)^{SH}] was confirmed to form insoluble aggregates by shaking at 37°C overnight. We have then chosen simvastatin, alfacalcidol, and miltefosine as representatives of the three groups mentioned above and tested their efficacy to suppress the formation of amyloid-like insoluble aggregates derived from apo-SOD1(G37R)^{SH}. Almost all fractions of apo-SOD1(G37R)^{SH}, however, became insoluble even in the presence of those three representative drugs (**Figure 5A**). Furthermore, in order to test if inhibitory effects of those drugs on the protein aggregation are limited to SOD1, we examined the aggregation of huntingtin with an elongated polyQ tract, which is a pathological hallmark of Huntington disease. As shown in **Figure 5B**, the translation product of exon 1 in the huntingtin gene with 42 consecutive glutamines [HTT^{EX1}(42Q)] formed insoluble aggregates in a sigmoidal kinetics; however, no inhibitory effects of the drugs on

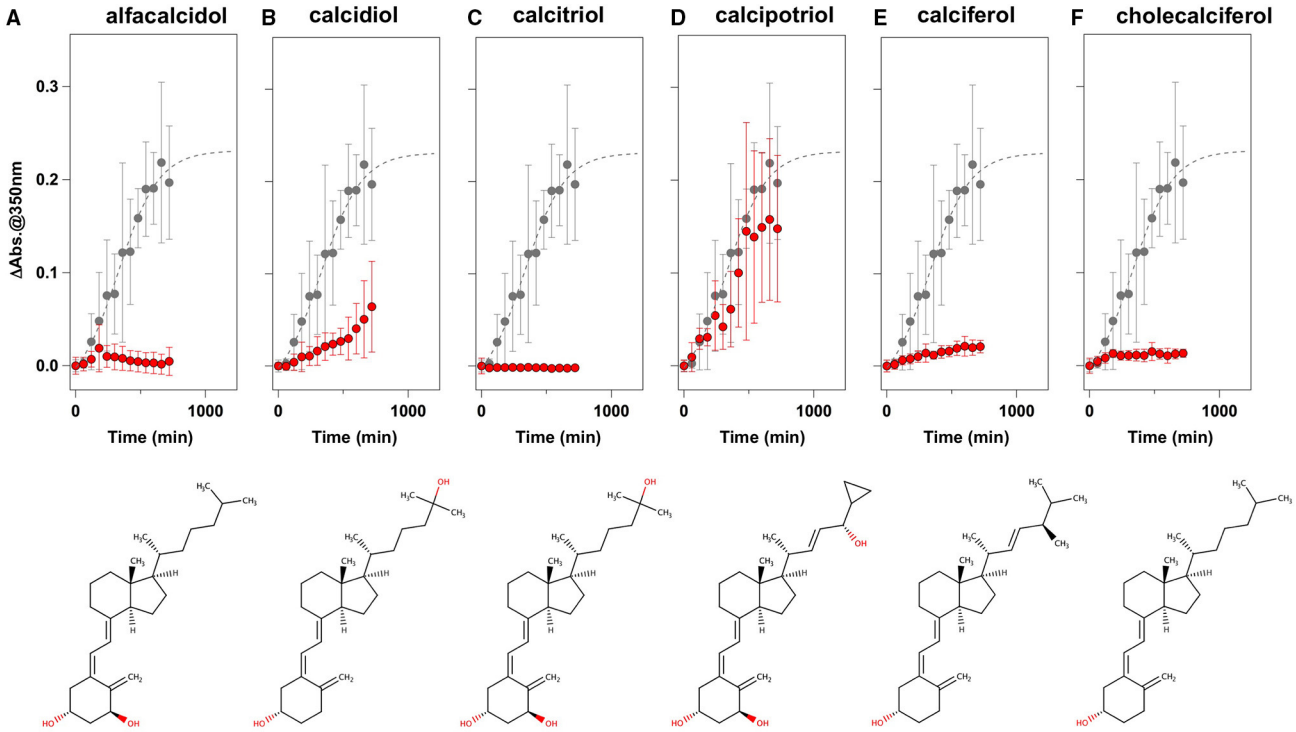

FIGURE 3 | Vitamin D derivatives as potent inhibitors for the formation of insoluble apo-SOD1(G37R)$^{S\text{-}S}$ aggregates. (A–F) The turbidity increase of 20 μM apo-SOD1(G37R)$^{S\text{-}S}$ in the presence of 1 M Gdn is shown in the presence of the following compounds (red filled circles): **(A)** alfacalcidol, **(B)** calcidol, **(C)** calcitriol, **(D)** calcipotriol, **(E)** calciferol, and **(F)** cholecalciferol. In each panel, the aggregation kinetics without any drugs was shown as gray filled circles. The kinetics was monitored by changes in the solution turbidity (the absorbance at 350 nm), and the final concentration of drugs added was 20 μg/mL. Experiments were repeated more than three times to estimate error bars (standard deviation). Structures of the chemical compounds were also shown below the panels.

the aggregation of HTT^{EX1}(42Q) were confirmed. Furthermore, the three representative drugs inhibited the turbidity increase in the aggregation of apo-SOD1$^{S\text{-}S}$ with the other ALS-causing mutation, G85R (data not shown). These results thus show that the drugs (simvastatin, alfacalcidol, and miltefosine) can effectively and also specifically suppress the formation of insoluble S-S oligomers derived from apo-SOD1$^{S\text{-}S}$ proteins. Nonetheless, it remains obscure how those drugs interact with SOD1 to keep it soluble.

The Drugs Inhibit the Interactions between Misfolded SOD1 Molecules Leading to Formation of Insoluble Aggregates

We first supposed that the drugs might prevent apo-SOD1(G37R)$^{S\text{-}S}$ from aggregation/oligomerization by stabilizing its folded conformation, and we thus examined effects of the drugs on the thermostability of apo-SOD1(G37R)$^{S\text{-}S}$ by using differential scanning calorimetry (DSC). The melting temperature, T_m, of apo-SOD1(G37R)$^{S\text{-}S}$ was, however, unaffected by the drugs: 42.2°C in the absence of any drugs; 41.6, 41.9, and 42.2°C in the presence of simvastatin, alfacalcidol, and miltefosine, respectively. It is thus unlikely that the drugs interact with the folded apo-SOD1(G37R)$^{S\text{-}S}$ to stabilize it.

While the drugs completely suppressed the formation of insoluble S-S oligomers, we noted that distinct, albeit slight, amounts of disulfide cross-linked oligomers were observed also in the soluble fraction in the presence of the drugs (**Figure 4**). Furthermore, the SOD1 band around 20 kDa was blurred in the presence of all drugs tested (indicated by arrows in **Figure 4**), suggesting the disulfide shuffling within a SOD1 molecule (**Figure 1B**). Therefore, the drugs might not act on the folded conformation of apo-SOD1$^{S\text{-}S}$ so as to inhibit the disulfide shuffling; rather, the drugs would prevent aberrant interactions among the disulfide-shuffled SOD1s that possibly lead to the formation of insoluble aggregates. In order to resolve those blurred bands, the soluble fractions of apo-SOD1$^{S\text{-}S}$ shaken at 1200 rpm in the presence and absence of the drugs for 2 h were examined with SDS-PAGE using a polyacrylamide gel containing 5 M urea. As shown in **Figure 6A**, multiple bands with distinct electrophoretic mobilities (at least four major bands) became apparent after agitation of apo-SOD1(G37R)$^{S\text{-}S}$ regardless of the presence or absence of the drugs. By treatment of the samples with the reducing agent, DTT, the multiple bands were collapsed into the single band corresponding to that of SOD1^{SH} (data not shown), corroborating that the multiplicity of bands in **Figure 6A** is caused by the intramolecular disulfide shuffling. Given little effects of the drugs on the band multiplicity, the drugs did not

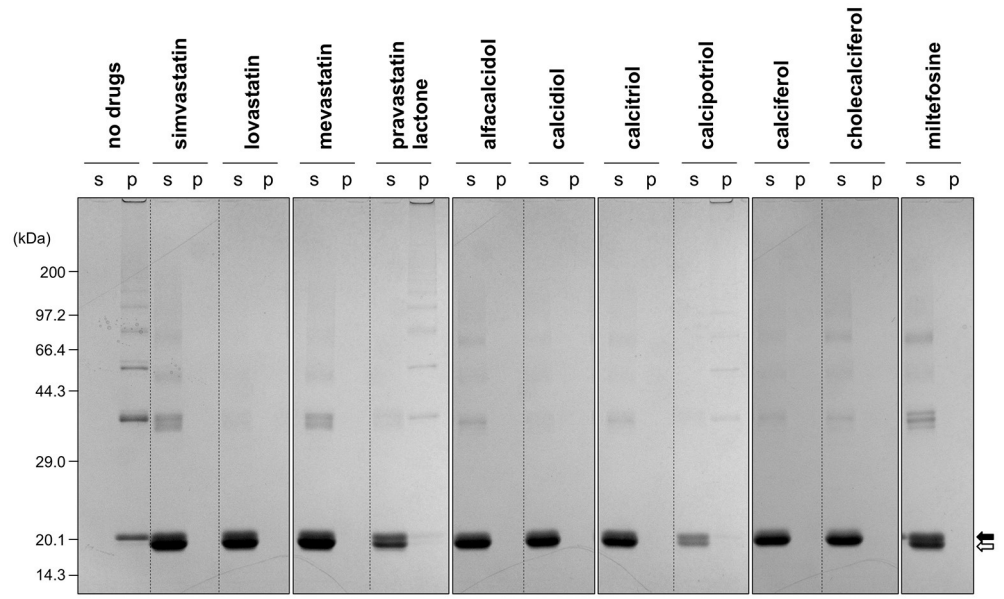

FIGURE 4 | Formation of insoluble SOD1 oligomers was efficiently suppressed by the hit compounds. As shown in **Figures 2**, **3**, 20 μM apo-SOD1(G37R)$^{S\text{-}S}$ was shaken at 37°C for 12 h in the NNE buffer containing 1 M Gdn in the presence of the indicated drugs (20 μg/mL) and then fractionated into soluble supernatant (s) and insoluble pellet (p) by ultracentrifugation. Both fractions were then analyzed by non-reducing SDS-PAGE using a 12.5% polyacrylamide gel. The position of the band corresponding to SOD1 with and without the canonical disulfide bond was indicated by open and filled arrows, respectively.

TABLE 1 | Expected values for water solubility of drugs examined in this study.

Drugs	M.W.[a]	Water solubility		Data source
		g/L	μM	
Simvastatin	418.6	7.7×10^{-4}	1.8×10^{0}	ChemIDplus[b]
Lovastatin	404.5	2.1×10^{-3}	5.3×10^{0}	ChemIDplus[b]
Mevastatin	390.5	4.8×10^{-3}	1.2×10^{1}	ChemIDplus[b]
Pravastatin lactone	406.5	2.4×10^{-2}	5.9×10^{1}	ChemIDplus[b]
Alfacalcidol	400.6	1.6×10^{-3}	4.1×10^{0}	DrugBank[c]
Calcidol	400.6	2.2×10^{-3}	5.5×10^{0}	DrugBank[c]
Calcitriol	416.6	6.7×10^{-3}	1.6×10^{1}	DrugBank[c]
Calcipotriol	412.6	1.4×10^{-2}	3.3×10^{1}	DrugBank[c]
Calciferol	396.7	4.3×10^{-4}	1.1×10^{0}	DrugBank[c]
Cholecalciferol	384.6	3.8×10^{-4}	1.0×10^{0}	DrugBank[c]
Miltefosine	407.6	2.2×10^{-4}	5.0×10^{-1}	DrugBank[c]
		2.5×10^{0}	6.1×10^{3}	Data sheet[d]

[a] *Molecular weight.*
[b] *http://chem.sis.nlm.nih.gov/chemidplus/.*
[c] *http://www.drugbank.ca.*
[d] *https://www.caymanchem.com/pdfs/63280.pdf.*

suppress abnormal shuffling of the disulfide bond within an apo-SOD1(G37R)$^{S\text{-}S}$ molecule.

Shuffling of the disulfide bond in SOD1 proteins can be more directly examined with a disulfide mapping analysis using MALDI-TOF mass spectrometry followed by the limited tryptic digestion. In the absence of Gdn, tryptic digestion of apo-SOD1(G37R)$^{S\text{-}S}$ produced mass peaks at *m/z* 4350 and 4507, which correspond to the peptides containing the canonical disulfide bond between Cys 57 and Cys 146 (**Figure 6B**, w/o Gdn). In contrast, several other mass peaks were emerged at *m/z* 4038 and 4607, when the apo-SOD1(G37R)$^{S\text{-}S}$ sample agitated in the presence of 1 M Gdn was trypsinized (**Figure 6B**, no drugs). These mass peaks correspond to the peptides containing abnormal disulfide bonds between Cys 6 and Cys 57 (*m/z* 4038) and between Cys 111 and Cys 146 (*m/z* 4607), consistent with the shuffling of the disulfide bond. These four mass peaks observed at *m/z* 4038, 4350, 4507, and 4607 disappeared upon treatment of the samples with DTT before the measurement (data not shown), supporting that the observed mass peaks represent the peptides crosslinked *via* an intramolecular disulfide bond(s). In the presence of the drugs, nonetheless, the mass peaks of those peptides containing abnormal disulfide bonds were still observed (**Figure 6B**), confirming that the drugs were unable to suppress the disulfide shuffling process within a SOD1 molecule.

The drugs we found here can almost completely suppress the formation of insoluble SOD1 aggregates cross-linked *via* disulfide bonds. The drugs were not able to inhibit the disulfide shuffling within a SOD1 molecule but could act on the soluble disulfide-shuffled SOD1 molecules to stop further aggregation into the insoluble species (**Figure 6C**). Soluble SOD1 oligomers have been shown to exhibit significant toxicities toward cultured cells (Luchinat et al., 2014; Proctor et al., 2016), while identities of the soluble oligomers in the previous studies would not match those of soluble disulfide-shuffled SOD1 in our current study. Actually, it remains obscure whether the misfolded SOD1 with an intramolecularly-shuffled disulfide bond is monomeric, dimeric, or oligomeric. Potential toxicities

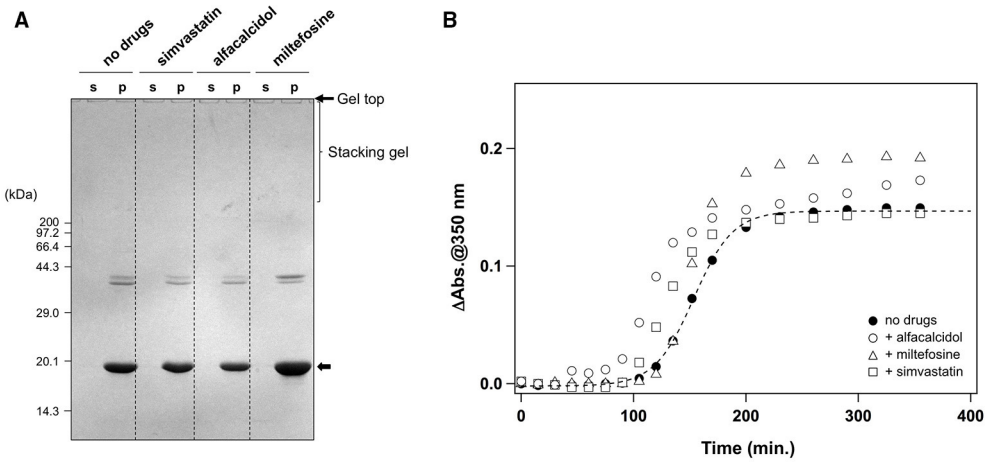

FIGURE 5 | Specificity of the hit compounds for the inhibition of apo-SOD1(G37R)$^{S\text{-}S}$ oligomerization. (A) 20 μM apo-SOD1(G37R)^{SH} in the NNE buffer with 5 mM DTT was shaken at 1200 rpm at 37°C in the presence or absence of the indicated drugs (20 μg/mL). After 24 h of agitation, the samples were fractionated to soluble supernatant (s) and insoluble pellets (p) by ultracentrifugation and then analyzed by non-reducing SDS-PAGE using a 12.5% polyacrylamide gel. **(B)** Effects of the drugs (20 μg/mL) on the aggregation kinetics of 20 μM HTT^{EX1}(42Q) were monitored by solution turbidity (absorbance at 350 nm): no drugs (filled circles), alfacalcidol (open circles), miltefosine (open triangles), and simvastatin (open squares).

of the soluble SOD1 species with a shuffled disulfide bond will also need to be examined, and our drugs might aggravate but not ameliorate the disease symptoms by stabilizing the soluble misfolded SOD1. Nonetheless, insoluble S-S oligomers are also observed as pathological species in the ALS-model mice; therefore, the drugs modulating the pathway for the formation of S-S oligomers will give pharmacological insights into the pathogenesis of *SOD1*-ALS.

Caveats for the Development of Pharmaceuticals for SOD1-ALS Based upon the Drugs Found in This Study

Among the drugs reported here, statins have been reported to associate with the occurrence of neuromuscular degenerative disease and an ALS-like syndrome, albeit controversial (Edwards et al., 2007; Sorensen and Lash, 2009; Zheng et al., 2013). Actually, prescription of statins for men and women in their 60 s dramatically increased from 1991 to 1998 (Magrini et al., 1997; Riahi et al., 2001), but no similar increase of ALS incidence was observed (Fang et al., 2009). Side effects of statin medications include muscle toxicity such as myopathy (Sathasivam and Lecky, 2008), and limited evidence for neurotoxic effects of statins has been reported (Kiortsis et al., 2007). Nonetheless, a strong association between statin medications and functional decline/muscle cramping in patients with ALS has been reported (Zinman et al., 2008). While it remains unknown if statins are beneficial for ALS patients with *SOD1* mutations, administration of the statin (simvastatin) to *SOD1*-ALS model mice expressing human SOD1 with G93A mutation (G93A mice) was found to accelerate the disease progression and shorten the survival (Su et al., 2016). Given that a high level of lipids in serum is also proposed to be neuroprotective in ALS cases (Dupuis et al., 2008; Yoshii et al., 2010), treatment of ALS patients with statins inhibiting the biosynthesis of cholesterol should be cautious.

In contrast, vitamin D has been proposed as a potential therapy in ALS (Gianforcaro and Hamadeh, 2014), and several mechanisms describing positive effects of vitamin D on ALS have been suggested (Gianforcaro and Hamadeh, 2014). Among those, supplementation of vitamin D has been found to decrease the levels of pro-inflammatory cytokines such as TNF-α and would thereby reduce neuroinflammation in ALS (Gianforcaro and Hamadeh, 2014). Also, vitamin D has been suggested to have roles in muscle cell proliferation and differentiation and thus improve musculoskeletal functions (Gianforcaro and Hamadeh, 2014); indeed, vitamin D_3 supplementation to the ALS patients reduced their decline in the ALSFRS-R score (Karam et al., 2013), which is a functional rating scale, and levels of vitamin D (serum calcidiol) appear to correlate with the ALS prognosis (Camu et al., 2014). Furthermore, vitamin D receptor-knockout mice exhibited significant impairment of locomotor and muscular functions, supporting a role of vitamin D in the maintenance of motor neurons (Burne et al., 2005). Deficiency of vitamin D_3 in G93A mice was found to improve early disease severity and delays disease onset but with decline in the motor performance (Solomon et al., 2011); instead, supplementation of high doses of vitamin D_3 to G93A mice improved their paw grip endurance and motor performance but with limited effectiveness on the disease course (Gianforcaro and Hamadeh, 2012; Gianforcaro et al., 2013). It is thus interesting to test in the future if vitamin D and/or its derivatives interact with mutant SOD1 to suppress the misfolding process and reduce their neurotoxicity in model mice.

Miltefosine is an antimicrobial drug that exhibits activity against parasites, pathogenic bacteria, and fungi (Dorlo et al., 2012), while no reports have been published on its efficacy to ALS and other neurodegenerative diseases.

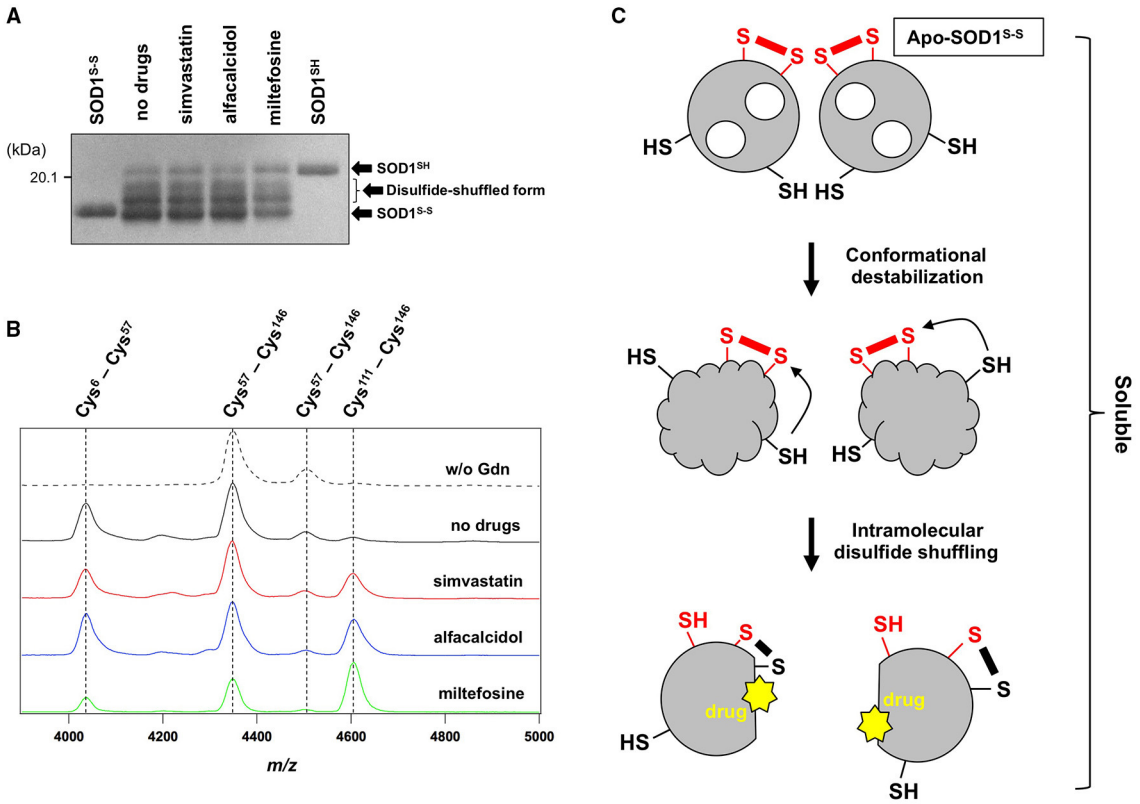

FIGURE 6 | The drugs could not inhibit the disulfide shuffling within an apo-SOD1(G37R)$^{S-S}$ molecule. (A) Apo-SOD1(G37R)$^{S-S}$ (20 μM) was agitated for 2 h in the presence of 1 M Gdn with and without the indicated drugs, and the soluble fraction obtained with ultracentrifugation was analyzed by non-reducing SDS-PAGE using a 12.5% polyacrylamide gel in the presence of 5 M urea. As controls, SOD1^{SH} and SOD1^{S-S} were also loaded on a gel. **(B)** After agitated for 2 h at 37°C in the presence of 1 M Gdn, the soluble fractions of apo-SOD1(G37R)$^{S-S}$ were trypsinized and analyzed by MALDI-TOF mass spectrometry (see Materials and methods). Reductant-sensitive mass peaks observed at *m/z* 4038, 4350, 4507, and 4607 were assigned to the peptides containing a disulfide bond between Cys 6 and Cys57, Cys 57 and Cys 146, Cys 57 and Cys 146, and Cys 111 and Cys 146, respectively. **(C)** Schematic representation of the SOD1 aggregation pathway inhibited by the drugs. Conformational destabilization of apo-SOD1^{S-S} triggers the intramolecular shuffling of the disulfide bond, and the drugs in this study are considered to interact with the disulfide-shuffled conformation of SOD1 and suppress the interaction of those disulfide-shuffled SOD1 proteins that leads to the formation of insoluble aggregates.

As summarized in the PubChem compound database (http://pubchem.ncbi.nlm.nih.gov), miltefosine has been reported to show toxicity toward some of human cells such as cancer cells, macrophages, and erythrocytes; therefore, a potential toxicity of miltefosine against neurons should be evaluated.

While the drugs found here (statins, vitamin D derivatives, and miltefosine) cannot be directly used for clinical treatment of *SOD1*-ALS, those drugs are found to specifically interact with a misfolded conformation of mutant SOD1 and thereby suppress the formation of insoluble oligomers/aggregates *in vitro* (**Figure 6C**). More effective and safer compounds with the ability to suppress the aggregation of SOD1 could hence be developed based upon our drugs and also be useful in evaluating the toxicity of misfolded/aggregated SOD1 in cultured cells to eventually modulate the disease course of *SOD1*-ALS cases.

AUTHOR CONTRIBUTIONS

YF directed the project, analyzed the data and wrote the manuscript. IA, KT, and ET performed experiments and analyzed the data. AM and SA performed DSC experiments and analyzed the data. All authors reviewed the manuscript.

FUNDING

This work was supported by Grants-in-Aid 16H04768 for Scientific Research (B) (to YF), 15H01566 for Scientific Research on Innovative Areas (to YF), 15K14480 for Challenging Exploratory Research (to YF), and 15H06588 for Young Scientists (Start-up) (to ET) from the Ministry of Education, Culture, Sports, Science, and Technology of Japan and also in part by Cooperative Research in Joint Studies at Institute for Molecular Science, Japan.

REFERENCES

Abel, O., Powell, J. F., Andersen, P. M., and Al-Chalabi, A. (2012). ALSoD: a user-friendly online bioinformatics tool for amyotrophic lateral sclerosis genetics. *Hum. Mutat.* 33, 1345–1351. doi: 10.1002/humu.22157

Andersen, P. M., and Al-Chalabi, A. (2011). Clinical genetics of amyotrophic lateral sclerosis: what do we really know? *Nat. Rev. Neurol.* 7, 603–615. doi: 10.1038/nrneurol.2011.150

Antonyuk, S., Strange, R. W., and Hasnain, S. S. (2010). Structural discovery of small molecule binding sites in Cu-Zn human superoxide dismutase familial amyotrophic lateral sclerosis mutants provides insights for lead optimization. *J. Med. Chem.* 53, 1402–1406. doi: 10.1021/jm9017948

Auclair, J. R., Boggio, K. J., Petsko, G. A., Ringe, D., and Agar, J. N. (2010). Strategies for stabilizing superoxide dismutase (SOD1), the protein destabilized in the most common form of familial amyotrophic lateral sclerosis. *Proc. Natl. Acad. Sci. U.S.A.* 107, 21394–21399. doi: 10.1073/pnas.1015463107

Banci, L., Bertini, I., Blazevits, O., Calderone, V., Cantini, F., Mao, J., et al. (2012). Interaction of cisplatin with human superoxide dismutase. *J. Am. Chem. Soc.* 134, 7009–7014. doi: 10.1021/ja211591n

Benmohamed, R., Arvanites, A. C., Kim, J., Ferrante, R. J., Silverman, R. B., Morimoto, R. I., et al. (2011). Identification of compounds protective against G93A-SOD1 toxicity for the treatment of amyotrophic lateral sclerosis. *Amyotroph. Lateral Scler.* 12, 87–96. doi: 10.3109/17482968.2010.522586

Bruijn, L. I., Houseweart, M. K., Kato, S., Anderson, K. L., Anderson, S. D., Ohama, E., et al. (1998). Aggregation and motor neuron toxicity of an ALS-linked SOD1 mutant independent from wild-type SOD1. *Science* 281, 1851–1854. doi: 10.1126/science.281.5384.1851

Burne, T. H., Mcgrath, J. J., Eyles, D. W., and Mackay-Sim, A. (2005). Behavioural characterization of vitamin D receptor knockout mice. *Behav. Brain Res.* 157, 299–308. doi: 10.1016/j.bbr.2004.07.008

Camu, W., Tremblier, B., Plassot, C., Alphandery, S., Salsac, C., Pageot, N., et al. (2014). Vitamin D confers protection to motoneurons and is a prognostic factor of amyotrophic lateral sclerosis. *Neurobiol. Aging* 35, 1198–1205. doi: 10.1016/j.neurobiolaging.2013.11.005

Chattopadhyay, M., Durazo, A., Sohn, S. H., Strong, C. D., Gralla, E. B., Whitelegge, J. P., et al. (2008). Initiation and elongation in fibrillation of ALS-linked superoxide dismutase. *Proc. Natl. Acad. Sci. U.S.A.* 105, 18663–18668. doi: 10.1073/pnas.0807058105

Deng, H. X., Shi, Y., Furukawa, Y., Zhai, H., Fu, R., Liu, E., et al. (2006). Conversion to the amyotrophic lateral sclerosis phenotype is associated with intermolecular linked insoluble aggregates of SOD1 in mitochondria. *Proc. Natl. Acad. Sci. U.S.A.* 103, 7142–7147. doi: 10.1073/pnas.0602046103

Dorlo, T. P., Balasegaram, M., Beijnen, J. H., and De Vries, P. J. (2012). Miltefosine: a review of its pharmacology and therapeutic efficacy in the treatment of leishmaniasis. *J. Antimicrob. Chemother.* 67, 2576–2597. doi: 10.1093/jac/dks275

Dupuis, L., Corcia, P., Fergani, A., Gonzalez De Aguilar, J. L., Bonnefont-Rousselot, D., Bittar, R., et al. (2008). Dyslipidemia is a protective factor in amyotrophic lateral sclerosis. *Neurology* 70, 1004–1009. doi: 10.1212/01.wnl.0000285080.70324.27

Edwards, I. R., Star, K., and Kiuru, A. (2007). Statins, neuromuscular degenerative disease and an amyotrophic lateral sclerosis-like syndrome: an analysis of individual case safety reports from vigibase. *Drug Saf.* 30, 515–525. doi: 10.2165/00002018-200730060-00005

Fang, F., Valdimarsdóttir, U., Bellocco, R., Ronnevi, L. O., Sparén, P., Fall, K., et al. (2009). Amyotrophic lateral sclerosis in Sweden, 1991-2005. *Arch. Neurol.* 66, 515–519. doi: 10.1001/archneurol.2009.13

Furukawa, Y. (2012). "Protein aggregates in pathological inclusions of amyotrophic lateral sclerosis," in *Amyotrophic Lateral Sclerosis*, ed M. H. Maurer (Rijeka: InTech), 335–356.

Furukawa, Y., Anzai, I., Akiyama, S., Imai, M., Cruz, F. J., Saio, T., et al. (2016). Conformational disorder of the most immature Cu, Zn-superoxide dismutase leading to amyotrophic lateral sclerosis. *J. Biol. Chem.* 291, 4144–4155. doi: 10.1074/jbc.M115.683763

Furukawa, Y., Fu, R., Deng, H. X., Siddique, T., and O'Halloran, T. V. (2006). Disulfide cross-linked protein represents a significant fraction of ALS-associated Cu, Zn-superoxide dismutase aggregates in spinal cords of model mice. *Proc. Natl. Acad. Sci. U.S.A.* 103, 7148–7153. doi: 10.1073/pnas.0602048103

Furukawa, Y., Kaneko, K., Yamanaka, K., O'Halloran, T. V., and Nukina, N. (2008). Complete loss of post-translational modifications triggers fibrillar aggregation of SOD1 in familial form of ALS. *J. Biol. Chem.* 283, 24167–24176. doi: 10.1074/jbc.M802083200

Furukawa, Y., and O'Halloran, T. V. (2005). Amyotrophic lateral sclerosis mutations have the greatest destabilizing effect on the apo, reduced form of SOD1, leading to unfolding and oxidative aggregation. *J. Biol. Chem.* 280, 17266–17274. doi: 10.1074/jbc.M500482200

Furukawa, Y., Torres, A. S., and O'Halloran, T. V. (2004). Oxygen-induced maturation of SOD1: a key role for disulfide formation by the copper chaperone CCS. *EMBO J.* 23, 2872–2881. doi: 10.1038/sj.emboj.7600276

Genç, B., and Özdinler, P. H. (2014). Moving forward in clinical trials for ALS: motor neurons lead the way please. *Drug Discov. Today* 19, 441–449. doi: 10.1016/j.drudis.2013.10.014

Gianforcaro, A., and Hamadeh, M. J. (2012). Dietary vitamin D3 supplementation at 10x the adequate intake improves functional capacity in the G93A transgenic mouse model of ALS, a pilot study. *CNS Neurosci. Ther.* 18, 547–557. doi: 10.1111/j.1755-5949.2012.00316.x

Gianforcaro, A., and Hamadeh, M. J. (2014). Vitamin D as a potential therapy in amyotrophic lateral sclerosis. *CNS Neurosci. Ther.* 20, 101–111. doi: 10.1111/cns.12204

Gianforcaro, A., Solomon, J. A., and Hamadeh, M. J. (2013). Vitamin D(3) at 50x AI attenuates the decline in paw grip endurance, but not disease outcomes, in the G93A mouse model of ALS, and is toxic in females. *PLoS ONE* 8:e30243. doi: 10.1371/journal.pone.0030243

Karam, C., Barrett, M. J., Imperato, T., Macgowan, D. J., and Scelsa, S. (2013). Vitamin D deficiency and its supplementation in patients with amyotrophic lateral sclerosis. *J. Clin. Neurosci.* 20, 1550–1553. doi: 10.1016/j.jocn.2013.01.011

Kiortsis, D. N., Filippatos, T. D., Mikhailidis, D. P., Elisaf, M. S., and Liberopoulos, E. N. (2007). Statin-associated adverse effects beyond muscle and liver toxicity. *Atherosclerosis* 195, 7–16. doi: 10.1016/j.atherosclerosis.2006.10.001

Luchinat, E., Barbieri, L., Rubino, J. T., Kozyreva, T., Cantini, F., and Banci, L. (2014). In-cell NMR reveals potential precursor of toxic species from SOD1 fALS mutants. *Nat. Commun.* 5, 5502. doi: 10.1038/ncomms6502

Magrini, N., Einarson, T., Vaccheri, A., Mcmanus, P., Montanaro, N., and Bergman, U. (1997). Use of lipid-lowering drugs from 1990 to 1994: an international comparison among Australia, Finland, Italy (Emilia Romagna Region), Norway and Sweden. *Eur. J. Clin. Pharmacol.* 53, 185–189. doi: 10.1007/s002280050360

McCord, J. M., and Fridovich, I. (1969). Superoxide dismutase. An enzymic function for erythrocuprein (hemocuprein). *J. Biol. Chem.* 244, 6049–6055.

Mitomi, Y., Nomura, T., Kurosawa, M., Nukina, N., and Furukawa, Y. (2012). Post-aggregation oxidation of mutant huntingtin controls the interactions between aggregates. *J. Biol. Chem.* 287, 34764–34775. doi: 10.1074/jbc.M112.387035

Nowak, R. J., Cuny, G. D., Choi, S., Lansbury, P. T., and Ray, S. S. (2010). Improving binding specificity of pharmacological chaperones that target mutant superoxide dismutase-1 linked to familial amyotrophic lateral sclerosis using computational methods. *J. Med. Chem.* 53, 2709–2718. doi: 10.1021/jm901062p

Proctor, E. A., Fee, L., Tao, Y., Redler, R. L., Fay, J. M., Zhang, Y., et al. (2016). Nonnative SOD1 trimer is toxic to motor neurons in a model of amyotrophic lateral sclerosis. *Proc. Natl. Acad. Sci. U.S.A.* 113, 614–619. doi: 10.1073/pnas.1516725113

Rakhit, R., Crow, J. P., Lepock, J. R., Kondejewski, L. H., Cashman, N. R., and Chakrabartty, A. (2004). Monomeric Cu,Zn-superoxide dismutase is a common misfolding intermediate in the oxidation models of sporadic and familial amyotrophic lateral sclerosis. *J. Biol. Chem.* 279, 15499–15504. doi: 10.1074/jbc.M313295200

Ray, S. S., Nowak, R. J., Brown, R. H. Jr., and Lansbury, P. T. Jr. (2005). Small-molecule-mediated stabilization of familial amyotrophic lateral sclerosis-linked superoxide dismutase mutants against unfolding and aggregation. *Proc. Natl. Acad. Sci. U.S.A.* 102, 3639–3644. doi: 10.1073/pnas.0408277102

Ray, S. S., Nowak, R. J., Strolovich, K., Brown, R. H. Jr., Walz, T., and Lansbury, P. T. Jr. (2004). An intersubunit disulfide bond prevents *in vitro* aggregation of a superoxide dismutase-1 mutant linked to familial amyotrophic lateral sclerosis. *Biochemistry* 43, 4899–4905. doi: 10.1021/bi030246r

Renton, A. E., Chiò, A., and Traynor, B. J. (2014). State of play in amyotrophic lateral sclerosis genetics. *Nat. Neurosci.* 17, 17–23. doi: 10.1038/nn.3584

Riahi, S., Fonager, K., Toft, E., Hvilsted-Rasmussen, L., Bendsen, J., Paaske Johnsen, S., et al. (2001). Use of lipid-lowering drugs during 1991-98 in Northern Jutland, Denmark. *Br. J. Clin. Pharmacol.* 52, 307–311. doi: 10.1046/j.0306-5251.2001.01439.x

Rodriguez, J. A., Shaw, B. F., Durazo, A., Sohn, S. H., Doucette, P. A., Nersissian, A. M., et al. (2005). Destabilization of apoprotein is insufficient to explain Cu,Zn-superoxide dismutase-linked ALS pathogenesis. *Proc. Natl. Acad. Sci. U.S.A.* 102, 10516–10521. doi: 10.1073/pnas.0502515102

Rosen, D. R., Siddique, T., Patterson, D., Figlewicz, D. A., Sapp, P., Hentati, A., et al. (1993). Mutations in Cu/Zn superoxide dismutase gene are associated with familial amyotrophic lateral sclerosis. *Nature* 362, 59–62. doi: 10.1038/362059a0

Sathasivam, S., and Lecky, B. (2008). Statin induced myopathy. *BMJ* 337:a2286. doi: 10.1136/bmj.a2286

Solomon, J. A., Gianforcaro, A., and Hamadeh, M. J. (2011). Vitamin D3 deficiency differentially affects functional and disease outcomes in the G93A mouse model of amyotrophic lateral sclerosis. *PLoS ONE* 6:e29354. doi: 10.1371/journal.pone.0029354

Sørensen, H. T., and Lash, T. L. (2009). Statins and amyotrophic lateral sclerosis–the level of evidence for an association. *J. Intern. Med.* 266, 520–526. doi: 10.1111/j.1365-2796.2009.02173.x

Stevens, J. C., Chia, R., Hendriks, W. T., Bros-Facer, V., Van Minnen, J., Martin, J. E., et al. (2010). Modification of superoxide dismutase 1 (SOD1) properties by a GFP tag–implications for research into amyotrophic lateral sclerosis (ALS). *PLoS ONE* 5:e9541. doi: 10.1371/journal.pone.0009541

Su, X. W., Nandar, W., Neely, E. B., Simmons, Z., and Connor, J. R. (2016). Statins accelerate disease progression and shorten survival in SOD1 mice. *Muscle Nerve* 54, 284–291. doi: 10.1002/mus.25048

Toichi, K., Yamanaka, K., and Furukawa, Y. (2013). Disulfide scrambling describes the oligomer formation of superoxide dismutase (SOD1) proteins in the familial form of amyotrophic lateral sclerosis. *J. Biol. Chem.* 288, 4970–4980. doi: 10.1074/jbc.M112.414235

Wright, G. S., Antonyuk, S. V., Kershaw, N. M., Strange, R. W., and Samar Hasnain, S. (2013). Ligand binding and aggregation of pathogenic SOD1. *Nat. Commun.* 4, 1758. doi: 10.1038/ncomms2750

Yoshii, Y., Hadano, S., Otomo, A., Kawabe, K., Ikeda, K., and Iwasaki, Y. (2010). Lower serum lipid levels are related to respiratory impairment in patients with ALS. *Neurology* 74, 2027–2028. doi: 10.1212/WNL.0b013e3181e03bbe

Zheng, Z., Sheng, L., and Shang, H. (2013). Statins and amyotrophic lateral sclerosis: a systematic review and meta-analysis. *Amyotroph. Lateral Scler. Frontotemporal Degener.* 14, 241–245. doi: 10.3109/21678421.2012.732078

Zinman, L., Sadeghi, R., Gawel, M., Patton, D., and Kiss, A. (2008). Are statin medications safe in patients with ALS? *Amyotroph. Lateral Scler.* 9, 223–228. doi: 10.1080/17482960802031092

Conflict of Interest Statement: The authors declare that the research was conducted in the absence of any commercial or financial relationships that could be construed as a potential conflict of interest.

Advantages of publishing in Frontiers

OPEN ACCESS
Articles are free to read, for greatest visibility

COLLABORATIVE PEER-REVIEW
Designed to be rigorous – yet also collaborative, fair and constructive

FAST PUBLICATION
Average 85 days from submission to publication (across all journals)

COPYRIGHT TO AUTHORS
No limit to article distribution and re-use

TRANSPARENT
Editors and reviewers acknowledged by name on published articles

SUPPORT
By our Swiss-based editorial team

IMPACT METRICS
Advanced metrics track your article's impact

GLOBAL SPREAD
5'100'000+ monthly article views and downloads

LOOP RESEARCH NETWORK
Our network increases readership for your article

Frontiers
EPFL Innovation Park, Building I • 1015 Lausanne • Switzerland
Tel +41 21 510 17 00 • Fax +41 21 510 17 01 • info@frontiersin.org
www.frontiersin.org

Find us on